Regulation of telomere length in mammalian cells

Ruman Rahman

Thesis presented for degree of
Doctor of Philosophy

The University of Edinburgh

2007

Declaration

I declare that the work presented in this thesis is my own, except where otherwise stated. All experiments were designed by myself in collaboration with my supervisor Dr. Wei Cui. No part of this thesis has been, or will be, submitted for any other degree, diploma or qualification.

Ruman Rahman
November 2006

Acknowledgements

I am gratified to my supervisor Dr. Wei Cui for her advice, encouragement, patience and expert guidance throughout the last three years and for simply making my doctoral studies such an enjoyable time. I would also like to thank my University of Edinburgh supervisors Prof. Ian Wilmut and Prof. John Ansell, who kindly reviewed my progress each year. Thanks are also due to all members of the Geron lab at Roslin, for much advice and encouragement during this time. A special thank you is reserved for Dr.Nick Forsythe for a plethora of technical and scientific advice regarding my experimental work.

I would like to acknowledge and give many thanks for Prof. Lea Harrington and Natalie Erdmann for inviting me to Toronto for two weeks in order to familiarize with the Quantitative-FISH technique. A further acknowledgement is due to Ling Mo for generation of the GRN25 transgenic lines in our laboratory and finally to the von Zglinicki laboratory in Newcastle for conducting oxidative stress analysis on some of the lines investigated during this project.

I would like to give a very special thank you to my parents and my partner for their love, moral support, encouragement and helping me stay focused and positive these last three years.

Finally, I would like to thank Prof. John Clark, initially my primary supervisor, who sadly passed away at the end of my first year of study. That year was sufficient for John, through his wonderful scientific thinking and manner, to have been an inspiration for me that I will take forward hereafter.

" We must, however, acknowledge, as it seems to me, that man with all his noble qualities... still bears in his bodily frame the indelible stamp of his lowly origin ".

Charles Darwin

Abstract

Mammalian telomere length is regulated in a dynamic manner through multi-factorial elements. This project focuses on specific aspects of both extrinsic and intrinsic factors that govern telomere length.

Expression of the human telomerase reverse transcriptase (hTERT) gene in sheep fibroblasts reconstitutes telomerase activity and extends their lifespan. Although stabilization of telomere length is directly correlated to hTERT expression level, this was not reflected in telomerase activity. Data presented here shows that overexpression of non-catalytic domains decreased telomerase activity, compromised senescence bypass status and did not enhance telomere maintenance, which may result from competitive binding to sheep TR molecules and/or disruption of hTERT homodimeric structure. These results are consistent with the notion that telomere maintenance requires a functional telomerase complex which contains an inter-dependent hTERT homodimeric structure.

The single-stranded 3' G-rich overhang has been implicated as a key feature with a telomeric end-protection configuration. Data presented here show that the 3' overhang is eroded during culture of sheep fibroblasts, indicating that the 3' overhang length shortens prior to replicative senescence in cultured sheep fibroblasts. Furthermore, a correlation between hTERT expression level, karyotypic stability and 3' overhang length is observed.

This project also demonstrated the first application of the Quantitative-FISH (Q-FISH) and Telomere-Oligonucleotide Ligation Assay (T-OLA) techniques in the sheep model system.

CONTENTS

CHAPTER 6 TELOMERE-OLIGONUCLEOTIDE LIGATION ASSAY AND LOW OXYGEN CULTURE IN OVINE FIBROBLASTS

List of Figures

List of Tables

CHAPTER 1: INTRODUCTION

1.1 A preface to telomere and telomerase biology

Often in nature things are not how they at first appear: a rock on the seafloor may be a poisonous fish and a beautiful flower in a garden may be a carnivorous insect lying in wait for prey. At one time, the DNA at the ends of chromosomes seemed to be static, yet in most organisms that have been studied, these tips, called telomeres, are actually ever changing; they shorten and lengthen repeatedly. Modern interest in telomeres and telomerase has its roots in experiments carried out in the 1930s by two remarkable geneticists: Barbara McClintock, then at the University of Missouri at Columbia, and Hermann J. Muller, then at the University of Edinburgh. Working separately and with different organisms, both investigators realized that chromosomes bore a special component at their ends that provided stability. Muller coined the term "telomere," from the Greek for "end" (telos) and "part" (meros). McClintock noted that without these end caps, chromosomes stick to one another, undergo structural changes and misbehave in other ways (McClintock 1939). Fast forward to the present day and we regard telomeres as key genetic elements in the regulation of the cellular ageing process, with telomere shortening in part, serving as a 'molecular clock' for replicative lifespan certainly *in vitro* and plausibly *in vivo*. Paradoxically a finite cellular lifespan may represent a primitive eukaryotic tumour suppression mechanism. In support of this, Mother Nature's counter mechanism to increase replicative lifespan, an enzyme known as telomerase, is not detected in most adult somatic tissues, but yet readily activated in the vast majority of tumours studied to date and is ever present in germline cells. Hence ageing and cancer may be two sides of the same coin, with telomeres and telomerase being more than mere bit part players. The net result over the past 25 years is seminal biological observations in the

field hinting at the possibility and feasibility of targeting both telomeres and telomerase components for therapeutic gain. Namely, strategies to target and inhibit telomerase in cancer settings and conversely to reactivate telomerase in tissues impacted upon by cellular ageing, have been a recent lure.

1.2   Telomere structure

1.2.1   Eukaryotic telomeres

Telomeres are specialized and essential DNA-protein complexes located at the ends of linear chromosomes, the nucleotide sequences of which were first revealed in 1978 by Elizabeth Blackburn, who found that the telomeres of the ciliated protozoan, *Tetrahymena thermophila*, consisted of a simple sequence of hexameric repeats of the nucleotides TTGGGG (Blackburn E.H & Gall, J.G 1978). In all vertebrates, telomere repeats are conserved as TTAGGG (Meyne et al., 1989) and similarly consist of proteins and reiterated Guanosine-rich repeats. The majority of telomeric DNA is double helical, with the GT-rich sequence paired with its CA complement, but in all eukaryotes studied, this G-rich 3'-end of the DNA protrudes as a single-stranded overhang. In humans, telomeres are comprised of a ~ 3-20kb array of duplex TTAGGG repeats, ending in a 100-500 nucleotide 3' protrusion (Harley et al., 1990; reviewed in de Lange 2004; Fig.1.1). Telomeres are essential elements that protect chromosomal termini from nuclease degradation and interchromosomal fusion and promote proper portioning of chromosomes during mitosis and meiosis, thereby contributing to genomic stability, (Counter et al., 1992, Hackett et al., 2001).
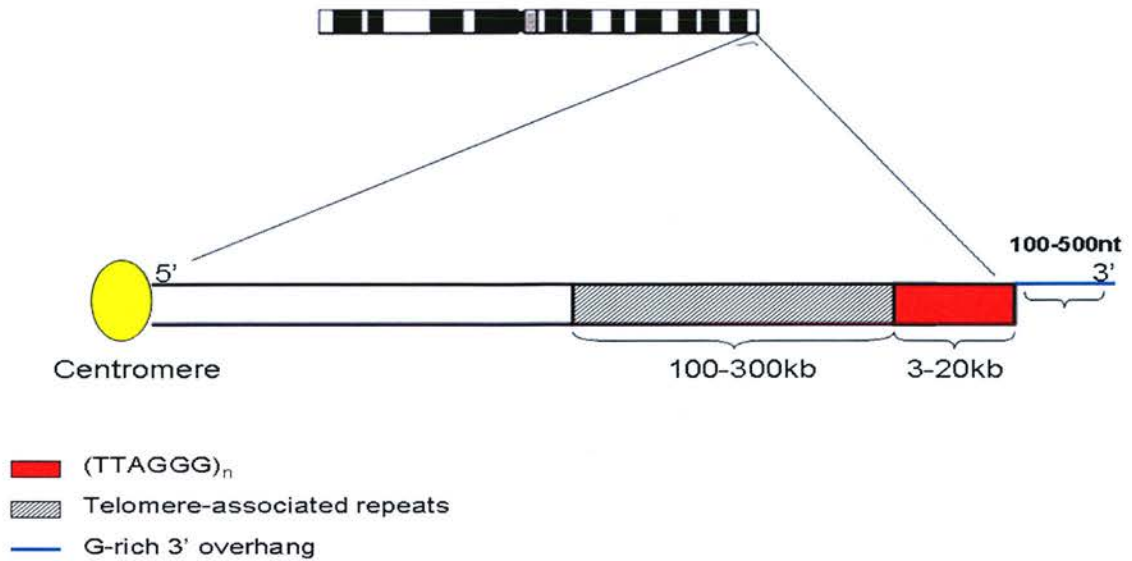
Figure 1.1 Classical human telomere structure. A typical human telomere (3-20kb) is depicted showing upstream sub-telomere associated repeats and downstream 3' protrusion of the G-rich strand.

1.2.2   Telomere structure – the new synthesis

Despite the important role of proper telomere function, it has become increasingly clear that telomeres do not simply function as a buffer zone that prevents loss of essential sequences. A large body of evidence dating back to the work of McClintock (McClintock 1939) is more consistent with the view that the telomeric complex allows cells to distinguish random chromosome breaks and natural chromosome ends. The classical view of linear chromosomes did not easily explain how telomeres are presumably 'protected' from DNA damage repair machinery. A recent seminal study from Jack Griffith and Titia de Lange revealed how mammalian chromosomes may overcome this burden: these studies used electron microscopy to demonstrate how the 3' single-strand telomeric overhang may invade the duplex repeat array thus

forming a Terminal (T)-loop structure at chromosomal termini and a displacement (D) loop further upstream (Griffith et al., 1999, commentary in Greider 1999). This proposed structure would give a mechanistic basis for how telomere ends may be protected from DNA damage surveillance systems (Fig. 1.2).
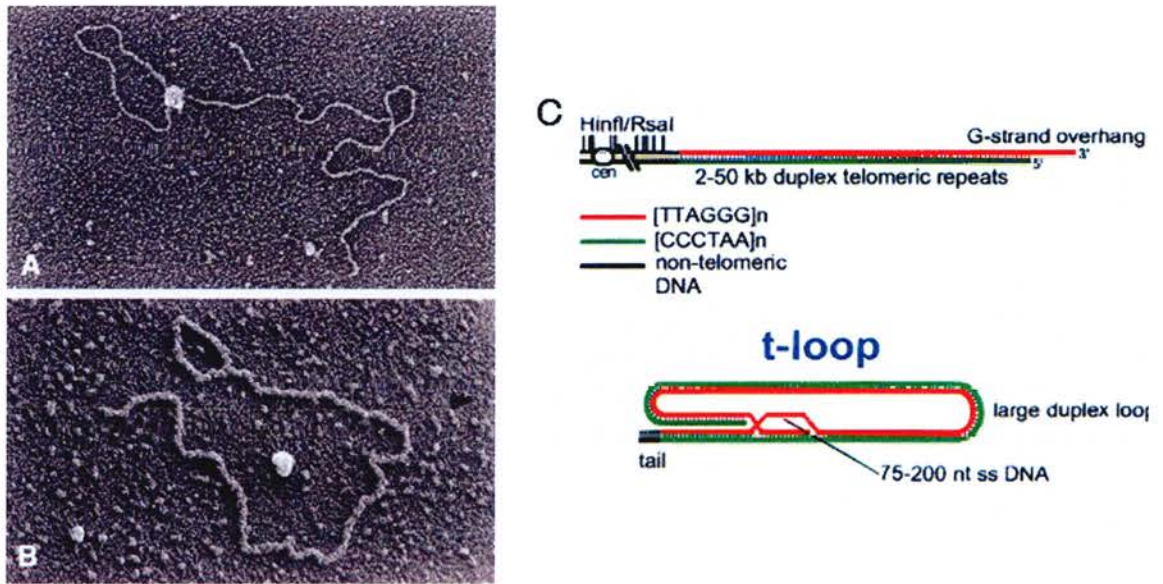
Figure 1.2. Mammalian telomeres end in a large duplex loop. (A-B) A telomeric DNA model containing 3kb of unique sequence DNA followed by ~2kb of TTAGGG repeating sequence with a 150-200nt 3' G-strand overhang. (DNA analyzed from HeLa cells). (C) The classical linear view of mammalian telomeres has been rejected in favour of a proposed T-loop structure whereby the single-stranded 3' overhang from the G-rich strand invades the telomere double-strand array, thus forming a telomere end-capping structure (figure adopted from Griffith, J.D et al 1999).

1.3   Telomere end-protection

1.3.1   Telomeric-loop (T-loop)

Telomere integrity thus plays a crucial role in the capacity for continuous cell proliferation. Both extrinsic and intrinsic factors facilitate in maintaining this integrity of telomeres. Furthermore, chromosome termini must be 'capped' in order to protect chromosomal ends from nuclease degradation, interchromosomal end fusions and improper recombination and repair, thereby contributing to genomic stability. Conversely, telomeres can lose integrity via loss of protection of the end structure (uncapped telomeres), which triggers immediate telomere instability, or by gradual attrition of telomeric DNA (loss of telomerase function). At the time of their switch to linear genomes, eukaryotes must have evolved a mechanism to manage their chromosome ends, creating two major problems: the first was the 'end replication' dilemma discussed in section 1.4.2 and the second problem lies in the ability of cells to distinguish natural chromosomal ends from sites of DNA damage. The finding that mammalian telomeres terminate in a duplex loop (T-loop), where most of the 3' overhang is tucked inside the telomere double-stranded array (Griffith et al., 1999; Fig. 1.2) hints at the structural basis for this end-protection function. Indeed T-loop structures are a conserved feature of telomere structure and are found not only in vertebrates, but also in ciliates (Murti K, G & Prescott D, M 1999) and trypanosomes (Munoz-Jordan et al., 2001). The size of the T-loop is highly variable and might not be important for telomere function. More likely the key function of the T-loop is the sequestration of the 3' overhang. Thus T-loops seem to be a good strategy to protect chromosome ends from fusion. In support of this, electron

microscopy observations on chicken erythrocyte and mouse lymphocytes, revealed that the T-loop is wrapped in telomere chromatin fibres in the form of closed terminal loops, which correspond to the T-loop structures adopted by telomere DNA (Nikitina T. & Woodcock C. 2004). Wrapping the T-loop in chromatin proteins probably hides the 3'-overhang from agents that detect free ends. However, how T-loops might allow cells to distinguish chromosome ends from DNA damage is less clear. We must also infer that the T-loop (or any non-canonical end structure) is to some extent dynamic at least through S-phase transition, to permit the telomerase complex (a specialized cellular ribonucleoprotein (RNP) reverse transcriptase complex consisting of an RNA template unit (TR) and a core catalytic subunit with reverse transcriptase activty (TERT), that synthesizes $TTAGGG_n$ telomeric repeats onto chromosomal ends (Greider & Blackburn 1987, Lingner et al., 1997, discussed in detail in section 1.8) and associated factors access to the telomere substrate (Mastuomi et al., 2003). Indeed the Bloom's syndrome helicase (encoded by the BLM gene that is defective in Bloom's syndrome), homologous to the RecQ subfamily of helicases, which functions as a 3'-5' DNA helicase *in vitro* and which requires a short 3' region of single-stranded DNA to unwind G4 DNA (four-stranded DNA), has been thus implicated to function at the telomere substrate (Sun et al., 1998, Huber et al., 2002). A number of key questions remain to be resolved regarding telomeric loops: what are the factors regulating T-loop dynamics; what percentage of mammalian telomeres carries this structure; does T-loop size vary between and within chromosomes in a chromosome complement; is the T-loop altered at replicative senescence? The latter hypothesis will be discussed in section 1.5.3. Moreover, a recent observation implicated T-loops as presenting a danger to

chromosome ends: low levels of telomeric circles were detected in normal human cells, indicating that telomere deletion by homologous recombination may be a feature of normal telomere metabolism (Wang et al., 2004). Hence protective T-loops may themselves represent a telomeric double-edged sword.

1.3.2   Telomere-associated factors and end capping

The ability of telomeres to evade the DNA-damage response is a consequence of their association with a set of protein complexes that protect chromosome ends and maintain telomere homeostasis. Loss of these factors leads to telomere uncapping and subsequent telomere dysfunction (reviewed in Harrington 2004). Some of these protecting factors bind along the duplex array of telomeric repeats whereas others bind to single-stranded telomeric DNA. Among these proteins, Telomere-repeat binding factor 1 (TRF1) and Telomere-repeat binding factor 2 (TRF2) directly bind double-stranded telomere DNA and interact with a number of proteins to maintain telomere structure (de Lange 2002, Iwano et al., 2004, and reviewed in Kim S, H et al., 2002). These two factors differ in their N-termini, which are rich in either acidic residues (TRF1) or basic residues (TRF2) and have both been shown to homdimerize through their Myb-related DNA-binding domains (Chong et al., 1995, Broccoli et al., 1997).

TRF1 was the first mammalian telomeric protein isolated, based on its *in vitro* specificity for double-stranded TTAGGG repeats (Zhong et al., 1992) and it has been shown that the amount of telomere-bound TRF1 correlates with telomere length. Overexpression of TRF1 shortened telomeres in human cells, whereas dominant-

negative TRF1 led to elongated telomeres (van Steensel et al., 1997, Smith, S. et al., 2000, Smogorzewska et al., 2000). Additionally, conditional TRF1 null mutant mouse embryonic stem (ES) cells showed growth defects and chromosomal instability (Iwano et al., 2004). Thus TRF1 binding to double-stranded telomere DNA functions as a negative regulator of telomere length and confers telomere end-protection.

TRF2 was subsequently identified as a paralog in the mammalian genic database. Based on *in vitro* and *in vivo* studies, TRF2 promotes T-loop formation by binding near the 3' telomeric overhang and is thus implicated in remodeling telomeres into T-loops (Griffith et al., 1999, Stansel et al., 2001). Overexpression of dominant-negative TRF2 activates the ATM/p53 or p16/RB pathways and induces cellular senescence or apoptosis (Karlseder et al., 1999, Smogorzewska et al., 2002). Moreover, inhibition of TRF2 induces end-to-end fusions and chromosomal instabilities (van Steensel et al., 1998, Karlseder et al., 2002). These data strongly suggest that TRF2 is a key player in functional telomere structure.

In addition to TRF1 and TRF2, several other associated telomeric proteins have been shown to be regulators of telomere length, such as POT1, RAP1, TPP1 - previously called PTOP1 (Liu D et al., 2004) - and TIN2 (de Lange 2002, Kim SH et al., 1999 & 2004, Liu, D. et al., 2004, Ye, J. & de Lange 2004). Both inhibition of endogenous POT1, RAP1, TPP1 and TIN2 expression through RNAi and expression of dominant-negative forms of these four proteins have been demonstrated to result in elongated telomeres in cultured cells (Loayaza et al., 2003, Ye, J. et al., 2004,

O'Connor et al., 2004, Ye J. et al., 2004). These observations suggest that POT1, RAP1, TPP1 and TIN2 may function in the same pathway and all therefore appear to facilitate negative regulation of telomere length. All four proteins directly or indirectly, associate with TRF1 or TRF2 (Ye, J. et al., 2004, Liu, D. et al., 2004, Li, B et al., 2000). The convergence of this data indicated that the TRF1/2 proteins may interact with each other and with the POT1, RAP1, TIN2 and TPP1 proteins to form a multi-subunit complex at mammalian telomeres. Co-immunoprecipitation experiments validated this hypothesis to show that TRF1 and TRF2 are in fact subunits of a telomere-associated high molecular weight complex, recently termed 'shelterin', also previously referred to as the mammalian 'telosome', (Liu, D. et al., 2004 and reviewed in de Lange 2005; discussed in section 1.3.4).

TRF1 has been shown to associate with additional factors called Tankyrase 1 and 2 (Smith S. et al., 2000). These are poly(ADP-ribose) polymerases that target TRF1 and induce progressive telomere lengthening via the dissociation of TRF1 from telomeric structures in human cells in a reaction that requires the catalytic activity of the PARP domain (Cook et al., 2002). Thus, Tankyrase 1 and 2 contribute to telomere homeostasis through its indirect function as a positive regulator of telomere length.

1.3.3 POT1-RAP1-TIN2-TPP1-mediated telomere regulation

Experiments deciphering the specific roles of POT1, RAP1, TIN2 and TPP1 aid our understanding of how a multi-subunit protein complex at the telomere substrate may regulate telomere length.

POT1

As the TRF1 complex binds to the duplex DNA of the telomere, it was unclear how it can affect telomerase, which acts on the single-stranded 3' overhang. TRF1 mediated-regulation of telomere length implies that this complex functions as a measuring device to assess telomere length. However, for telomere length homeostasis to be effective, information about the length of the telomere needs to be relayed from the TRF1 complex to the single-stranded part of the telomere. Recently it was shown that the TRF1 complex interacts with the single-stranded telomeric DNA-binding protein, 'protection of telomeres 1' (POT1) – and that human POT1 controls telomerase-mediated telomere elongation (discussed in section 1.8). hPOT1 was identified based on sequence homology to telomere-end-binding factors in unicellular eukaryotes (Baumann et al., 2001) and is the most conserved of the telomere-associated factors. A mutant form of hPOT1 lacking the DNA-binding domain, abrogated TRF1-mediated control of telomere length and induced rapid and extensive telomere elongation. (Loyaza et al., 2003). That hPOT1 binds to single-stranded telomere DNA exclusively, suggests two possible mechanisms for its role in telomere regulation: the TRF1 complex may recruit hPOT1 to the telomeric chromatin and facilitate its accumulation on the single-stranded DNA at the nearby telomere terminus. Once tethered there, hPOT1 may sequester the telomere terminus and thus directly block telomerase from elongating the telomeric DNA; alternatively, the recruitment hPOT1 to the telomeric chromatin could facilitate its binding to the single-stranded DNA (D-loop) at the base of the T-loop, thus stabilizing telomeres in the T-loop configuration and thereby inhibiting telomerase by indirect sequestration of the 3' terminus. Intriguingly, recent evidence has suggested that hPOT1 may in

fact permit telomerase-mediated telomere elongation at the telomere substrate due to a configuration change of hPOT1 (Songyang Z. et al. personal communicaton). Whether hPOT1 functions as both a positive and a negative regulator of telomerase will have to be validated with additional experiments. POT1 may also highlight a specific caveat of the mouse as a human model for telomere end capping, plus a general caveat in extrapolating across species with respect to telomere-associated proteins. Although POT1 deficiency in the mouse initiated DNA damage checkpoint activation and erroneous homologous recombination at telomeres, recent reports have demonstrated that there are two distinct POT1 paralogues (*Pot 1a* and *Pot1b*) in the mouse in contrast to a single POT1 locus in the human genome. *Pot1a* knockout results in embryonic lethality whereas *Pot1b* knockout mice are viable and fertile. In the absence of both proteins, 70-80% of telomere protection is lost; this proportion falls to 30% when only *Pot1a* is deleted, whereas *Pot1b* does not have any affect on its own (Wu L. et al., 2006, Hockemeyer et al., 2006). Therefore the relationship between POT1a and POT1b in repressing the DNA damage signal is not simple and the mechanism remains to be reconciled.

RAP1

'Human Repressor activator protein 1' (hRap1) was discovered in a yeast two-hybrid screen with TRF2 as bait (Li B. et al., 2000) and shown to interact with multiple proteins that are involved in DNA damage response pathways, including Rad50, Mre11, Ku70/86, and Tankyrase 1 PARP. Rad50 and Mre11 are members of the MRN complex which, similar to the Ku70/86 complex, is known to regulate double-stranded DNA break repair and homologous recombination (Connely et al., 2002,

reviewed in Hopfner et al., 2002), whereas Tankyrase 1 PARP modulates chromatin structure in response to stress (Smith S. et al., 2001). Thus, hRap1 together with TRF2 may function to recruit the DNA damage response proteins for telomere maintenance. The exact role of these DNA-damage-response proteins at mammalian telomeres remains to be determined. Interestingly, knockdown of endogenous hRap1 expression by small hairpin interference RNA resulted in longer telomeres, implicating hRAP1 as a negative regulator of telomere length (Connely et al., 2002).

TIN2

TIN2 was identified using a two-hybrid screen with TRF1 as bait (Kim S-H et al., 1999). Truncated TIN2 proteins extended telomeres, thus implicating this factor as a negative regulator of telomere length (Kim S-H et al., 1999). TRF1 may recruit TIN2 to the telomere, where TIN2 acts to dampen telomere elongation by telomerase. In support of this notion, TIN2 has been shown to modulate the Tankyrase 1 PARP in the TRF1 complex, suggesting that TIN2 could facilitate the stable association of Tankyrase 1 with the TRF1 complex (Ye J. et al., 2004) and conversely the controlled dismantling of the telomeric complex during S phase. The temporary removal of the TRF1 complex may be necessary for replication fork progression and telomerase-mediated telomere elongation.

TPP1

TPP1 previously known as TINT1 (Houghtaling et al., 2004), PTOP (Liu D 2004) and PIP1 (Ye J. et al., 2004) has been shown (in conjunction with TIN2) to be required to bridge the TRF1 and TRF2 subcomplexes. Specifically, TPP1 helps to

stabilize the TRF1-TIN2-TRF2 interaction and promote a six-protein complex formation. Consistent with this model, overexpression of TPP1 enhanced TIN2-TRF2 association. Conversely, knocking down TPP1 reduced the ability of endogenous TRF1 to associate with the TRF2 complex (O' Connor et al., 2006). Such coordinated interactions among TPP1, TIN2, TRF1, and TRF2 may ensure robust assembly of the Shelterin complex, telomere targeting of its subunits, and ultimately, regulated telomere maintenance.

Collectively, these factors contribute to telomere homeostasis by either positively or negatively regulating telomere length, mainly through governing the accessibility of telomerase to the 3' terminus (reviewed in Evans & Lundblad 2000). Further studies will be required to fully understand how these factors (and others?) and their homeostatic feedback loops, co-ordinate the regulation of mammalian telomere length.

1.3.4   The shelterin protein complex

The elucidation of specific roles of telomere-specific proteins aids our understanding of systemic telomere length regulation – undoubtedly novel factors yet to be identified may have direct or indirect roles in telomeric regulation. The shelterin complex was so coined by Titia de Lange (de Lange 2005) with analogy to other chromosomal protein complexes such as condensin and cohesion. Three shelterin subunits, TRF1, TRF2 and POT1 directly recognize TTAGGG sequences and are interconnected by three additional shelterin subunits, TIN2, TPP1 and Rap1. These factors combine to allow cells to distinguish telomeres from sites of DNA damage.

Shelterin components are defined by their exclusive functional role at telomeres, although a number of non-shelterin components (thus categorized due to their additional non-telomeric functions) directly interact with shelterin and contribute to telomere function (discussed in section 1.6.2). Shelterin determines the structure of the telomere terminus, it is implicated in the generation of T-loops and it controls the synthesis of telomeric DNA by telomerase (Fig. 1.3).
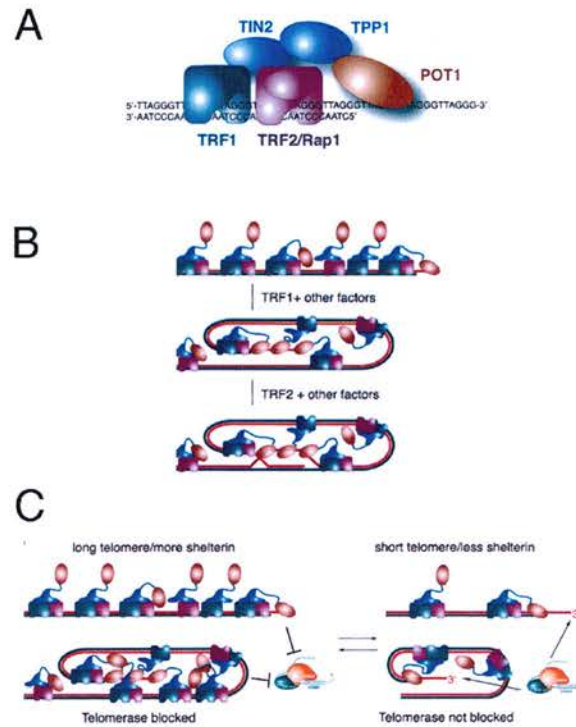
Figure 1.3. Proposed modeling of telomeres by shelterin. (A) Schematic of shelterin on telomeric DNA. For simplicity, POT1 is only shown as binding the single-strand site closest to the duplex telomeric DNA (D-loop), although it can bind to the single-strand 3' end. (B) Speculative model for shelterin-mediated T-loop formation. TRF1 has the ability to loop and pair telomeric DNA and TRF2 can mediate T-loop formation (both *in vitro*). (C) Model for telomere length regulation by shelterin. As the t-loop configuration is unlikely to be a substrate for telomerase, telomeres are shown in the 'open' state, which could be generated during S phase. The number of shelterin complexes may be proportional to the amount of telomere. Long telomeres may have more shelterin bound, increasing the loading of POT1 onto the 3' overhang and thus blocking telomerase action (*left*). Conversely, short telomeres with less shelterin, reduce the chance that POT1 loads onto the 3'overhang, leading to a greater chance that telomerase can elongate the telomere (*right*) (modified from de Lange 2005).

Since the TRF1, TRF2 (both homodimers and double-strand binding) and POT1 (single-strand binding) subunits are connected through protein interactions, shelterin has the capacity to recognize telomeric DNA with at least five DNA-binding domains. As a consequence, shelterin is uniquely qualified to distinguish telomere ends from all other DNA ends (de Lange 2005). Evidence for DNA remodeling activities comes from *in vitro* studies demonstrating that TRF2 can remodel an artificial telomeric substrate into loops (Griffith et al., 1999, Stansel et al., 2001). As this reaction is not efficient, it is likely that TRF2 requires the assistance of other factors to generate T-loops *in vivo*. Regarding the proposed function of telomere synthesis control, it is easy to speculate how the single-strand binding activity of POT1 could block telomerase from gaining access to the 3' telomeric terminus and *in vitro*, such inhibitory activity has been noted (Kelleher et al., 2005, Lei et al., 2005). Based on these data, the current model predicts that the amount of shelterin on a telomere determines the likelihood that its POT1 component can position itself on the 3' terminus and block telomerase, thus providing one mechanistic description of how telomerase regulation is governed.

1.4   Telomeres and cellular ageing

1.4.1   Cellular ageing and the Hayflick limit

Almost 45 years ago, Leonard Hayflick discovered that cultured human cells have limited replicative capacity to undergo rounds of DNA replication and divide, after which cells enter an irreversible non-dividing state termed 'replicative senescence' (a

cellular growth arrest also now referred to as the M1 stage (Shay & Wright 2005). In the absence of cell-cycle checkpoint pathways (e.g. p53 and or p16/Rb), cells bypass M1 senescence and telomeres continue to shorten, eventually resulting in crisis (also called the M2 stage). M2 is characterized by many 'uncapped' chromosome ends, end-fusions, chromosome breakage fusion-bridge cycles, mitotic catastrophe and a high fraction of apoptotic cells (Shay & Wright 2005). The widespread phenomenon of cultured diploid cells to undergo a specific number of population doublings has become known as the 'Hayflick limit' (Hayflick & Moorehead 1961), which specifically describes the finite capacity of normal cells as opposed to cancerous cells which usually become immortal. The existence of an intrinsic cellular counting mechanism was further implied by Hayflick's observation that cryogenically preserved cells can 'remember' how many times they have divided when they were frozen (Hayflick 1984). This putative molecular event counter was designated the 'replicometer' by Hayflick and in 1975, Woodring Wright showed that the molecular replicometer and cellular control of ageing was located in the nucleus (Wright & Hayflick 1975).

1.4.2   The 'end-replication' problem

Although the presence of telomeres on chromosome tips had been noted previously, (McClintock 1939), the property and function of these structures was unclear. The molecular basis of the replicometer was theorized independently by Alexy Olovnikov (Olovnikov 1973) and James Watson (Watson 1972) in the early 1970s when DNA replication mechanisms were better understood. It was realized that the properties of DNA replication prevent the ends of linear DNA to be fully copied and

thus telomere sequences may be lost during each successive round of cell division. The first hints that human telomeres might shorten appeared in 1986 when it was shown that telomere lengths are not the same in all tissues (Cooke et al., 1986). These studies culminated in the demonstration that telomeres shorten as normal human fibroblasts divide in culture (Harley et al., 1990). That telomere shortening is indeed a faithful cell division counter was recently demonstrated by results showing that replicative lifespan and telomere shortening rate in sheep fibroblast strains are not altered by nuclear transfer and cloning of foetuses, although foetal development resets the telomere clock (Clark et al., 2003).

The molecular basis of telomere shortening was referred to as the 'end replication' problem by James Watson. During DNA replication, the leading strand is synthesized as a continuous molecule that can potentially replicate through to the termini of a linear template. DNA polymerase requires an RNA primer to initiate synthesis in the 5'-3' direction. The lagging strand however, is synthesized as a discontinuous set of short Okazaki fragments, each requiring a new primer to be laid down on the template, that are then ligated to form a continuous strand. Without DNA to serve as template for a new primer, the replication machinery is unable to synthesize the sequence complementary to the final primal event. The result is the "end-replication problem" in which a telomere segment is lost at each round of DNA replication (Fig. 1.4). The leading strand is subsequently processed after completion of S phase to generate a 3' overhang.
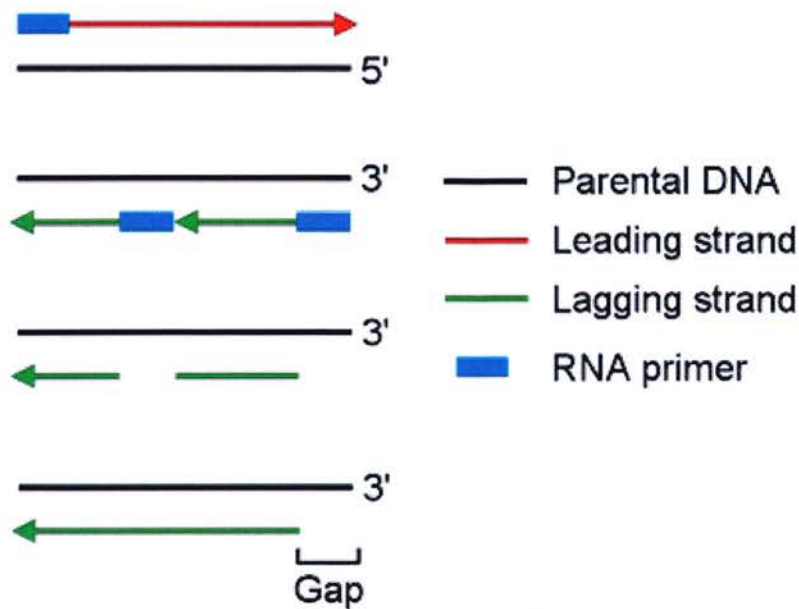
Figure 1.4. The end replication problem. Continuous replication of the leading strand proceeds to chromosomal termini. Discontinuous replication of the lagging strand through a series of Okazaki fragments results in a gap at the 5' end of the C-rich strand after removal of the last RNA primer.

The lowest shortening rates in human fibroblasts are around 10-20bp per population doubling (Lorenz et al., 2001). This shows that polymerase can position the most distal primer very close to the physical end of the chromosome. However the length of the G-rich telomeric overhang in some human cells has been shown to be 100-500nt in length (Makarov et al., 1997, Wright et al., 1997, McElligott et al., 1997, Stewart et al., 2003), suggesting that either the final RNA primer for lagging strand synthesis is not placed at the very distal end of the G-rich strand or that nucleolytic processing of the C-rich strand is extensive. Possible roles of oxidative stress and culture shock upon telomere shortening will be discussed in section 1.5.4.

1.5   <u>Replicative senescence</u>

The paradigm of cellular replicative senescence currently resides as a circular argument of cause and consequence – it remains unclear as to what factors are ultimate causes and what factors are proximate causes of senescence. Conventional dogma (section 1.4.1) states that telomere shortening provides the counting mechanism for the cellular 'mitotic clock'. In this regard, replicative senescence occurs as a consequence of progressive shortening of the TTAGGG repeat tract at chromosome ends (Hayflick & Moorehaed 1961, Harley et al., 1990, Bodnar et al., 1998, Wight & Shay 2002), when telomere length falls below a critical threshold to preserve replicative capacity that is presumably species- and cell-type specific. Human telomeres are programmed to lose ~100 base pairs per population doubling (PD), resulting in senescence after ~50 PDs (Harley et al., 1990, Counter et al., 1992, Shay & Wright 2000). This shortening rate is faster than expected from the end-replication problem (~10-20bp; Watson 1972, Olovnikov 1973, Lundbald et al., 1989, Singer et al., 1994; section 1.4.2), suggesting active nucleolytic attack on chromosome ends. Replicative senescence can be induced by either the p53 or the p16-retino blastoma (RB) tumour suppressor pathways, the breakdown of which may be the basis for the escape from *in vitro* cellular senescence and subsequent immortalization (Shay et al., 1991, Hara et al., 1991). In mammalian cells, telomeric foci containing multiple DNA damage response factors are assembled in a subset of senescent cells and signaled through ATM kinase to p53, upregulating p21 and causing G1 phase growth arrest (Herbig et al., 2004). But how these pathways are activated in cells with short telomeres though, is not known. Of what upstream

molecular trigger of senescence may these associated pathways be subsequently activated?

1.5.1   'Subset of short telomeres' hypothesis

The understanding that one of the major functions of telomeres is to hide the ends of the chromosomes from being recognized as double-strand breaks needing repair (de Lange 2002), has led to the hypothesis that a DNA damage signal from 'too-short' telomeres causes cellular senescence (Greider 1990, Harley 1991; section 1.7). This concept is reinforced by demonstrations that at senescence, DNA sequences adjacent to telomeres co-precipitate with γH2AX antibodies (di Fagagna et al., 2003) and that induced telomere dysfunction can cause telomere co-localization with DNA damage foci (Takai et al., 2003). Cell biological approaches have shown that the shortest telomeres determine the onset of replicative senescence in human cells (Ouelette et al., 2000, Steinert et al., 2000), an observation confirmed with respect to end-to-end fusions in murine cells (Hemann et al., 2001). However the pending question was whether specific telomeres produced this result, as these studies did not distinguish between one or a few short telomeres and did not identify specific telomeres involved. This was the rationale for a study to obtain direct evidence about the role of specific telomeres in senescence. Using quantitative *in situ* analysis of telomere lengths in normal human fibroblasts, this pivotal study showed that the shortest telomeres (as judged by a signal-free end using a telomere-specific probe) co-localized with γH2AX-positive DNA damage foci in senescent cells. Furthermore, in normal fibroblasts where cell cycle arrest has been blocked, 10% of telomeres with the shortest ends are involved in 90% of all end-fusions (Zou Y. et al., 2004). This finding argues against the existence of a sentinel telomere or random telomeres to

monitor telomere shortening but rather that a subset of telomeres is being used to time the onset of replicative senescence in the population of cells. Presumably a short telomere has to find a partner to form an end-association before growth arrest occurs, which would invoke more than one short telomere. An interesting side observation to this latter study indicated that ~85% of metaphase spreads from near-senescent cultures contained more than one signal-free end. This establishes that normal cells are still able to divide in the presence of telomeres sufficiently short to produce no hybridization signal (which may not be short enough to initiate a DNA damage response). This does however underline a caveat – signal-free ends are an arbitrary assignment due to technical limitations that does not necessarily imply a true absence of telomere repeats.

1.5.2   The 'altered telomere state' hypothesis

A general counter argument to telomere loss on one or more chromosomes as being the ultimate trigger of replicative senescence states that the main event heralding the end of replicative life of cells is a failure in the protective function of critically shortened telomeres. Clues for this trajectory come from studies manipulating the duplex binding protein TRF2, known to protect chromosome ends from end-to-end fusions (Broccoli et al., 1997, Bilaud et al., 1997, van Steensel et al., 1998, Karlseder et al., 1999, de Lange 2001). Overexpression of TRF2 increased the rate of telomere shortening in primary human cells without accelerating senescence. Thus TRF2 protected critically short telomeres from fusion by repressing chromosome end-to-end fusions in pre-senescent cultures (Karlseder et al., 2002). If the senescence signal were due to one or more chromosome ends lacking telomeric DNA altogether, TRF2

would not be expected to repress this signal and alter the senescence checkpoint. The implication is that critically shortened telomeres in senescent cells no longer bind sufficient TRF2 to achieve a protective state such as the T-loop configuration. Alternatively, binding of TRF2 may facilitate the recruitment of other proteins required for telomere end-protection and suppression of senescence. Therefore it follows that replicative senescence may be induced by a change in the protected status of shortened telomeres rather than a complete loss of telomeric DNA.

1.5.3 The '3' telomeric overhang' hypothesis

With the development of the Telomere-Oligonucleotide Ligation Assay (T-OLA), the G-rich strand 3' overhang has been subject to measurement (section 2.2.17). Using this approach, a recent study argued for evidence indicating that the telomeric 3' overhang is eroded at replicative senescence in primary human cells (Stewart et al., 2003). This data suggested that during senescence, most overhangs drop to below 100nt, potentially disrupting the T-loop or another non-canonical telomeric end structure. The kinetics of overhang loss differed from those of overall telomere shortening. Telomere shortening rate in the lines studied were in accordance with shortening rates reported previously (Harley et al., 1990, Allsopp et al., 1995, Huffman et al., 2000). In contrast telomeric overhang lengths remained constant during early and mid-point passages of culture and dropped abruptly at senescence (Stewart et al., 2003). Thus the authors claimed that overhang length is not a direct reflection of overall telomere length, but rather that overhang loss is the specific molecular alteration that occurs at the telomere in association with replicative senescence. This challenges the paradigm of telomere shortening as the molecular

clock that limits cellular lifespan. Nevertheless, it is imperative to state that others have shown using the same cell type as used in this study, that the 3' telomeric overhang is eroded only at crisis and therefore represents a consequential event to upstream senescence activation (Chai et al., 2005). This may represent technical variations between laboratories or may reflect clonal variations of the particular cell lines studied. For the role of the 3' overhang in replicative senescence (causal or consequential) to be fully understood, studies on telomeric overhang will have to incorporate a number of cell types and be widespread across species. With the conservation of telomere repeat tract sequences across eukaryotes and the functional similarity with key associated proteins and telomerase, it is tempting to speculate that the molecular trigger of replicative senescence is a general one.

1.5.4   The 'physiologic stress' hypothesis

The simple 'mitotic' clock' hypothesis cannot easily accommodate the marked intrinsic heterogeneity of replicative lifespan that is evident among the individual cells of a population in culture (Smith J. et al., 1980, Jones R. et al., 1980, Martn Ruiz et al., 2004). It is this heterogeneity within a population that indicated that the correlation between average telomere length and population doubling might not be sufficient to sustain the notion of telomeres as replication counters at the individual cell level. There is good evidence to show that the telomere-driven checkpoint is not the only one, if activated, to induce a senescence-like growth arrest. For example, human epithelial cells encounter a telomere-independent p16-dependent growth arrest that may be triggered due to sub-optimal culture conditions (Stampfer et al. 2003). Overexpression of oncogenes such as activated RAS or RAF, induces a

senescence-like growth arrest in primary human and mouse cells (Lin A. et al., 1998, Dimri et al., 2002, Ferbeyre et al., 2002). In addition, DNA-damaging stress induces cellular growth arrest, which may originate from different types of radiation (Herskind et al., 2000), drugs generating DNA double-strand breaks (Robles et al., 1998) and different means to generate oxidative stress such as increasing ambient oxygen tension (Balin et al., 1977, von Zglinicki et al., 1995) and treatment with hydrogen peroxide (Chen Q. et al, 1994, Frippiat et al, 2001). Thereby with increasing replicative age cells become more sensitive to environmental stress, in part due to changes in gene expression (Luce et al., 1992, Cristofalo et al., 1989). Semantics plays a part regarding descriptions of 'senescence'. Telomere-independent growth arrest, which reflects inadequate culture conditions, has been referred to as STASIS by Woodring Wright and Jerry Shay to distinguish between true senescence as determined by the replicometer.

Molecular oxygen plays a pivotal role in cellular respiration and is an absolute requirement for aerobic life; however, it is also toxic. Oxygen toxicity is believed to result from changes in the rates of cellular generation of reactive oxygen species (ROS). Faster telomere shortening rates (than that predicted from the end-replication problem) have been observed in human cell lines which have high levels of peroxide, indicating less efficient anti-oxidant defence (Lorenz et al., 2001, von Zgliniicki et al., 2000). The clear implication is that the contribution to telomere loss caused by oxidative damage is, in many cases, much greater than the contribution from the end-replication problem (reviewed in von Zglinicki 2003 and 2003). Ageing and telomere

shortening in bulk culture may therefore reflect a consequential event of the balance between oxidative stress and anti-oxidative defence.

Cause and consequence?

Collectively the current evidence regarding the causal and consequential events of cellular replicative senescence resides in a circular event. My opinion is that a subset of short telomeres, once a critical minimum length is reached, is the ultimate trigger of replicative senescence. Deprotection of telomere terminal structures due to sufficient shortening of the 3' overhang would therefore be viewed as a consequential epi-phenomenal event of overall telomere shortening in this subset. Loss of a T-loop configuration would presumably be necessary and sufficient to allow p53-dependent and associated senescence program pathways to be activated via signaling stemming from the terminal and exposed telomere substrate. However the evidence is convincing that telomere shortening counts not only mitotic divisions but also cumulative mutations that are dependent on culture shock conditions. Therefore we may consistently observe telomere-driven senescence occurring prematurely *in vitro* owing to imperfect protection from damage such as that induced by oxidative stress. From an evolutionary perspective, telomere-driven senescence becomes more plausible as a tumour suppressor mechanism if it limits proliferation not merely as a result of a predetermined number of cell divisions but also in response to possible damage to the genome.

1.5.5   Telomere length and cell viability

It is widely regarded that loss of telomere function can lead to genetic instability and cancer progression – whether short telomeres *per se* predispose cells to be cancerous is unclear. Whereas normal cells maintain chromosome stability, cancer cells are characterized by chromosomal changes (Lengauer et al., 1997), the sort of which was elucidated by McClintock, in studies observing the consequence of telomere loss (McClintock 1939). In a population of cells, there is a distribution of telomere lengths collectively representing each individual chromosome end, the establishment and maintenance of which requires telomerase. While the consequences of telomere dysfunction are well characterized (section 1.6.2), the primary determinant of the cellular response to global telomere shortening is poorly understood. One hypothesis is that average telomere length contributes to the cellular responses to telomere shortening (Blackburn 2000). In support of this idea, average telomere length has been shown to correlate with the lifespan of human cells in culture (Allsopp et al., 1992, 1995) and numerous studies have argued that it is the average telomere length in a cell that determines the proliferative potential of a cell line in the absence of telomerase (Lansdorp 2000, Martens et al., 2000). These models anticipate that as telomeres shorten, the probability of all telomeres losing function increases. An alternative hypothesis is however emerging from more recent studies. Rather than average telomere length, it is predicted that individual telomeres are recognized as DNA damage and it is those that elicit a cellular response. Support for this comes from studies using transgenic mice that are null for the telomerase RNA subunit gene, mTR, ($mTR^{-/-}$) or are heterozygous ($mTR^{+/-}$). Inter-generational crosses ($mTR^{+/-}$) revealed that telomerase-mediated restoration of telomere function occurs without a

considerable increase in average telomere length (Hemann et al., 2001). Although a wild-type telomere length distribution was not restored in the F1 generation, telomere function was restored. Similarly, studies using mouse embryonic stem (ES) cells heterozygous for the telomerase reversere transcriptase gene, TERT, ($mTERT^{+/-}$) argued for the preferential maintenance of critically short telomeres (Yie L 2002). Here, although average telomere length in $mTERT^{+/-}$ ES cells declined to a similar level as $mTERT$-null ES cells, $mTERT^{+/-}$ ES cells retained a minimal telomeric DNA signal at all chromosome ends. Consequently no end-to-end fusions and genomic instability was observed in the latest passages of these lines. This further revealed a distinct dosage requirement for the maintenance of long and short telomeres – despite haploinsufficiency for the maintenance of long telomeres, $mTERT^{+/-}$ mice retain minimal telomere DNA at all chromosome termini and did not exhibit the infertility typical of telomerase-deficient strains (Erdmann et al., 2004). Thus, the essential role of telomerase may not be the maintenance of an average telomere length, but rather the maintenance of telomere function at critically shortened telomeres. In this regard critically short telomeres are both necessary and sufficient for telomere dysfunction to manifest. Moreover, it has been shown that chromosomes frequently involved in fusions have the shortest telomeres (Blasco et al., 1997). This preferential elongation of short telomeres to maintain cell viability and chromosome stability, may explain previous findings in which limiting amounts of telomerase maintained telomere lengths at the shortest telomeres, despite decreases in overall telomere length within the population (Chiu C. et al., 1997, Zhu J. et al., 1999 Ouelette et al., 2000). This process may represent an uncoupling of telomere length maintenance from the maintenance of telomere function. If distinctions between long

and short telomeres are to be made, the presumable inference is that telomerase has a sophisticated mechanism to preferentially elongate short telomeres that are close to a minimum threshold required for chromosome stability.

1.6   Telomere length and organismal ageing

Although it is well established that telomere length is a crucial factor in cellular replicative senescence, it will be of greater importance to determine whether organisms with longer telomeres live longer. An insight regarding this question comes from studies in *C. elegans* where overexpression of the telomere single-strand binding protein HRP-1, by gradually increasing telomere length, resulted in worms with a longer lifespan. This was confirmed as due to longer telomeres rather than overexpression of HRP-1 *per se* as nontransgenic progeny who retained the longer telomeres, also lived longer (Fiset et al., 2001, Joeng et al., 2004). Additionally, it has been observed that telomeres shorten more slowly in long-lived birds than in short-lived ones (Hausmann et al., 2003). It will be interesting to determine whether this holds true for mammals; the mouse may not be a suitable model for such a study due to their long telomeres, so long-term studies in domesticated animals such as sheep may be more informative. Recently it was shown that people with long telomeres, although with independent genetic backgrounds, have lower mortality rates than those with short telomeres (Cawthon et al., 2003). Furthermore, not only is there evidence that human chromosome-specific telomere lengths may be inherited (Londono-Vallejo et al., 2001, Graajkaer et al., 2003 & 2004) but, by directly comparing telomere lengths in children and their parents, that allele-specific telomere lengths are transmitted by meiosis (Graajkaer et al., 2006). It will be

necessary to replicate these sorts of studies in numerous population cohorts of large population size but the implication is that telomere length may be a predisposition to certain age-related diseases in organs impacted upon by senescence and may thus serve as one predictor of longevity. Lengthening telomeres in adult somatic cells by a means that does not result in deleterious side effects, could in theory help mammals, including humans, to live longer, or certainly compress the period of morbidity in the elderly.

1.7   Telomeres, genome stability and the DNA damage response

It was long suspected that telomeres remain 'hidden' from DNA damage signaling pathways. Evidence that dysfunctional telomeres activate the DNA damage response pathway first emerged from experiments in which the TRF2 shelterin subunit was inhibited with a dominant-negative allele (van Steensel et al., 1998). The loss of TRF2 function results in telomeric-end fusions and activates the ATM kinase (Ataxia-Telangiectasia Mutated) DNA damage response pathway, leading to p53 up-regulation and p21-mediated G1/S cell cycle arrest and consequent apoptosis (Karlseder et al., 1999). Interestingly activation of the ATM pathway was not due to the secondary damage that can be generated when cells with dicentric chromosomes progress through mitosis (formed by end-to-end fusion). Rather, it is the damage at the telomere itself that appears to activate the ATM pathway. Telomere dysfunction can lead to either apoptosis or senescence depending on the cell type; upon TRF2 inhibition, human fibroblasts undergo senescence whereas apoptosis is a more prominent outcome in lymphocytes and epithelial cells (Karlseder et al., 1999).

The argument that deprotected telomeres activate the DNA damage response has been strengthened by the direct observation of DNA damage factors at telomeres. After inhibition of TRF2 or when telomeres become critically short, 53BP1, γ-H2AX, phosphorylated ATM and the Mre11/Rad50/Nbs1 (MRN) complex, accumulate at chromosome ends (di Fagagna et al., 2003, Takai et al., 2003). The cytological structures formed by these DNA damage factors are referred to as 'Telomere dysfunction Induced Foci' (TIFs) (Takai et al., 2003). TIFs are also formed when other shelterin components such as TIN2 and POT1 are inhibited (Kim S-H et al., 2004, Hockemeyer et al., 2005; Fig. 1.5). Intriguingly, there is current evidence suggesting that the converse holds true, where telomeric proteins are involved in a DNA damage response elsewhere in the genome. TRF1, TRF2 and TIN2 appear to be involved in an early DNA damage response after induction of double-strand breaks at defined regions within the nuclei of human fibroblasts (Bradshaw.P et al, personnal communication).
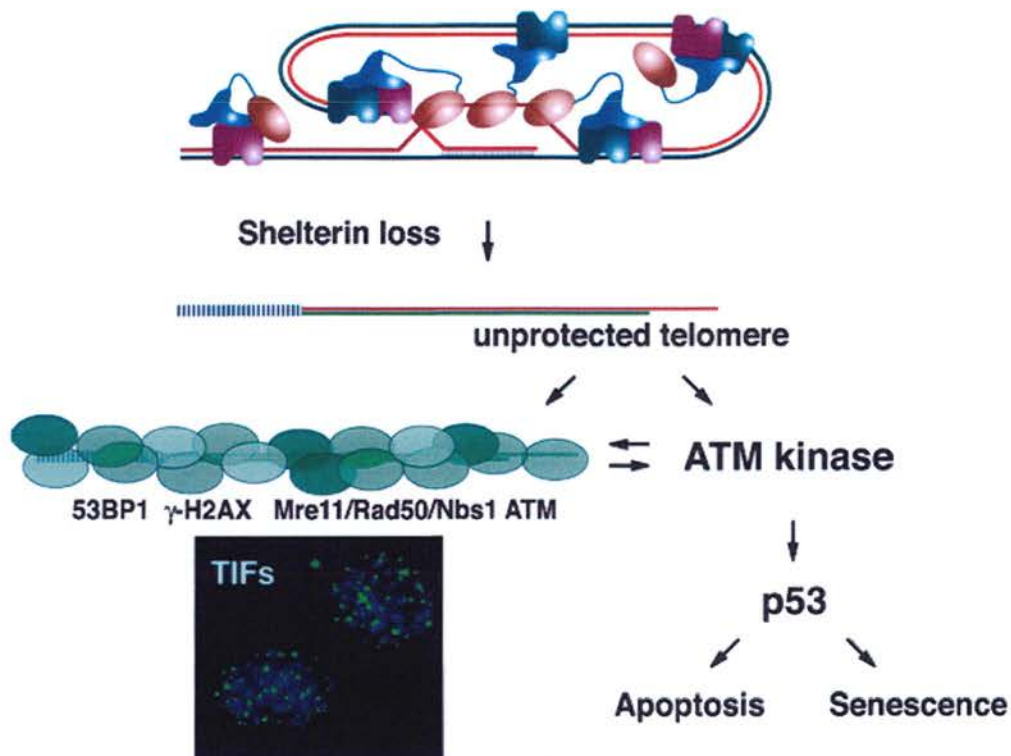
Figure 1.5. DNA damage response at dysfunctional telomeres. Telomeres lose end-protection after inhibition of shelterin subunits (e.g. TRF2, TIN2 and POT1) or due to telomere erosion. Upon loss of protection, telomeres become associated with DNA damage response factors, forming Telomere dysfunction Induced Foci's (TIFs). Telomere damage activates the ATM kinase which leads to a p53-dependent G1/S cell cycle arrest and can induce either apoptosis or senescence (from de Lange 2005).

Of particular interest is the presence of the MRN complex at the telomere substrate and indeed the Mre11, Rad50 and Nbs1 proteins have been shown to co-purify with TRF2 (Zhu X. et al., 2000). These proteins were previously characterized for their role in non-homologous end joining (NHEJ), a process that can result in the ends of two telomeres joining to form a dicentric chromosome (reviewed in Harrington 2004). In addition, homologous recombination (HR) between telomeres could generate aberrant telomere length and recombination between telomeres and interstitial telomeric sequences could result in deletions, inversions and translocations. Presumably base excision repair, nucleotide excision repair and

mismatch repair are used to maintain fidelity of the TTAGGG repeat sequence, just as they function for bulk DNA. In support of this, the recombination/repair protein RAD51D has shown to be present at mammalian telomeres and required for telomere maintenance (Tarsounas et al., 2004). It remains to be established whether recombination is required for telomere elongation or for protection of the telomeric single-strand overhang. This leads to the question of how shelterin in conjunction with DNA repair factors, functions to prevent improper recombination and repair? The obvious suggestion is that telomeres are protected from these events by the shelterin-mediated T-loop configuration (Fig. 1.6). In this regard, RAD51D-mediated telomere maintenance would be via its role in telomere capping.
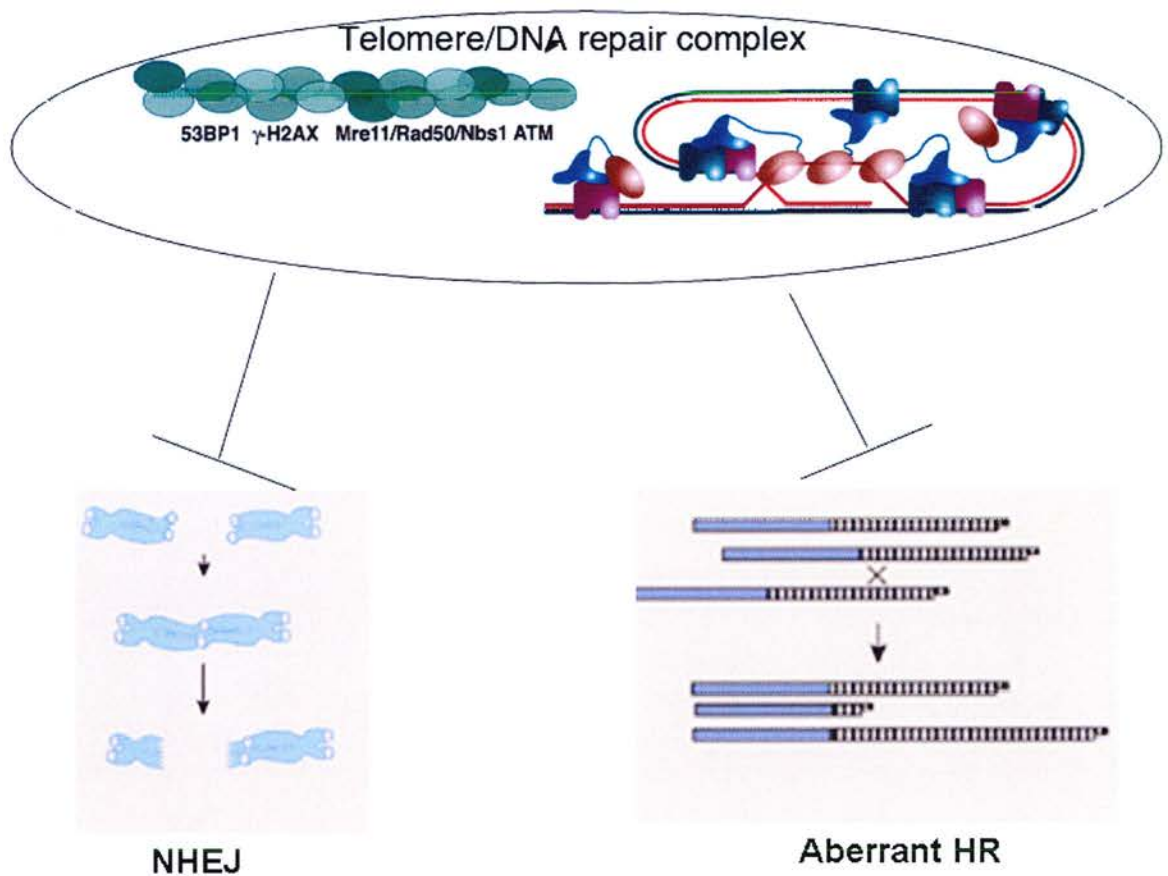
Figure 1.6. Proposed model of how telomere ends may avoid a DNA damage response. Shelterin DNA-binding factors and the DNA-repair factors they recruit to mammalian telomeres may function to inhibit, rather than promote a variety of repair processes, such as Non-homologous End Joining (NHEJ) and aberrant homologous recombination (HR) (adapted from de Lange 2005 and Wright & Shay 2005).

Collectively the data argue that dysfunctional telomeres are detected by the canonical DNA damage response and there is no evidence that a telomere-specific checkpoint or specific signaling pathway is invoked. Hence, damaged telomeres do appear to share molecular characteristics of a localized DNA damage response. The evidence indicates that the shelterin complex is not a static structural component of the telomere, but rather a protein complex with DNA remodeling activity that acts in

coercion with several associated DNA repair factors to alter the structure of telomeric DNA, thereby protecting chromosome ends. So, although telomerase is generally required for the synthesis of telomeric repeats, the enzyme is not required for telomere protection *per se* as long as there is enough telomeric DNA (Blasco et al., 1997). A recent seminal observation has shown that chromosome ends of normal human primary fibroblasts are recognized as double-strand breaks at the G2 phase and recruit the ATM, NBS1 and Mre11 DNA damage response factors (Verdun et al., 2005). This leads to the intriguing hypothesis that a localized DNA damage response at 'functional' telomeres after replication may be necessary and essential for recruiting the processing machinery that promotes formation of a chromosome end protection complex.

1.8   Telomere homeostasis and telomerase

1.8.1   Telomerase holoenzyme structure

If short telomeres limit the rate of cell growth, there had to be a counter-mechanism to the telomere problem in the germline cells and potentially highly proliferative tissues (e.g. stem cells, some progenitors,) of higher organisms and in immortal and cancerous cells. The solution again originated in studies with *Tetrahyema* by Carol Greider and Elizabeth Blackburn (Greider & Blackburn 1985), where Greider and Blackburn discovered the enzyme 'telomerase' that maintains and elongates telomeres. Telomerase was later found in extracts of immortal human cell lines

(Morin et al., 1989) and in most human tumours (Kim N-W et al., 1994) and is now known to be almost universally conserved in eukaryotes.

Telomerase is a specialized cellular ribonucleoprotein (RNP) reverse transcriptase complex that synthesizes $TTAGGG_n$ telomeric repeats onto chromosomal ends (Greider & Blackburn 1987, Lingner et al., 1997). Telomerase consists minimally of two main components that are required for core enzymatic activity. These are a telomerase RNA (TR), used as a template to dictate the addition of *de novo* telomeric repeats onto the 3' end and a catalytic protein subunit with reverse transcriptase activity (TERT). It has recently been shown that human telomerase is a multimer containing two cooperating hTR molecules (Wenz et al., 2001) and generally thought to most likely contain two hTERT molecules. The human telomerase holoenzyme is large (~1000kDa; Schnapp et al., 1998) and mammalian telomerase activity is associated with a number of proteins that may be implicated in ribonucleprotein assembly, processing and stability such as: TP1 (Harrington et al., 1997); p23 and Hsp90 (Holt et al., 1999); Est2 (Lingner et al.,1997 and Mitchell et al., 1999); (see section 1.8.2). However, human telomerase that is affinity purified under stringent salt conditions has a molecular mass of 600kDa, consistent with a minimal complex composed of two hTERTs and two hTRs (Wenz et al., 2001). The secondary structure of telomerase RNA was proposed based on phylogentic comparative analysis. Four structural domains were conserved across vertebrates - the pseudoknot domain, the CR4-CR5 domain, the Box H/ACA domain and the CR7 domain. Each conserved structural domain in the consensus structure might play a distinctive role in either the function, stability, processing, or localization of telomerase RNA. These

regions are also good candidates as binding sites for TERT or other telomerase accessory proteins (Romero & Blackburn 1991, Chen J. et al., 2000, reviewed in Nugent & Lundblad 1998 and Smogorzewska & de Lange 2004). Indeed some studies have implicated the pseudoknot and CR4-CR5 domains as essential for telomerase activity that interact separately with hTERT (Chen J. et al., 2002, 2003 and 2003, Martin-Rivera et al., 2001, Tesmer et al., 1999). Studies from *Tetrahymena* have shown that the templating region of the telomerase RNA can be dissected into two functionally seperable regions (Autexier et al., 1994 and 1995, Gilley et al., 1996). The hTERT gene is located on the distal arm of chromosome 5p and is in fact the most distal marker (Meyerson et al., 1997, Bryce et al., 2000, Shay & Wright 2000). The hTERT promoter contains a number of regulatory sites including two c-Myc binding sites (Wang J. et al., 1998) and may also contain a site that negatively regulates its expression in a p53-dependent manner (Kanaya et al., 2000). In support of the notion that proper hTERT function may also require a homodimeric structure, studies have shown that two separate catalytically inactive hTERT proteins can complement each other in *trans* to reconstitute telomerase activity (Beattie et al., 2001, Arai et al., 2002). hTERT has been shown to consist of two physically separable functional domains: a polymerase domain, containing RNA interaction domain 2 (RID2), reverse transcriptase (RT) and C-terminal sequences, and a major accessory domain consisting of RNA interaction domain 1 (RID1) (Moriarty et al., 2004; Fig 1.7). Further support of this notion of an hTERT multimer was provided by a study using recombinant hTERT which demonstrated that hTERT monomers oligomerize and that two independent regions are required for its oligomerization and telomerase activity (Arai et al., 2002). Mutation screens of

hTERT are permitting a dissection of the functional organization of the subunits of this unique reverse transcriptase. Both N-terminal and C-terminal subunits of hTERT contain regions essential for *in vitro* and *in vivo* enzymatic activity, and both regions contain a DAT domain that "dissociates activities of telomerase", mutations in which render the hTERT enzyme catalytically active but unable to function *in vivo* (Armbruster et al., 2001 and 2004, Bachand et al., 2001, Banik et al., 2002, Huard et al., 2003). These findings support the notion that hTERT subunits out with the RT domain are necessary for both enzymatic activity and telomere maintenance.
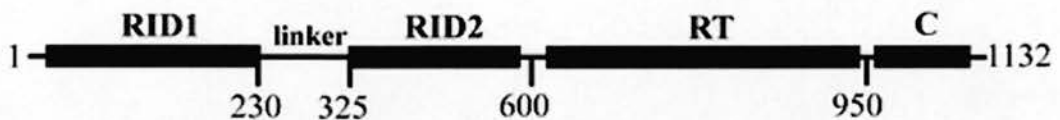
Figure 1.7. A schematic depicting conserved hTERT regions. The hTERT N-terminus can be subdivided into two regions, RNA interaction domains 1 and 2 (RID1 and RID2, respectively), which are separated by a nonconserved linker that is not required for telomerase activity (Armbruster B 2001, Moriarty T 2002, Xia, J 2000). This forms two physically separable domains of hTERT, the polymerase domain (RID2, RT, C) and major accessory domain (RID1). Numbers indicate the amino acid boundaries defined from recent studies. A 'dissociates activities of telomerase' (DAT) domain is found in both the RID1 motif of the N-terminal domain and in the C-terminal domain. *RID1/2, RNA-interacting domain 1/2; RT, reverse transcriptase domain; C, Carboxy-terminal* (adopted from Moriarty T, J. 2004).

1.8.2   Telomerase complex: associated proteins

A large numebr of telomerase-associated proteins have been identified in ciliates, yeasts and vetrtebrates. However, only a few are common to all telomerases and discussion here will be restricted to those. One of the first TERT interacting proteins identified was the p23 chaperone (Holt et al., 1999), which is required, along with

Hsp90, for the efficient assembly of active telomerase both *in vitro* and *in vivo*. Contrary to the association of chaperones with most proteins, p23 and Hsp90 remain stably associated with active telomerase following assembly and may therefore contribute additional regulatory functions at telomeres (Forsythe et al., 2001).

A number of additional proteins may regulate TERT activity through direct binding. Ku is a heterodimer composed of two subunits – Ku70 and Ku80 – that binds to DNA in a sequence dependent manner. In all systems studied, Ku has been shown to facillitate the repair of DNA double-strand breaks by non-homologous end joining (NHEJ) (Downs et al., 2004). Interestingly, the human heterodimeric Ku complex was shown to be linked to telomere maintenance through its interaction with telomeric DNA and TRF1 and TRF2 (Downs et al., 2004). More recent studies suggest that the complex can also independently associate with hTERT and hTR. Ku binds specifically to a stem-loop in the telomerase RNA and may promote the localization of telomerase to telomere termini (Chai W. et al., 2002, Ting NSY et al., 2005).

hEST1A and hEST1B are both human homologs of the yeast telomerase subunit EST1p. Yeast EST1p mediates the recruitment of telomerase to telomere ends by binding to both telomerase RNA and CDC13p, a telomere end-binding protein (Pennock et al., 2001). However, direct interaction between Est1p and yeast TERT has not been detected. In contrast, both hEST1A and hEST1B were shown to bind hTERT independently of the RNA subunit when expressed *in vitro* (Snow et al., 2003) Only hEST1A has been functionally linked to telomere maintenance *in vivo*;

overexpression of hEST1A results in telomere uncapping and elevated levels of chromosomal fusion and, in combination with hTERT overexpression, can provoke substantial telomere elongation (Snow et al., 2003).

1.8.3　Telomerase-mediated telomere maintenance

The processive addition of telomeric repeat sequences by telomerase is repetitive, whereby telomerase undergoes a translocation reaction and repositions the 3' end of the telomeric DNA in concert with recognition of the 3' template boundary (see Fig. 1.8). In humans, the telomerase holoenzyme is preferentially expressed in germ-line cells and in early embryonic tissues but is not detected in most somatic cells (Wright et al., 1996), although it has recently been shown to be present at low levels in cycling human fibroblasts (Mastuomi et al., 2003). hTERT has been indicated as a key factor limiting telomerase activity in human somatic cells because the RNA subunit is constitutively expressed at a low basal level in cells (Feng et al., 1995). However studies from the mouse have shown that the expression of telomerase RNA template, but not telomerase reverse transcriptase, is limiting for telomere length maintenance *in vivo*. TERT$^{+/-}$ heterozygotes had no detectable defect in telomere elongation compared to wild-type controls, whereas TR$^{+/-}$ heterozygotes were deficient in telomere elongation, indicating that both TR and TERT are essential for telomere maintenance and elongation but that gene copy number and transcriptional regulation of TR, but not TERT, are limiting for telomerase activity *in vivo*. (Lingner et al., 1997, Chiang et al., 2005). In addition the telomerase RNA template has been shown to be a determinant of telomere repeat extension rate in humans (Drosopoulos et al., 2005). The caveat in this mouse study concerns the fact telomerase is

expressed at high levels in an array of somatic murine tissues (Greenberg et al.,

1998), hence a deficient phenotype in mTERT$^{+/-}$ may not be evident.

Figure 1.8. Model for processive elongation by telomerase. Reiterative extension of telomeric DNA is postulated to entail (*a*) binding of telomeric DNA to the TR unit RNA template and to other domains of the RNP (e.g. the anchor site(s)); (*b*) successive addition of nucleotides to the 3'end of the DNA; (*c*) upon reaching the 5' template boundary, translocation and repositioning of the 3' end of telomeric DNA in concert with recognition of the 3' template boundary; and (*d*) subsequent repeat rounds of elongation. (Figure adopted from Autexier & Lue 2006).

When it was demonstrated that human primary fibroblasts could be immortalized by

transfection of human TERT (hTERT), the catalytic subunit of telomerase (Bodnar et

al., 1998), telomere shortening was firmly established as a biological clock for cellular senescence. However, it has more recently become clear that it is unlikely to be telomere shortening *per se* that triggers a senescent arrest, but rather that other non-canonical structures and a number of extrinsic factors may be key determinants regarding the onset of senescence (section 1.5). In this respect, telomere shortening may be a proximate rather than an ultimate cause of cellular senescence.

1.9   Extra-curricular roles of telomerase

The possibility of telomere-independent telomerase function is intriguing. Various lines of evidence suggest that telomerase may have yet undiscovered roles. As discussed previously, despite the ample telomere reserve in murine cells, telomerase is upregulated in a spectrum of tumour types (Blasco 1996, Greenberg et al., 1999, Cao Y. et al., 2002; reviewed in Chang S. et al., 2002), suggesting that telomerase may confer enhanced proliferative and survival potential during tumourigenesis, independent of its role in telomere maintenance. Similarly, telomerase extends the lifespan of virus-transformed human cells without net telomere lengthening, indicating a protective function of telomerase that allows cell proliferation (Zhu J et al., 1999), perhaps by conferring karyotypic stability by 'capping' chromosomes. Furthermore, descriptive studies have shown hTERT localization not only in the nucleus, but in the cytosol, reinforcing the notion of telomere-independent functions (reviewed in Chung H 2005).

On the basis that low levels of hTERT are detected in S phase of normal human fibroblasts (Mastuomi et al., 2003), a recent study investigated the effects of hTERT

suppression in these cells. Strikingly, an impaired DNA damage was observed in response to ionizing radiation, implicating hTERT as a critical regulator of the DNA damage response (Mastuomi et al., 2005). Moreover the sustained loss of hTERT expression through several rounds of cell division alters the overall state of chromatin into a configuration that inhibits the activation of the DNA damage response (Mastuomi et al., 2005). Hence hTERT may regulate the DNA damage response through its actions on chromatin structure, in a manner independent from its role in telomere maintenance.

Two recent seminal studies, through investigating the role of telomerase in stem cell compartments, showed that conditional transgenic induction of TERT in mouse skin epithelium causes a rapid transition from telogen (the resting phase of the hair follicle cycle) to anagen (the active phase), thereby facilitating robust hair growth. This new function for TERT does not require the telomerase RNA component, and therefore operates through a mechanism independent of its activity in synthesizing telomere repeats (Flores et al., 2005, Sarin et al., 2005; reviewed in Flores et al., 2006). Indeed changes in telomere length were absent from these overexpression studies. This study has been further exemplified in small intestinal stem cells, corneal stem cells and brain stem cell compartments (Blasco. M et al, personnal communication). These data indicate that, in addition to its well established role in extending telomeres, TERT can promote proliferation and mobilization of resting stem cells through a non-canonical pathway. This raises the question as to what role telomerase may have during metastases?

1.10   Telomerase, telomeres and cancer

Due to the degree of conservation of telomere repeat sequences across phyla ($TTAGGG_n$ in vertebrates and $TTTAGGG_n$ in many plants; reviewed in Fajkus et al., 2005), it is tempting to suggest that telomere-dependent replicative senescence may be the hallmarks of a primitive tumour suppressor mechanism that may pre-date sophisticated protein-mediated tumour suppression. A pre-programmed cessation of proliferation would inevitably protect against uncontrolled cell growth and unwanted genetic abnormalities. Presumably, the pre-determined replicative capacity of early multicellular organisms provided a safe buffer zone in which to propagate their selfish genetic units of inheritance. This window for replicative capacity would thus be stable and selected for, with this tumour suppressor strategy inadvertently leading to cellular ageing and possibly contributing to organismal ageing – a cellular double-edge sword. However, it is important to stress, with respect to our own species that although replicative senescence may *be* a potent tumour suppressor mechanism, this may be an inadvertent phenomena and unlikely to have been an adaptation; we may simply be observing this phenomenon due to our current longevity compared to our early *Homo sapiens* ancestors.

1.10.1   Telomerase reactivation

It is easy to speculate that cell division is potentially a risky strategy and organisms with renewable tissues have evolved to limit the maximal number of permissible cell divisions. Presumably the optimal cell turnover for the expected lifespan of humans has been reduced to a number set in the wild (i.e. Stone Age *Homo sapiens)*. Modern

medicine has allowed us to live far longer than is necessary for high reproductive fitness (Selfish Gene theory – Richard Dawkins, 1976) and therefore cancer is a phenomenon that may have no scope to be selected against.

Cancer is a disease of cellular ageing and impaired genome stability – and several lines of evidence have confirmed that the maintenance of telomeres and reactivation of telomerase participate actively in the pathogenesis of cancer (reviewed in Maser et al., 2002, Mastuomi & Hahn 2003, Shay & Wright 2005 and Bailey et al., 2006). Although telomere shortening appears to limit replicative lifespan of human cells and suppress cell transformation, telomere shortening also eventually leads to critically short telomeres and the onset of M2 stage crisis. Whereas most cells that enter crisis are eliminated by apoptosis (Shay & Wright 1989, era-Bloch et al., 2002), sporadic cells ($\sim 1 \times 10^{-7}$) survive crisis and become immortal (Shay & Wright 1989). Such immortal cells typically exhibit aneuploidy and extensive chromosomal translocations indicating that telomeres lose their protective function at lengths associated with crisis (Counter et al. 1992). Crucially, telomeres in ~90% of cancers studied are maintained by the activation of telomerase (Kim N W et al., 1994, Counter et al., 1994). This stabilization of telomere length permits immortalization and facilitates further malignant progression. Although catalytic activity is necessary, telomere elongation alones seems insufficient to explain the requirement of telomerase in a tumour setting, as average stabilized telomere lengths are often shorter that the corresponding wild-type tissue (Hastie et al., 1990, Counter et al., 1994). At present the additional mechanism(s) by which telomerase activation contributes to tumourigenicity remains undefined. It has been proposed that lines

with catalytically active hTERT are more resistant to apoptosis (Gorbunova et al., 2002, Forsythe H. et al., 2002) and/or that catalytically active hTERT may serve as a physical cap for the (exposed?) telomere (Zhu J et al., 1999, Blackburn 2001). Thus telomere shortening and telomerase activation can act both to suppress and facilitate tumour development depending on the timing and context of these related events – a molecular double-edged sword (Fig.1.9).

1.10.2   Alternative Lengthening of Telomeres (ALT) pathway

Although most human cancers use telomerase as their telomere maintenance mechanism, some (~7-10%) use an alternative lengthening of telomeres (ALT) mechanism (Fig. 1.9). The latter especially include specific subtypes of soft tissue sarcomas where ALT occurs most often in tumors with complex karyotypes, astrocytic brain tumors and osteosarcomas (Bryan T. et al., 1997, Muntoni et al., 2005). Some ALT cells have atypical features, suggesting that there is more than one ALT mechanism. ALT cells are characterized by high rates of telomeric recombinational exchange (Dunham et al., 2000). One of the hallmarks of the ALT mechanism is the presence of ALT-associated PML bodies (APBs), which are subnuclear structures where PML protein colocalizes with telomeric DNA, telomere-binding proteins and several proteins involved in DNA synthesis and recombination (Yeager et al., 1999). The latter include the Mre11/Rad50/Nbs1 (MRN) complex which appears to be required for ALT. The existence of ALT raises the possibility that telomerase-positive tumors undergoing anti-telomerase therapies may escape by activating the ALT pathway (reviewed in Stewart 2005).
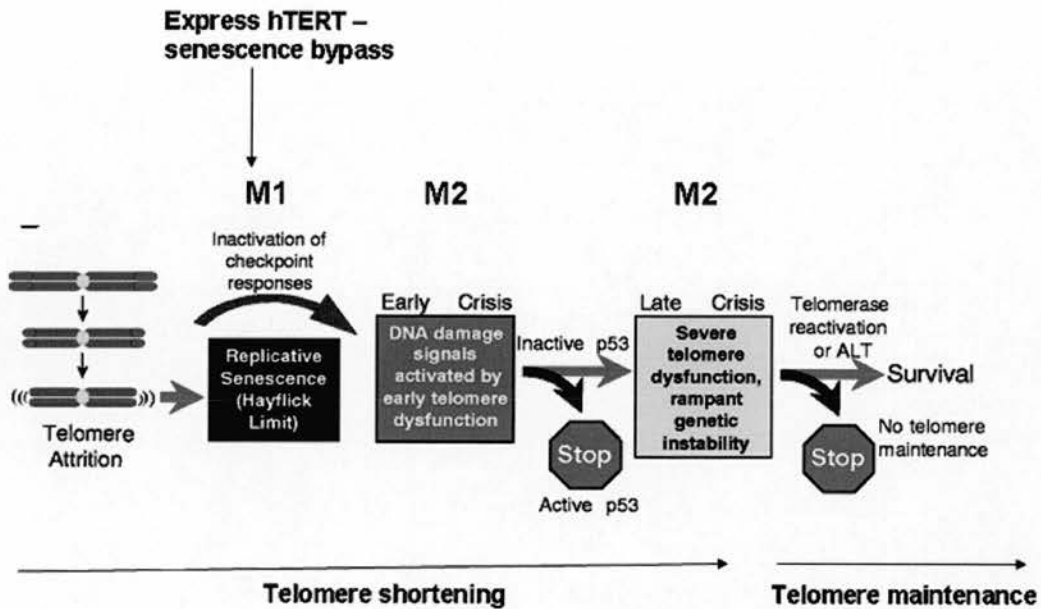
Figure 1.9. A model for crisis induced by telomere attrition. Shortened telomeres elicit replicative senescence *in vitro*, blocking further proliferation unless checkpoint responses are disrupted. Continued cell division will eventually cause telomere dysfunction and crisis. The early stage of crisis can be averted by loss of p53. Eventual emergence from late stage crisis requires not only p53 inactivation but the acquisition of telomere maintenance mechanisms, be it telomerase-dependent or telomerase-independent. (Adapted from Maser & de Pinho 2002 and Shay & Wright 2005).

1.10.3   Lessons from the mouse

A telomerase-deficient mouse model was generated by the elimination of the gene encoding the murine Terc (TR) gene (reviewed in Blasco 2003). Only a limited number of generations of these mice could be derived before loss of viability due to telomere exhaustion and increased end-to-end fusions (Blasco et al., 1995 and 1997; Herrera et al., 1999). Terc $^{-/-}$ mice show telomere dysfunction pathologies in most tissues and is characterized by decreased cell proliferation and/or increased apoptosis (Rudolph et al., 1999, Franco et al., 2002, Samper et al., 2002). As human telomeres (~15kb) are much shorter than those of the laboratory mouse (~50kb) and as

telomerase is absent in most human somatic tissues, telomere shortening in humans may lead to a similar failure of the organism as that described in the late generation telomerase-deficient mouse. Importantly, telomerase introduction in these mice is able to elongate critically short telomeres thus preventing the pathologies associated with end-to-end fusions (Samper et al., 2001). This hints at the possible use of telomerase in gene therapy of premature ageing syndromes such as Werner syndrome (reviewed in Collins et al., 2002) and dyskeratosis congenita (DC) (Vulliamy et al., 2001 and 2004), the latter of which is a multi-system bone marrow failure syndrome that may be X-linked (mutation in the DKC1-encoded protein) or autosomal dominant (mutation in Terc) (Walne et al., 2005), resulting in short telomeres.

Telomerase activity is upregulated during murine tumourigenesis despite mice having long telomeres (Broccoli et al., 1996, Artandi et al., 2002) suggesting that telomerase may promote tumourigenesis at two levels: by signaling proliferation and promoting growth independently of telomere length, and by rescuing tumour cells with critically short telomeres.

1.10.4   Telomeres and telomerase in cancer stem cells

Recent evidence suggests that only a subset of cells within some tumours, the so-called cancer stem cells, may drive the growth and metastasis of these tumours. Thus tumours are regarded as heterogeneous in nature rather than a homogenous population of rapidly dividing cells. The first evidence of a putative tumour-initiating cell came from studies of the haematopoietic system and the identification of leukaemic stem cells (Lapidot et al., 1994, Bonnet et al., 1997; reviewed in

Harrington 2004 and Huntly & Gilliland 2005). The identification of tumour-initiating cells in solid tumours such as brain (Singh S et al., 2003, 2004) and breast (Al-Hajj M. et al., 2003) shatters much dogma in the field of cancer biology and the implications of the cancer stem model are profound. A key upstream mutation(s) causing the breakdown of self-renewal regulation may until now have been overlooked. If cancer stem cells represent the sole population with tumourigenic potential then the failure of conventional chemotherapy may be readily explained; like their normal stem cell counterpart, cancer stem cells most probably exist in a quiescent state, removed from the cycle of division and thus are not targeted by chemotherapeutic drugs that target rapidly dividing cells. In this regard, non-tumourigenic progeny from the cancer stem cell will be killed, but the small population of cancer-initiating cells will remain, hence relapse. Nevertheless, it is still a matter of debate whether solid cancers derive from stem cells or their progenitors that have acquired the ability to self-renew through mutation. It may well be that the cancer cellular culprit differs in each tumour setting as each is dependent on a tissue-specific microenvironment.

In light of these findings it appears of great importance to elucidate the role of telomeres and telomerase in cancer stem cells. In one respect, telomere shortening might be involved in the development of chromosomal instability and transformation of stem cells. In another respect, tumour stem cells might require telomerase activation to achieve immortal self-renewal capacity (reviewed in Ju Z 2006). The fact that stem cells and tumour cells express similar levels of telomerase indicates that somatic cells may be target cells for malignant transformation (Morrison et al.,

1996). The identification of better surface markers on cancer-initiating populations, that could help unequivocally identify a 'cancer stem cell', could help to characterize telomerase activity and telomere shortening in these compartments. Since telomere dynamics represents the mitotic history of highly proliferating organs, analyzing telomere length, telomerase activity and cytogenetic profiles may be helpful to exploit the origin of tumour-initiating cells and the history of tumour formation.

Finally from a clinical view, it will be vital to determine whether telomeres and telomerase represent promising targets to attack cancer stem cells. Two concepts are promising: (i) telomerase is an attractive target for inhibition strategies that may limit proliferation and induce apoptosis in cancer stem cells. Preliminary studies of telomerase inhibition in a variety of tumor cell types have been conducted using the novel telomerase template antagonist GRN163L (Asai et al., 2003, Djojosubroto et al., 2005). The caveat of course is that normal tissue stem cells express telomerase, so a specific targeting method will be required; (ii) stabilization of telomeres in pre-malignant diseases may inhibit the evolution of chromosome instability and transformation of cancer stem cells. The obvious paradox here is that this strategy will require controlled reactivation of telomerase. Thus the telomere and telomerase model for cancer stem cell initiation may supplement one of the most intriguing areas of future cancer research.

1.11   An historical perspective

1.11.1   On the origins of telomeres

It is vital to invoke an evolutionary perspective to understand the role of telomeres in the evolution of genomes, chromosomes, terminal sequences, genes and proteins. The current study of telomere biology may be sophisticated, but studies beyond model organisms are required to give a broader perspective on those features of telomeres that are organism-specific and those that are conserved. The increasing interest in telomerase-independent systems might be instrumental in our understanding of why and how natural selection favoured linear chromosomes over their circular counterparts in nuclei of eukaryotic cells. One intriguing hypothesis that has been debated, suggests that the replication strategies of mitochondrial telomeres represent an evolutionary paradigm for the emergence of linear eukaryotic chromosomes during a 'pre-telomerase' era. This postulates that a selfish element replicating via a rolling-circle mechanism could generate terminal arrays of tandem repeats at chromosomal termini of early eukaryotes (reviewed in Fajkus et al., 2005, Nosek et al., 2006). Why linear chromosomes may have been an adaptation is unclear. Primordial telomeric structures may then have recruited telomerase, which provided a more robust method of maintaining chromosomal ends and out-competed evolutionary ancient mechanisms. The elucidation of the T-loop structure not only at mammalian chromosomal termini, but that of the ciliate *Oxytricha fallax* (Murti K. et al., 1999) and the flagellate protozoan *Trypanosoma brucei* (Munoz-Jordan et al., 2001), raises the tempting suggestion that early eukaryotes could have stabilized their chromosome ends using the T-loop structure or one similar.

1.11.2   On the origin of telomerase

The clues to the origins of telomerase come from its structural conservation: telomerase contains conserved domains with all known reverse transcriptases with phylogenetic analysis revealing that the major branch in which telomerase resides contains the eukaryotic retrotransposable elements without long-terminal repeats, known as the non-LTR retrotransposons (Nakamura T. et al., 1997 & 1998). As to which arose first, telomerase or retrotransposons, the debate continues (reviewed in Eickbush et al., 1997 and Nakamura T. 1998). Although the origin of telomerase may thus be traced back to the RNA world (de Lange 2004), this does not necessarily imply that the enzyme maintained telomeres in ancestral eukaryotes. The evolutionary success of telomerase in the eukaryotic world might have been due not only to the efficient synthesis of telomeric arrays but also due to its extracurricular telomere-independent activities that may have increased cellular viability (section 1.8). A fascinating experiment has been suggested, based on the introduction of telomerase into natural telomerase-deficient cells, such as *D. melanogaster* (representing a lineage in which telomerase was lost) (Nosek J 2006). Would telomerase out-compete the telomerase-independent mechanisms? Would the reprogrammed strains differ in their relative fitness? Telomerase is arguably one of the earliest proteins to have been selected for in the eukaryotic kingdom, probably due to the array of functions it mediated to ensure cellular viability. Studies of telomerase in a plethora of extant eukaryotes will further elucidate the exact historical accounts of both telomerase and telomeres.

1.12 Current Project

1.12.1 Using sheep to study telomere and telomerase biology

Previous work conducted in our laboratory has demonstrated that sheep fibroblasts are similar to human fibroblasts in respect to replicative senescence and telomere and telomerase biology. Sheep fibroblasts have a limited proliferative lifespan which seems to be controlled by the telomere mitotic clock. In addition, hTERT is compatible with sheep TR and associated machinery, thus providing an alternative mammalian model system to study telomere/telomerase biology. Introduction of hTERT into primary foetal sheep fibroblasts, restores telomerase activity, extends proliferative lifespan and maintains senescence bypass (Cui et al., 2002). However, stabilization of telomere length and karyotypic stability was directly proportional to the levels of hTERT expression. Unexpectedly this was not reflected in an assay for telomerase repeat addition activity, with all lines analyzed showing comparable activtity. Therefore it is not clear whether non-catalytic domains of hTERT have a telomere maintenance function distinguishable from enzymatic activity, or whether the hTERT catalytic domain alone is the key rate-limiting factor.

A second study on sheep fibroblasts conducted in our laboratory showed that two lines derived from the same breed (Black Welsh), differed dramatically in their proliferative lifespan (Cui et al., 2003). Both lines showed comparable average telomere length after derivation and also at replicative senescence; however these lines differed in their proliferative capacities by ~3-fold. The major limitation in this analysis was inference based on calculation of average telomere length, taking the

population as a whole. Recent advances in telomere detection have permitted a quantitative approach to calculate telomere length based upon signals from individual telomeres. This method allows analysis of telomere length heterogeneity, manifest as a result of varying shortening rates with respect to subsets of telomeres. It was therefore imperative to use this strategy to descriptively address telomere shortening in these two sheep primary lines, taking into consideration shortening of individual telomeres, and relate this to the previous observation of differences in proliferative lifespan.

Further recent advances in the telomere biology field have both permitted analysis of the G-rich single-strand 3' overhang and implicated this structure as a key factor with respect to telomere capping. However, it is unclear whether the 3' overhang alters during cellular proliferation or has a causal or consequential role regarding replicative senescence. To address these issues, the sheep lines in our laboraotory again provide a valuable tool; 3' overhang length can be measured during proliferation of normal sheep fibroblasts to assess alterations to the 3' overhang length. Furthermore, hTERT-immortalized sheep fibroblasts can be used to address if there is any direct or indirect relationship between hTERT expression and 3' overhang length.

1.12.2   Project objectives

Regulation of telomere length in mammalian cells is a multi-factorial process involving not only a host of telomere- and telomerase-associated factors, but also the dynamic physical configuration of chromosomal termini. Hence both extrinsic and intrinsic factors inter-dependently contribute to maintain telomere metabolic homeostasis. To gain insight into both avenues:

1)   The human telomerase catalytic subunit (hTERT) was studied to determine whether hTERT reverse transcriptase domain is rate-limiting with respect to telomere maintenance and senescence bypass, or whether there is evidence for a telomere maintenance function that can be distinguished from enzymatic activity. Furthermore, the consequences of long-term culture with hTERT-transfected transgenic lines were considered.

2)   A descriptive study of telomere shortening in primary sheep fibroblasts was conducted, taking into account individual telomere length heterogeneity. This study demonstrated the application of using Quantitative-FISH (Q-FISH) in the sheep model system, thus highlighting the technical advantages over previous methods for telomere length analysis.

3)   The 3' telomeric overhang was analyzed during culture of primary sheep fibroblasts to determine if the 3' overhang erodes throughout replicative lifespan and if so, whether a relationship between 3' overhang shortening rate and telomere shortening rate can be deduced. Furthermore, the 3' overhang was studied in the context of hTERT-immortalized sheep fibroblasts to infer the relationship between hTERT expression level and 3' overhang length.

CHAPTER 2

MATERIALS AND METHODS

2.1 General molecular biology materials

Bacterial Transformation and culture

Luria-Bertani (LB) Medium

1% Bacto-trptone (Difco), 0.5% Bacto-yeast extract (Difco), 125nM sodium chloride (NaCl).

Luria-Bertani (LB)-Agar

LB medium containing 1.5% agar (Difco).

SOC-medium

2% Bacto-tryptone, 0.5% Bacto-yeast extract, 10mM NaCl, 2.5mM potassium chloride (KCL), 20mM Mg^{2+} stock (1M $MgCl_26H_2O$/ 1M $MgSO_47H_2O$), 20mM glucose (Fisons).

Ampicillin selection

Stock solution 100mg/ml, used at 100μg/ml concentration.

Agarose gel electrophoresis

10x TAE Buffer

0.4M Tris-HCl pH 8.0, 0.01M EDTA, 0.2M acetic acid.

5x DNA Gel Loading Buffer (Sigma)

0.05% Bromophenol blue, 40% sucrose, 0.1 M EDTA Ph 8.0 and 0.5% SDS.

DNA Lysis

TNE DNA lysis Buffer

100mM Tris-HCl pH 8.5, 5mM EDTA, 0.2% SDS, 200mM NaCl, 100μg/ml Proteinase
K, 20μg/ml RNase.

Senescence-associated β-gal staining solution

X-gal

1mg/ml X-gal (Promega), 40mM Na_2HPO_4/citrate pH 6.0, 5mM potassium ferricyanide,
5mM potassium ferrocyanide, 150mM NaCl, 2mM $MgCl_2$ and made up to 10ml with
nuclease-free water.

TRAP assay (Chemicon)

1x.CHAPS Lysis Buffer

10mM Tris-HCl pH 7.5, 1mM $MgCl_2$, 1mM EGTA, 0.1mM Benzamidine, 5mM β-
mercaptoethanol, 0.5% CHAPS, 10% glycerol.

10x TRAP Reaction Buffer

200mM Tris-HCl pH 8.3, 15mM $MgCl_2$, 630mM KCL, 0.5% Tween 20, 10mM EGTA.

<u>50x dNTP Mix</u>

2.5mM each of dATP, dTTP, dGTP and dCTP.

<u>PCR Grade Water</u>

Protease, DNase and RNase-free; deionised.

<u>10x TBE Buffer</u>

0.89M Tris-HCl pH 8.0, 0.89M borate, 0.02M EDTA.

<u>40% Polyacrylamide Stock Solution</u>

Pre-mixed, 40% liquid acrylamide (19:1 acrylamide:bis-acrylamide ratio) (Electran)

<u>10% Ammonium Persulfate (APS)</u>

10% $(NH_4)_2S_2O_8$ (Electran)

<u>TEMED (</u>Tetramethylethylenediamine)

$C_6H_{16}N_2$ (Electran)

TRF Telomere Length assay

HCl Solution

0.25M HCl

Denaturing Solution

0.5M NaOH, 1.5M NaCl.

Neutralization Solution

0.5M Tris-HCl, 3M NaCl pH 7.5.

20x SSC

3M NaCl, 0.3M sodium citrate pH 7.0.

Miscellaneous Reagents

Sterile PBS

0.16M NaCl, 0.003M KCl, 0.008M disodium hydrogen phosphate, 0.001M potassium dihydrogen phosphate.

TE Buffer

10mM Tris-HCl pH 8.5, 1mM EDTA.

2.2 Molecular biology methods

2.2.1 Preparation of genomic DNA from cultured cells

Cells were harvested and lysed overnight in 700µl TNE DNA lysis buffer (see 2.1) and DNA extracted using the Phase-Lock Gel (PLG) method (Eppendorf). 700µl cell lysis was transferred to a 2ml PLG tube and an equal volume of phenol added. Tubes were thoroughly inverted to form a transiently homogenous suspension, prior to centrifugation at 13000rpm for 5 minutes. The aqueous phase was transferred to a fresh PLG tube and an equal volume of chloroform added. Tubes were again thoroughly inverted prior to centrifugation at 13000rpm for 5 minutes. The aqueous phase was transferred to a fresh 1.5ml tube and an equal volume of cold isopropanol added. DNA was visible upon inversion of the tube and transferred to a fresh 1.5ml tube. DNA was resuspended in 50-150ml of TE buffer (see 2.1) dependent on the size of DNA pellet incubated at 4°C to ensure complete resuspension.

2.2.2 Restriction endonuclease digestion

Digestion of pGEM-T Easy Sub-cloning Vector

1µg of plasmid pGem-T Easy (Promega) DNA was digested with 10 units EcoR1 restriction enzyme in a microcentrifuge tube using the supplied manufacturer's buffer (Buffer H). The reaction volume was 10µl and incubation was conducted at 37°C for 1 hour, 30 minutes.

Linearization Digests of pWGB25 and pWGB23

Prior to transfection with pWGB25 (mutant hTERT plasmid; section 2.9.1) and pWGB23 (EGFP-mock control plasmid; section 2.9.1), plasmids were linearized by a single-cut digestion at a non-essential region as follows: 70 units of Pci (New England Biolabs) was used to digest 66.5µg pWGB25 DNA in a reaction volume of 70µl, using 7µl of the buffer supplied by the manufacturer (10x NEBuffer 3). 80 units of BglII (Roche) was used to digest 54µg of pWGB23 DNA in a 100µl reaction volume using 10µl of the buffer supplied by the manufacturer (10x Buffer M). Samples were incubated at 37°C for 2-3 hours until complete digestion was observed by agarose gel electrophoresis.

2.2.3 Agarose gel electrophoresis

Agarose powder was dissolved in 1X TAE (0.8-2.0%) by microwave heating and allowed to cool. Ethidium bromide was added to a final concentration of 0.5µg/ml, prior to pouring the gel onto a horizontal electrophoresis set-up. DNA samples were mixed with 5x DNA loading buffer (see 2.1) prior to loading onto gels; at least one lane was reserved for 5µl of a molecular weight marker (Hyperladder Type I, Roche). An electrical current between 85 and 100 volts was applied. Following electrophoresis, DNA was visualized using a UV transilluminator and images captured using Multi-Analyst software (BioRad).

2.2.4 Purification of DNA fragments from agarose gels

DNA fragments electrophoresed through an agarose gel were excised using a clean sharp scalpel (visualized under long-wavelength UV light) and transferred to a microcentrifuge tube. The gel slice was processed using a QIAquick column (Qiagen) in accordance with the manufacturer's instructions. The weight of agarose was determined and 3 volumes of Buffer QG were added to 1 volume of gel (e.g. 300µl buffer to 100mg gel). This mixture was incubated at 50°C for 10 minutes and vortexed at intervals until the gel slice had dissolved. 1 gel volume of isopropanol was added to the mixture and the sample transferred to a QIAquick column held within a 2ml collection tube. The column was microcentrifuged at 10000g for one minute to bind the DNA. This step was repeated a second time to increase DNA yield, after which the flow-through was discarded. The column was washed with 750µl Buffer PE for 5 minutes to remove any residual agarose and excess salts, followed by a third 1 minute microcentrifugation. Flow-through was discarded and the column re-centrifuged to remove any remaining buffer. The column was placed in a clean 1.5ml centrifuge tube and 40µl of elution buffer added. The column was allowed to stand for 1 minute prior to a final centrifugation for 1 minute to elute the DNA.

2.2.5 DNA quantification

Spectrophotometric measurements were used to determine both the quantity and the quality of DNA preparations. Typically a DNA sample was diluted 1:200 with TE buffer and the absorbance read at 260nm to give the concentration of nucleic acid in the sample. An optical density (OD) of 1 corresponds to approximately 50µg/ml of double-stranded DNA. The ratio between readings at 260nm and 280nm provided an estimation of the purity and hence quality of the DNA preparation. Pure DNA has an OD_{260}/OD_{280} ratio of 1.8-2.0. Spectrophotometric measurements were verified by agarose gel electrophoresis using 1-2µl of DNA.

2.2.6 Preparation of total RNA from cultured cells

Total RNA was extracted using the RNeasy kit (Qiagen) according to the manufacturer's guidelines. Cells grown on a monolayer were harvested, washed twice with PBS (see 2.1) and disrupted by addition of 350µl Buffer RLT (Qiagen). Samples were homogenized by passing a 0.9mm diameter gauge needle through the lysate 5-7 times. 350µl of 70% ethanol was added to the homogenized lysate and mixed well by pipetting. 700µl of the sample was applied to an RNeasy mini column placed in a 2ml collection tube and centrifuged for 15 seconds at 13000rpm and flow-through discarded. At this stage, samples were DNase treated: 10µl DNase 1 stock solution was added to 70µl Buffer RDD (Qiagen RNase-free DNase set) and mixed gently by inverting the tube. The DNase 1 incubation mix (80µl) was added directly onto the RNeasy silica-gel membrane and placed on the benchtop for 15 minutes. 350µl Buffer RW1 (Qiagen) was added to

the column and centrifuged for 15 seconds at 13000rpm and flow-through discarded. The RNeasy column was transferred to a fresh 2ml collection tube and 500μl of Buffer RPE (Qiagen) was added to the column and centrifuged for 15 seconds at 13000rpm to wash the column. After discarding flow-through this wash step was repeated with a 2 minute centrifugation. To elute RNA, the RNeasy column was placed in a fresh 1.5ml tube and 40μl RNase-free water applied directly onto the silica-gel membrane.

2.2.7 RNA quantification

Spectrophotometric measurements were used to determine both the quantity and the quality of RNA preparations. Typically an RNA sample was diluted 1:200 with TE buffer and the absorbance read at 260nm to give the concentration of nucleic acid in the sample. An optical density (OD) of 1 corresponds to approximately 40μg/ml of single-stranded DNA. The ratio between readings at 260nm and 280nm provided an estimation of the purity and hence quality of the DNA preparation. Pure RNA has an OD_{260}/OD_{280} ratio 1.8-2.0. Spectrophotometric measurements were verified by agarose gel electrophoresis using 1-2μl of RNA.

2.2.8 First-strand cDNA synthesis

The AMV Reverse Transcriptase (RT) (Roche) was used to catalyze the synthesis of single-stranded cDNA from total isolated RNA. A total reaction volume was prepared using the following components: 1.5-2.5μg RNA diluted to a final volume of 9μl using

RNase-free water (diluted RNA incubated at 65°C for 15 minutes), 4μl 5x RT buffer (Roche), 1μl oligo(dT)$_{15}$ random primers (Roche), 4μl 5mM dNTP and 1μl RNase Inhibitor (Roche). The 20μl reaction was incubated at 30°C for 8 minutes followed by 42°C for 1 hour and 95°C for 5 minutes. Samples were centrifuged briefly and stored at -20°C.

2.2.9   Reverse-transcription polymerase chain reaction

Each reverse-transcription polymerase chain reaction (RT-PCR) was conducted in a 50μl reaction volume using the following components: 100ng-200ng of template cDNA (typically 1-2μl) made up to 38.5μl using PCR grade water, 5μl 10x PCR buffer (Roche), 4μl 2.5mM dNTP, 1μl forward primer, 1μl reverse primer and 0.5μl *Taq* Polymerase (Roche). Thermal cycle conditions to amplify total hTERT transgene levels, mutant hTERT transgene level alone and endogenous sheep GAPDH were set as follows: 94°C for 45 seconds, 60°C for 30 seconds (annealing) and 72°C for 45 seconds. Thermal cycle number used was 30 for hTERT and 26 for GAPDH. An annealing temperature of 61°C was used to detect hTERT 3'UTR in an amplification reaction using 30 cycles, and an annealing temperature of 54°C used to detect human GAPDH in an amplification reaction using 26 cycles. 10μl of RT-PCR product was used for agarose gel electrophoresis to visualize amplified DNA.

To distinguish between the mutant hTERT transgene and endogenous hTERT transcript in HEK 293-transfected cells, a set of primers were designed whereby the reverse

primer amplifies from within the SV40 polyadenylation signal in the mutant hTERT vector (pWGB25, see Appendix 1), generating an amplified product of ~600bp, the forward primers amplifying from within the mutant hTERT transgene. Thermal cycle conditions were set as follows: 94°C for 45 seconds, 55°C for 30 seconds (annealing) and 72°C for 45 seconds, for 26 cycles.

Primer sequences for RT-PCR:

i) Total hTERT transgene (wild-type and mutant)

hTERT-W1- 5'-AGCGACTACTCCAGCTATG-3' (Forward)

hTERT –W2- 5'-GTTCTTGGCTTTCAGGATGG-3' (Reverse)

Predicted product size – 325bp

ii) Mutant hTERT transgene alone

Mu-hTERT-F 5'-ACGGTGTGCACCAACATCTA-3' (Forward)

Mu-hTERT-R 5'-TGAAATTTGTGATGCTATTGCT-3' (Reverse)

Predicted product size – 598bp

iii) hTERT 3'UTR

Ex15F 5'-CATTCCTGCTCAAGCTGACTCGAC-3' (Forward)

3'UTR R 5'-CCTCAGACTCCCAGCCGTGCG-3' (Reverse)

Predicted product size – 350bp

iv) <u>Sheep GAPDH</u>

sGAPDH-F- 5'-TGTCCGTTGTGGATCTGACC-3' (Forward)

sGRAPH-R- 5'-CGTACCAGGAAATGAGCTTGAC-3' (Reverse)

Predicted product size – 224bp

v) <u>Human GAPDH</u>

rGAPDHF 5'-TGAGTATGTCGTGGAGTCTAC-3' (Forward)

rGAPDHR 5'-GGCCATGTAGGCCTAGAGGTC-3' (Reverse)

Predicted product size – 750bp

2.2.10 Polymerase chain reaction

Polymerase chain reaction (PCR) was conducted to amplify the GAPDH locus. A 50μl reaction volume was used incorporating the following components: 10ng-100ng of template genomic DNA (typically 1-2μl) made up to 38.5μl using PCR grade water, 5μl 10x PCR buffer (Roche), 4μl 2.5mM dNTP, 1μl forward primer, 1μl reverse primer and 0.5μl *Taq* Polymerase. Thermal cycle conditions to amplify the endogenous sheep GAPDH locus were set as follows: 94°C for 45 seconds, 60°C for 30 seconds (annealing) and 72°C for 45 seconds. GAPDH primers used as described in section 2.2.9.

2.2.11 Protein lysis (Western Blot)

Protein lysis was carried out on harvested cells using 300µl RIPA Buffer (Chemicon) containing 50mM NaCl, 25mM Tris pH 8.2, 0.5% Nonidet P40, 0.5% deoxycholate, 0.1% SDS and 0.1% Azide. Upon addition of RIPA lysis buffer, samples were vortexed for 1-2 minutes and passed through a 0.6mm needle to homogenize. Samples were centrifuged at 14000rpm at 4°C for 20 minutes and stored at -80°C.

2.2.12 Protein concentration (Western Blot)

A Bovine Serum Albumin (BSA) standard curve was set up to determine protein concentration of samples. Typically a BSA standard range of 0-5µg/µl was used where 10µl of each BSA concentration was mixed with 190µl bicinchoninic acid (BCA) working reagent (Pierce). RIPA buffer was used to dilute BSA standards to the desired concentration. To 2µl of each protein lysis sample, 8µl of water and 190µl BCA working reagent were added. All standards and samples were prepared in a 96-well plate and incubated at 37°C for 30 minutes. A spectrophotometer plate reader was used to read absorbance at 562nm. All samples were measured in triplicate and average 562nm absorbance measurement of the blank standards, subtracted from average measurements of each particular sample. A standard curve was prepared by plotting the average blank-corrected 562nm measurement for each BSA standard vs. its concentration in µg/ml. This standard curve was used to determine the protein concentration of each unknown sample.

2.2.13   Western Blot analysis

A total of 40μg protein from each sample was used to prepare a boiling mix containing 3x sample loading buffer (62.5mM Tris-HCl pH 6.8, 2% SDS, 10% glycerol, 50mM DTT and 0.1% bromophenol blue) and water to give a final volume of 20μl. This mix was boiled at 100°C for 10 minutes prior to separation on a 7.5% vertical polyacrylamide separating gel (40% acrylamide mix, 10% SDS, 1.5mM Tris pH 8.8 and water). A 4% polyacrylamide mixture (40% acrylamide mix, 10% SDS, 0.5mM Tris pH 6.8 and water) was used as the stacking gel. All wells were flushed with isopropanol after adding gel mixtures and flushed with water twice after gels had set. Polyacrylamide gel electrophoresis (PAGE) was conducted at 150V for approximately 1 hour using 10x running buffer (0.25M Tris, 1.92M glycine, 1% SDS). 25μl of the Rainbow molecular weight marker (Amersham) was run on either side of the sample lanes. Protein was transferred at 4°C overnight onto a nitrocellulose membrane using 10x blotting buffer (0.25M Tris, 1.92M glycine pH 8.3). Membranes were blocked for 1 hour in PBS containing 0.1% Tween (PBST) and 10% milk prior to incubation with rabbit monoclonal anti-hTERT primary antibody Y182 (Abcam) overnight at 4°C using a 1:100 dilution. Membranes were washed twice with PBST/10% milk, followed by washing twice with PBST alone and twice again with PBST/10% milk, followed by incubation with goat anti-IgG HRP-conjugated secondary antibody (Dako) at a dilution of 1:2500 for 30 minutes at room temperature. Proteins were detected using an ECL chemiluminescence HRP detection substrate (Millipore). Briefly, 3ml luminol and 3ml peroxide were mixed and poured onto the nitrocellulose membrane prior to 5 minutes

incubation at room temperature. Blots were drained, covered with acetate and exposed to autoradiography film for 30 seconds to 20 minutes. Membranes were stripped for 1 hour using buffer consisting of 62.5M Tris pH 6.8, 2% SDS and 100mM β-mercaptoethanol, and washed twice with PBST followed by blocking in PBST/10% milk for 2 hours. Blots were re-probed using mouse monoclonal anti-β-actin antibody (Santa-Cruz) at a 1:10000 dilution to detect β-actin, serving as an internal/loading control. Membranes were washed once with PBST/10% milk, followed by washing once with PBST alone and once with PBST/10% milk, followed by incubation with goat anti-mouse HRP-conjugated secondary antibody (Dako) at a 1:2500 dilution. Membranes were exposed to autoradiography film as described previously.

2.2.14 Protein lysis and concentration (Telomere Repeat Amplification Protocol Assay)

Harvested cells were lysed using 40μl 1x CHAPS buffer (Chemicon) and divided into 10μl aliquots. Cells were snap frozen on dry ice immediately proceeding lysis to ensure stability of the telomerase protein/RNA complex. A BSA standard was set up similar to that described in section 2.2.12. A BSA concentration range of 0.125-2μg/μl was used using 1x CHAPS buffer as the diluent. 10μl of each standard was added to 250μl Coomassie reagent (Pierce). For each protein sample, 1μl was added to 9μl 1X CHAPS buffer and 250μl Coomassie reagent. Protein concentration was determined in a 96-well plate which was incubated for 15 minutes at room temperature with gentle shaking. Absorbance at 595nm was calculated using a spectrophotometer plate reader and a

standard curve prepared by plotting the average blank-corrected 595nm measurement for each BSA standard vs. its concentration in µg/µl. This standard curve was used to determine the protein concentration of each unknown sample.

2.2.15   TRAP assay

TRAP assay (Chemicon) was conducted according to procedures previously described (Kim et al., 1997). Protein lysate was diluted to a concentration of 0.1-0.5µg/µl and 1µl used to set up a reaction mix consisting of 40.6µl of PCR grade water and 8.4µl of TRAP PCR mix (5µl 10x TRAP buffer, 1µl TS primer, 1µl Primer mix, 1µl 50x dNTP, 0.4µl *Taq* polymerase). 1µl of cell lysate (0.1-0.5µg) was heated in a 0.5ml tube at 85°C for 10 minutes to heat inactivate telomerase and thus serve as a control for heat sensitivity. Telomerase extension was achieved by heating samples at 30°C for 30 minutes. Amplification of the telomerase product was subsequently carried out using a thermal cycle of 94°C for 30 minutes, followed by 59°C for 30 minutes, repeated 30 times. 10µl of 5x DNA loading buffer (Sigma) was added to each PCR product before telomerase products (25µl per well), including heat inactivation controls, were resolved on 10% polyacrylamide vertical gels (0.5x TBE, 10% acrylamide mix, 0.1% APS, 0.01% TEMED, adjusted to 50ml with nuclease-free water) using 0.5x TBE as running buffer. TRAP gels were run at 240V for approximately 2 hours or until the loading dye had completely run off the bottom of the gel. 20µl of DNA molecular marker VIII

(Roche) was loaded onto lanes either side of TRAP products. TRAP gels were washed briefly in 1x TE buffer followed by staining for 30 minutes in the dark with SyBR Green 1 (Roche) solution (10μl SyBR Green 1, 100ml 1x TE buffer). TRAP gels were scanned using an FX phosphoimager and semi-quantitative analysis conducted using Multi-analyst software.

2.2.16 Competitive inhibition TRAP assay

TRAP assay was conducted as described in section 2.2.14, incorporating two independent lysate samples. Initially various ratios of the two competing samples were used but yet ensuring a final protein concentration of 1μg/μl; e.g. 0.5μg:0.5μg or 0.25μg:0.75μg. This strategy was modified to compare samples at 5 to 20-fold excess of protein; e.g. 0.1μg:5μg or 0.1μg:20μg.

2.2.17 Telomere Restriction Fragment length assay

Genomic DNA from cultured cells was isolated as described in section 2.2.1. Telomere length was determined by telomere restriction fragment (TRF) Southern blot analysis with a digoxigenin labelled (TTAGGG)$_3$ probe (Roche) as described previously (Harley et al., 1990) and using the manufacturer's guidelines. A frequent cutter restriction enzyme mix consisting of 0.75μl (30U) Rsa1 (Roche), 0.75μl (30U) Hinf1 (Roche), 2.5μl Buffer A (Roche) and 0.5μl RNase A, was added to 2-4μg genomic DNA and made up to a final volume of 25μl for each sample tested. After overnight digestion at 37°C, 3μl Xylene Cyanol dye (Mol. Bio. Laboratories) was added to each sample and

samples electrophoresed on a 0.8% agarose gel, initially at 100V for 20 minutes, prior to approximately 16 hours overnight at 30V. A digoxygenin-labelled (DIG) high molecular weight marker (Roche) was freshly prepared for each gel as follows: 4μl DIG marker, pre-heated at 65°C for 10 minutes, was added to 4μl Xylene Cyanol dye and 12μl nuclease-free water. 10μl of DIG marker was loaded on either side of samples. At this stage, DNA was visualized under UV light to determine degree of migration on the gel. Prior to Southern Blot transfer, gels (DNA side up) were depurinated in 0.25M HCl (10 minutes), rinsed twice with deionised water, denatured using 1.5M NaCl/0.5M NaOH (2x 15 minute washes), again rinsed twice with deionised water and neutralised using 0.5M Tris/1.5M NaCl pH 7.5 (2x 15 minute washes). Southern transfer of DNA fragments was achieved by inverting the gel onto 3M Whatman blotting paper and placing a positively charged nylon membrane on top of the gel, followed by 3M Whatman paper and a heavy weight. 20x SSC buffer was used to facilitate the transfer and blots allowed to transfer overnight. Prior to hybridization, membranes were X-linked using a UV cross-linker and washed briefly in 2x SSC. Pre-hybridization was performed using 15ml DIG Easy Hyb solution (Roche) for 1 hour at 42°C, whilst rolling. Hybridization was performed using 15ml DIG Easy Hyb solution and 3μl telomere-specific probe (Roche) overnight at 42°C. Membranes were washed prior to DNA detection using the following regime: 100ml 2x SSC/0.1% SDS (2x 5 minutes at room temperature with shaking), 50ml 0.2SSC/0.1% SDS (2x 15 minutes at 50°C and rolling), 100ml 1x Washing Buffer (Roche) (5 minutes at room temperature with shaking), 100ml 1x Maleic Acid Buffer/1x Blocking serum (Roche) (30 minutes at room temperature with shaking). After washes, membranes were incubated with Anti-DIG-Alkaline

Phosphatase solution (Roche; 10μl Anti-DIG-AP and 100ml 1x Maleic Acid Buffer/1x Blocking serum) followed by washing with 100ml 1x Washing Buffer (2x 15 minutes at room temperature with shaking). Membranes were finally washed with 100ml 1x Detection Buffer (Roche) (5 minutes at room temperature with shaking) prior to adding CDP chemiluminescence substrate (Roche) drop-wise onto membranes. Membranes were wrapped in Saran Wrap and exposed to X-ray film for 30 seconds to 3 minutes. TRF telomere length was determined using Multi-Analyst 1.1 software.

2.2.18 Telomere-Oligonucleotide Ligation Assay

Telomere-oligonucleotide ligation assay (T-OLA) was adapted from (Cimino-Reale et al., 2001). 1.85MBq of ^{32}P radioisotope (Amersham) was used to label 10pmol of telomere G-rich strand specific oligonucleotide (CCCTAA)$_4$ or mismatch control oligonucleotide (CCCTTA)$_4$ (MWG Biotech). The end-labelling reaction was catalyzed using 10U T4 Polynucleotide Kinase (PNK) (Roche) using 1x T4 PNK Buffer (Roche) in a total reaction volume of 25μl. Samples were incubated at 37°C and reactions allowed to proceed for 45 minutes, followed by incubation at 68°C for a further 15 minutes. To remove unincorporated labelled nucleotides, samples were first adjusted to 50μl with 150mM STE Buffer (NaCl/TE) and passed through a G-50 Micro Column (Amersham) at 2800rpm for 2 minutes. A similar set up was used to label 750ng of dephosphorylated DNA Molecular Weight Marker VIII (Roche) with 0.925MBq of ^{32}P, in a reaction volume of 10μl. For hybridization of oligonucleotides to undenatured

genomic DNA, 1pmol G-rich or mismatch-labelled oligonucleotide was added to 10μg RNase-treated DNA and 1x *Taq* Ligase Buffer (Roche), adjusted to a final volume of 20μl. Hybridization reactions were incubated at 52°C for 16-20 hours. Samples were briefly centrifuged prior to a ligation reaction using 30U *Taq* Ligase (Roche) at 52°C for 5 hours. Ligated products were ethanol precipitated by adding 80μl nuclease-free water, 11μl 5M NaCl and 250μl 100% ethanol. Samples were incubated at -80°C overnight and centrifuged at 13000rpm for 50 minutes to precipitate ligated DNA. Products were washed with 70% ethanol and re-suspended in 10μl nuclease-free water at 52°C for 2-3 hours. DNA was denatured by adding 10μl of formamide based denaturing buffer (Ambion) and incubated at 100°C for 5 minutes. A vertical denaturing polyacryamide gel (6M Urea, 5% acrylamide, 1xTBE, 0.3% APS, 0.04% TEMED adjusted to 100ml with deionised water) was used to resolve ligated DNA products, with 5μl of each sample loaded per lane and 2μl of marker loaded on lanes either side of samples. 0.5x TBE was used as running buffer and gels run at 2500V for approximately 2-3 hours. Gels were transferred to Whatman filter paper, dried using a gel drier (80°C for 30 minutes) and exposed to autoradiography film. To ensure equal DNA loading, 10ng of every T-OLA sample was used as a template for genomic PCR reactions to detect the GAPDH gene. T-OLA images were analysed by Multi-Analyst software.

2.3 <u>Histological methods</u>

2.3.1 Detection of β-galactosidase activity

Cells grown on monolayers were prepared by washing x2 with PBS, fixed with 3% formaldehyde and washed again x2 with PBS. Senescence-associated β-gal staining was detected by adding 5ml fresh X-gal solution (Promega) (see section 2.1) and incubating cells for approximately 16 hours at 37°C.

2.4 <u>Bioinformatics methods</u>

2.4.1 BLAST and Multiple Sequence Alignment analysis

A BLASTN nucleotide search was conducted using the NCBI search engine, with the sequence of ligated inserts (approximately 250bp) as a query sequence. Databases of all mammalian species available were compared to identify percentage homology with the prospective sheep gene sequence of interest. A ligated insert of known sequence (hTERT fragment from the HEK293 line) was also sent to DNASeq for validation and the nucleotide sequence (~300bp) used to BLAST all eukaryotic databases to determine percentage of TERT sequence homology across species.

2.5 Quantitative methods

2.5.1 Quantitative-Fluorescence In-Situ Hybridization (Q-FISH) analysis

Q-FISH analysis was conducted on metaphase images (section 2.10.2) using TFL-Telomere TeloQuant Analysis software (Peter Lansdorp laboratory, Vancouver, Canada). The Open Lab 2D microscope image processing software was used to capture FISH images using an exposure time of 0.99 seconds. Images of DAPI-stained chromosomes and Cy3-stained telomere repeats were captured independently. Approximately 350-400 chromosomes were accounted for with respect to each cell line, representing 7-10 metaphase spreads. This permitted valid statistical analyses. A minimum telomere threshold value of 2 (arbitrary numerical value) was set for TeloQuant analysis. Due to the denatured appearance of sheep metaphase chromosomes, a paint tool (Photoshop) was used to define borders of individual chromosomes and thus allow the software to distinguish chromosomes for telomere quantification. An arbitrary value is assigned to each telomere end - Telomere Fluorescence Units (TFU) - with TFU being directly proportional to the size of the individual telomere repeat length. (NB: Zero TFU is not necessarily regarded as a telomere signal free end (SFE), but rather reflects a telomere signal below the threshold of this software). TFU values were categorized into 'bins' at intervals of 50 using Microsoft Excel Software and a 'frequency' command used to

represent number of telomeres with TFU values within a given category.The data was plotted either directly or as a percentage of telomere ends per category.

2.5.2 Densitometric analysis (RT-PCR)

For the GRN clones, RNA expression levels were quantified by densitometry using Multi-Analyst software and normalized to GAPDH. Relative stoichiometry was inferred by assigning a value of 1 to the GRN23(C1) mock vector control and calculating total hTERT expression as relative.

To calculate relative inhibition of endogenous hTERT in HEK 293 cells transfected with a mutant hTERT transgene, endogenous hTERT RNA levels were normalized to GAPDH and relative inhibition calculated relative to the untransfected control.

2.5.3 Densitometric analysis (TRAP)

Telomerase activity in GRN clones was quantified using Multi-Analyst software, as the ratio of the intensity of the telomere repeat ladder over the intensity of the 36bp internal control band. Relative TRAP activity was calculated relative to the GRN23(C1) mock vector control.

2.5.4 Densitometric analysis (TRF)

Mean TRF telomere length was calculated using Multi-Analyst software according to the following formula:

$$TRF = \Sigma(OD_i)/ \Sigma(OD_i/L)$$

where OD_i is the chemiluminescent signal and L_i is the length of the TRF fragment at position i. The calculation takes into account the higher signal intensity from larger TRF fragments due to multiple hybridization of the telomere-specific hybridization probe. A power regression standard using the DIG molecular weight marker is used to determine the actual telomere length, and average background subtracted for each sample.

2.5.5 T-OLA G-rich size distribution analyses

T-OLA images were analysed by Multi-Analyst 1.1 software. The relative frequency of overhangs of different length was obtained by normalizing the intensity of each single band to the sum of intensity of all the bands of the ladder. This densitometric analysis was performed for at least three different experiments for each cell line to calculate standard deviations of the mean relative frequencies.

2.6 Cell culture materials

Basic sheep fibroblast medium

Glasgow minimal essential medium (GMEM; Invitrogen) supplemented with 10% foetal calf serum (FCS; Globepharm), 2mM L-glutamine, 1mM sodium pyruvate and 1x non-essential amino acids (all Gibco).

Basic human fibroblast and HEK 293 medium

Dulbecco's modified eagles medium (DMEM; Invitrogen) supplemented with 10% foetal calf serum (FCS; Glopepharm), 2mM L-glutamine, 1mM sodium pyruvate and 1x non-essential amino acids (all Gibco).

Sterile PBS

As described in section 2.1

Trypsin/EDTA solution (Sigma)

0.5g/l porcine trypsin and 0.2g/l EDTA in Hanks' Balanced Salt solution with phenol red.

1x Freeze mix

90% GMEM and 10% dimethyl sulfoxide (DMSO; Sigma).

G418 (Geneticin)

50mg/ml stock solution (Invitrogen) diluted to working concentration of 400-750µg/ml.

2.7 Cell culture methods

2.7.1 Maintenance of primary cell lines

Sheep fibroblasts, BW6F2 and BWF1, were isolated from a day 35 Black Welsh eviscerated foetus as described previously (Wilmut et al., 1997). Cells were cultured in Glasgow minimal essential medium (Sigma), supplemented with 2mM L-glutamine, 1mM sodium pyruvate, 1x non-essential amino acids and 10% foetal calf serum (GlobePharm) in a humidified incubator at 37°C, 5% CO_2 and 21% O_2 using a 25 or 75cm^3 plastic tissue culture flask. Human BJ-hTERT foreskin fibroblasts and HEK 293 cells were cultured in a similar fashion but using DMEM (Invitrogen). Cells were supplemented with fresh medium every two days and serial passage performed upon 90% confluency as follows: culture media was aspirated and cells washed with PBS to remove traces of serum. Cells were then incubated with 1-3ml of Trypsin-EDTA (Sigma) for 2-3 minutes at 37°C and further encouraged to detach by gently tapping the side of the flask. Immediately after detachment, serum-containing medium was added to inactivate trypsin and cells harvested by centrifugation at 1000rpm for 4 minutes. Supernatant was discarded and cells resuspended in fresh serum-containing medium before transfer to a new flask at the desired ratio, typically 1:6. For an accurate estimation of cell number, harvested cells were resuspended in 5-10ml of medium, mixed thoroughly and counted using a haemocytometer. A total of 64 squares were

counted (4 grids, 16 squares each), averaged and cell number determined using the following formula:

Cells/ml =

$$\Sigma \, [(\text{Grid A } 1\text{-}16) + (\text{Grid B } 1\text{-}16) + (\text{Grid C } 1\text{-}16) + (\text{Grid E } 1\text{-}16)/4] * 10^4,$$

Culture of Black Welsh sheep fibroblasts in hypoxic conditions was achieved using a specialized air-tight chamber supplemented with 2% O_2 regularly.

2.7.2 Freezing and resuscitating cells

Subconfluent monolayer cultures were harvested as previously described (section 2.8.1) and pellets resuspended in 1x freezing mix (section 2.7). 1ml aliquots were frozen overnight at -80°C before being transferred to $N_2(l)$ for long-term storage. Cells recovered from long-term storage were thawed rapidly at 37°C and resuspended in appropriate basic culture medium. Cells were then pelleted at 1000rpm for 4 minutes to remove traces of DMSO, plated on complete growth medium and refreshed after 24 hours.

2.7.3 Growing cells under a selection regime

For GRN sheep fibroblasts clones, cell monolayers were passaged 1:6, 24 hours prior to adding selection. Cells were cultured with basic culture medium (section 2.7), supplemented with 400µg/ml Geneticin (Invitrogen) or 1µg/ml Puromycin (Invitrogen),

to select for G418- and puromycin-resistant cells that express mutant (and EGFP mock control) and wild-type hTERT transgenes respectively. Cells were cultured for 10-14 days, serially passaged when required and supplemented with fresh selection medium.

To isolate HEK 293 cells transfected with mutant hTERT or mock EGFP vector (section 2.9.1), cells were cultured with basic culture medium (section 2.7) and supplemented with 400-750µg/ml Geneticin (Invitrogen). After four days culture, cells from each experimental set-up were pooled and expanded as one population, grown for approximately four weeks under a selection regime, and protein lysate and RNA collected at intervals.

2.7.4 Population doubling (PD) rate calculation

Each GRN sheep fibroblast clone was expanded to confluency in a T75 tissue culture flask, from which 3×10^5 cells were plated into a T25 culture flask and growth curves commenced at this point. Cells were sub-cultured twice weekly and maintained at log phase growth. Population doubling rate was calculated according to the following formula:

$$PD = \log E/S / \log 2,$$

where E = end count and S= start count.

2.8 Transgene introduction - methods of transfection

2.8.1   Electroporation

The GRN(25), GRN(23) and BW6F2(25) sheep fibroblast lines were generated previously in our laboratory by Ling Mo. To generate bi-transgenic lines that express both wild-type and mutant hTERT transgenes, the GRN1-1 line was transfected with pWGB25. GRN1-1 represents a hTERT-immortalized line that exhibits low levels of wild-type hTERT and pWGB25 (7.3kb, see Appendix 1; constructed by Dr. Wei Cui) contains mutant hTERT cDNA driven by the phosphoglycerate kinase (PGK) promoter and mutated at three bases in three distinct reverse transcriptase (RT) motifs, thus rendering the hTERT transgene catalytically dysfunctional. RT-domain mutations were as follows: Arginine was substituted at amino acid position 631 with Alanine (R631A), Aspartic acid at position 712 with Alanine (D712A) and Aspartic acid at position 868 with Alanine (D868A). (Plasmid GRN380, containing mutant hTERT cDNA was kindly provided by Geron Corp.) To generate an EGFP mock vector control line, GRN1-1 was transfected with pWGB23 (4.7kb, see Appendix 1; constructed by Dr. Wei Cui). pWGB23 contains an EGFP cDNA driven by the phosphoglycerate kinase (PGK) promoter. To generate a cell line control, the parental sheep fibroblast line, BW6F2, was transfected with pWGB25 to generate a transgenic line that exhibits mutant hTERT expression alone. All transfections were conducted using 10µg of plasmid DNA and via the electroporation method under a condition of 400V, 250uF. The GRN1-1 line was

transfected at passage 27 and BW6F2 transfected at passage 8. All transfected cells were placed under a G418 selection regime using 400µg/ml Geneticin and stable clones showing good morphology were picked and expanded in a T25 flask. Clones were denoted passage 1 (post-transfection) at this stage.

2.8.2 Lipofectamine 2000-mediated transfection

Lipofectamine 2000 (Invitrogen) was used to transfect HEK 293 cells with either the pWGB25 mutant hTERT plasmid or pWGB23 EGFP mock vector control. Lipofectamine 2000 is a cationic lipid formulation that may be used to efficiently transfect cells on a monolayer or in suspension. All transfections were carried out in a 6-well format with cells seeded at a density of 5×10^4, 1×10^5 or 2×10^5. DNA to lipofectamine ratio used was either 1:2.5 (4µg DNA: 10µl lipofectamine) or 1:3 (4µg DNA: 12µl lipofectamine). The transfection procedure was as follows: 4µg DNA was diluted in 240µl Opti-MEM 1 reduced serum medium w/o serum (Invitrogen) and mixed gently. An appropriate volume of Lipofectamine 2000 (10 or 12µl) was diluted in 240µl Opti-MEM 1 and incubated for 5 minutes at room temperature. Diluted DNA and Lipofectamine 2000 was combined by gentle pipetting and incubated for 20 minutes at room temperature. Complexes (500µl) were added carefully in a drop-wise fashion to each well and mixed gently by rocking the plate. Cells were incubated at 37°C for 5 hours whence fresh medium was applied. 400µg/ml Geneticin was supplemented to fresh medium 24 hours post-transfection. A Lipofectamine 2000-only transfection was used as a negative control. Cells were passaged upon confluency and split into 3 x T75

flasks for each transfection set-up. After 7 days, all HEK 293-mutant hTERT and HEK 293-EGFP- transfected populations were pooled and expanded. Transfection efficiency was judged by viewing EGFP-transfected clones under UV light. At day 14 post-transfection, Geneticin concentration was increased to 750μg/ml and cell populations expanded. RNA and protein was collected at 1 week intervals for a period of 4 weeks.

2.9   Fluorescence-in situ hybridization (FISH)

2.9.1   Preparation of cells in fixative

Cells were cultured to 100% confluency prior to splitting to ensure synchronous release from contact inhibition. Fixative was applied 26 hours post-transfection, during log-phase growth. Typically, cells were washed with PBS, trypsinized and harvested by centrifugation at 1500rpm for 5 minutes. Medium was removed and cells resuspended in fresh 10ml 0.6% tri-sodium citrate (hypotonic solution), added drop-wise whilst vortexing. Tubes were incubated for 15 minutes at room temperature to allow cells to swell. Cells were again centrifuged at 1500rpm for 5 minutes and supernatant discarded. 6ml fresh fixative (3:1 methanol: acetic acid) was added drop-wise whilst vortexing and tubes centrifuged at 1500rpm for 5 minutes. This fixation step was repeated twice. Cells were resuspended in 500μl fixative, whereby the suspension appears milky, and stored at -20°C.

2.9.2 Preparation of metaphase spreads

Microscopic slides were immersed in 50ml 100% ethanol/1ml concentrated HCL, kept in 50ml Glass Hellendahl jars. Prior to use, slides were immersed in distilled and then deionised water and then incubated at 37°C for 5 minutes. The surface of slides was made moist by breathing and 2-3 drops of cell fixative suspension gently dropped onto slides at a 45°C angle. Slides were moved to a vertical position immediately after drops had landed to remove excess solution. Slides were allowed to dry at room temperature for 15 minutes after which metaphase quality and quantity was viewed under a microscope using a 10x and 20x phase light objective

2.9.3 FISH

Detection of telomeres in metaphase chromosomes was carried out using the Telomere PNA FISH/Cy3 kit (Dako). This procedure uses a 24-mer Cy3-conjugated peptide nucleic acid probe (PNA) (a synthetic DNA/RNA analogue) specific to TTAGGG telomere repeat sequences. (Pre-treatment and all treatment stages were carried out in 50ml glass Hellendahl jars). A pencil was used to mark an area of approximately 20 x 20mm length on metaphase slides, where high quality of spreads was evident. Pre-treatment was conducted as follows: slides were immersed in TBS (Dako) for 2 minutes followed by immersion in 3.7% formaldehyde (diluted with TBS) for 2 minutes and again immersed in TBS (2x 5 minutes). Slides were then immersed in pre-treatment solution (Dako) for 10 minutes (diluted 1:2000 with TBS) and washed in TBS (2x 5 minutes). Slides were finally immersed in a cold ethanol series (70%, 85% and 100%

ethanol; 3x 2 minutes) and left to dry vertically at room temperature for 5 minutes. Denaturation and hybridization were conducted as follows: 10µl Telomere PNA/Cy3-conjugated probe was applied to the marked area on slides and covered with a plastic coverslip. Slides were placed in a pre-heated incubator (adjusted to 80°C) for 3 minutes and placed in a dark box at room temperature for 30 minutes to allow hybridization. Slides were washed in 50ml Rinse Solution (Dako) for 1 minute to remove coverslips prior to immersion in 50ml Wash Solution (Dako) at 65°C for 5 minutes. Slides were washed in a cold ethanol series as before and left to dry vertically at room temperature for 5 minutes. For mounting and counterstaining, 2x 10µl of 0.1µg/ml DAPI (Vectashield) was applied onto each slide and a glass coverslip placed on top. Slides were left for 15 minutes to allow counterstain colour to develop before performing fluorescence microscopy using a 100x oil objective with a propidium iodide filter (similar wavelength to a Cy3 filter).

2.10   <u>Statistical methods</u>

<u>Standard deviation</u>

Standard deviation of the mean was calculated where appropriate using the following formula:

$$\sigma = \sqrt{\Sigma(x-y)^2/N}$$

where x = individual scores, y = mean of individual score and N is the total number of scores.

<u>Q-FISH statistics</u>

The Chi Squared test was used to determine whether or not the two sheep fibroblast lines used for study (BWF1 and BW6F2) significantly differed with respect to telomere length - Telomere Fluorescence Units (TFU) - as determined by Q-FISH. In addition, Chi Squared was performed for telomere length values within each line to show that telomere shortening significantly differs from early to late passage. The basic formula used for statistical analysis was as follows:

$$X^2 = \Sigma \frac{(\text{Observed frequency} - \text{Expected frequency})^2}{\text{Expected frequency}}$$

TFU values were placed into categories with intervals of 50 TFU (e.g. – 50, 100, 150….900) and percentage of telomere ends per category plotted. However this resulted in the number of categories exceeding the upper limit of that required for an acceptable degree of freedom for the Chi Squared analysis. Therefore the TFU categories were grouped as follows: 50-200; 201-400; 401-600; 601-900. The 50-200 TFU category represents the shortest telomeres and the 601-900 TFU represents the longest telomeres in this setting. With this reduced number of grouped categories, Chi Squared was performed to test significance of telomere lengths within and between the cell lines.

CHAPTER 3: ANALYSIS OF

CATALYTICALLY DYSFUNCTIONAL HTERT

IN PRIMARY OVINE FIBROBLASTS AND

HEK 293 TUMOUR CELLS

3.1   Introduction

As previously discussed in section 1.4, TERT has been implicated as a key factor limiting telomerase activity in human somatic cells, because the RNA subunit is constitutively expressed at a low basal level in cells (Feng et al., 1995). This hypothesis is supported by the observation that ectopic expression of human TERT (hTERT) in primary human fibroblasts restored telomerase activity, extended telomeres and indefinitely prolonged cellular lifespan (Bodnar et al., 1998, Counter et al., 1998). It has been accepted generally that telomere length in mammals is regulated by a homeostatic mechanism that is governed in part by telomerase and a telomere-specific protein complex recently termed 'Shelterin', which consists of TRF1, TRF2, TIN2, Rap1, TPP1 and POT1 (de Lange 2005). However, telomere length is not always maintained in cells with reconstituted telomerase, indicating that telomerase activity does not necessarily imply telomere maintenance (Ouelette et al., 1999, Cui et al., 2002). Similarly the telomeres of many tumour cell lines are shorter than those of corresponding normal cells, despite the fact that the tumour cells have high levels of telomerase activity (Hastie et al., 1990, Counter et al., 1994). Telomerase-mediated telomere maintenance rather than telomerase expression *per se*, may be one key normal cellular lifespan-limiting factor. In the last decade, murine models have been instrumental in demonstrating the impact of telomerase function in the context of a whole organism. Mice with inactivated TR or TERT exhibit gradual telomere attrition and long-term viability of the strain is compromised due to infertility (Blasco et al., 1997, Erdmann et al., 2004). Conversely mice with ectopic TERT show telomere extension, increased cell proliferation and a

higher incidence of tumour formation (Oh et al., 2001, Artandi et al., 2002). However, telomerase-deficient mice do not recapitulate the whole spectrum of human pathologies. For example mTR knockout mice only show a phenotype after 6 or 7 generations, whereas by contrast, hTR haploinsufficiency in humans is lethal at foetal stage (Vulliamy et al., 2001). These discrepancies may be explained by the fact that laboratory mouse (*Mus musculus*) telomeres are long (30kb to more than 200kb) and hypervariable (Prowse et al., 1995, Starling et al, 1990) compared to human telomeres (5-15Kb) (Kipling et al., 1990). Moreover in most human tissues, telomerase is not readily detectable (Kim N-H et al., 1994), whereas telomerase activity is found in most mouse tissues (Greenberg et al., 1998). Therefore, another animal model other than mouse is necessarily required. Previous work in our laboratory has shown that sheep (*Ovis aries)* fibroblasts share a lot of similarities with human in respect to telomere and telomerase biology. Sheep fibroblasts have a defined *in vitro* lifespan, their telomeres shorten at rates comparable to that reported in humans, and ectopic expression of hTERT effectively immortalizes the cells (Cui et al., 2002 & 2003, Clark et al., 2003).

The hTERT-immortalised sheep fibroblasts showed that at higher levels of hTERT expression, full length telomeres are maintained and karyotypic stability is preserved. By contrast, at lower levels, telomere erosion and genomic instability occur to an extent that is directly attributable to the level of hTERT expression – however, telomerase activity was comparable between these lines (Cui et al., 2002). This further highlights the complex relationship between telomerase function and telomere maintenance. One question arising is whether non-catalytic domains in hTERT have any function(s) with

respect to telomere maintenance, be it direct (e.g. proper telomerase assembly; substrate binding) or indirect (e.g. recruitment of telomerase-associated factors), independent of reverse transcriptase-mediated telomere maintenance; however it is conceivable that hTERT catalytic domain expression level solely is rate determining for telomere repeat processivity. An alternative hypothesis regarding telomerase-mediated telomere maintenance follows from the postulation of a dimeric model of TERT in order for proper telomerase function (Prescott & Blackburn 1997). This model of a dimeric telomerase complex predicts that telomerase function and telomere maintenance may be compromised if the complex is disrupted, where both TERT molecules may function inter-dependently.

In order to address both these issues, a catalytically dysfunctional hTERT transgene was expressed in an hTERT-immortalized primary sheep foetal fibroblast line in which telomeres stabilize at an average length much shorter than the untransfected parental line. This system provides an opportunity to study effects of over-expression of hTERT non-catalytic domains on telomerase activity and telomere maintenance. This strategy thereby presents a window in which telomere maintenance function may be attributed to hTERT that can be distinguished from enzymatic activity. Conversely the presence of a catalytically dysfunctional hTERT should further understanding of whether proper hTERT function requires an inter-dependent hTERT dimer with two intact reverse transcriptase motifs. In this regard both mutant/wild-type telomerase heterodimers and mutant/mutant telomerase homodimers may compete with and compromise wild-type/wild-type telomerase homodimeric function.

Additionally, catalytically dysfunctional hTERT was transfected into a telomerase positive primary human tumour line, in order to assess the effects of mutant hTERT on endogenous hTERT function. This strategy underlines the anti-telomerase dominant negative strategies proposed to target telomerase in a tumour setting.

3.1.1   Hypothesis

1)   hTERT reverse transcriptase activity is rate-limiting with respect to hTERT-mediated telomere maintenance.

2)   Introduction of mutant hTERT in tumour cells inhibits endogenous telomerase activity through dominant-negative and/or competitive interactions.

3.1.2   Chapter aims

1)   To familiarize with techniques to measure telomere length and telomerase activity.

2)   To determine whether mutant hTERT has the capacity to restore telomerase activity and affect proliferative lifespan.

3)   To determine whether hTERT non-catalytic domains have a role in telomere maintenance that can be distinguished from enzymatic activity in telomerase positive cells.

4)   To gain insight into proper telomerase function with respect to hTERT interacting monomers.

5)   To analyze the effects of introducing catalytically dysfunctional hTERT into a telomerase positive human tumour cell line.

3.2   Results

3.2.1   Generation of stably transfected clonal lines

A hTERT-immortalized BW6F2 sheep fibroblast clonal line (GRN1-1) and its parental cells, BW6F2, were transfected with a mutant hTERT construct or a mock vector construct containing GFP (section 2.9.1). To select for and generate stable clones, the constructs also contain a neomycin cassette (transfections and generation of lines conducted by Ling Mo, previously in our laboratory). A 7.3 kb mutant hTERT construct was used for the study, containing three *in vitro* induced amino acid substitutions (R631A, D712A and D868A) and driven by the PGK promoter. For mock controls, a 4.6kb EGFP construct was used using the same vector backbone (Fig. 3.1).
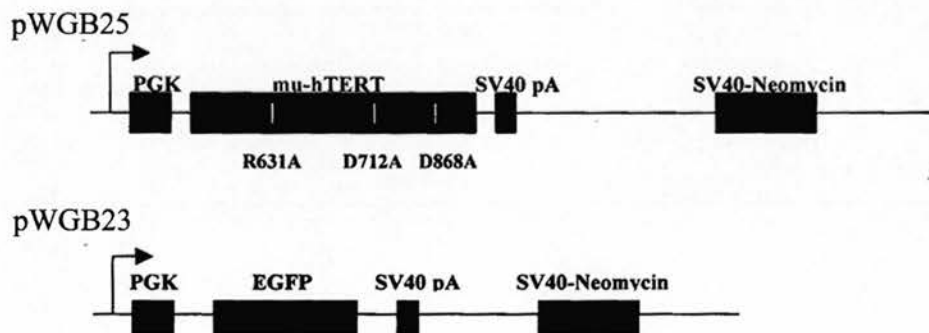
Figure. 3.1: Schematic of pWGB transgenic constructs. (Top) pWGB25 mutant hTERT (7.3Kb) with amino acid substitutions indicated. (Bottom) pWGB23 EGFP mock vector (4.6Kb). The PGK promoter, SV40 polyadenylation signal and neomycin selection cassette are indicated for both constructs.

After selection, multiple clones were picked up from transfected GRN1-1 cells both with pWGB25 and 23 constructs. However, a lower number of clones were formed from

parental BW6F2 cells. Only two clones BW6F2 (25)-7 and -8 were able to be expanded

from pWGB25 transfection, for further analysis.

3.2.2 Mutant hTERT cannot restore telomerase function

To address whether mutant hTERT alone can reconstitute telomerase activity, the effect

of mutant hTERT expression on telomerase activity was first addressed in the parental

sheep fibroblast line, BW6F2, using the Telomere Repeat Amplification Protocol

(TRAP) assay (section 2.215). Telomerase activity is not induced by catalytically

inactive mutant hTERT expression in primary sheep fibroblasts even though mutant

hTERT expression was high in the BW6F2(25)-8 clone (Fig. 3.2).
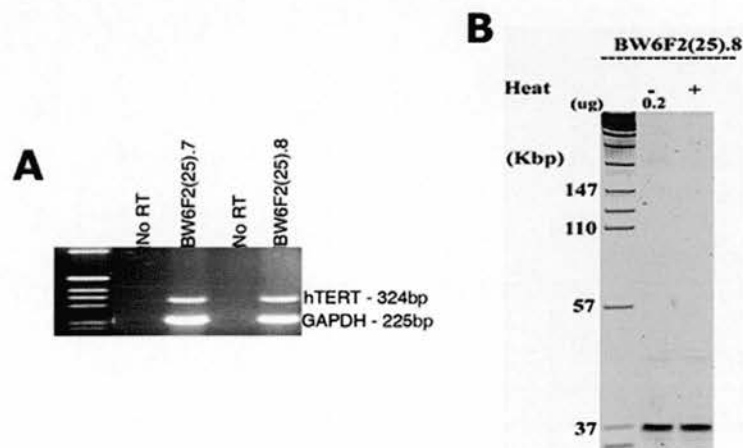
Figure 3.2: Telomerase activity in primary sheep fibroblasts transfected with mutant hTERT. (A) Expression of mutant hTERT in primary sheep fibroblasts. The BW6F2 parental sheep fibroblast line was transfected with a catalytically dysfunctional mutant hTERT alone. Two clones, BW6F2(25)-7 and BW6F2(25)-8, showed high levels of mutant hTERT expression. No DNA contamination was detected in RNA samples lacking reverse transcriptase. PCR reactions were conducted at 30 cycles. (B) No telomerase activity is detectable in the parental sheep fibroblast line transfected with the pWGB25 mutant hTERT transgene alone. 0.2µg of BW6F2(25).8 total protein extract was used for TRAP. Heat inactivated and internal standard control is shown.

This proved that telomerase activity is totally abolished by mutating three amino acids in three distinct reverse transcriptase motifs of the hTERT catalytic domain and that a functional hTERT catalytic domain is required for telomerase activity. In addition, the transfected cells did not proliferate vigorously and senesced after several passages (Fig. 3.7A) similar to EGFP transfected clones. These results confirmed that the three point mutations in distinct reverse transcriptase motifs of hTERT had abolished its catalytic function and that the mutant hTERT does not have the ability to reconstitute telomerase activity.

3.2.3   RNA expression analysis in transfected GRN1-1 clones

The effect of mutant hTERT expression on telomerase activity was next addressed in hTERT-immortalised sheep fibroblasts using the Telomere Repeat Amplification Protocol (TRAP) assay (section 2.215). Variable levels of the catalytically dysfunctional hTERT transgene expression were evident in the pWGB25 stably transfected clones of the hTERT-immortalized foetal sheep fibroblast line, GRN1-1. Due to only three base pairs differing between wild-and mutant- hTERT, we were unable to differentiate between their expression levels with current available techniques. Thus, expression of total hTERT mRNA was analysed by semi-quantitative Reverse Transcriptase-PCR (section 2.2.8 and 2.2.9). As all lines were derived from a clonal cell line GRN1-1 and have similar levels of wild-type hTERT, the excess of TERT above that of the controls was mainly attributed to mutant hTERT levels.

The results showed that five clones (GRN25-1, GRN25-5, GRN25-6, GRN25-7 and

GRN25-9) expressed high levels of mutant hTERT expression (Fig.3.3, lanes 1-5)

relative to the wild-type hTERT expression level of mock vector controls, GRN23-C1

and GRN23-C4 (Fig.3.3 lanes 7-8). In the GRN25-10 line, steady-state mRNA level of

hTERT was too low to be detected under these conditions.
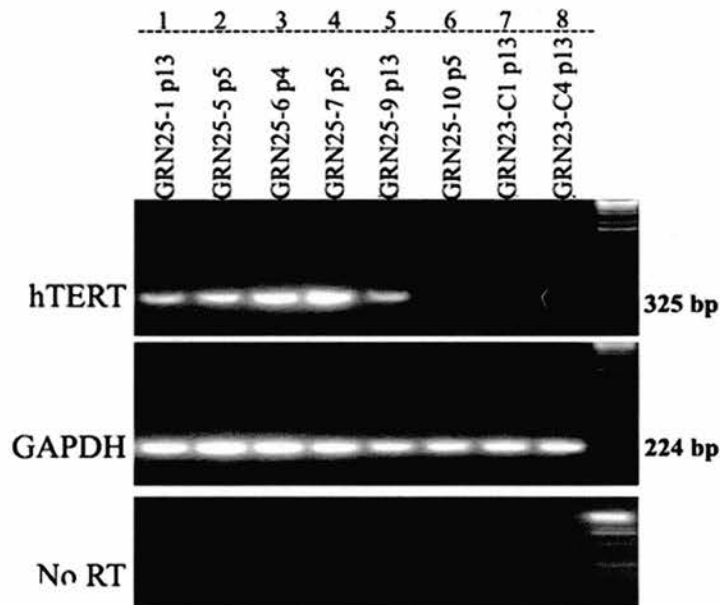
Figure 3.3: **Analysis of mutant hTERT mRNA expression levels.** (B) Expression of mutant hTERT in hTERT-immortalized (GRN) sheep fibroblasts. Five mutant hTERT-transfected clones show high levels of mutant hTERT mRNA with GRN25-6 and GRN25-7 exhibiting the highest levels. All PCR reactions were conducted at 30 cycles and GAPDH serves as the loading control. No DNA contamination was detected in RNA samples lacking reverse transcriptase. Passage number post-transfection is indicated.

Relative stoichiometry of mutant to wild-type hTERT was inferred by calculating band

intensity using Multi-Analyst software with a relative value of 1 assigned to the

normalized mean intensity of the mock controls. On this basis, we grouped the GRN

clones into two classes according to the level of total TERT expression: medium (7.7, 9.0 and 9.4 fold excess in lines GRN25-1, GRN25-5 and GRN25-9 respectively) and high (12.6 and 14.1 fold excess in lines GRN25-6 and GRN25-7 respectively). Relative expression of the GRN25-10 was below the mock control level (0.6).

In summary, by transfecting a 7.3kb mutant hTERT construct, we generated GRN(25) lines that over-express hTERT relative to immortalized BW6F2 sheep fibroblasts. Crucially these lines over-express intact non-catalytic domains but express a catalytic domain mutated at three distinct reverse transcriptase motifs. These lines provide an opportunity to investigate a putative role for hTERT non-catalytic domains with respect to telomere maintenance, distinguishable from enzymatic activity.

3.2.4   Protein expression analysis

Western Blot analysis was conducted as described in section 2.2.13. Protein expression levels revealed a more complex pattern. GRN23-C1 exhibits wild-type hTERT expression alone, whereas GRN25 lines show total hTERT expression (wild-type and mutant). GRN25-1, GRN25-6 and GRN25-9 have the highest levels of total hTERT expression (3.3-fold higher than mock control). GRN25-5 and GRN25-7 had lower levels of total hTERT expression (2.6-fold and 2.0-fold higher then control) (Fig 3.4). Clones GRN25-1 and GRN25-9 show higher protein levels relative to the other clones than would be predicted by RNA expression analysis. Conversely GRN25-7 has much lower levels of protein than expected.
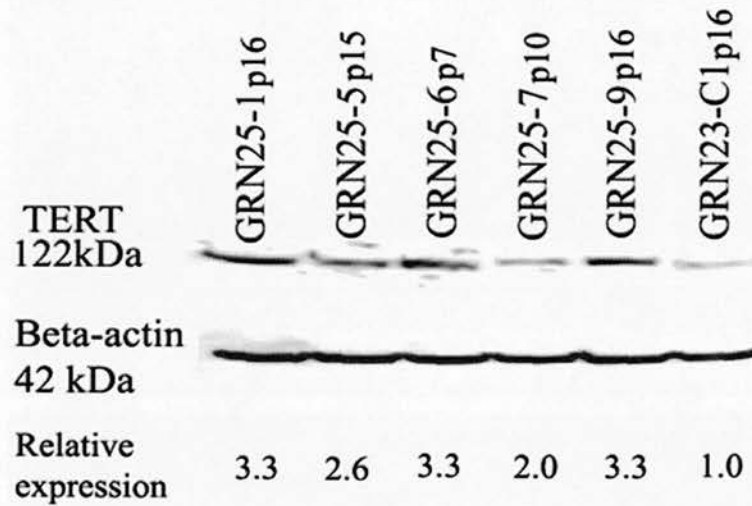
Figure 3.4: Protein expression analysis in GRN clones. Western blot showing hTERT protein expression. Protein (40µg) was separated on 7.5% SDS-PAGE and blotted onto nitrocellulose membrane. The blot was incubated with anti-hTERT antibody Y182 (Abcam) followed by incubation with HRP-conjugated secondary antibody. The signals were visualized using an ECL detection kit. The hTERT protein is shown as 122kDa. Relative expression to GRN23-C1 mock control is shown in panel below. Beta-actin is shown as an internal control to verify equal amounts of protein loaded.

Superficially, this may appear to reflect differences in translation efficiency, but the effect of mutant hTERT is likely to be a factor. If mutant hTERT compromises cellular proliferation and senescence bypass status, then the existence of a heterogeneous population rather than the presumed clonogenic population may result in subsets of cells with low or no levels of mutant hTERT, having a growth advantage. This scenario will be discussed in section 3.2.3 and Chapter 4.

3.2.5 Telomere Repeat Amplification Protocol (TRAP) analysis on hTERT-immortalized lines

Telomere Repeat Amplification Protocol (TRAP) assay was next carried out on the mutant hTERT stable-transfected GRN clonogenic lines. The analysis showed that the four lines (GRN25-1, GRN25-5, GRN25-9 and GRN25-10) which exhibited low to medium levels of mutant hTERT expression, showed comparable telomerase activity to the GRN23-C1 mock vector control (Fig. 3.5, lanes 1-2 and 5-6). By contrast, in the lines exhibiting higher levels of mutant hTERT, (GRN25-6 and GRN25-7), telomerase activity was almost undetectable (Fig.3.5, lanes 3-4).These results indicate that the catalytically dysfunctional mutant hTERT may function to inhibit telomerase activity. This abrogation of telomerase catalytic activity appears a direct function of mutant hTERT expression levels, with only the two lines with highest levels of the mutant transgene expression, showing compromised telomerase activity.

A

Cell Line	GRN (25).1	GRN (25).5	GRN (25).6	GRN (25).7	GRN (25).9	GRN (25).10	GRN (23).C1
Heat	- +	- +	- +	- +	- +	- +	- +
Protein (ug)	0.1	0.1	0.1	0.1	0.1	0.1	0.1

147
110
57

IC   37
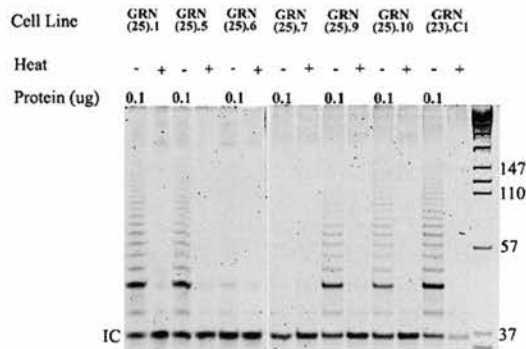
B
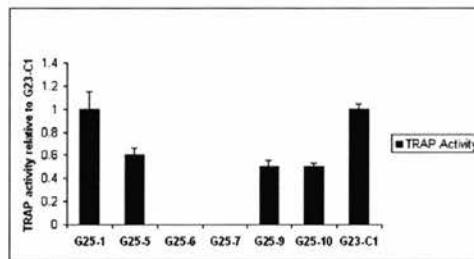
Figure 3.5: Telomerase activity in hTERT-immortalized sheep fibroblasts. (A) Reconstituted telomerase activity in hTERT-immortalized GRN25 clones. Telomerase activity was measured by TRAP assay with 0.1µg of total protein of each cell extract. Telomerase activity in four lines (GRN25-1, GRN25-5, GRN25-9 and GRN25-10) is comparable to that of the mock control (GRN23-C1). Telomerase activity is inhibited in the GRN25-6 and GRN25-7 lines, which have the highest levels of mutant hTERT expression relative to the other clones. Heat inactivated and internal standard controls are indicated. (B) TRAP activity relative to the G23-C1 mock vector control. Densitometric analysis was used to compare relative levels of TRAP activity based on the intensity and length of the TRAP product, normalized to the internal control. TRAP activity is completely inhibited in the GRN25-6 and GRN25-7 clones, whereas relative activity is 50 – 100% in all other clones. (NB: TRAP was conducted at the same passage number as for RT-PCR analysis; Fig.3.3).

Low levels of telomerase activity was however detected in the GRN25-6 and GRN25-7 lines when total protein extract was increased 5-fold from 0.1μg to 0.5μg (Fig. 3.6). Nevertheless, telomerase inhibition through dominant-negative and/or competitive inhibition effects, are still noticeable; the 36-bp internal standard is present in these samples whereas they are absent in all other GRN clones, including the GRN23 mock controls, except GRN25-1. This indicates sufficiently high levels of telomerase activity in the majority of GRN clones, to out-compete the shared forward primer used in TRAP to amplify both the TRAP product and the internal standard. Of note is the telomerase inhibition evident in GRN25-1, not detected in the previous TRAP (Fig. 3.5). The discrepancy may be accounted for by this initial TRAP assay being conducted ~6PDs prior to TRAP assay conducted using 0.1μg. This hints at high levels of mutant hTERT post-transfection in the GRN25-1 line, resulting in early telomerase inhibition, followed by restoration of telomerase activity to levels comparable to mock controls in a short period of serial culturing.
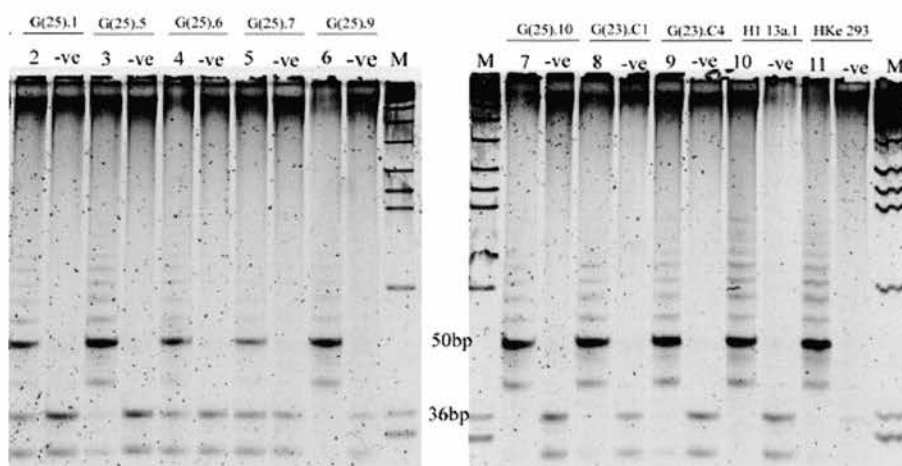
Figure 3.6: TRAP analysis on hTERT-immortalized clones using a 5-fold increase (0.5µg) of protein lysate. Trace telomerase activity is evident in GRN25-1, GRN25-6 and GRN25-7, whereas very high levels of activity are present in all other GRN clones. This is inferred by the TRAP product and also the presence/absence of the 36-bp internal standard. The H1 human ES line and HEK293 tumour line are included as positive controls for the assay. Heat inactivated controls are indicated.

This indicates the complexity of telomere and telomerase dynamics per population doubling and highlights a caveat of studying this dynamic interplay via molecular snapshots of time.

3.2.6   Analysis of extensive culture period

3.2.6.1   Calculation of proliferation rate

Since the TRAP assay results showed that telomerase activity in the mutant clones was inhibited, the effects of mutant hTERT on cell growth and proliferation was next examined by recording their growth curves. The BW6F2(25)-7 and BW6F2(25-8 sheep

fibroblast clones, transfected with mutant hTERT alone did not proliferate vigorously and senesced after several passages at around day 50-60 of the culture regime (Fig. 3.7a).

All GRN clones, except GRN25-7, grew uncompromised with a steady rate of proliferation during the 160 days of the growth curve recording period, with about one population doubling every 19 hours. There is no significant difference to the overall proliferation profile between these clones and control GRN23 clones which only expressed wild-type hTERT (Fig. 3.7a). The reconstituted telomerase activities were sufficient to bypass senescence in all clones in spite of the GRN25-6 and GRN25-7 clones exhibiting telomerase inhibition. This indicates that trace telomerase expression may be sufficient to maintain a senescence bypass status, presumably due to telomerase maintaining telomere length in the subset of shortest telomeres, thus avoiding activation of a p53-mediated growth arrest.

3.2.6.2   *Senescence-associated β-galactosidase staining*

In the GRN25-7 clone however, a period of slower proliferation was evident at around 3 weeks of continuous culture, in which population doubling rate slowed to over 40 hours (Fig. 3.7b).Concurrent with this, a subset of cells within the population adopted a morphology of bigger and flat appearance with clearly visible microtubules, a characteristic of the senescent phenotype. This subset of cells represented around 30% of the total population. To further confirm that these cells were senescent, the senescence-associated β-galactosidase (SA-β-gal) staining assay was applied to the GRN25-7 cells

and the results indicated positive staining as expected (Fig. 3.7c). Approximately 50% of cells within the population showing a senescent-like phenotype, stained positive for SA-β-gal, i.e. half the population. This may reflect the fact that only senescent cells stain positive, whereas pre-senescent cells, although displaying a similar phenotype, did not express the particular stress marker(s) to result in a positive histochemical stain. This raises the question of whether β-galactosidase is a truly accurate marker for cellular replicative senescence?
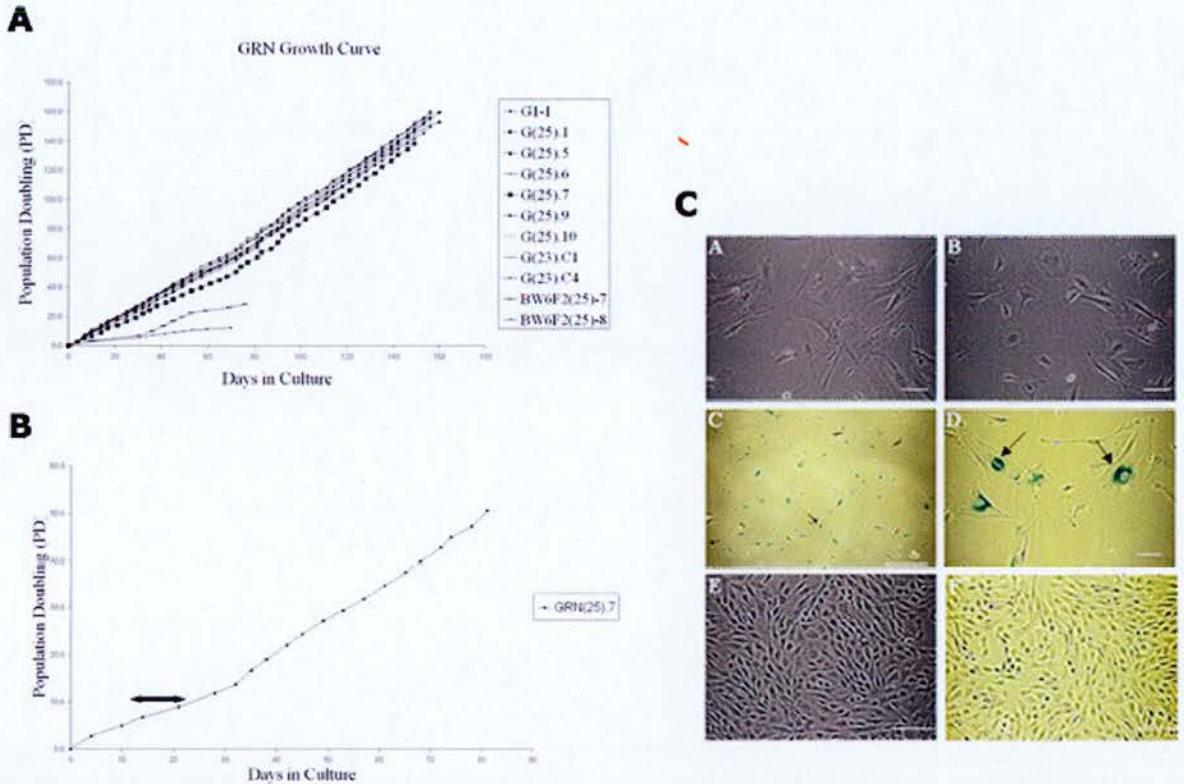
Figure 3.7: Effects of mutant hTERT expression on cellular proliferation and senescence. (A) General proliferation profile of GRN clones. GRN25 and GRN23 clones maintained a steady population doubling rate throughout the 160-day culture period and accumulated 138-160 population doublings. The overall profile of the growth curves does not differ significantly. All clones underwent 150-160 population doublings except GRN25-7, for which the total population doubling was 138. The BW6F2(25)-7 and BW6F2(25)-8 control clones express mutant hTERT alone and accumulated 28 and 12 population doublings respectively. Both lines ceased proliferating by ~50-60 days post-commencement of the growth curve. (B) GRN25-7 lag phase. Proliferation rate of GRN25-7 slowed dramatically during a 14-day period during which the cell population doubled only five times. Arrows denote lag phase. (C) SA-β-Gal staining in the GRN25-7 clone. Senescent morphology was evident during early stages (7 population doublings) of extended culture (*A-B*). Incubation with fresh senescence-associated β-Gal (SA-β-Gal) resulted in positive histochemical staining at pH 6.0 (*C-D*) Photos were taken 16 hours post-incubation. Arrows indicate senescent cells. As a negative control GRN25-5 from a late stage of culture (140 population doublings) was also incubated with SA-β-Gal, (*E-F*). Magnifications: A, B and D, x10; C, E and F x4. Scale bar for A, B and D denotes 100 μM and 500μM for C, E and F. (Growth profiles of the BW6F2(25) clones were generated by Ling Mo).

3.2.7 Telomere Restriction Fragment (TRF) length analysis

The most obvious function of active telomerase is to add telomeric repeats to telomere ends to prevent telomere attrition each time a cell divides. However, it is unclear if it is exclusively the catalytic domain of hTERT that is rate-limiting in this aspect or whether non-catalytic motifs may play functional roles, be it directly or indirectly, in repeat addition processivity. Previous studies have indicated that forced expression of hTERT, although extending proliferative lifespan, did not maintain telomere length (Zhu J. et al., 1999, Ouelette et al., 2000). In particular, a prior study in sheep primary fibroblasts showed that stabilization of telomere length and karyotypic stability are directly correlated with the level of hTERT gene expression, even though telomerase activity was comparable within these lines (Cui et al., 2002). This led to the hypothesis that hTERT non-catalytic motifs may play a role in telomere maintenance that may be distinguished from enzymatic activity.

To assess the effect of over-expressing non-catalytic hTERT domains on telomere maintenance, we cultured mutant TERT-transfected immortalized GRN clones for an extensive period of ~160 days. Telomere length was measured by Southern Blot (section 2.2.16) with a $(TTAGGG)_3$ probe, and the mean TRF was calculated at multiple time points (0, 70 & 130 days) during long term culture for each cell line. The results showed that after ~70 days in culture, telomere lengths shortened in all cell lines (Fig.3.8A and Table 3.1). However, GRN25-1 and GRN25-7 exhibited significantly shorter mean telomere length (6.7 kb and 7.7 kb, respectively) in comparison with GRN23 control

cells (9.2kb and 10.1kb, p=0.02). The remaining GRN25 clones (GRN25-5, 9.5kb; GRN25-6, 10.6kb; GRN25-9, 9.1kb and GRN25-10, 9.2kb) showed similar telomere shortening as the GRN23 controls (p = 0.95). This pattern of telomere shortening persisted throughout the culture period and mean TRF lengths in all GRN clones were stabilized after approximately 100 population doublings post-transfection. Stabilized mean TRF length in clones GRN25-5, GRN25-6 and GRN25-9 were within the range of 6.6-7.1kb, and did not differ significantly to the 7.0 and 7.2kb of GRN23 mock controls (p = 0.29), whereas the mean TRF lengths in GRN25-1 and GRN25-7 were eventually stable at 5.2 kb and 6.3kb, significantly shorter than that in the mock controls (p = 0.0002) (Fig. 3.8B and Table 3.1).
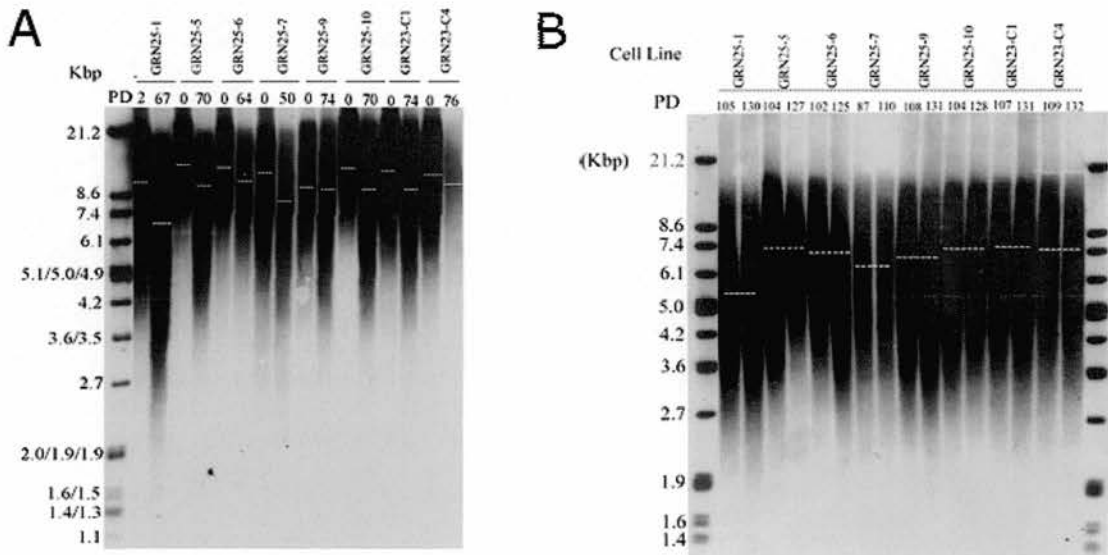
Figure 3.8: Telomere restriction fragment length in mutant hTERT-expressing clones after period of extensive culture. Telomere length was measured using Telomere Restriction Fragment (TRF) Southern Blot analysis with a $TTAGGG_3$ probe. Samples were analysed at intervals throughout a 160-day culture period. (A) TRF analysis from early and middle passage. No significant enhanced telomere maintenance is evident at this stage with GRN25-5 (9.5Kb), GRN25-6 (10.6kb), GRN25-9 (9.1kb) and GRN25-10 (9.2kb) showing comparable mean TRF length to GRN23-C1 (9.2kb) and GRN23-C4 (10.1kb) mock vector controls. Aggravated telomere attrition is evident in the GRN25-1 (6.7kb) and GRN25-7 (7.7Kb) clones. (B) TRF analysis from late passage. Mean TRF length in all GRN clones are maintained at a stabilized length after approximately 100 population doublings. GRN25-1 and GRN25-7 show significantly shorter stabilized mean telomere lengths (5.2 kb and 6.3kb respectively) compared to the GRN23-C1 (7.0kb) and GRN23-C4 (7.2kb) mock transfected controls, whereas GRN25-5 (7.1kb), GRN25-6 (6.9kb), GRN25-9 (6.6kb) and GRN25-10 (7.1kb) show comparable mean stabilized lengths. Calculated mean telomere lengths are depicted by white lines and are stated in Table 1. PD, Population Doublings.

GRN Cell Line	Population Doubling (PD)	Days in Culture	Mean TRF (Kbp)
G25-1	2	4	11.0
	67	79	6.7
	130	133	5.2 a
G25-5	0	0	14.0
	70	81	9.5
	127	135	7.1 a
G25-6	0	0	13.5
	64	79	10.6
	125	134	6.9 a
G25-7	0	0	11.6
	50	81	7.7
	110	135	6.3 a
G25-9	0	0	9.2
	74	81	9.1
	131	133	6.6 a
G25-10	0	0	13.7
	70	81	9.2
	128	134	7.1 a
G23-C1	0	0	12.2
	74	81	9.2
	131	134	7.2 a
G23-C4	0	0	11.0
	76	81	10.1
	132	133	7.0 a

Table 3.1: Summary of mean TRF length in hTERT-immortalized sheep fibroblasts. [a] Represents mean TRF length at which telomeres stabilize.

From the analysis of telomere length after long term culture of hTERT-immortalized clones with varying levels of catalytically dysfunctional mutant hTERT expression, no enhanced telomere maintenance function is evident. For the majority of lines, there is no significant difference in mean telomere restriction fragment length after culture, when compared to mock controls. Thus we do not find evidence to support the notion that hTERT non-catalytic motifs have a role in telomere maintenance that can be readily distinguishable from hTERT enzymatic activity.

These results indicate that high levels of mutant hTERT expression might accelerate the telomere shortening in GRN25-1 and GRN25-7 cells probably as a consequence of inhibited telomerase activity. Aggravated telomere attrition in GRN25-1 reveals a more complex pattern whereby telomerase inhibition was evident at PD 0 but relieved at PD 6. The possibility of transgene silencing and selection upon a heterogeneous population will be discussed in Chapter 4. Furthermore, the other high expressing mutant hTERT clone GRN25-6, did not appear to have accelerated telomere shortening in spite of the clear inhibition of telomerase activity. These results indicate that telomere length regulation is more complicated and consideration has to be given to the multiple extrinsic and intrinsic factors involved.

3.2.8   Competitive inhibition TRAP

To address the molar stochiometry of mutant hTERT and wild-type hTERT in this context, a TRAP assay was designed (section 2.2.15) to analyze the particular threshold upon which the mutant hTERT exerts an inhibition effect on the hTERT-immortalized line chosen for study here. This assay was referred to as a 'competitive inhibition TRAP' although the term will be used to include inhibition and/or dominant-negative effects. As the GRN25 clones express both wild-type and mutant hTERT, the GRN23-C1 line was chosen to monitor hTERT inhibition as this line exhibits wild-type hTERT expression alone. The BW6F2(25)-8 line was used as the source of high level mutant hTERT, as this line does not express wild-type hTERT which would confound results. A presumption in this approach states that the expression level of mutant hTERT in the

BW6F2(25)-8 line is similar to that of the GRN25-6 and GRN25-7 line in which the dominant-negative/competitive inhibition effect was evident. Although this may not be the case, the rationale for the competitive inhibition TRAP was to obtain an approximate threshold at which mutant hTERT excess conferred an inhibitory effect on wild-type hTERT expression levels and hence on wild-type hTERT function.

Initially, the assay was conducted using a maximum 5-fold excess of mutant hTERT to wild-type hTERT protein lysate, thereby constituting the upper limit of recommended total protein lysate amount for the TRAP assay (0.5μg). As no inhibition was evident within this molar ratio imbalance (Fig 3.9a), mutant hTERT to wild-type molar ratio was increased up to 200-fold. Although complete inhibition was evident when mutant hTERT was in excess by between 150-200-fold (Fig. 3.9b), the internal control standard was not amplified in the PCR reaction indicating saturating levels of mutant hTERT levels in the total lysate. Although mutant hTERT levels at such an excess would be expected to promote an inhibitory effect, the competitive inhibition TRAP does not give an accurate level of the mutant hTERT:wild-type hTERT relative stoichiometry due to the absence of the internal control.
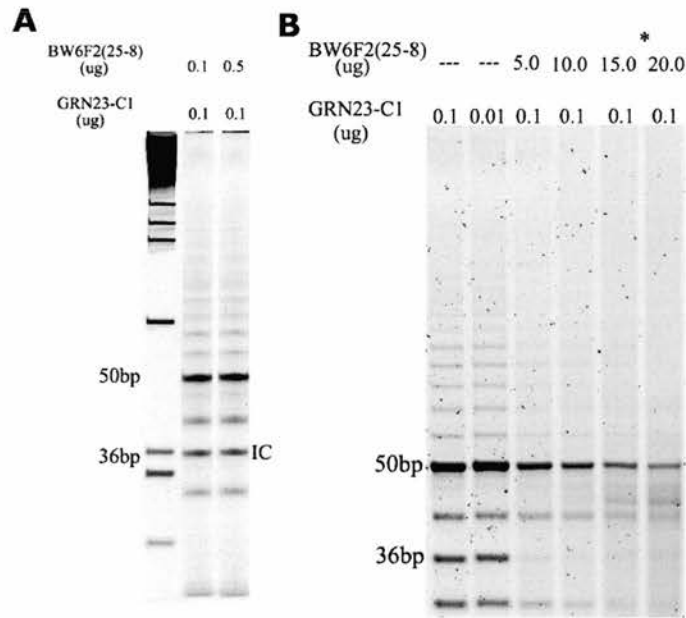
Figure 3.9: Competitive inhibition TRAP assay. A 5-fold Excess of mutant hTERT does not result in inhibition of wild-type hTERT telomerase activity (A). A molar ratio of between 150-200-fold excess results in complete inhibition of telomerase activity (B), but with the failure of the 36-bp internal standard to be amplified.

3.2.9   Transfection of mutant hTERT into HEK 293 cells

Due to the observed effect of a catalytically dysfunctional mutant hTERT exerting a dominant-negative/competitive inhibition effect on wild-type hTERT, thus compromising telomerase activity and function, the natural progression was to try and abrogate telomerase activity in a tumour setting. The HEK 293 tumour line was chosen for this study as this line exhibits high levels of telomerase activity (Fig. 3.6). The working hypothesis states that introduction of the mutant hTERT transgene will inhibit endogenous hTERT protein monomers from acting at the telomere substrate through a

dominant-negative/competitive inhibition mechanism. If endogenous telomerase activity is inhibited, HEK 293 cells may be forced into replicative senescence or to an apoptotic fate, plausibly due to lack of telomere maintenance in the subset of the shortest telomeres in the population. This would support the many documented strategies to inhibit telomerase in a tumour setting using a dominant-negative approach.

3.2.9.1   *Selection of 293 transfected cells*

HEK 293 cells were transfected with the pWGB25 vector containing mutant hTERT cDNA and the PWGB23 EGFP-containing mock vector and selected for as described in section 2.9.2. Upon 7 days of selection, populations were pooled and expanded as one mixed population. Transfection efficiency was judged by monitoring EGFP expression in the mock controls. (NB: This is an approximation of transfection efficiency regarding the mutant hTERT construct as the vector size is much larger compared to the mock EGFP construct). At this stage, heterogeneous EGFP expression was evident in the mock controls with EGFP expression absent in many cells. Approximately 40% of cells were EGFP positive. A similar number of cell death/survival was evident in the mutant hTERT-transfected cells. At 14 days post-transfection the pooled populations were placed under a more stringent selection regime (section 2.9.2) and expanded for four weeks with RNA expression analyzed throughout this period (see section 3.2.7.2). During this stage, EGFP positive cells represented ~75% of the total population in the mock-transfected line and analysis at this stage clearly showed that even in the 75% GFP positive cells the levels of GFP expression were variable (Fig. 3.9 A-C). Cell

survival rate under this selection regime was comparable for the mutant hTERT-transfected lines (Fig. 3.10 D-E).
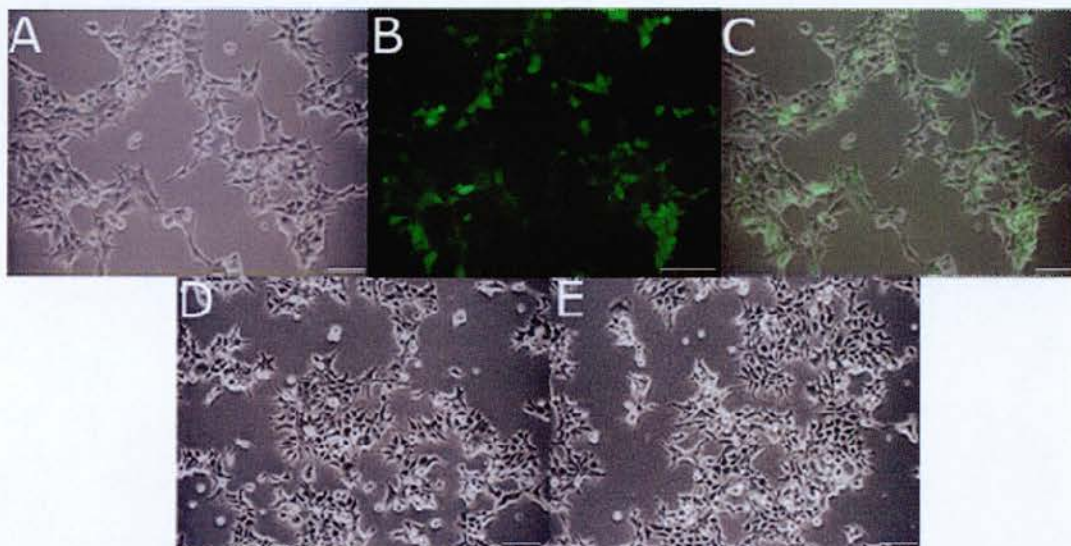
Figure 3.10: HEK 293 cells transfected with mutant hTERT or EGFP mock control. Images were taken 21 days post-transfection and represent pooled populations under a stringent selection regime. (A-C) HEK 293 cells transfected with EGFP: A, phase-light; B, EGFP; C, merged. (D-E) HEK 293 cells transfected with mutant hTERT. Scale bar represents 100μM.

3.2.9.2   RNA expression and telomerase activity analysis of transfected HEK 293 cells

RT-PCR analysis was conducted as described in section 2.2.9. Primers to detect the mutant hTERT transgene were designed whereby a portion of the SV40 polyadenylation signal was amplified in addition to a portion of the mutant hTERT transgene. As the SV40 polyadenylation signal is not present endogenously, this strategy allowed the mutant hTERT transgene to be distinguished from the endogenous hTERT in 293-

transfected cells. RNA was collected at the beginning of the stringent selection regime and each week for a period of four weeks thereafter. The primers chosen to conduct analysis on endogenous hTERT were located in the hTERT 3'UTR region, therefore allowing the endogenous hTERT to be distinguished form the transgenic hTERT. A clear reduction in the endogenous hTERT expression levels in HEK 293 cells transfected with the mutant hTERT construct, is evident after 7 days and persists through to the 14-day stage (Fig. 3.11a). This is concurrent with high levels of mutant hTERT transgene levels evident at the 7 day-stage (Fig. 3.11c). However by day 28, endogenous hTERT levels are restored to that of the untransfected HEK 293 cells (Fig. 3.11a), consistent with a reduction in mutant hTERT levels by this stage (Fig. 3.11c)
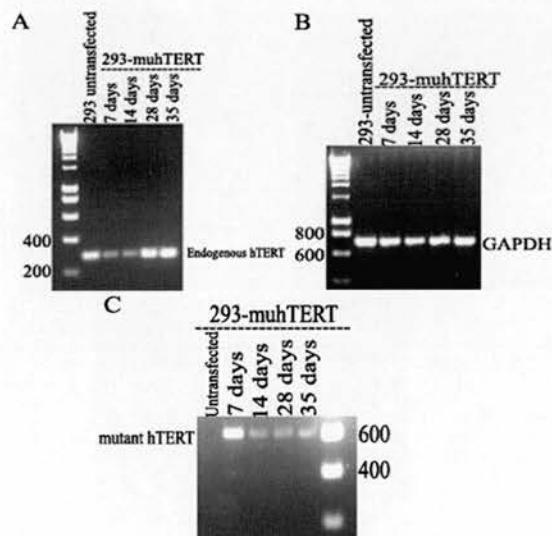
Figure 3.11: Endogenous and mutant hTERT RNA expression levels in HEK 293 cells transfected with a mutant hTERT transgene. (A) Endogenous hTERT gene expression. mRNA expression is considerably reduced by day 7 of a stringent selection regime, with levels being restored to that comparable to the untransfected control by day 28. (B) GAPDH RNA expression levels. GAPDH levels at the same stage showing equal loading for RT-PCR analysis. (C) mutant hTERT RNA expression levels. Consistent with the endogenous hTERT RNA expression profile, mutant hTERT RNA expression levels are high after day 7, followed by a considerable reduction by day 14 that persists throughout the remaining period monitored.

As endogenous hTERT levels were not completely abrogated, telomerase activity is not compromised in the mutant hTERT transfected lines. Telomerase activity is comparable to the untransfected HEK 293 cells at all stages analyzed (Fig. 3.12). This is consistent with the data presented in section 3.2.5.
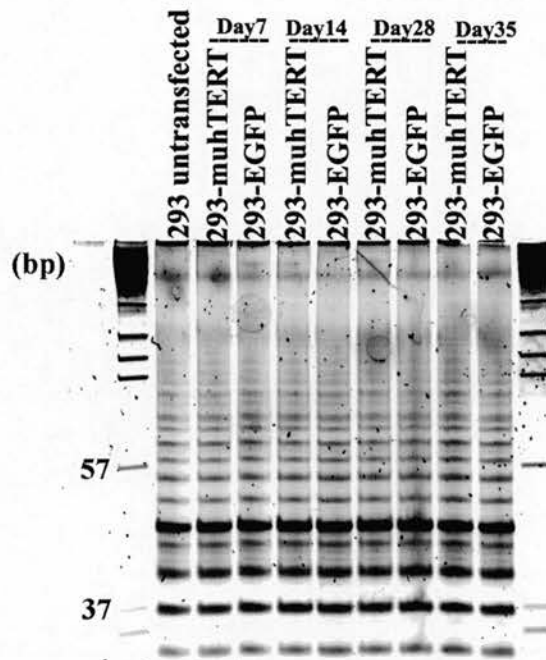
Figure 3.12: Telomerase activity in 293 cells transfected with mutant hTERT. Telomerase activity was measured at various stages during a 35 day period after expanding populations that survived the selection regimes. No difference between telomerase activity in the untransfected 293 cells and those transfected with mutant hTERT is evident. Mock transfected EGFP populations are shown. TRAP was conducted using 0.1µg.

These results reflect the heterogeneous nature of these transfected populations similar to the GFP tranfectants. Although endogenous hTERT levels are reduced after introduction of the mutant hTERT transgene, a subset cells within the population may have mutant

hTERT levels that are insufficient to confer a dominant-negative effect upon translation of the mutant protein. Therefore these cells may have a growth advantage over a subset of cells which suffer a dominant-negative effect, presuming that this effect results in cells proliferating more slowly relatively. This notion is supported by the observation that there was almost no cell death during this culture period under stringent selection, indicating that cells that exhibited high levels of mutant hTERT expression did not die but rather may have been selected against during serial passaging.

3.3   **Discussion**

The relationship between telomerase enzymatic activity and telomere maintenance has been poorly understood in the field of telomere biology. It has consistently been reported that telomerase activity per se does not lead to the maintenance of telomeres, both in normal and abnormal cellular contexts (Ouelette et al., 1999, Hastie et al., 1990, Counter et al., 1994). Our laboratory have previously used primary sheep (*Ovis aries*) fibroblasts to study hTERT function with respect to telomere maintenance, in order to provide an alternative mammalian model to the laboratory mouse. In this setting, stabilization of telomere length and karyotypic stability are directly correlated to the level of hTERT gene expression. However this was not reflected in telomerase activity as detected by the *in vitro*-based TRAP assay (Cui et al., 2002). This led to the speculation as to whether the hTERT reverse transcriptase catalytic domain was the key rate-determining subunit within the telomerase complex with respect to telomere maintenance, or whether non-catalytic hTERT domains play a role in telomere maintenance that can be distinguished from enzymatic activity. To address these questions, a strategy was devised to ectopically express a catalytically dysfunctional hTERT transcript in a primary sheep fibroblast line that exhibits low levels of hTERT expression, insufficient to prevent telomere erosion and the onset of karyotypic instability. This provides a system in which to descriptively study both the dimeric function of hTERT and the effects of hTERT non-catalytic domain over-expression.

RNA expression analysis showed that two clones exhibited high levels of mutant hTERT and three clones exhibited moderate levels. This was readily translated to the analysis of TRAP activity as lines with moderate levels of mutant hTERT showed comparable levels of telomerase activity to the mock control, whereas lines with high levels of mutant hTERT showed inhibition of telomerase activity likely due to possible dominant-negative and/or competitive inhibition effects between the wild-type and mutant hTERT protein. Thus mutant hTERT expression compromised wild-type telomerase activity in a manner directly attributable to mutant hTERT expression level. When TRAP assay was conducted using a 5-fold increase in protein lysate however, low levels of telomerase activity was evident in lines with high levels of mutant hTERT transcript, thus highlighting a critical caveat when considering dominant-negative strategies to target hTERT in tumours. It was striking to note that when TRAP analysis, conducted at stages that differed by ~6 PDs was compared, one line (GRN25-1) showed a dominant-negative affect at the earlier time-point but which was not evident 6PDs later. This indicates that wild-type telomerase activity was inhibited in a subset of cells within this population but due to a heterogeneous population, this subset was rapidly selected against, whereby a subset(s) with levels of mutant hTERT insufficient to confer inhibitory effects were selected for. This observation is consistent with the idea that high levels of mutant hTERT may have adverse effects on cellular proliferation and may indeed inhibit cell growth.

An extensive culture period of 160 days allowed the effects of mutant hTERT expression to be studied in a cellular context. No significant change in the general

proliferation profile was evident between mutant hTERT-transfected and mock-transfected clones. Proliferation rate throughout culture was similar for all clones and calculated to be on average one population doubling per 19 hours, except GRN25-7 which exhibited a period of slower proliferation between days 14-28 of the culture period. Population doubling rate during this period slowed dramatically in this clone, to one population doubling per 3-4 days. This was concurrent with a senescent morphology within a subset of cells (30%) within the population. Approximately half of this population stained positively for the senescence-associated histochemical marker β-galactosidase. This data indicates that sufficiently high expression of catalytically dysfunctional hTERT inhibits proper telomerase function, presumably due to restriction of functional homodimers at the telomere substrate. However, this was only reflected in a subset of cells within the GRN25-7 population, with the bulk of the population exhibiting a selective advantage thereafter, resulting in a comparable proliferation rate to all other clones. Only in this context is it possible to attempt to reconcile protein expression data. Protein levels of mutant hTERT within the GRN25-7 line were much lower than expected from the RNA expression analysis and TRAP activity. However as protein analysis was conducted ~9 PDs later than RNA and TRAP analysis, the lower levels of mutant hTERT protein may reflect selection within this 'mixed' population, with a subset of cells exhibiting high levels of mutant hTERT initially, being selected against.

It has been reported that stochastic variation of this nature may account for heterogeneous populations *in vitro* that are inaccurately termed 'clonal' (Martin-ruiz et al., 2004). In this context, a subpopulation of cells with compromised telomerase function would be selected against during long-term culture. It has been documented that TERT may regulate cellular survival and proliferation independent of enzymatic activity in tumour cells (Cao Y. et al., 2002). This data however, indicates that in primary fibroblasts, pro-survival functions of hTERT are a direct function of catalytic activity. Consistent with this, the parental sheep fibroblast line used for this study, transfected with catalytically dysfunctional hTERT alone, ceased to proliferate and entered replicative senescence after ~50 days culture.

Mean TRF length calculation at mid point and late stage of the extended culture period revealed comparable mean telomere length during culture and also comparable stabilized mean telomere length between the majority of clones and mock controls. Maintenance at a stabilized mean telomere length and the persistent check on entry to replicative senescence, is therefore most likely due to wild type expression level in these clones, as in mock controls. Significant telomere attrition however, was evident in two of three clones with high levels of mutant hTERT expression (GRN25-1 & GRN25-7). Telomeres in these clones eventually reached mean stabilized lengths much shorter than those in mock controls. These results seem to be directly attributable to mutant hTERT expression. Mutant hTERT/mutant hTERT and mutant hTERT/wild-type hTERT dimeric complexes are likely to be in much greater abundance than wild-type/wild-type dimers within these lines (Fig. 3.13). Inhibition of telomerase activity and increased

telomere attrition are therefore likely to be due to the compromising of wild-type homodimeric function at the telomere substrate due to the molar ratio imbalance of hTERT complexes. This is consistent with the notion that hTERT homodimers are necessary to form a functional telomerase complex at the telomere substrate, where catalytic domains of both hTERT molecules may function inter-dependently. On this basis, the GRN25-1 clone which showed telomerase inhibition at the beginning of the growth curve but restoration of telomerase levels after ~6 PDs, may have experienced aggravated telomere attrition at an early stage. However, there is no evidence for any lengthening of telomeres (with respect to average telomere length) after restoration of telomerase activity. Surprisingly one clone with high mutant hTERT expression level and subsequent abrogation of telomerase activity, showed comparable stabilized mean telomere length to mock controls. This highlights the limitation of *in vitro* based telomerase activity assays to assess proper telomerase function; as telomere length is not controlled by telomerase (TERT and TR) alone but requires other telomerase associated proteins and telomere binding proteins, such as POT1, TRF1 and TRF2, differences in expression level of these factors may account for this discrepancy. For example, TRF1 is known to negatively regulate telomere length (Ohki et al., 2004) and therefore differences in expression level of TRF1 may be one factor that accounts for this discrepancy. Generally the heterogeneous nature of the lines used in this study may exhibit varied expression levels of telomere-associated proteins that contribute to telomere homeostasis.

Wt hTERT/Wt hTERT **Mt hTERT/Mt hTERT** **Wt hTERT/Mt hTERT**

Functional complex **Non-functional complex** **Non-functional complex**
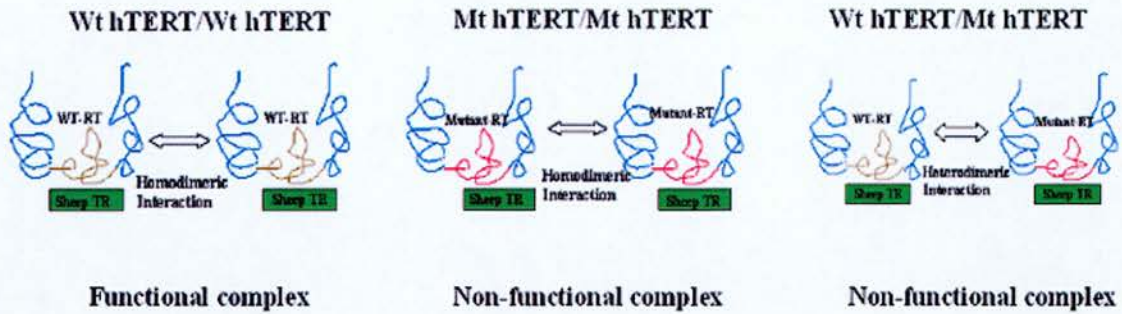
Figure 3.13: Functional dimerization model of hTERT. hTERT-mediated interactions in the GRN sheep fibroblast clones favour the homodimeric model of hTERT first postulated by Prescott, J. and Blackburn, E. in 1997. On this premise, only wild-type hTERT homodimeric interactions can contribute to a functional telomerase complex (left). Catalytically defective mutant hTERT homodimers (middle) and wild-type/mutant hTERT heterodimers (right) result in a non-functional telomerase complex with respect to telomere repeat addition processivity, suggesting that the hTERT catalytic domain is the rate-limiting factor. Blue, hTERT non-catalytic domains; Brown, wild-type reverse transcriptase domain; Red, mutant reverse transcriptase domain; Green box, sheep TR.

Collectively there is no evidence to indicate that non-catalytic hTERT domains contribute to telomere maintenance in a manner distinguishable from catalytic domain mediated telomerase activity. Rather, these data support the notion that telomere maintenance requires a functional telomerase complex with hTERT monomers likely interacting in an inter-dependent manner. Furthermore the result demonstrates that although hTERT non-catalytic domains may be necessary for telomerase assembly and processivity at the telomere substrate, they are not rate-determining. The catalytic domain of hTERT appears to be a crucial rate-determining factor regarding processivity (Rahman et al., 2006); however a more thorough understanding of telomerase- and telomere-associated factors will be required to understand fully the interplay that governs telomere homeostasis *in vitro* and *in vivo*. Consistent with the work from other

laboratories, these results also show a potential interest of using dominant-negative mediated anti-telomerase gene therapy to treat cancer but consideration has to be taken on how to ensure sufficiently high levels of mutant hTERT expression in a tumour line, that is also persistent throughout treatment. Data presented here show that even trace telomerase activity may be sufficient to maintain a check on replicative senescence and/or apoptotic pathways. Furthermore, the heterogeneous nature of populations *ex vivo* will have to be realized during conceptual models of anti-telomerase therapy.

CHAPTER 4

TRANSGENE SILENCING AND

FUNCTIONAL CONSEQUENCE OF LONG-

TERM CULTURE

4.1   <u>Introduction</u>

Data presented in Chapter 3 suggest that 'clonogenic' sheep fibroblast lines used for this analysis, are not exactly homogenous regarding transgene expression, as was initially regarded, particularly after long-term culture. These cells became heterogeneous in nature within the particular population. This is a theme that is recurrent within studies of clonally-derived cell lines as an *in vitro* tool. Many authors have stated reservations regarding *in vitro* artifacts that are hoped will reflect *in vivo* settings. The difficulties in recreating a proper biochemical and physiological niche *in vitro* is a severe obstacle at present and we cannot profess to be culturing cells in an accurate tissue and cellular microenvironment.

Transgenic technology *in vitro* presents an additional caveat whereby the monitoring of long-term consequences of transgene expression is vital, especially with respect to the potential of gene therapy. Can we presume that transgene expression levels are sustained throughout a long culture period incorporating over 100PDs? Can we presume that transgene expression is constant in every cell in the population? Therefore as the GRN sheep fibroblasts used for this analyses were cultured for ~160 days, the natural follow-up was to analyze the functional consequences of transgene expression during long-term culture. This not only provides an opportunity to gain further insight into this concept from a technical point of view but also presents additional information regarding alterations to total hTERT transgene expression and to telomerase activity, furthering understanding of the effects of mutant hTERT in hTERT-immortalized sheep fibroblasts.

A distinct limitation in studying the sheep as a mammalian model for telomerase and telomere biology and function is the absence of the gene sequences for sheep TERT as well as telomere binding proteins. Therefore it is difficult at present to provide direct evidence for possible activation or up-regulation of the endogenous sheep TERT transcript. Rather the convergence of various lines of data relating to the consequences of long-term culture may be used to provide indirect evidence of the functional presence or absence of sheep TERT. As the transgenic constructs used for this study were transfected into the GRN1-1 line, previously shown to express levels of hTERT insufficient to maintain full-length telomeres and prevent the onset of karyotypic instability (Cui et al., 2002), it is plausible to hypothesize that endogenous TERT may be switched on during long-term culture of the GRN25 fibroblasts. In this regard, sheep TERT activation may be concurrent with the functional immortalization of these lines and may facilitate the maintenance of a senescence-bypass status. This concept does not necessarily imply that these lines are transformed; it is accepted that telomerase itself does not cause growth deregulation, unlike classical oncogenes, therefore additional alterations in the genome are required to transform a cell that is telomerase positive (reviewed in Harley et al., 2002).

4.1.1 Hypothesis

1)   GRN sheep fibroblast lines consist of a heterogeneous population upon which selection pressures bias a particular subset(s) upon serial culture. Cells with compromised telomerase activity therefore would be selected against.

2)   Endogenous sheep TERT is activated as a consequence of long-term culture, reflected by an increase in telomerase activity.

4.1.2 Aims

1)   To gain a thorough understanding of the consequences of mutant and wild-type hTERT transgene expression levels during an extensive culture period; verify whether transgene expression persists, varies or is lost.

4.2   Results

4.2.1   RNA expression analysis after long-term culture

Semi-quantitative RT-PCR analysis was carried out on GRN clones at ~day100 to determine total hTERT transgene expression levels at this stage (section 2.2.8 and 2.2.9). The null hypothesis states that there is no difference in total hTERT transgene levels at this stage when compared to the initial stage of RNA analysis, prior to commencement of the extensive culture period. Surprisingly, RT-PCR analysis revealed almost complete absence of any hTERT transcript, indicating that the mutant hTERT transcript is completely silenced by this stage (Fig. 4.1). Trace hTERT message was detectable in three clones, including one of the mock controls. It is unclear whether this reflects the wild-type hTERT or mutant hTERT transgene (or both).
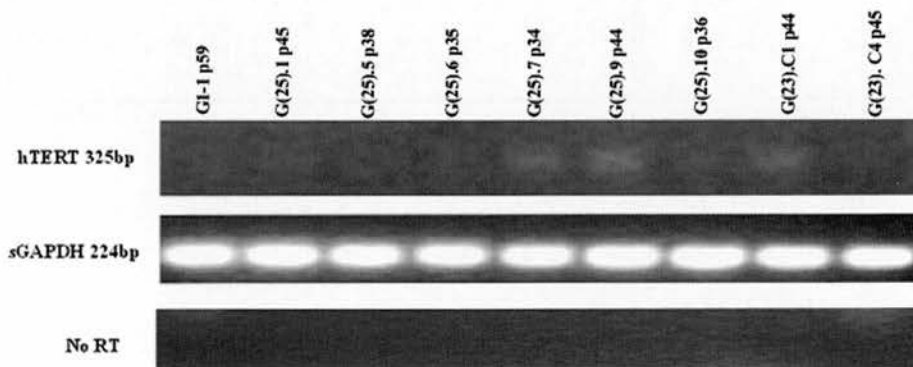
Figure 4.1: hTERT RNA expression analysis in hTERT-immortalized fibroblasts after ~ 100 days culture. RT-PCR analysis showing total hTERT expression levels in GRN hTERT-immortalized sheep fibroblasts. Total hTERT transcript is completely absent in the majority of lines, with trace expression evident in GRN25-7, GRN25-9 and the GRN23-C1 mock control. GRN1-1 represents the hTERT-immortalized parental line, into which either mutant hTERT or EGFP was transfected. GAPDH internal controls and no reverse transcriptase controls are shown. PCR was conducted at 30 cycles.

As this analysis was conducted at the ~100 day stage, in comparison to day 0 previously (Fig. 3.1), it is unclear as to how early or late the mutant hTERT transgene has been silenced. Therefore RNA collected from an earlier stage (~day 80) was retrospectively analyzed for hTERT RNA expression levels. At this stage, the GRN clones exhibited readily detectable levels of total hTERT message, but which was much lower than that evident at the initial stage of analysis (Fig. 4.2). Levels of total hTERT were comparable across all the GRN lines, although the GRN23-C4 mock control showed slightly higher expression.
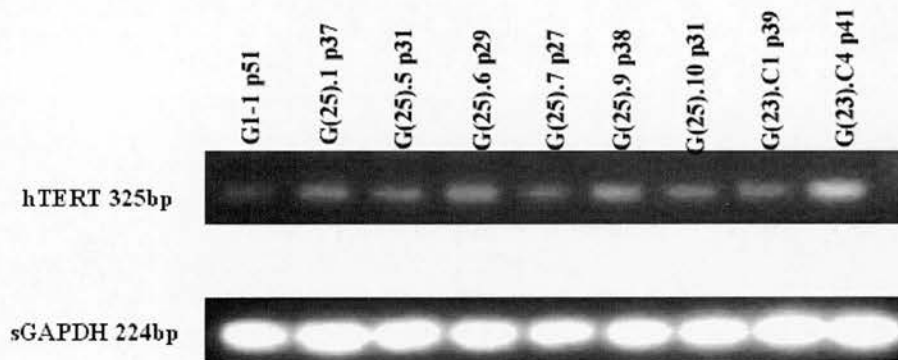
Figure 4.2: hTERT RNA expression analysis in hTERT-immortalized fibroblasts after ~ 80 days culture. RT-PCR analysis showing total hTERT expression levels in GRN hTERT-immortalized sheep fibroblasts. Total hTERT expression levels are comparable across all the GRN25 clones, but slightly higher in the GRN23-C4 mock control. GAPDH internal controls and no reverse transcriptase controls are shown. PCR was conducted at 30 cycles.

This observation suggests that the mutant hTERT transgene may be silenced by this stage in a proportion of cells within each population, but that mutant hTERT expression persists in another subset(s) of cells within the same population. Of note is the level of hTERT expression in the GRN23 mock controls relative to the GRN25 lines. GRN23-C1 shows comparable hTERT expression to the GRN25 lines, whereas GRN23-C4 shows a slightly higher level. This difference may be accounted for by

differences in cDNA loading as GAPDH levels appear higher in the mock controls. Therefore total hTERT levels may in fact be comparable across all lines. As the mock controls express wild-type hTERT alone, the comparable hTERT levels across the GRN25 lines, may thus reflect wild-type hTERT levels, suggesting that mutant hTERT may have been already lost by this stage of the culture period. To better illustrate hTERT transgene silencing, semi-quantitative analysis was conducted by calculating densitometry of normalized hTERT expression bands. Analysis from day 80 and day 100 of the culture period were compared to the initial expression levels at day 0 (section 3.2.1.2), prior to the start of long-term culture. Densitometric analysis illustrates complete hTERT silencing by day 100. At day 80 most lines show a clear reduction in hTERT expression most probably due to silencing in a subset of cells. Unexpectedly, wild-type hTERT expression in the mock controls appears to increase at the day 80 stage, prior to complete silencing by day 100 (Fig. 4.3).
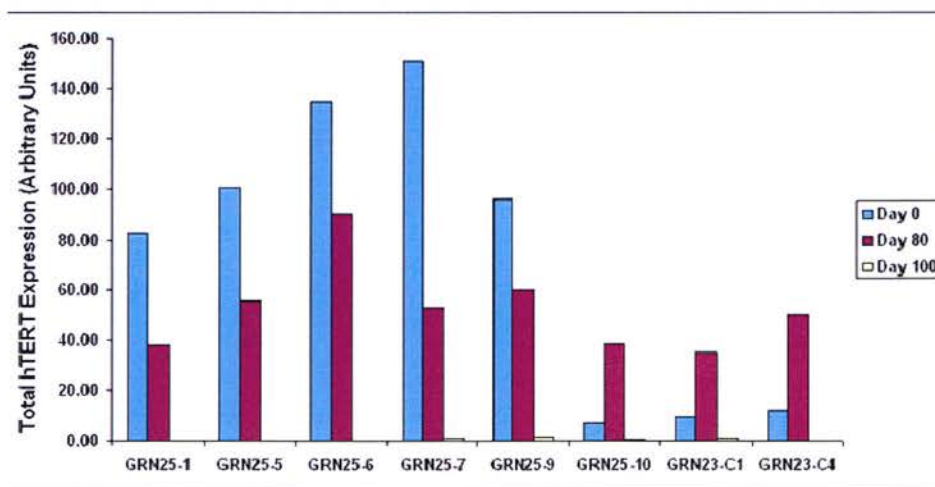
Figure 4.3: Semi-quantitative analysis of hTERT expression. At day 0, the vast majority of hTERT expression is due to mutant hTERT in the GRN25 clones. By day 80, mutant hTERT transgene silencing is evident in a proportion of cells in each line. By day 100 complete transgene silencing of mutant hTERT is evident in all GRN25 clones. Wild-type hTERT expression appears to increase by day 80 in the GRN23 mock controls prior to complete silencing in day 100.

4.2.2   Selection regime for mutant hTERT transcript

To infer whether the mutant hTERT transcript was completely absent, representative GRN clones at late passage were placed under a neomycin selection regime (as described in section 2.8.3), set at the initial concentration (400µg/ml) at which these clones were selected post-transfection. The presumption here states that the if the neomycin selection cassette is silent/absent, then due to the close proximity of the mutant hTERT transgene, it too will be silenced/absent. No cell death was evident until cells were passaged 48 hours after applying Geneticin selection. By ~day 6 of the selection regime, all lines exhibited widespread cell death with no cells surviving by ~day 14 in the GRN25-1 line and the GRN1-1 and GRN23-C1 controls (Fig. 4.4a). GRN1-1 serves as a negative control for the selection regime as this line has no neomycin transgene. A minority of cells survived selection in the GRN25-6 and GRN25-7 lines and this selected subset repopulated the population, with confluency reached by ~day 13 (Fig. 4.4b).

Figure 4.4: GRN culture under neomycin selection. Late passage hTERT-immortalized GRN clones were cultured under a 400µg/ml neomycin selection regime for ~2 weeks. No cells survived neomycin selection by day 14 in the GRN25-1 line and GRN1-1 and GRN23-C1 controls (Top panel). After an initial period of gross cell death in the GRN25-6 and GRN25-7 lines, a subset of cells were selected for and repopulated the population to confluence by ~day 13 (Bottom panel). Scale bar represents 500µM.

This observation suggests that the neomycin cassette has been silenced during long-term culture, with cells where this phenomenon has occurred being selected for. The obvious inference is that mutant hTERT and EGFP transgenes have therefore also been silenced in the GRN25-1 and GRN23-C1 clones respectively. This suggests that in GRN25-1 cells in which silencing of the neomycin (and hence mutant hTERT)

transgene has occurred, this has thus resulted in a growth advantage in that particular subset of cells. The resistance in a minority of cells within the GRN25-6 and GRN25-7 populations, indicate that a subset of cells expressed sufficient levels of neomycin to confer resistance and most probably low levels of mutant hTERT.

RT-PCR analysis was conducted on the neomycin-selected GRN25-6 and GRN25-7 lines and compared to an earlier stage where mutant hTERT silencing was evident, to determine if mutant hTERT had been selected for. RNA expression of hTERT shows a slight increase in mutant hTERT transcript in the neomycin-selected lines (Fig. 4.5). The neomycin cassette was only detected in the GRN25-6 line at this stage, indicating that only trace neomycin is sufficient to confer the resistance in GRN25-7 as no transcript was detected in the GRN25-7 line.
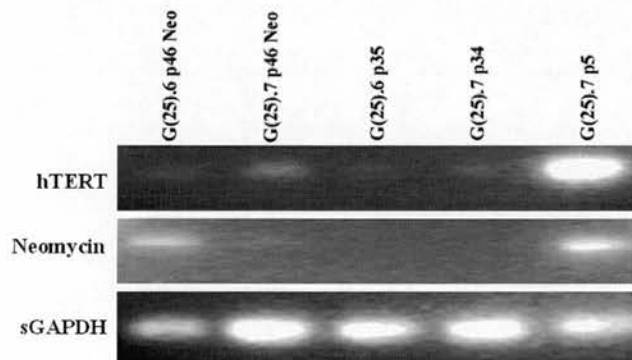
Figure 4.5: Total hTERT RNA expression analysis on neomycin-selected lines. Total hTERT levels are slightly higher in the neomycin-selected lines compared to an earlier passage where no transcript is evident. The GRN25-7 line at the beginning of the extensive culture period is shown as a positive control.

4.2.3 Monitoring of EGFP expression in mock-transfected clones

The GRN23 EGFP mock-transfected controls were monitored for EGFP expression under UV light. The GRN23-C1 control line, exhibited no EGFP expression after the extended culture period. This line was shown previously to exhibit EGFP expression prior to long-term culture (Fig. 4.6b). In contrast, the GRN23-C4 control line, exhibited a mosaic pattern of EGFP expression, ranging from high levels in some cells, to complete absence in others (Fig. 4.6a). However, silencing of the EGFP transgene in the GRN23-C1 line is not expected to have conferred a growth advantage upon those cells as such, as EGFP is expected to exert a negligible effect on cellular viability and proliferation. Rather it is likely that silencing has occurred in all cells within the population. The EGFP cassette is still present in the GRN23-C4 line, although expression is mosaic. Excluding variation in these lines due to a stochastic manner, the key variable is the site of integration of the EGFP and neomycin-resistant transgenic loci. This observation, taken together with those of section 4.2.2, is consistent with the notion that the GRN lines are heterogeneous in nature, rather than homogenous/truly clonal.
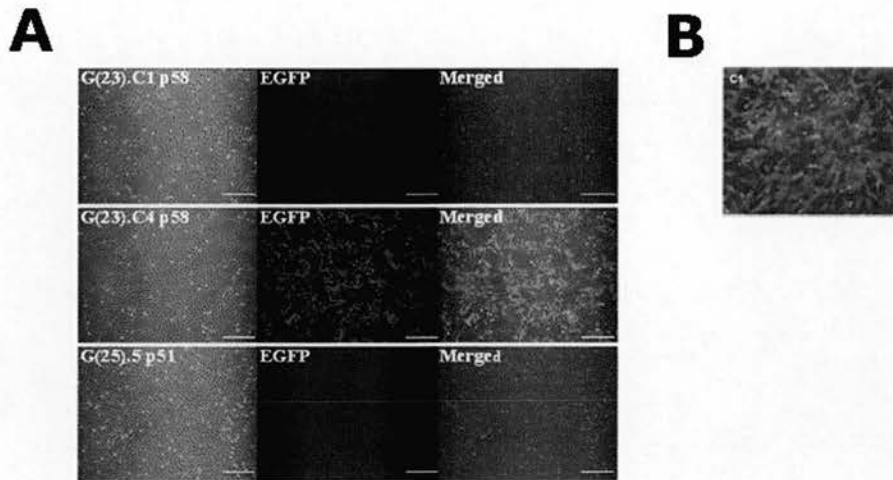
Figure 4.6: EGFP expression in GRN23 mock-transfected clones after extensive culture period. (A) EGFP expression is completely absent in the GRN23-C1 clone at this stage, whereas a mosaic pattern of EGFP expression is present in the GRN23-C4 clone, ranging from high expression to no expression in subsets of cells within the population. The GRN25-5 line at a similar stage of the culture period is shown as a negative control. Scale bar represents 500μM. (B) EGFP expression evident in the GRN23-C1 clone prior to the extensive culture period. (EGFP image for (B) taken by Ling Mo).

4.2.4   Selection regime for wild-type hTERT transcript

As a puromycin-resistant cassette was present in the transgenic loci containing wild-type hTERT, a puromycin selection regime using the same concentration used to initially select for the hTERT-immortalized GRN1-1 clone (0.75μg/ml), was used to determine indirectly if the wild-type hTERT transcript was still present after long-term culture. By day 5, no cells survived this regime in any of the representative lines analyzed, indicating that the puromycin cassette and through inference, the wild-type hTERT transcript, had been silenced in a subset(s) of cells (Fig. 4.7).
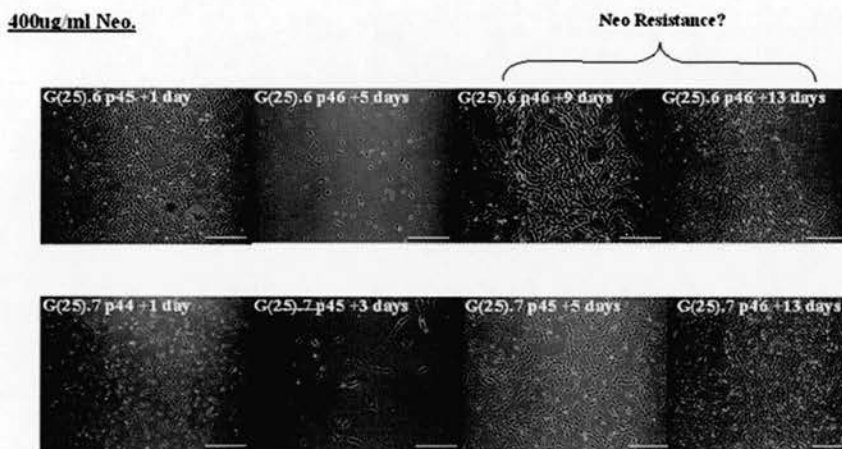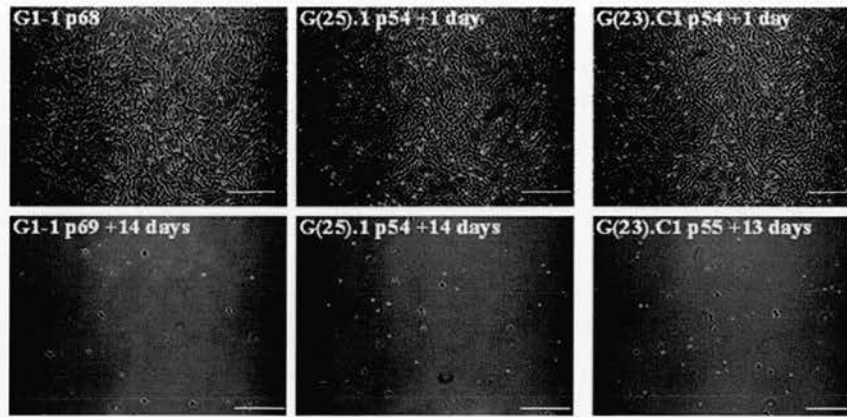
0.75ug/ml Puro.
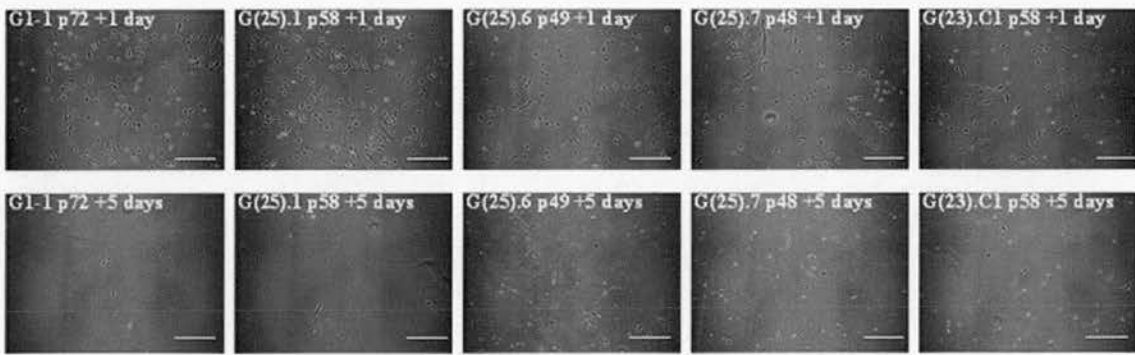
Figure 4.7: GRN culture under puromycin selection. Late passage hTERT-immortalized GRN clones were cultured under a 0.75µg/ml puromycin selection regime. No cells survived the selection regime after a period of 5 days. Scale bar represents 500µM.

Although wild-type hTERT is lost through serial culturing by this stage, the GRN lines still maintain a consistent proliferation profile and thus maintain a senescence bypass status. Furthermore, telomerase is active and telomeres are stabilized and maintained at this stage. This would not be expected if hTERT was not expressed and telomerase did not function to maintain telomeres, at least at the subset of the shortest telomeric substrates, unless endogenous sheep TERT is activated. This data indirectly implicates endogenous sheep TERT as being activated and functioning as a pro-survival factor, acting at the telomere termini to maintain telomere length and to keep senescence checkpoint pathways at check.

4.2.5   TRAP analysis after long-term culture

To investigate whether telomerase activity altered during this period of extensive culture, TRAP analysis was conducted on the GRN clones at late-passage using the same concentration of protein lysate (0.1µg/µl) used for the initial TRAP analyses

prior to the culture period. This ensures a direct comparison of TRAP activity at the different stages of analysis.

TRAP analysis at ~day 100 shows that telomerase activity has considerably increased by this stage. This is indicated by the loss of the 36-bp internal standard in the reaction due to primer competition; i.e. high levels of telomerase results in a telomeric substrate product that utilizes, most if not all, of the forward primer (Fig. 4.8a). Of note is the high level of telomerase activity detected in lines GRN25-6 and GRN25-7, previously shown to be effected by a dominant-negative/competitive inhibition interaction. This is consistent with the data indicating silencing of the mutant hTERT transgene. However as the previous data also indicated that the wild-type hTERT transgene has been silenced, telomerase activity would not be expected in this context, at least not telomerase activity due to hTERT. This result therefore indirectly supports the notion that endogenous sheep TERT is activated in the GRN lines by this stage, and is therefore the source of TRAP activity in the assay. (NB: Due to the conservation of the telomeric repeat sequence in mammalia, TERT from any mammal would be expected to elongate the telomeric substrate used for TRAP assay).

However, to confirm that telomerase activity had indeed increased after the period of long-term culture, a systemic TRAP assay was conducted by preparing protein lysate and measuring concentration of samples systemically from both the early and late stage. On the basis of this analysis it is difficult to state whether telomerase activity has increased at the later stage, as telomerase activity and the internal standard are

comparable across the lines. The analysis confirms the alleviation of telomerase

inhibition conferred by mutant hTERT in the GRN25-6 and GRN25-7 lines (Fig.

4.8b). Taken together, TRAP analysis demonstrates that telomerase activity is high in

all GRN lines after ~ 100 days in culture, suggesting that the source of this activity

may be the endogenous TERT protein, rather than the hTERT transgenic protein.
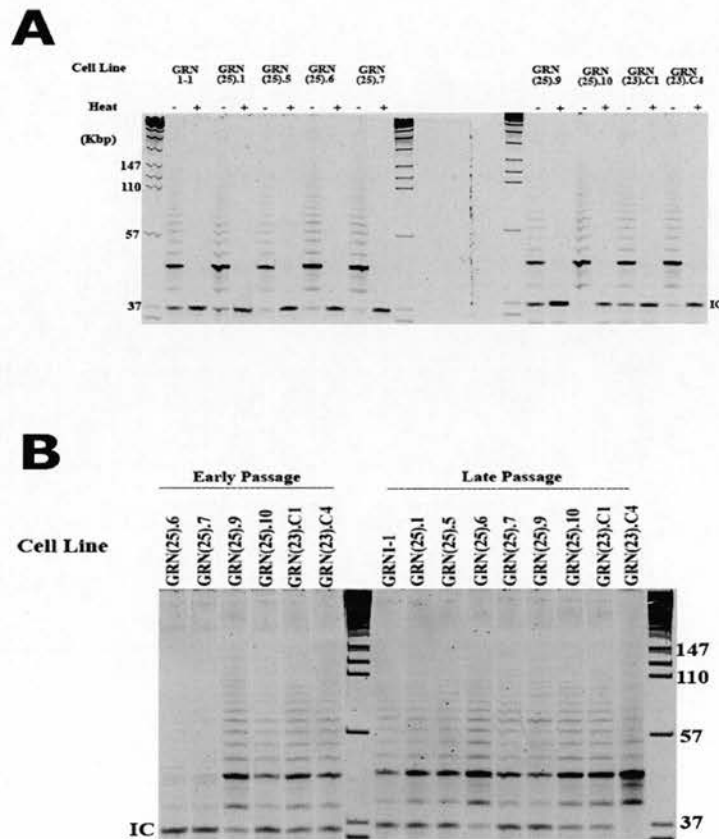
Figure 4.8: TRAP assay on GRN lines after period of extensive culture. (A) TRAP analysis on GRN lines at ~day 100 of the extensive culture period and using 0.1µg/µl. Telomerase activity is high and comparable in all lines, adjudged by the TRAP product ladder and the loss of the 36-bp internal standard. Heat inactivated controls are shown. (B) Systemic TRAP analysis. Protein measurement and TRAP analysis was conducted in a systemic fashion using lysate from an early stage of culture and after ~ 100 days. Telomerase activity is comparable in all GRN lines at late passage and this activity level is similar to the majority of lines at the early stage. Release of telomerase inhibition in the GRN25-6 and GRN25-7 lines is evident.

The lack of the sheep TERT sequence hampers any study attempting to identify its activation and subsequent biological role. The data presented here indirectly implicates endogenous sheep TERT as being activated after a sustained period of culture.

4.3   Discussion

The heterogenic nature of the hTERT-immortalized lines (GRN) used for this study was presented in Chapter 3, with particular regard to the GRN25-7 line which exhibited the highest levels of mutant hTERT at the particular molecular snapshot analyzed. The obvious implication was that mutant hTERT compromised active hTERT in this line through competitive binding to the wild-type hTERT or the telomere substrate. This would then have lead to an adverse affect on cellular proliferation as observed with a subset of cells within the population entering a senescence-induced growth arrest. However the majority of cells within the population maintained a normal fibroblastic morphology and maintained an uncompromised growth rate, thus eventually being selected for due to the growth advantage conferred. This led to speculation as to whether heterogeneity evident in GRN25-7 is initially directly attributable to the effects of mutant hTERT expression, followed by selection upon serial passage as a consequence of long-term culture, in excess of 100PDs.

Initially, total hTERT transgene expression was monitored, with the null hypothesis stating that hTERT transgene expression will be comparable to levels evident prior to

the extended culture period. Strikingly by day ~100, almost no hTERT message is evident in any of the GRN lines, including mock controls. Expression analysis at ~day 80 showed comparable levels of hTERT expression across all lines, although this was much lower than levels detected in the five lines adjudged to express medium to high mutant hTERT expression prior to the extensive culture period (section 3.2.1). This hints at the heterogeneous nature of these lines, whereby mutant hTERT may have been silenced in a subset of cells within a population, a subset unto which a growth advantage is conferred thereafter. Mutant hTERT expression may then still be evident by day ~80 as a subset of cells within the population still retains mutant hTERT expression; however, by day ~100, it appears the subset with 'silenced' mutant hTERT has overwhelmed the population. That the mutant hTERT transgene was indeed silenced, was indirectly confirmed by culturing GRN cells at this late stage under a neomycin selection regime, as the mutant hTERT cDNA will be in close proximity to the neomycin resistant cassette upon integration. Only cells from the GRN25-6 and GRN25-7 populations survived this regime – nevertheless only a very sparse subset of cells survived selection and eventually repopulated the population. Therefore even in these lines, it appears the mutant hTERT transgene is silenced in the majority of cells. The subset conferring neomycin resistance may truly reflect a subset of cells where mutant hTERT is still active, although the caveat of only a few neomycin molecules conferring resistance to Geneticin, must be considered.

Surprisingly, when the mock controls were monitored at this stage for expression of the EGFP transgene, one clone showed a mosaic pattern of expression (GRN23-C4)

whilst the other clone showed complete abrogation of expression (GRN23-C1). This indicates complete silencing of the transgene in GRN23-C1 as high EGFP expression was evident prior to the extensive culture period. This silencing phenomenon appears to be an inherent consequence of serial passaging during an extensive period, as EGFP expression *per se* would not be expected to have any compromising effects on cellular growth and viability, regardless of whether expression was heterogeneous within a given population. Therefore this implicates that although mutant hTERT may have adverse affects on cellular growth, this is confounded by the possibility that transgene silencing may have occurred in these lines purely as a result of culture and selection bias as a result. If this were the case then the wild-type hTERT transgene would also be expected to be silenced in the GRN lines. When grown under a puromycin selection regime to infer presence of wild-type hTERT, no cells from any representative line survived. Thus wild-type hTERT is also silenced in these lines. However, senescence bypass has been shown to be uncompromised in these lines during this stage (section 3.2.4), raising the question of whether the endogenous sheep TERT is activated and functioning to check senescence pathways and maintain telomere length in the subset of shortest telomeres. Indirect evidence for this is presented through TRAP analysis after the extensive culture period; telomerase activity is high and comparable across all the GRN lines, with restoration of telomerase activity in GRN25-6 and GRN25-7 after the initial period of telomerase inhibition. If the wild-type hTERT transgene were indeed silenced in these lines, telomerase activity would be expected to be absent. Therefore activation of endogenous sheep TERT is implicated here, as the sheep telomerase complex would be expected to elongate the telomeric substrate used in the TRAP assay. Any

study attempting to address this issue is hampered by the lack of the sheep TERT coding sequence.

In light of evidence presented here that demonstrates silencing of the hTERT transgenes, results discussed in chapter 3 may be viewed within this context. In particular, telomerase inhibition in GRN25-1 at the earliest stage TRAP (section 3.2.3), followed by restoration of activity to levels similar to mock controls after ~6 PDs, may be explained due to transgene silencing. It is likely that mutant hTERT expression levels were sufficiently high (most likely comparable to levels in GRN25-6 and GRN25-7) so as to exert a dominant-negative/competitive inhibition effect at the early stage. However due to silencing of mutant hTERT in a subset of cells (or at least reduced expression levels), these cells were endowed with a growth advantage within the population. This may then explain the restoration of telomerase activity due to uncompromised function of wild-type hTERT, albeit after only ~6 PDs.

This study highlights the precarious nature of a sustained period of *in vitro* culture using transgenic lines and underlines the importance of maintaining stringent selection throughout the extensive culture period as well as frequent monitoring of whether transgene expression is persistent.

CHAPTER 5

QUANTITATIVE-FISH (Q-FISH) ANALYSIS

TO DETERMINE TELOMERE LENGTH

HETEROGENEITY IN NORMAL OVINE

FIBROBLASTS

5.1   Introduction

Telomere length regulation is controlled by a complex homeostatic mechanism that invokes both extrinsic factors such as telomerase and other telomere-associated factors, but also key intrinsic manifestations based on telomeric configuration structure and telomere length heterogeneity. Classical telomere length measurement has relied on a calculation of average telomere length based upon telomere restriction fragments (see section 2.2.16). Such analysis reflects the span of telomere lengths from a population as a whole; however our current understanding of telomere dynamics reveals a considerable degree of telomere length heterogeneity within any given karyotype, which importantly is of functional significance (see section 1.6.1). To address this technical issue, Peter Lansdorp and co-workers refined the fluorescence *in situ* hybridization (FISH) technique and established a method to robustly quantify individual telomere lengths on chromosome arms, providing a powerful tool to resolve telomere length at the individual chromosomal level (Lansdorp 1996). The method utilizes a fluorescence-tagged telomere repeat probe that is administered to metaphase spreads and fluorescence units from individual telomeres measured by dedicated software.

A descriptive study conducted in our laboratory previously reported considerable differences in proliferative lifespan of two normal sheep fibroblast lines –BWF1 and BW6F2- (Clark et al., 2003). Both these foetal fibroblast lines were independently isolated from the same genetic breed, Black Welsh (sheep breeds are essentially outbred and exhibit less than 1% co-ancestry within a breed). Both derived lines exhibited similar mean telomere restriction fragment lengths after isolation (BWF1,

18kb; BW6F2, 20kb) and at replicative senescence (BWF1, 11kb; BW6F2, 11kb). Intriguingly proliferative lifespan differed 3-fold between these two lines, with BW6F2 entering replicative senescence at ~112PD, whereas senescence in BWF1 was reached after ~34PD. This is directly correlated to the average telomere shortening rate in these lines, with BWF1 exhibiting an average shortening rate of 301bp/PD, whereas BW6F2 exhibited a shortening rate of 91bp/PD (Clark et al., 2003). What are the intrinsic factors that account for such a significant difference in average telomere shortening rate? Is this causal or consequential of proliferative lifespan? These issues are difficult to address mechanistically at present, reflected by the lack of reports documenting intrinsic or extrinsic determinants of telomere shortening rate. However with advances in the methods to quantitatively measure individual telomere lengths, descriptive studies may be undertaken to help begin to understand this process further. The key limitation of the previous study in our laboratory was that true telomere length heterogeneity was not accounted for and therefore only average shortening rate had been calculated. It is likely that average telomere shortening rate only indirectly indicates the functional consequence of telomere attrition. For example, telomere shortening rate within only a subset of telomeres may be directly correlated to the onset of replicative senescence rather than average telomere length in the karyotype *per se*. Therefore it was of interest to optimize Q-FISH methodology in the sheep system to attain a description of telomere shortening in the Black Welsh fibroblasts that takes into account true telomere heterogeneity and to calculate telomere shortening rate on this basis.

5.2.1 Hypothesis

1) Telomere shortening rates differ considerably *between* the BWF1 and BW6F2 lines; *within* each line telomere shortening rates are constant throughout (null hypothesis).

2) A subset of telomeres in both the BWF1 and BW6F2 lines exhibit a significantly faster telomere shortening rate than all other telomeres, but there are a greater proportion of telomeres representing this category ('short' telomeres) in the BWF1 line compared to the BW6F2. Thus it follows, that entry into replicative senescence is earlier in the BWF1 line due to the rapid shortening of telomeres within this subset

5.2.2 Chapter aims

1) To present the first demonstration of Q-FISH methodology in ovine cells

2) To provide descriptive analysis of telomere length heterogeneity within two primary ovine fibroblast lines derived from the same genetic background.

5.2 Results

5.2.1 Fluorescence *In-Situ* Hybridization (FISH)

FISH was conducted on metaphase spreads as described in section 2.10 and constitutes a key rate-determining step regarding Q-FISH analysis. Sheep chromosomes by their very nature are not as compact/condensed as mouse and human chromosomes and appear somewhat denatured in their appearance. Telomere-FISH can only serve to approximately judge individual telomere lengths by estimating the brightness of signals, for example a long telomere length showing brighter signal than a short one. It is evident that telomere FISH clearly shows telomere shortening in the BW6F2 and BWF1 sheep fibroblasts during *in vitro* culture from early through to late, pre-senescent passage (Fig. 5.1a and b). Fluorescent intensity is high and comparable between the lines at the early passage stage as expected. However, telomere FISH signals in BWF1 became invisible by passage 18 (PD29). In contrast, the signals in BW6F2 were still detectable until passage 37 (PD103). Therefore, the differences in telomere shortening rate become evident between the two lines. This is consistent with the results reported previously documenting differing proliferative capacities regarding these two lines (Clark et al., 2003).
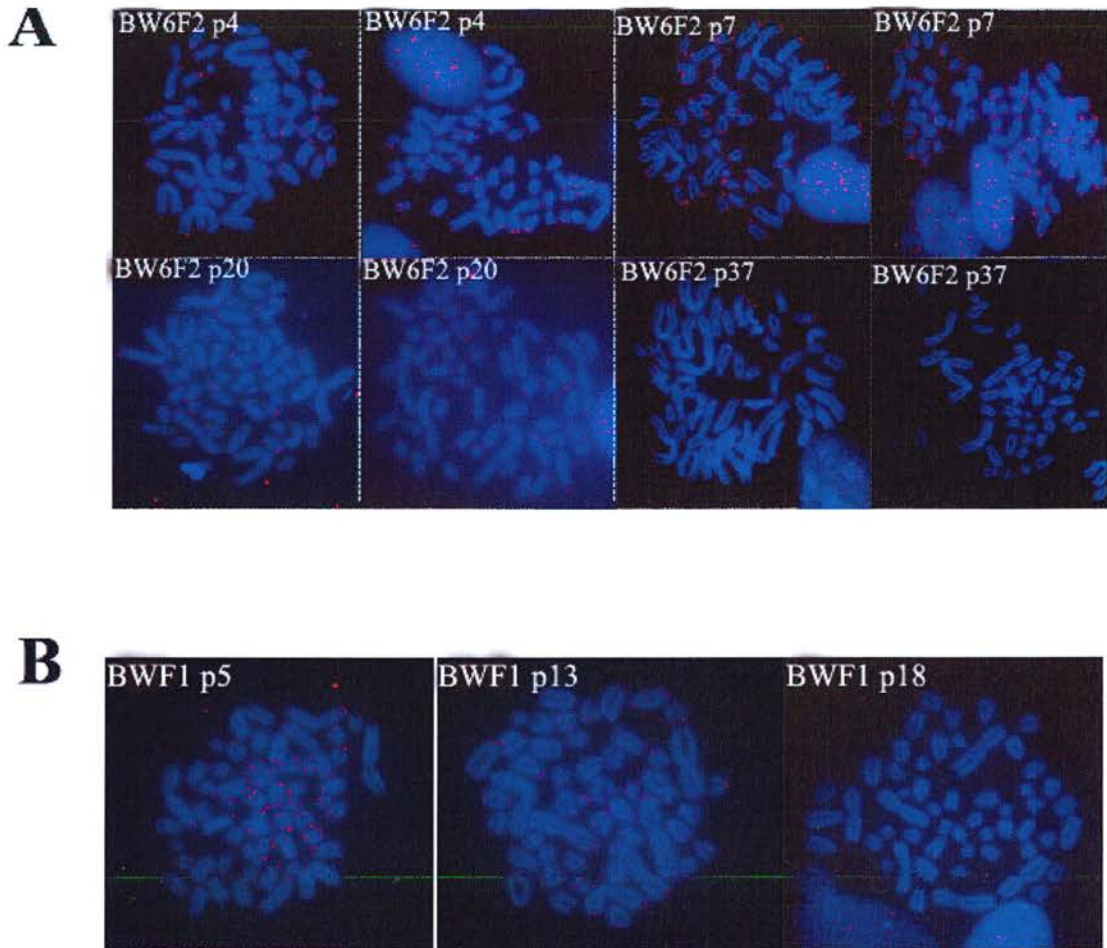
Figure 5.1: Telomere Fluorescence *In-Situ* Hybridization on metaphase spreads from BW6F2 and BWF1 ovine fibroblasts. Telomeric fluorescent signals progressively diminish in both the BW6F2 and BWF1 lines during culture, with the earliest passage generating the strongest telomere fluorescent signal. However, telomere length below the minimum length required to generate a signal under the conditions for image capture used here is reached by passage 37 (PD103) in BW6F2 (A), whereas a similar minimal telomere length is reached by passage 18 (PD29) in BWF1 (B), thus reflecting the intrinsic difference in telomere shortening rate between the two lines.

Observation of metaphase also provided scope to determine if the Black Welsh lines displayed a normal karyotype throughout culture. Sheep have 26 autosomes and two sex chromosomes (diploid chromosome number of 54), including six distinct large metrocentric chromosomes. Diploid chromosome number was ~54 (give or take 1-2 chromosomes that can be attributed to the preparation of the spread) in each

metaphase analyzed and neither variation in metrocentric chromosome number nor obvious abnormal chromosomes (such as dicentric), were evident within any metaphase. Therefore there are no gross abnormal chromosomal changes evident within the BW6F2 and BWF1 lines to confound analysis.

5.2.2   Metaphase manipulation using TFL-TELO software

It is difficult to distinguish between subtle differences in telomere length and more accurately quantify them with FISH alone. To allow for an accurate comparison on telomere length within each line and between lines, dedicated software called TFL-TELO Q-FISH, was applied. However, due to the rather 'puffy' denatured morphology of sheep chromosomes, Q-FISH software currently available cannot distinguish individual chromosomes from one another and therefore, upon the superimposing of DAPI stained chromosomes and Cy3-conjugated telomeres, cannot assign numerical values to fluorescent-tagged telomere repeat sequences (Fig. 5.2a). This problem can be overcome by 'drawing' around the edges of each chromosome using an appropriate drawing tool in Photoshop. This allows each chromosome edge to be defined, enabling the software to recognize individual chromosomes within each metaphase spread (Fig. 5.1b). It is difficult practically to obtain fluorescent values for every telomere end, particularly the very weak signals, but using this modified approach, it is possible to record values for the vast majority of ends. Therefore, if a sufficient number of chromosomes from a number of metaphase spreads are counted, then Q-FISH analysis using this approach can be valid. Thus, it is possible to quantitatively analyze telomere-FISH fluorescent signal intensities using ovine metaphase spreads.
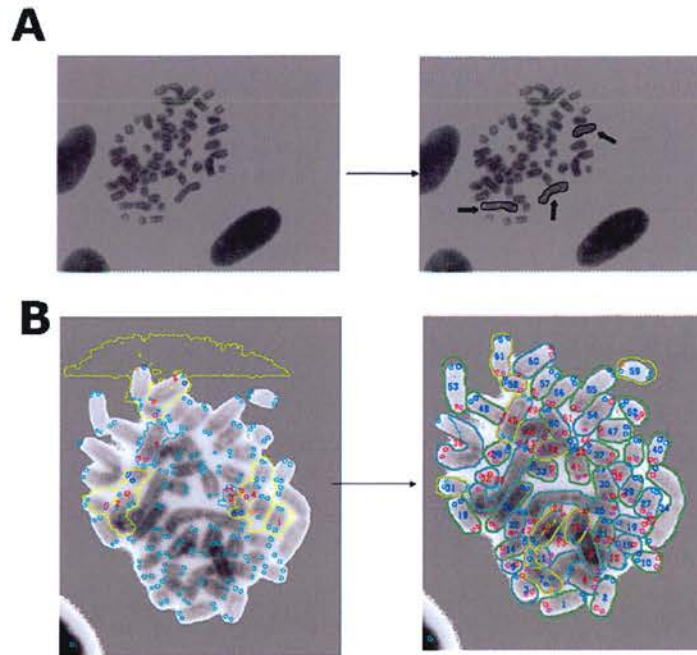
Figure 5.2: Manipulation of ovine metaphase spreads. Due to the denatured morphology, characteristic of sheep chromosomes (A, *left)*, current Q-FISH software cannot distinguish between individual chromosomes (B, *left)*. Therefore each chromosome image must be defined using an appropriate drawing tool, (A, *right*; indicated by arrows). Q-FISH software can then be used to analyze the manipulated metaphase spread and calculate telomere length based on arbitrary fluorescence units (B, *right*). Chromosome number assignment denoted is also arbitrary. Coloured circles represent individual telomeres on each chromosomal arm; fluorescent signal intensities (proportional to telomere length) that are above the minimum detection level, are categorized into five subgroups (high to low) and assigned one of five different coloured circles.

5.2.3   Quantitative-FISH analysis

Approximately 8-10 metaphase spreads were analyzed for every cell line/passage studied. The latest passage for both the BWF1 and BW6F2 cell line, provided the fewest high quality spreads suitable for Q-FISH analysis, owing to the low signal intensities due to very short telomeres at this stage. The number of chromosomes counted for each line analyzed is shown in Table 5.1. As the number of quality metaphase spreads with sufficient signal intensities was low for the BW6F2 p37 line,

only 95 chromosomes could be counted. Therefore this line will be excluded for the overall Q-FISH profile analysis (see Appendix 3 for profile that includes this line).

Cell line	Number of chromosomes counted
BW6F2 p4 (PD8)	329
BW6F2 P7 (PD15)	323
BW6F2 P20 (PD52)	321
BW6F2 P37 (PD 103)	95
BWF1 p5 (PD4)	380
BWF1 P13 (PD19)	337
BWF1 P18 (PD29)	286

Table 5.1: Number of chromosomes analyzed by Q-FISH for each cell line.

Due to the quality of sheep metaphase spreads, a number of telomere end signals are not detected due to overlapping arms, therefore accounting for all signal free ends (SFE) would result in an overestimation as many of these telomeres would be expected to have signal intensities detected by the Q-FISH software. Therefore the category of SFE will be excluded for the general descriptive analysis of the Q-FISH profile, (see Appendix 4 for profiles including the SFE category). Furthermore, rather than directly plot crude signal intensities, a better representation will be deployed here, one which plots the percentage of telomere ends per category. Category here refers to the Telomere Fluorescence Units (TFU) that is arbitrarily assigned by the software, which is directly proportional to telomere length. (The absolute values of TFU recorded, are presented in the Appendix 2 section).

The general pattern of telomere shortening as determined by the Q-FISH method is comparable between the two Black Welsh lines (Fig. 5.3). However the specific profiles differ in a manner that may be interpreted to give a descriptive account of the rate of shortening and the percentage of telomere ends at particular lengths at each

molecular snapshot. At the early stage of analysis, BW6F2 (p4; PD8) (Fig. 5.3a and c) shows a wider and hence more heterogeneous distribution than BWF1 (p5; PD4) (Fig. 5.3b and d). BWF1 has a higher percentage of telomere ends at the low intensity categories than BW6F2. This pattern persists as cells from these lines proliferate, with BW6F2 maintaining a more heterogeneous distribution of telomere length than BWF1. This analysis also shows that telomere shortening rate is more pronounced at an early stage in BW6F2 as shortening rate between p4 (PD8) and p7 (PD15) was more dramatic than the rate between p7 (PD15) to p20 (PD52). Although telomere length profiles are similar between these two stages, results are confounded somewhat by the lack of 'true' SFE data. Nevertheless, using SFE data generated from this analysis, BW6F2 p20 shows a much greater degree of telomere ends at the <50 TFU category, approximately 2-fold higher (see Appendix 3). This is suggestive of a subset of telomeres shortening at a faster rate than the rest of the telomeres in a given cell at this stage. Conversely, the data suggests that telomere shortening rate in BWF1 is more homogenous, which is reflected by only a slight increase in the proportion of SFE detected at each stage (see Appendix 4).
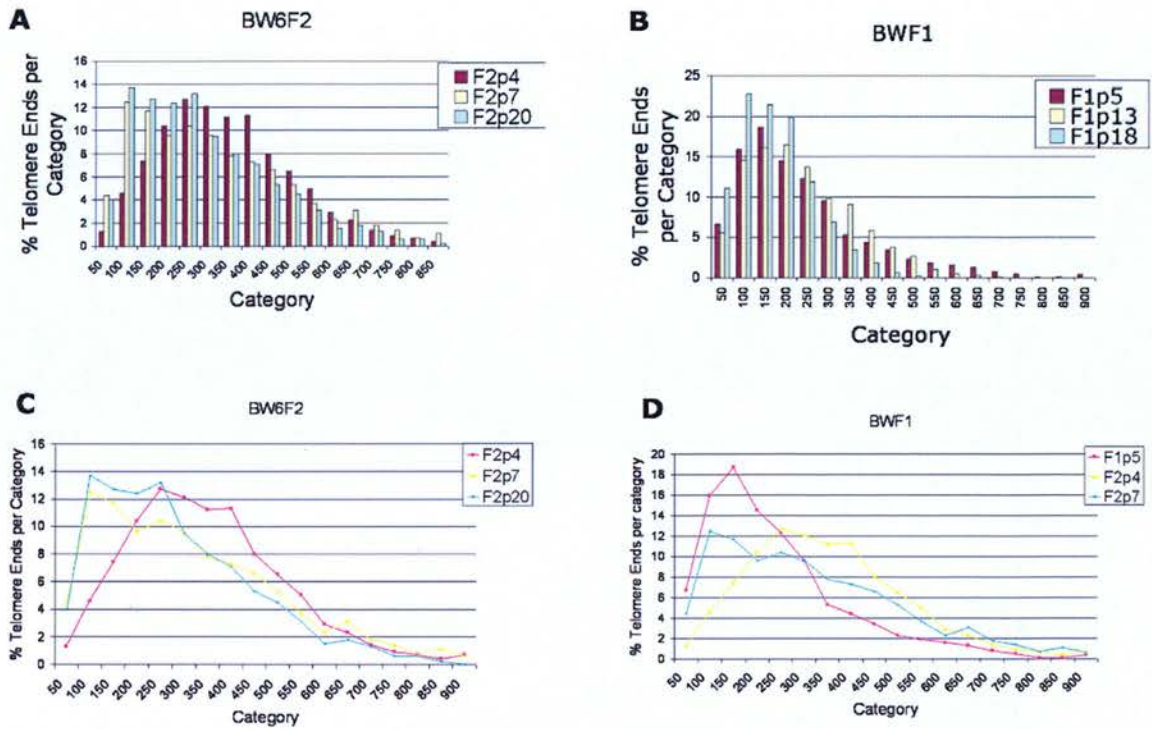
Figure 5.3: Q-FISH profiles of Black Welsh sheep fibroblasts. Histograms and line graphs showing percentage of telomere ends per category, with category reflecting arbitrary telomere fluorescence units as measured by the Telo-TFL Q-FISH quantitative software. A more heterogeneous telomere length profile is evident in BW6F2 (A and C), compared to a relatively more homogenous distribution in the BWF1 line (B and D). A greater proportion of telomeres correspond to low telomere fluorescent unit categories in BWF1 throughout the culture period.

5.2.4   Gated Q-FISH analysis

To better present telomere length determined by Q-FISH analysis, categories were gated to show percentage of telomere ends per gated category (Table 5.2). This approach shows clearly that BWF1 has a greater percentage of telomere ends of the shortest telomere length category (category 50-200) and conversely a much lower percentage of telomere ends of the longest telomere length categories (category 450-600 and 650-900). Interestingly, both the BWF1 and BW6F2 lines show a comparable percentage of telomere ends representing the 250-400 TFU categories, a category that reflects the highest proportion of telomere ends at the early passage.

A

Category	BW6F2 p4	BW6F2 p7	BWF2 p20	BW6F2 p37
50	1.3	4.4	4.0	26.0
100	4.6	12.5	13.7	34.9
150	7.4	11.7	12.7	21.3
200	10.4	9.6	12.4	10.1
250	12.7	10.4	13.2	4.7
300	12.1	9.6	9.5	1.2
350	11.2	7.8	8.0	0.6
400	11.3	7.3	7.1	0.6
450	8.0	6.6	5.3	0.0
500	6.5	5.3	4.5	0.6
550	5.0	3.7	3.1	0.0
600	2.9	2.3	1.5	0.0
650	2.3	3.1	1.8	0.0
700	1.4	1.8	1.3	0.0
750	0.9	1.4	0.6	0.0
800	0.7	0.7	0.6	0.0
850	0.4	1.1	0.2	0.0
900	0.7	0.6	0.0	0.0

% Telomere Ends per category

Gate 1 (Category 50-200)
Gate 2 (Category 250-400)
Gate 3 (Category 450-600)
Gate 4 (Category 650-900)

B

Category	BWF1 p5	BWF1p13	BWF1p18
50	6.7	5.6	11.1
100	15.9	14.6	22.8
150	18.7	16.1	21.4
200	14.5	16.5	19.8
250	12.3	13.7	11.9
300	9.6	9.9	6.9
350	5.3	9.1	3.4
400	4.4	5.9	1.8
450	3.4	3.8	0.6
500	2.3	2.7	0.2
550	1.9	1.0	0.0
600	1.6	0.5	0.0
650	1.3	0.3	0.0
700	0.8	0.1	0.0
750	0.5	0.0	0.0
800	0.1	0.0	0.0
850	0.1	0.0	0.0
900	0.4	0.0	0.0

% Telomere Ends per category

Gate 1 (Category 50-200)
Gate 2 (Category 250-400)
Gate 3 (Category 450-600)
Gate 4 (Category 650-900)

	Category 50-200	Category 250-400	Category 450-600	Category 650-900	(Category 50-400)	(Category 450-900)
BW6F2 p4	25.7	47.3	22.4	6.4	71.0	28.8
BW6F2 p7	38.2	35.1	17.9	8.7	73.3	26.6
BW6F2p20	42.8	37.8	14.4	4.5	80.6	18.9
BW6F2p37	92.3	7.1	0.6	0.0	99.4	0.6

% Telomere Ends per gated category

	Category 50-150	Category 200-400	Category 450-600	Category 650-900	(Category 50-400)	(Category 450-900)
BWF1p5	41.3	46.1	9.2	3.2	87.4	12.4
BWF1p13	52.8	38.6	8.0	0.4	91.4	8.4
BWF1p18	75.1	24.0	0.8	0.0	99.1	0.8

% Telomere Ends per gated category

Table 5.2: Percentage of telomere ends per gated category. BW6F2 exhibits a greater proportion of telomere ends at the 450-600 and 650-900 TFU categories. Conversely, BWF1 exhibits a greater proportion of telomere ends at the 50-200 TFU category throughout the culture period analyzed. Both lines have a comparable proportion of telomere ends representing the 250-400 TFU categories.

The heterogenic dynamics of telomere shortening rate can be inferred on the basis of this analysis. Whereas a comparable proportion of telomeres at early passage (BW6F2 p4, 47%; BWF1 p5, 46%) are of lengths calculated as 250-400 TFU, telomere shortening is more pronounced in a subset of telomeres in BWF1 and BW6F2. This accounts for telomeres that correspond to 50-200 TFU even at this early passage. But crucially, there is approximately twice the percentage of telomere ends at this 'short' telomere category in BWF1 (~41%) compared to BW6F2 (~24%). This suggests that although both lines consist of a subset of telomeres within

the population that have a more pronounced telomere shortening rate relative to the rest of the population, the proportion of telomeres exhibiting such a rate is substantially higher in BWF1 compared to BW6F2.

The initial descriptive gated categories reveal a subset of telomeres within the BWF1 line that exhibited more pronounced telomere shortening If only two TFU categories are regarded, representing simply 'long' and 'short' telomeres (category 50-400 TFU and category 450-900 TFU respectively), the comparative distribution of telomere length heterogeneity can be more readily appreciated. (NB: This categorization is simply the two categories either side of the median TFU calculated for these lines.) Although 'long' and 'short' telomeres are a subjective measure in this context, the relative distribution is what matters. This analysis shows that at an early stage, similar for both lines (BWF1 p5; BW6F2 p4), ~87% of telomeric ends are 'short' within the BWF1 line, whereas ~71% of telomeric ends fall within this category for BW6F2. This conversely results in more than twice the number of 'long' telomere ends within the BW6F2 (~29%) line compared to BWF1 (~13%). This pattern persists throughout the proliferative lifespan of these lines, with ~99% of telomeric ends exhibiting 'short' telomeres in the BWF1 p18 line, whereas ~81% of telomeres are 'short' in the BW6F2 p20 line (Table. 5.3).

	Category 50-400 TFU	Category 450-900 TFU
BWF1 p5	87.4%	12.6%
BWF1 p13	91.4%	8.6%
BWF p18	99.1%	0.9%
BW6F2 p4	71.0%	29.0%
BW6F2 p7	73.3%	26.7%
BW6F2 p20	80.6%	19.4%

Table 5.3: Percentage of telomere ends within gated categories representing 'short' and 'long' telomeres. A greater proportion of telomere ends represent the 'short' telomere category in the BWF1 line compared to BW6F2 at the initial stage of analysis. This pattern of distribution persists throughout the culture period analyzed.

To confirm that the differences in telomere length within passages of each line and between the two lines are significant, a Chi Squared test (see section 2.11) was conducted on the values representing the percentage of telomere ends per TFU category. For the telomere length distribution within the BWF1 line, a Chi Squared value of 20.1 was calculated using 6 degrees of freedom. This reflects a p value of less than or equal to 0.01 (99% confidence level), hence the telomere lengths are significantly different. Similarly for the BW6F2 line, a Chi Squared value of 54.5 was obtained (p value less than or equal to 0.001; 99.9% confidence level). When comparing telomere lengths between the two lines, a Chi Squared value of 65.1 was obtained ((p value less than or equal to 0.001; 99.9% confidence level). Therefore telomere lengths within each line measured from early to pre-senescent passage, are significantly different, as is telomere length distribution between the two lines.

5.2.5 Calculation of telomere shortening rate

To accurately determine telomere shortening rate, absolute TFU and population doublings incurred has to be considered. This allows for a calculation of overall mean telomere shortening rate (Total TFU/PD) as well as shortening rate between each particular stage of analysis (e.g. early to middle passage). It must be stated that calculation of telomere shortening rate deployed here, excludes the category of SFE due to the limitations previously noted. Due to the low sample size of the BW6F2 p37 pre-senescent passage, that line will be omitted from this calculation. Regardless of these limitations, calculation of telomere shortening rate based on a quantitative assessment of telomere signals, can further our understanding of intrinsic telomere dynamics when comparing the BW6F2 and BWF1 lines. An objective description of telomere shortening rate, regarding individual telomere ends is a more robust method of analysis than a rather subjective calculation of mean telomere length within a population across particular snapshots in time. To determine mean TFU for each passage based on the Q-FISH output, the total number of telomere ends (frequency of events) for each TFU value (category) was calculated to give the weighted frequencies for each telomere end. The sum of weighted frequencies divided by the sum of frequencies gave the mean TFU for each passage. The total PDs were taken from a previous report from our laboratory (Clark 2003).

Cell line	Mean TFU	TFU Shortening	Cumulative PD	Total PD	Shortening rate (TFU/PD)	Mean shortening rate (Total TFU/Total PD)
BWF1 p5	255	-	4	-		
BWF1 p13	236	19	19	15	1.3	
BWF1 p18	173	63 (Total = 82)	29	10 (Total = 25)	6.3	**3.3**
BW6F2 p4	351	-	8	-		
BW6F2 p7	331	20	15	7	2.9	
BW6F2 p20	292	39 (Total = 59)	52	37 (Total = 44 PD)	1.1	**1.3**

TFU = Arbitrary Telomere Fluorescence Units
NB: Data excludes SFE category and also omits the BW6F2 p37 line (low sample size)

$$\frac{\text{Mean shortening rate BWF1}}{\text{Mean shortening rate BW6F2}} = \frac{3.3}{1.3} \quad \sim \textbf{2.5-fold difference}$$

Table 5.4: Calculation of mean telomere shortening rate based upon TFU. Mean telomere shortening rate based upon TFU shortening, is approximately 2.5-fold greater in the BWF1 line. However, there is a wide distribution of telomere shortening rate from the overall mean shortening rate, when different stages of the culture period are considered. BWF1 incurs a shortening rate of 1.3TFU/PD between p5 and p13 and increases dramatically to 6.3TFU/PD between p13 and p18. Conversely, mean shortening rate for BW6F2 is 2.9TFU/PD between p4 and p7 and slows to 1.1TFU/PD between p7 and p20.

The analysis shows that telomere length, based upon mean TFU, is substantially higher in the BW6F2 line; e.g.- mean TFU is 351 for BW6F2 p4, whereas mean TFU is 255 for BWF1 p5 (Table 5.4). Total telomere shortening (TFU shortening or more accurately, signal decrease of telomere fluorescence units) is greater in BWF1 than BW6F2 (TFU shortening of 82 and 59 respectively) over the culture period analyzed (Table 5.4). Taking into account the PDs accumulated within each line, telomere shortening rate based upon TFU shortening rate can be calculated between each stage (early, middle and late passage). The result shows that the two Black Welsh lines differ not only regarding overall telomere shortening rate, but also at which stage

telomere shortening rate is more pronounced or less pronounced relatively. BWF1 incurs a mean telomere shortening rate of 3.3 TFU/PD, whereas BW6F2 incurs 1.3 TFU/PD (Table 5.4). This amounts to a ~2.5fold difference in overall mean telomere shortening rate. This is close to the ~3-fold difference in mean telomere shortening rate reported previously, based on telomere restriction fragment length analysis (~91bp/PD for BW6F2; ~300bp/PD for BWF1) (Clark 2003). However the mean telomere shortening rate within these lines is not homogenous throughout the culture period; rather shortening rate dramatically alters at different stages, depending on the line in question. Between p5 (PD4) and p13 (PD19), BWF1 exhibits a mean telomere shortening rate of 1.3TFU/PD, whereas between p13 and p18 (PD29), mean telomere shortening rate is substantially more pronounced – 6.3TFU/PD (Table 5.4). Surprisingly, although there is a clear alteration in rate of telomere shortening in the BW6F2 line, the shortening rate is more pronounced at an early stage. Between p4 (PD8) and p7 (PD15), BW6F2 exhibits a shortening rate of 2.9 TFU/PD, whereas this rate decreases to 1.1 TFU/PD at p20 (52PD) (Table 5.4) Thus TFU calculations based upon Q-FISH profiles, suggest heterogeneous telomere shortening rates within the Black Welsh lines, with a more pronounced shortening rate being incurred much later in BWF1 than BW6F2. It is interesting to observe the degree by which telomere shortening rate alters within the BWF1 line. Telomere attrition is more pronounced by approximately ~5-fold between the two stages analyzed, (1.3TFU/PD to 6.3 TFU/PD). Conversely, telomere attrition rate slows by ~3-fold between the two stages analyzed within the BW6F2 line.

5.3   <u>Discussion</u>

This analysis is the first demonstration of the Q-FISH technique in ovine metaphase spreads and shows how individual telomere repeats may be quantitatively assessed. Thus it is possible to present a highly specific description of telomere shortening dynamics using the Q-FISH method. This study, regards alterations in overall telomere length profiles and of mean telomere shortening rate dynamics, taking into account quantitative values form individual telomeres. It may be more informative to *directly* monitor telomere shortening rate within individual telomere ends, but to do so would require labeling sheep chromosomes in a manner that allows them to be distinct from one another. This would include the ability to identify sheep chromosomes by eye prior to overlaying images using the Q-FISH software, thus accounting for telomere shortening in say sheep chromosome 6 during proliferative lifespan.

There are however a number of limitations using the TFL-TELO Q-FISH software. Firstly, sheep chromosomes cannot be treated with colcemid, which is the conventional method for treating mouse and human cells prior to metaphase preparation. Treatment with colcemid on sheep cells results in chromosomes fragmenting, the reason being unclear. Instead, sheep cells are released from contact inhibition due to 100% confluency, 24 hours prior to metaphase preparation. As colcemid acts to inhibit spindle formation, the absence of colcemid possibly results in many sheep cells not at the metaphase stage when cells are prepared for FISH analysis. This reduces the number of quality spreads. Secondly, sheep chromosomes are required to be manipulated prior to overlaying chromosome and telomere repeat

images. And finally, the minimum threshold for the software to detect telomere signals is set too high – this results in a read-out of SFE that do not necessarily reflect telomeres with no signal. The subsequent problem regarding this issue is that it is difficult to consider chromosome termini with very short telomeres, as they will all be categorized under SFE in combination with chromosomes that genuinely have no signal. Therefore at present, it is difficult to assess telomere lengths of the 'shortest' telomeres at replicative senescence. Nevertheless, a descriptive study of telomere length heterogeneity, within the permissible threshold of the software, is still informative, quantitative and gives a greater degree of resolution than TRF analysis on an entire population.

Generally, the Q-FISH profiles when plotted as the percentage of telomere ends per TFU category, shows BW6F2 to display a more heterogeneous profile than BWF1. Both lines show a reasonably normal distribution of telomere lengths; i.e. – a minority subset of telomeres with very long or very short telomeres, with the majority of telomeres representing an intermediate length. Therefore we can infer that average telomere length does not differ dramatically between these lines. However, the skew of this distribution is more biased towards shorter telomeres in BWF1, relative to BW6F2. Thus, BWF1 exhibits a Q-FISH profile that is relatively more homogenous than BW6F2. This distribution is better represented by gating TFU categories. Comparison of telomere ends per TFU category at the initial stage of analysis is revealing. Both BWF1 and BW6F2 have a comparable percentage of telomere ends at category 200-400 (46.1% and 47.3% respectively), a category that represents a relatively intermediate telomere length in this study. However, BWF1 at

this early stage exhibits 41.3% of telomeres in the 'shortest' TFU category (50-150 TFU), whereas only 23.7% of BW6F2 telomeric ends represent this category at a similar stage of analysis. This is a recurring pattern at each stage analyzed - BWF1 exhibits a greater proportion of 'short' telomeres. Therefore although the proportion of telomeres with average telomere length is inferred to be comparable, BWF1 exhibits a greater proportion of very short telomeres. This suggests rather superficially, that although replicative senescence may be triggered at a comparable 'mean' telomere length, the telomere shortening rate in a *subset* of telomeres within the BWF1 population may be a key determinant of the much earlier onset of senescence activation in this line. This pattern is descriptive evidence of intrinsic differences of telomere shortening rate between individual telomere ends within the BWF1 and BW6F2 lines, thereby rendering a rejection of the null hypothesis. Taking into consideration the previously reported PD rate for these lines (Clark 2003), a more accurate description of telomere shortening rate can be deduced. As expected, this reveals that BWF1 exhibits a more aggravated mean telomere shortening rate (based upon TFU shortening) relative to BW6F2. Mean telomere shortening rate is approximately 2.5-fold more pronounced in BWF1. However, the rate of BWF1 telomere shortening (6.3TFU/PD) is dramatically more pronounced at a later stage of culture (p13 to p18) than at an early stage (1.3TFU/PD; p5 to p13). The pattern is reversed in BW6F2 with telomere shortening rate more pronounced at an earlier stage (2.9TFU/PD; p4 to p7) than at a later stage (1.1TFU/PD; p7 to p20). It is important to note that even this more pronounced telomere shortening rate in BW6F2, is still only half the attrition rate of BWF1 at the later stage of culture. Interestingly, if absolute TFU is taken into consideration for each line, there are more

telomeres (relatively) with a high TFU (600 TFU or more) for BW6F2 than for BWF1, notably at the earliest stage analyzed (see Appendix 2 for absolute TFU values). This was not shown in previous methods to analyze telomere length based on TRF studies (Clark et al., 2003). This may reflect a limitation in using TRF analysis to measure telomere length compared to the quantitative approach as provided by Q-FISH.

These results hint at the functional consequence of BWF1 exhibiting a greater proportion of 'short' telomeres at similar stages of culture (i.e. – passage number). There is a suggestion that aggravated telomere attrition within the BWF1 line is directly attributable to the earlier onset of senescence and hence the reduced proliferative lifespan evident in this line. However using a descriptive approach such as this makes it difficult to infer a conclusion of causal or consequential relationships. Is the more pronounced telomere shortening rate in BWF1 a key determinant of a shorter proliferative lifespan relative to BW6F2? Or is telomere shortening rate in this context, consequential of alternative intrinsic and extrinsic factors that determine proliferative lifespan? Both these lines are derived from the same breed and therefore constitute similar genetic backgrounds. This probably accounts for the comparable average telomere lengths after derivation of the lines and upon onset of replicative senescence. However the intrinsic differences in telomere shortening rate may be due to more subtle differences in genetic profiles of these lines, such as gene expression levels and timing of expression. Although the very nature of *in vitro* culture systems confers various sources of stress upon cellular populations, these lines repeatedly show this intrinsic difference in telomere

shortening rate, implying that the cause of this difference is likely due to the inherent genetic make-up of the lines, rather than due to a stochastic variable.

Overall, Q-FISH provides a robust, reproducible and quantitative method to analyze individual telomere length to a high resolution. Moreover, it is likely that telomeres that are detected as 'short', i.e.- corresponding to ~50 TFU, may not have been readily detected by the TRF assays deployed previously, and so obscured results. Factors regulating telomere shortening rate remain one of the most elusive avenues in telomere biology research. One of the key limitations is that analysis is usually conducted at molecular snapshots in time rather than as a smooth temporal continuum. It will be important to determine telomere shortening at each round of cell division and for each telomere. Q-FISH profiles of telomere dynamics have showed that heterogeneity is apparent within telomere ends as proliferation progresses, therefore although average telomere shortening rate at any given point can be informative, individual telomere shortening rates will be crucial to our understanding of issues such as proliferative lifespan capacity and onset of replicative senescence.

CHAPTER 6

TELOMERE-OLIGONUCLEOTIDE

LIGATION ASSAY AND LOW OXYGEN

CULTURE IN OVINE FIBROBLASTS

6.1   Introduction

Two main mechanisms have been postulated to restrict lifespan of primary mammalian cells. The first suggests that cultured cells suffer from extrinsic physiologic stress and cumulative damage that ultimately trigger senescence (von Zglinicki et al., 2001 & 2003). The second proposes that an intrinsic counting mechanism triggers senescence after a predetermined number of cell generations (Hayflick 1961) that may be cell-type and species-specific. The 'telomere-length as a mitotic clock' hypothesis is based on the latter model whereby progressive telomere shortening induces senescence once one or more telomeres erode to a critical length (Harley et al., 1990, Zou Y. et al., 2004). Consistent with this hypothesis, expression of telomerase, which halts telomere erosion, prevents senescence (Bodnar et al., 1998). Critically, some important findings are not easily explained by the telomere length hypothesis; many normal cells enter senescence with relatively long telomeres and there are many examples of cells that have much shorter telomeres than those found in senescent cells, yet retain the ability to divide (Allsopp et al., 1995, Blackburn 2000). Thus, short telomeres *per se* are not incompatible with continued cellular division. In human chromosomes, the long terminal protrusions of single-stranded G-rich sequence have been reported to vary from 50nt to more than 500nt (Makarov et al., 1997, Stewart et al., 2003). It has been suggested that long TTAGGG single-strand protrusions, besides being an effective substrate for telomerase, may form several non-canonical structures. Seminal work involving electron microscope observation revealed that up to 42% of telomere ends form a large loop in a reaction that depends on the presence of a 3'-overhang (3'-OH) on the G-rich strand and

the telomeric double-stranded binding protein TRF2 (Van Steensel et al., 1998, Griffith et al., 1999). The free 3'end was shown to invade the duplex telomere array at the loop junction. This terminal structure, termed the T-loop, may explain how the extreme termini of chromosomes are distinguished from a DNA break, preventing an appropriate DNA damage response and avoiding G-rich strand degradation or end-to-end fusions of chromosomes. The elucidation of the T-loop poses several key questions: how does telomerase access the hidden chromosomal ends and what is the relationship between telomerase expression and 3'-OH length; is the t-loop structure altered at replicative senescence and if so, is this event a trigger of senescence or consequential? Regarding the latter hypothesis, it has been reported in normal human fibroblasts that the 3'-OH is eroded at replicative senescence and that this may be a molecular trigger of senescence (Stewart et al., 2003). However others have shown, using the same cell type, that 3'-OH is eroded only at crisis and therefore represents a consequential event to upstream senescence activation (Chai et al., 2005).

An intriguing hypothesis was furhter postulated by Jerry Shay and Woodring Wright, which states that telomere shortening rate is directly determined by 3'-OH length. In this respect, telomere erosion would be predicted to be directly proportional to 3'-OH loss after each round of cell division. The potential ability to manipulate this rate of shortening has profound implications both for slowing the rate of replicative ageing in normal cells and accelerating the rate of telomere loss in cancer cells in combination with anti-telomerase therapies. Further independent studies using a variety of human cell types and those from different mammalian species, will be required to fully understand

the molecular alteration of the 3'-OH during culture and to determine whether telomere shortening rate is detemined by the 3'-OH length.

The study presented here utilizes an alternative mammalian model, the sheep (*Ovis aries*), to study the relationship between G-rich 3'OH length and population doubling and also of the relationship of 3'-OH to telomere length and hTERT gene expression. As discussed in Chapter 5, the sheep breed studied here, exhibits similar *in vitro* telomere lengths after isolation of foetal fibroblast cell lines (~18kb and ~21kb), to that reported for somatic human cells (~5-15kb) (Kipling 1990). Moreover previous experiments in our laboratory have shown that ectopic expression of hTERT in sheep fibroblasts reconstitutes telomerase activity, extends lifespan and maintains senescence bypass (Cui et al., 2002). This study will use the Telomere-Oligonucleotide Ligation Assay (T-OLA) to investigate whether the G-rich 3'-OH alters during *in vitro* culture of normal sheep fibroblasts and if so, whether this is a direct correlate to telomere shortening rate. In addition, T-OLA will be conducted on hTERT-immortalized sheep fibroblasts to determine if there exists a relationship between 3'-OH length and hTERT gene expression level. A possible relationship between oxidative stress response capacity and telomere and 3'-OH shortening rate will also be addressed.

6.1.1 Hypothesis

1)   Telomere shortening rate is determined by 3'-OH length in primary sheep fibroblasts.

2)   3'-OH length correlates to both hTERT expression level and to telomere length; lines with high levels of hTERT expression maintain longer telomeres and longer 3'-OH than lines with lower levels of hTERT expression.

3)   Telomere shortening rate can be slowed when sheep fibroblast lines are grown under low oxygen (2%) conditions due to decreased oxidative stress.

6.1.2 Chapter aims

1)   To provide the first demonstration of the T-OLA technique in primary ovine cells.

2)   To investigate the relationship between 3'-OH length and telomere length in primary ovine cells. If telomere shortening rate is determined by 3'-OH length, the BWF1 line would be predicted to have longer 3'-OH.

3)   To investigate the relationship between 3'-OH length and hTERT expression level.

6.2   Results

6.2.1   T-OLA Optimisation

To assess the length of the telomeric overhang, the T-OLA assay was conducted as described in section 2.2.17 (Cimino-Reale et al., 2001). Specifically, radiolabeled oligonucleotides complementary to the telomeric overhang are annealed to genomic DNA, ligated and then electrophoretically separated. The length of ligation products and their signal intensity then reflect the length of overhangs in the sample. Firstly, T-OLA conditions were optimized in our laboratory using the BJ-hTERT immortalized primary human fibroblast line, previously reported by others. In our laboratory settings, the optimised amount of genomic DNA used for T-OLA was 10µg rather than 5µg previously documented. In addition, annealing temperature for hybridization of radiolabeled oligonucleotide to telomeric overhang was set at 52°C, rather than the previously documented 50°C. For ligation of hybridized products, 30U of *Taq* ligase was required for efficient ligation, rather than the 20U documented by others. A maximal 3'-OH signal of 324nt was detected for the BJhTERT line (Fig. 6.1), shorter than a previous recent report with respect to this line (Stewart et al., 2003). This may reflect intrinsic differences in these clonal lines across laboratory settings.
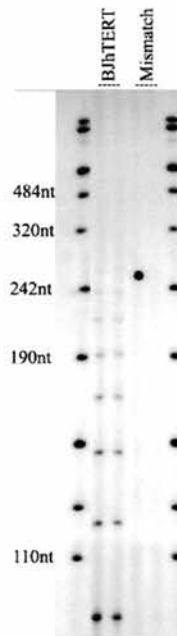
Figure 6.1: T-OLA optimization. T-OLA analysis of genomic DNA from human BJ fibroblasts immortalized with hTERT using radioactively labeled oligonucleotide of the sequence (CCCTAA)$_4$ or mismatch control (CCCTTA)$_4$. A maximal product of 324nt is detected.

6.2.2   T-OLA analysis of primary sheep fibroblasts

We sought to address whether the G-rich 3' telomeric overhang is altered during *in vitro* culture and whether this correlates to telomere shortening rate, in an alternative higher order mammalian species, the sheep (*Ovis aries*). Our laboratory previously reported two sheep fibroblast lines (BWF1 and BW6F2) which showed comparable telomere lengths after isolation and at replicative senescence, but which differed dramatically in replicative lifespan, due to intrinsic differences in telomere shortening rate (BWF1 exhibited a 3-fold shorter replicative lifespan) (Clark et al., 2003). T-OLA analysis was conducted to measure whether the 3' telomeric overhang is altered during *in vitro* culture of BWF1 and BW6F2 normal primary sheep fibroblasts and the experiment

repeated twice. Both lines showed progressive 3'-OH shortening of 72nt, from a

maximal T-OLA signal of 456nt at early passage to 384nt at late pre-senescent passage,

(Fig. 6.2a, and Table 6.1). However, this lower value of overhang length was detected

after 48 population doublings (PD) in BWF1 and 103 PD in BW6F2 (Fig 6.2b).
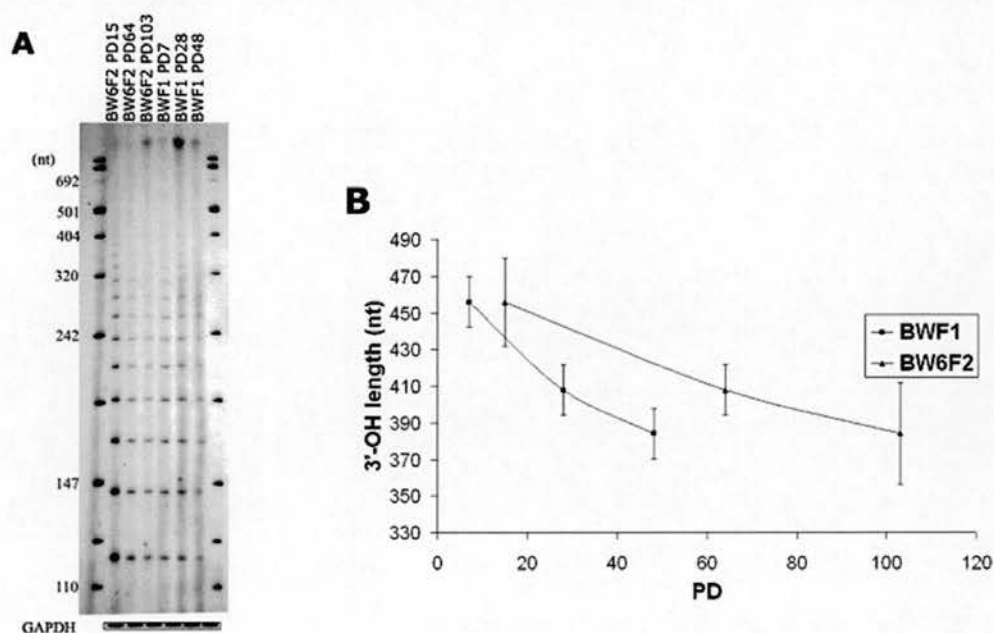
Figure 6.2: G-rich 3'-OH analysis of DNA from Black Welsh sheep fibroblasts (BWF1 and BW6F2). (A) T-OLA analysis of DNA at increasing PDs up till pre-senescence. A maximal T-OLA signal of 456nt at early passage and 384nt at late passage, is detected for each line. Genomic PCR of the GAPDH locus using 10ng template conducted on each sample is displayed on the lower panel. (B) However, 3'-OH shortening is more pronounced in BWF1 with the lower 3'-OH value of 384nt reached after 48PD in this line compared to 103PD in theBW6F2 line.

In order to determine the length distribution of the G-rich 3'-OH, repeated experiments

were performed on BWF1 and BW6F2 fibroblasts. For BWF1, 27 % of the G-rich tail

was in the class ranging from 240nt to 456nt at an early culture stage (PD7), falling to

22% at PD28 and 16% at PD48 (Fig. 6.3b). Comparably for BW6F2, 32% of the G-rich

tail ranged from 240nt to 456nt at PD15, 23% at PD64 and 17% at PD103 (Figure 6.3a).

A
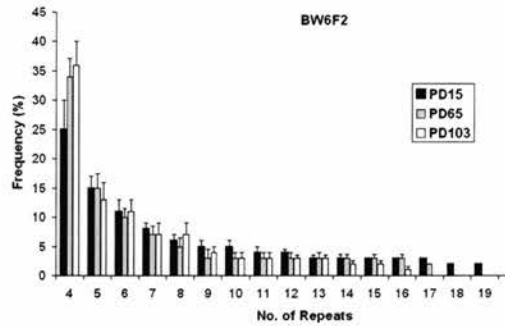
B
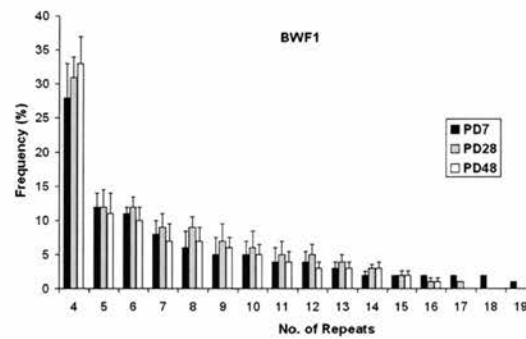
Figure 6.3: Distribution of G-rich 3' overhangs in cultured primary sheep fibroblasts. The band intensity of ligated products was calculated using Multi-Analyst 1.1 software. The frequency of overhangs of different length for (A) BW6F2 and (B) BWF1, was obtained by normalizing the intensity of each single band to the sum of intensity of all bands in the ladder at the PDs indicated. On the *x*-axis the numbers of oligonucleotides ligated by the T-OLA are reported.

Thus the data supports the conclusion that 3'-OH shortens during *in vitro* culture of

normal sheep fibroblasts.

6.2.3   TRF analysis of normal sheep fibroblasts

To establish whether 3'-OH shortening correlates to telomere length, telomere restriction

fragment length analysis was conducted on Black Welsh lines at the same stages as that

of T-OLA analysis and directly compared. Telomeric overhang shortening paralleled

mean telomere length shortening in both lines (Fig. 6.4a) and was found to be a

significant correlate ($r = 0.79$) in this setting (Fig 6.4b and Table 6.1).
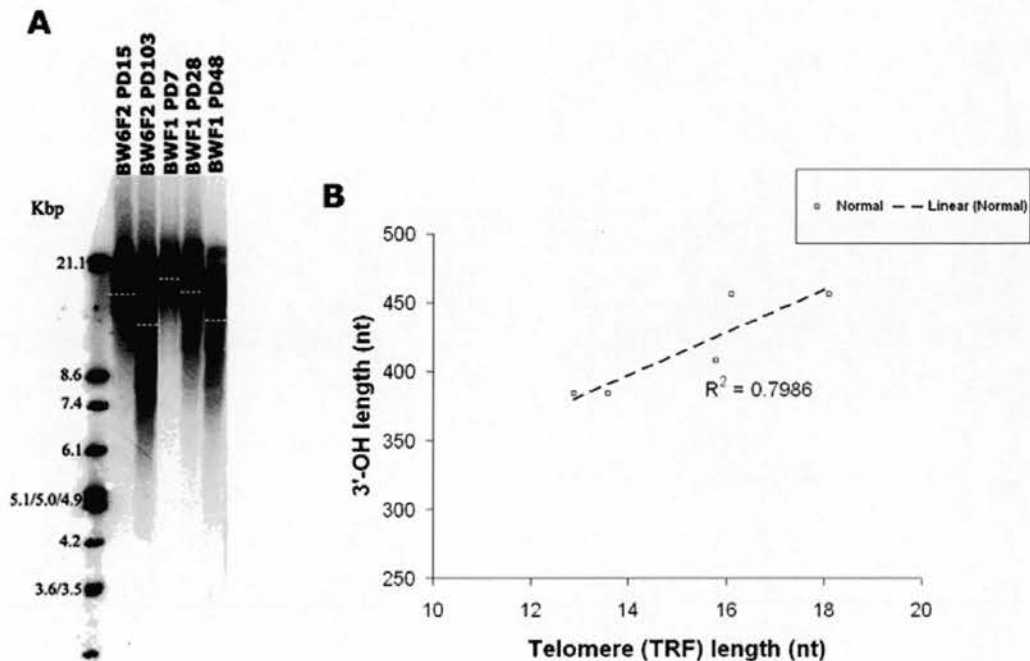
Figure 6.4: 3'-OH length correlates to telomere length in primary sheep fibroblasts.
(A) Denaturing TRF Southern-blot analysis of genomic DNA from Black Welsh lines at
the indicated PDs. (B) Direct correlation between 3'-OH length and mean TRF length.

The rate of 3'-OH shortening was next calculated and compared to the rate of telomere

shortening. Mean telomere shortening rate was calculated as 51.1bp/PD for BW6F2 and

128.0bp/PD for BWF1, approximately a 2.5-fold difference. This is similar to the

shortening rate reported previously (Clark et al., 2003). Comparably, mean 3'-OH

shortening rate was calculated as 0.8nt/PD for BWF6F2 and 2.88nt/PD for BWF1– a

3.5-fold difference. Of the total 72nt of 3'-OH eroded during the culture period analyzed,

1.11% on average is lost per PD in BWF6F2, whereas 4.0% is lost per PD in BWF1

(Table 6.1). Strikingly, of the total 4.5kb telomere erosion in BW6F2 during this culture

period, 1.13% is lost on average per PD, and of the 3.2Kb telomere erosion incurred in

BWF1, 4.0% is lost per PD. Although the percentage loss of mean telomere length and

telomeric overhang length is identical, it is difficult to determine if this is coincidental or

of functional importance. However, the findings indicate that mean telomere shortening

rate is related to mean telomeric overhang shortening rate in primary sheep fibroblasts in

this context. The data supports the conclusion that 3'-OH shortens during *in vitro* culture

of normal sheep fibroblasts and that 3'-OH shortening parallels telomere shortening.

However there is no evidence that this is a direct correlate; telomere shortening per PD

is significantly more pronounced than 3'-OH shortening per PD, thus the data does not

provide evidence for telomere shortening rate being directly proportional to the size of

the 3'-OH. It is important to state that maximal 3'-OH length reported here simply

reflects the maximal T-OLA signal obtained from the assay under these settings and

does not exclude the possibility of true 3'-OH length being longer.

Cell line	PD [a]	Mean TRF length (Kb)	3'-OH length (nt)	Mean TRF shortening rate (bp/PD)	Mean 3'-OH shortening rate (nt/PD)	% Mean TRF shortening/PD (kb/PD)/total telomere shortening	% Mean 3'-OH shortening/PD (nt/PD)/total 3'-OH shortening
BW6F2	15	18.1	456				
	64	15.8	408				
	103	13.6	384	51.1	0.8	1.13	1.11
BWF1	4	16.1	456				
	14	-	408				
	29	12.9	384	128.0	2.88	4.0	4.0

[a] Population doubling rate calculated from growth curve reported in (Clark 2003).

Table 6.1: Summary of TRF and T-OLA analysis on sheep fibroblast clones.

6.2.4   Culture of sheep fibroblasts under low oxidative stress

It has been suggested that telomeres measure stress and damage accumulation more readily than simple mitotic time and that telomere shortening may be stress-dependent due to a telomere-specific damage repair deficiency (von Zglinicki et al., 2002 & 2003). Previously a laboratory in Newcastle, UK, (von Zglinicki lab) have investigated whether response to oxidative stress may be a determinant of differences in telomere shortening and 3'-OH shortening rate evident in the BWF1 and BW6F2 normal sheep fibroblasts. Anti-oxidative defence capabilities was investigated in these lines by measuring peroxide levels under normal and hyperoxic culture conditions. Actual units of peroxide levels were similar for BWF1 and BW6F2 under normoxic conditions. However, under hyperoxic culture shock conditions, although peroxide levels rose significantly for both lines, levels were 3-fold more pronounced in BWF1 than for BW6F2 (see Appendix 5). This suggests that stochastic variations of mild oxidative stress may be one factor for the

shorter proliferative lifespan of BWF1. Therefore it was of interest to investigate whether culture in 2% low oxygen rather than 21% oxygen may overcome a possible stress-induced premature senescence in BWF1. BWF1 cells at PD20 were cultured in each oxygenated setting and PD calculated. Although proliferation rate of cells in 2% oxygen increased moderately after ~28PD, cells reached replicative senescence at the same proliferative age (~35PD) under both conditions (Fig 6.5). The outcome was similar for BW6F2, where cells under both oxygenated conditions reached senescence at ~100PD (data not shown). Therefore, culture in 2% oxygen failed to reduce the rate of telomere shortening in this setting.
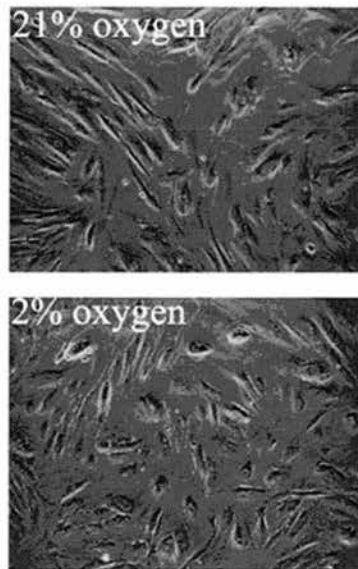
Figure 6.5: Culture in low percentage oxygen in BWF1 primary sheep fibroblasts. Senescent morphology was evident after ~35 PD for BWF1 cells cultured in 21% and 2% oxygen from ~20PD.

6.2.5   T-OLA analysis of hTERT-immortalized sheep fibroblasts

A recent reported has documented how the 3'-OH is found to be significantly shorter in samples derived from endometrial cancers compared to those derived from normal endometria (Hashimoto et al., 2005). This was the first report examining the 3'-OH of telomeric repeats in clinical cancer samples. Unexpectedly perhaps, this study failed to observe any correlation between the levels of telomerase activity and 3'-OH or telomere length. Furthermore it remains elusive as to whether there is a correlation between telomerase activity and 3'-OH in a normal cellular context. Previously our laboratory reported the generation and characterization of hTERT-immortalized primary sheep fibroblasts (GRN). In this scenario, telomere length stabilization and karyotypic stability were directly correlated to levels of hTERT expression as measured by absolute real time qRT-PCR (Cui et al., 2002, Table 6.2). To investigate the relationship between hTERT gene expression and telomeric overhang length, T-OLA analysis was conducted to measure the 3'-OH length in GRN hTERT-immortalized fibroblasts that had incurred in excess of 400PD; at this stage, telomeres were shown to be stabilized and lines with low levels of hTERT displayed 90-100% karyotypic abnormalities (Table 6.2). T-OLA indicates a strong relationship between hTERT expression and 3'-OH length: lines with >300 copies of hTERT mRNA per cell (GRN2-1 and GRN2-7) exhibited the longest maximal 3'-OH length at 504nt; lines with 0.5-87.5 copies of hTERT per cell (GRN2-5 and GRN2-8) had a shorter 3'-OH length of 432nt and lines with <0.5 copies of hTERT per cell (GRN1-1 and GRN2-13) exhibited the shortest 3'-OH length at 312nt (Fig.6.6a

and b; Table 6.2). In support of this, we found a significant correlation ($r = 0.70$) between hTERT expression and 3'-OH length (Fig 6.6c).
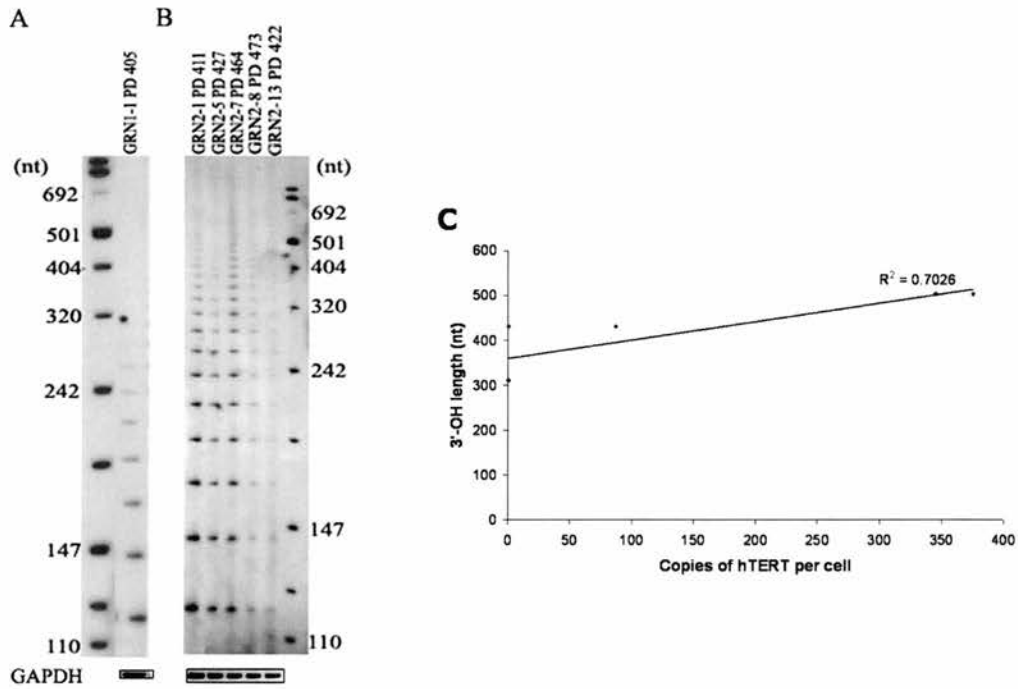
Figure 6.6 : Telomeric 3'-OH analysis from hTERT-immortalized sheep fibroblasts. (A) T-OLA analysis on GRN hTERT-immortalized sheep fibroblasts at culture stage in excess of 400PDs. GRN2-1 and GRN2-7 exhibited the longest maximal T-OLA signal (504nt). GRN1-1 and GRN2-13 exhibited the shortest signal (312nt).Genomic PCR of the GAPDH locus using 10ng template conducted on each sample is displayed on the lower panel.

GRN1-1 and GRN2-13 had considerably shorter stabilized telomere lengths (6.5 and 6.0kb) than all other lines investigated and correspondingly showed the shortest telomeric overhang length (312nt). Conversely, GRN2-1 and GRN2-7 showed the longest stabilized mean telomere lengths (17.2 and 18.0kb) and longest 3'-OH (504nt). GRN2-5 and GRN2-8 had telomere lengths (17.0 and 15.8kb) and 3'-OH lengths (432nt) at an intermediate length between these two classes (Fig. 6.7a and Table 6.2).

Furthermore, 3'-OH length correlated significantly ($r = 0.92$) to calculated stabilized

telomere length in hTERT-immortalized lines (Fig. 6.7b and Table 6.2).
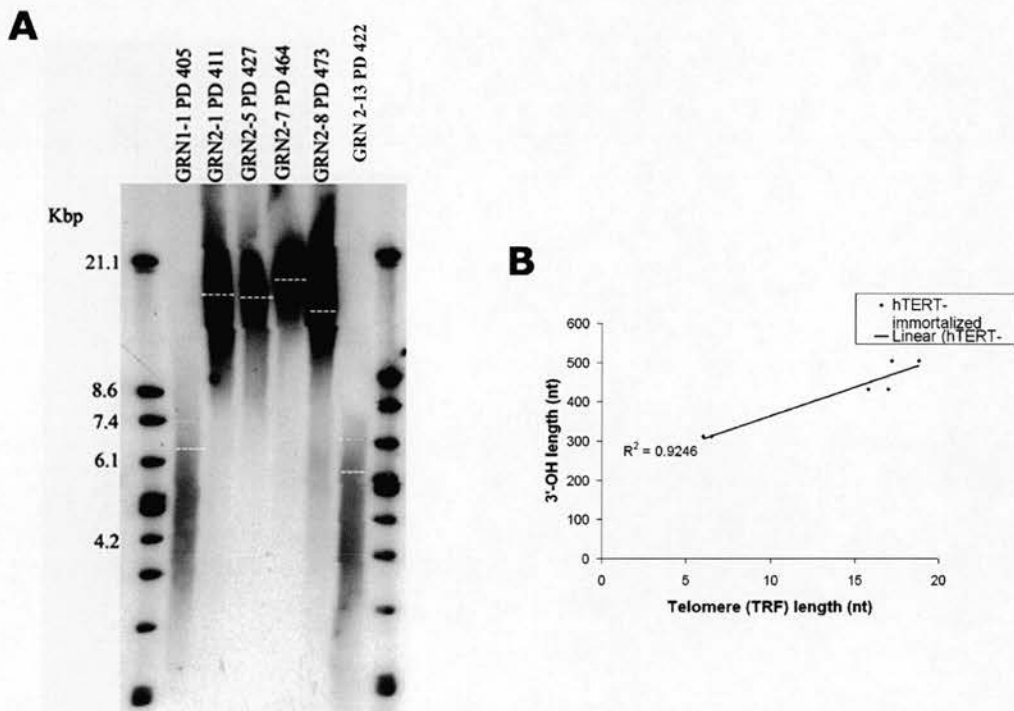
Figure 6.7: TRF analysis from GRN hTERT-immortalized sheep fibroblast lines.
All telomere restriction fragments shown represent stabilized telomere lengths with the
mean telomere length indicated. GRN1-1 and GRN2-13 have substantially shorter
telomere lengths (6.5 and 6.0kb respectively) than all other GRN clones, which exhibit a
mean telomere length range of ~16-18kb.

The frequency distribution of G-rich tails was calculated for the GRN clonal lines.

GRN2-1 and GRN2-7 exhibited 32% and 36% G-rich tails respectively for the overhang

class ranging from 312 to 504nt; conversely, GRN1-1 and GRN2-13 exhibited 4% and

6% of G-rich tails respectively within this range with GRN-5 and GRN2-8 exhibiting a

frequency between these two groups (24% and 25% respectively) (Fig 6.8).
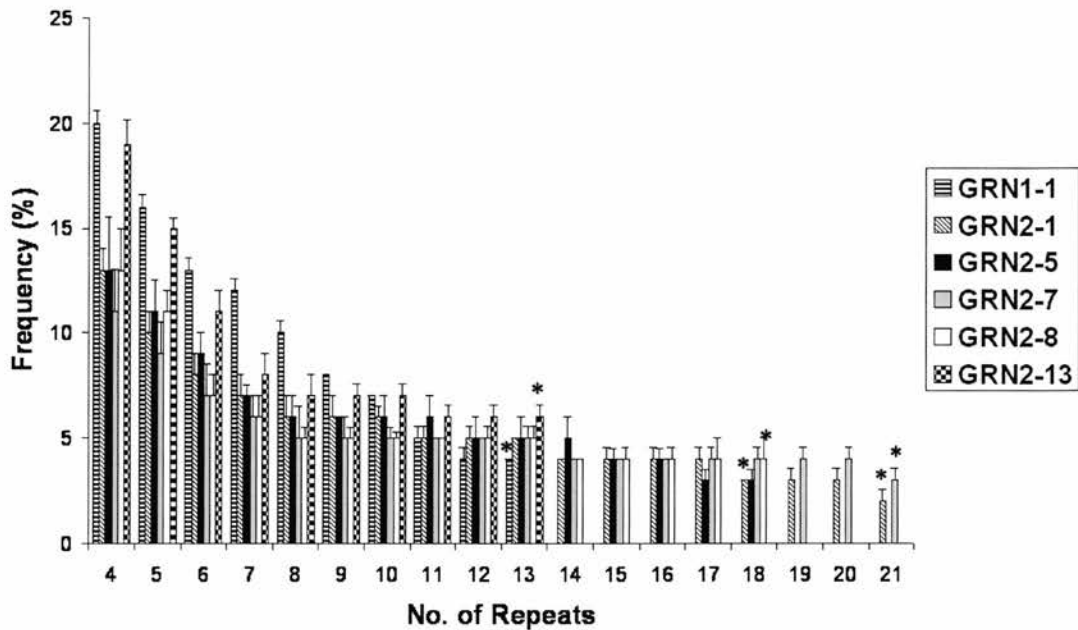
Figure 6.8: Frequency distribution of G-rich tails in hTERT-immortalized fibroblasts. Maximal T-OLA product at PDs indicated for each line is denoted by an asterisk. GRN2-1 and GRN2-7 exhibit the longest maximal telomeric overhang length and approximately one third of overhangs are within a size of 312-504nt. Conversely, GRN1-1 and GRN2-13 have the shortest maximal telomeric overhang length and approximately 5% of overhangs are within a size range of 312-504nt. GRN2-5 and GRN2-8 exhibit a maximal overhang length intermediate to these outliers.

Thus the data provide strong evidence for a relationship between hTERT expression level and 3'-OH length. However, whether this is a direct causal relationship or indirectly as a result of hTERT-dependent stabilized telomere length is unclear.

6.2.6 Relationship between 3'-OH and karyotypic stability

3' telomeric overhang length was further shown to be related to abnormal karyotype levels previously reported (Cui et al., 2002). GRN1-1 and GRN2-13 which showed the

shortest 3'-OH length, also displayed the highest degree of karyotypic instability at the PDs indicated – 93% and 100% abnormal karyotype respectively. GRN2-1 and GRN2-7, with the longest 3'-OH length, showed a more stable genome at similar PDs – 0% and 3% karyotypic abnormalities respectively. GRN2-5 and GRN2-8, with 3'-OH in between these two groups, showed 3% and 50% of abnormal karyotypes at similar PDs. This is a strong indication that 3'-OH length and not telomere length *per se* may contribute to chromosomal instability. In support of this notion, dicentric chromosomes, characteristic of end-to-end telomere fusions, were only apparent in GRN1-1 and GRN2-13, lines which had significantly the shortest 3'-OH length (Table 6.2) (Cui et al., 2002). The data suggests that a minimal length of 3'-OH may be necessary to confer genomic stability, likely due to the formation of a proper telomere end-capping structure such as the T-loop. In this regard, 3'-OH length below this threshold may be a determinant of the onset of karyotypic instability.

Cell line	PD[a]	Mean TRF (kb)[b]	3'-OH (nt)	Relative hTERT mRNA expression[c]	hTERT mRNA per cell[d]	% abnormal karytype[e]
GRN1-1	427	6.5	312	2.6	0.34	93
GRN2-1	408	17.2	504	5873.5	375.08	0
GRN2-5	416	17.0	432	1278.3	87.24	3
GRN2-7	421	18.0	504	5752.6	345.14	3
GRN2-8	408	15.8	432	8.1	0.58	50
GRN2-13	413	6.0	312	1.0	0.08	100

Table 6.2: Summary of TRF and T-OLA analysis on hTERT-immortalized sheep fibroblast clones; ([c, d and e] taken from Cui W. et al 2002).

6.3   Discussion

6.3.1   Analysis of primary sheep fibroblasts

This is the first report of 3' telomeric overhang analysis in primary sheep fibroblast lines and thus represents an alternative mammalian model in which to study function of the 3'-OH and its interplay with telomere-related factors. These observations demonstrate that 3'-OH length erodes during *in vitro* culture of normal primary sheep fibroblasts and that 3'-OH length correlates significantly ($r = 0.798$) to telomere (TRF) length. Previous reports using cultured human fibroblasts have argued for 3'-OH being eroded only at replicative senescence (Stewart et al., 2003) or at crisis (Chai et al., 2005). The gradual shortening of 3'-OH in sheep fibroblasts may reflect intrinsic cross-species differences. Both the BWF1 and BW6F2 sheep fibroblast lines studied here exhibit similar 3'-OH length at an early stage of culture (456nt) and at a pre-senescent stage (384nt). Therefore the telomere shortening does not seem to corrrelate directly with the size of 3'-OH. However, the rate of 3'-OH loss is more pronounced in BWF1 compared to BW6F2. This parallels telomere shortening rate and relates to a 2.5-fold shorter replicative lifespan in BWF1 compared to BW6F2. We further compared percentage of mean 3'-OH loss per PD between the two lines and show that 4.0% of total overhang erosion occurs per PD in BWF1 whereas the figure is 1.1% for BW6F2- approximately a 4-fold difference. Similarly, regarding percentage of mean telomere shortening per PD, 4.0% of total telomere loss, occurs per PD in BWF1 and 1.1% per PD in BW6F2 – again approximately a 4-fold difference. Thus, mean 3'-OH shortening rate per PD directly parallels mean telomere shortening rate in this setting. Although we find a correlation

between relative 3'-OH shortening and relative telomere shortening, there is a substantial discrepancy between actual mean telomere and 3'-OH shortening rate. Mean telomere shortening rate in BWF1 is ~128bp/PD, whereas mean 3'-OH shortening rate is ~2.9nt/PD. Similarly, the respective values are ~51bp/PD and 0.8nt/PD for BW6F2. Therefore although the 3'-OH and telomere duplex array both shorten during *in vitro* culture, the data shows that telomere shortening rate is not directly determined by 3'-OH erosion. One explanation of this apparent discrepancy is that 3'-OH shortening may reflect the end-replication problem, whereas overall telomere shortening better reflects other nucleolytic processing events as well as a function of (external) oxidative stress and (internal) anti-oxidant defence. In support of the latter argument, BW6F2 showed a substantially better response to hyperoxic culture conditions than BWF1. Therefore anti-oxidative capacity may be a key determinant of replicative lifespan and may transpire to overall telomere shortening rate. The dramatically shorter lifespan and more pronounced telomere shortening rate in BWF1 may hence be related to response to mild-stress in culture. On this basis it was reasoned that culture in low oxygen may slow BWF1 telomere shortening rate to levels comparable with BW6F2. However culture in a 2% low oxygen chamber, failed to increase replicative lifespan of BWF1 and BW6F2 fibroblasts. This may reflect the fact that these lines have adapted, genetically and epigenetically, to culture conditions of 21% oxygen and thus gene expression profiles may not be readily reversible. A definitive experiment would require culture in low oxygen directly after derivation of primary cells. It is also imortant to note that Black Welsh fibroblasts used in this study were isolated from the foetal carcass which is composed mainly of skin fibroblasts and was reported to be less sensitive to room

temperature oxygen levels. This may explain why there is no difference in anti-oxidative response between BWF1 and BW6F2 under normoxic conditions (see Appendix 5) and subsequently why there was no difference in proliferative lifespan observed under low oxygen conditions. Therefore it may not be surprising that *both* lines show reduced anti-oxidative capabilites under hyperoxic conditions (although BW6F2 fared better under hyperoxin conditions, peroxide levels still rose substantially).

6.3.2   Analysis of hTERT-immortalized sheep fibroblasts

The relationship between hTERT gene expression and 3'-OH length was next addressed. A recent previous report failed to find any significant correlation between levels of telomerase activity and 3'-OH in a tumour setting (Hashimoto et al., 2005), but no report has been documented regarding any relationship in hTERT-immortalized cells both *in vitro* and *in vivo*. Our laboratory previously analyzed Black Welsh sheep fibroblasts immortalized with ectopic hTERT and reported that telomere maintenance and karyotypic stability are directly correlated to levels of hTERT expression (Cui et al., 2002). The current analysis of 3'-OH in this setting revealed a significant correlation (r = 0.702) between maximal 3'-OH length and copies of hTERT mRNA per cell. The longest 3'-OH length, concurrent with near maximal mean telomere length and stable karyotype, was evident in lines exhibiting >300 copies of hTERT mRNA per cell. Conversely, shortest 3'-OH length, concurrent with shortest mean telomere length and grossly abnormal karyotype, was evident in lines exhibiting <0.5 copies of hTERT mRNA per cell. This is in accordance of RT-PCR data from others which indicate that

most cancer cells contain only a very few (<2 copies per cell) molecules of hTERT full-length mRNA (Yi X. et al., 2001). Thus, 3'-OH length in cells with low levels of forced hTERT mRNA expression may mimic the biological situation in most tumours. Stabilized mean telomere (TRF) length also showed a strong correlation ($r = 0.924$) to 3'-OH length in these cell lines. Thereby lines with high levels of hTERT expression exhibited near full length mean telomere length, more or less normal karyotype (0% abnormal in GRN2-1 and 3% abnormal in GRN2-7) and a maximal T-OLA product of 504nt after ~400PD. Conversely, lines with low levels of hTERT exhibited a mean stabilized telomere length shorter than the senescent length of the parental lines, grossly abnormal karyotype (93% in GRN1-1 and 100% in GRN2-13) and correspondingly a maximal T-OLA product of 312nt. Therefore telomeric overhang length appears to be related to the stability of the genome and attributable to levels of hTERT expression. Whether this is a direct relationship or indirectly as a function of hTERT-mediated telomere duplex repeat maintenance is unclear. The data presented here regarding 3'-OH shortening in normal sheep fibroblasts suggests that 3'-OH length in hTERT-immortalized fibroblasts is an indirect function of hTERT expression level and is determined by telomerase-mediated telomere maintenance.

Viewed together, the data indicates that the telomeric 3'-OH length of 504nt in fibroblasts immortalized with high levels of hTERT, may represent full length maximal 3'-OHs in Black Welsh fibroblasts *in vitro*. The 3'-OH length of 456nt at early stage BWF1 and BW6F2 fibroblasts presumably reflects 3'-OH erosion with PDs incurred up to that stage. Conversely, the 3'-OH length of 384nt evident at late pre-senescent stage

BWF1 and BW6F2 fibroblasts, may reflect a length close to a minimal length of 3'-OH required to maintain a T-loop structure and hence chromosomal stability and cell viability. In support of this, the GRN1-1 and GRN2-13 hTERT-immortalized lines, with a 3'-OH length of 312nt show a hugely abnormal karyotype. 3'-OH in these lines may have been permitted to shorten beyond the minimal 3'-OH length necessary for genomic stability, due to the forced expression of hTERT, ensuring bypass of replicative senescence activation pathways. It is plausible that 3'-OH length in these lines may be insufficient to allow the G-rich strand overhang to invade the duplex array to form a T-loop or any other non-canonical structure. In support of this, previous experiments in our laboratory showed these lines to exhibit a high degree of dicentric chromosomes (Cui et al., 2002), not apparent in any of the other lines, which indicates telomere end-to-end fusions, the likelihood of which may be increased by loss of a 3' telomere capping structure (Fig. 6.9). This scenario may represent a tumourigenic setting where 3'-OH length (and stabilized mean telomere length) is shorter than the corresponding wild-type tissue, thus resulting in loss of end-protection and facilitating chromosomal dysfunction that augments the tumour cells.
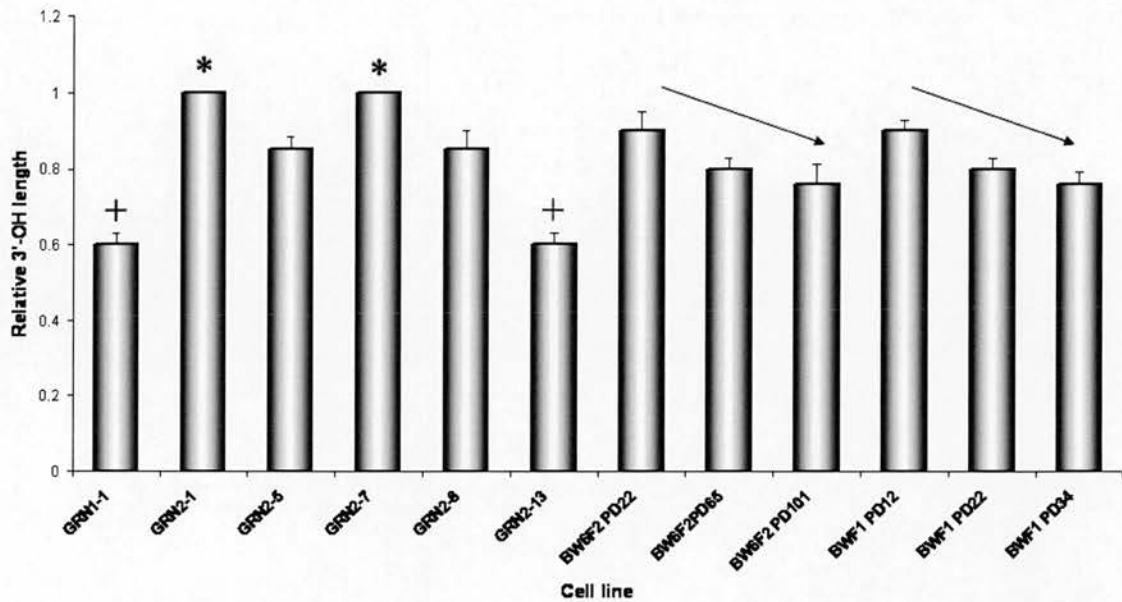
Figure 6.9: **Relative 3-OH length in normal and hTERT-immortalized sheep fibroblasts.** Maximal telomeric overhang is presented relative to the GRN2-1 and GRN2-7 lines (denoted by an asterisk), which showed the longest T-OLA product (504nt). G-rich strand shortening in normal fibroblasts is shown on the right of chart, denoted by arrows. 3'-OH length was calculated as 384nt for both BWF1 and BW6F2 at a pre-senescent stage. The shortest 3'-OH length was calculated for GRN1-1 and GRN2-13 (312nt) and is denoted by a cross and may represent 3'-OH lengths insufficient to permit a telomere end-capping structure such as the T-loop.

In summary, the data presented shows that 3'-OH length in primary sheep fibroblasts, rather than be maintained during culture, gradually erodes and that maximal 3'-OH length correlates to mean telomere length. More informatively, the relative rate of 3'-OH loss was found to directly correlate to the relative rate of overall telomere loss. In addition, the correlation of 3'-OH length to telomere length is a function of hTERT gene expression in hTERT-immortalized sheep fibroblasts. A high degree of karyotypic instability is prevalent in hTERT-immortalized cell lines with a 3'-OH length below that of late stage normal fibroblasts, thus implying that the 3'-OH-governed telomere end-

protection structure is required for maintenance of genomic stability. This raises the interesting question of whether telomerase mediated telomere repeat addition results in 3'-OH length, sufficient to form a T-loop structure in any cells at all within the context of a tumour? And if not, how does the pro-survival role of telomerase override the seemingly compromised state of cell viability, conferred due to loss of telomere end-protection and consequent karyotypic abnormalities?

.

CHAPTER 7

DISCUSSION

Regulation of telomere length in mammalian cells is a complex multi-factorial process involving not only a dynamic interplay of telomere- and telomerase-associated factors, but also the physical configuration of telomeric structure at chromosomal termini. Hence both extrinsic and intrinsic factors inter-dependently contribute to maintain telomere metabolic homeostasis. The project presented here has used an alternative mammalian model, the sheep (*Ovis aries*), to gain valuable insight into telomere length regulation, with respect to aspects of both extrinsic and intrinsic factors regulating mammalian telomere length. The justification of this model was provided by previous research in our laboratory which showed that sheep fibroblasts have a defined *in vitro* lifespan, sheep telomeres have been reported to shorten at rates comparable to that reported in humans, and ectopic expression of hTERT effectively reconstitutes telomerase activity and immortalizes the cells (Cui et al., 2002 & 2003, Clark et al., 2003). This presents some considerable advantages of using the sheep system, when compared to the classical model, mouse. In general telomere and telomerase biology may be more reflective of human in the sheep.

7.1   Extrinsic regulation of telomere length

A previous study in our laboratory monitoring sheep fibroblasts immortalized with ectopic hTERT, showed that telomere erosion and genomic instability occur to an extent that is directly attributable to the level of hTERT expression; at higher levels of hTERT expression, full length telomeres are maintained and karyotypic stability is preserved. By contrast, at lower levels of hTERT expression, telomeres erode and karyotypic abnormalities manifest. Surprisingly, telomerase activity was comparable between these lines (Cui et al., 2002). This highlights the complex relationship between telomerase function and telomere maintenance. Based on this evidence, two general hypotheses were formulated: i) do non-catalytic motifs of hTERT mediate regulation of telomere length in a manner that can be distinguished from hTERT catalytic activity? ii) or is the hTERT catalytic domain solely rate-determining with respect to telomerase-mediated telomere maintenance? In order to address both these issues, a catalytically dysfunctional hTERT transgene was expressed in an hTERT-immortalized primary sheep foetal fibroblast line in which telomeres stabilize at an average length much shorter than the untransfected parental line. This strategy thereby permitted both a window in which telomere maintenance function may be attributed to hTERT that can be distinguished from enzymatic activity, but also a system to test the effects of catalytically inactive hTERT on active telomerase activity.

The data presented showed that clones exhibiting high levels of mutant hTERT expression inhibited telomerase activity, whereas clones exhibiting lower levels did not. These results indicated that the inhibition effect of mutant hTERT has a threshold and that this is likely due to a dominant-negative and/or competitive inhibition effect between the wild-type and mutant hTERT proteins. Thus mutant hTERT expression compromised wild-type telomerase activity in a manner directly attributable to mutant hTERT expression level. When mutant hTERT expression is sufficiently higher than the wild-type, it competitively inhibits the binding of wild-type hTERT to telomerase RNA or the formation of TERT homodimers, hence inhibition of telomerase activity. However, when TRAP assay was conducted using 0.5µg rather than 0.1µg protein lysate, low levels of telomerase activity was detectable in cells with high expressing mutant hTERT. This low level of telomerase activity could be due to a small number of cells in which mutant hTERT was silenced or expressed at low levels and highlights a caveat of considering dominant-negative anti-telomerase intervention in tumour cells. Furthermore, sufficiently high levels of mutant hTERT expression were found not only to inhibit telomerase activity but also to affect cellular proliferation and telomere length, which may be a consequence of telomerase inhibition. Although the general proliferation rate throughout culture was similar for all clones, one clone, shown to exhibit the highest relative levels of mutant hTERT, exhibited a period of slower proliferation after only a short period in culture, concurrent with a senescent morphology and positive senescence-associated β-galactosidase staining within a subset of cells within the population. However, the remaining cells in the population where telomerase

inhibition was presumably not effected, thereafter incurred a growth advantage and were thus selected for. This highlights the difficulty in regarding lines derived from a single colony as truly 'clonal'. Stochastic variation of this nature may account for heterogeneous populations *in vitro* that are inaccurately termed 'clonal' (Martin-ruiz et al., 2004).

Significant telomere attrition was evident in two of three clones with high levels of mutant hTERT expression. Telomeres in these clones eventually reached mean stabilized lengths much shorter than those in mock controls. These results seem to be directly attributable to mutant hTERT expression. Mutant hTERT/mutant hTERT and mutant hTERT/wild-type hTERT dimeric complexes are likely to be in much greater abundance than wild-type/wild-type dimers within these lines. Inhibition of telomerase activity and increased telomere attrition are therefore likely to be due to the compromising of wild-type homodimeric function at the telomere substrate due to the molar ratio imbalance of hTERT complexes. This is consistent with the notion that hTERT homodimers are necessary to form a functional telomerase complex at the telomere substrate (Prescott & Blackburn 1997) where catalytic domains of both hTERT molecules may function inter-dependently.

The long-term monitoring of these hTERT-immortalized lines revealed a critical caveat regarding the precarious nature of a sustained period of *in vitro* culture using transgenic lines. After ~ 3 months of continuous propagation, almost no hTERT message (wild-type and mutant) was evident in any of the lines, including mock controls. This hints at

the heterogeneous nature of these lines, whereby mutant hTERT may have been silenced in a subset of cells within a population, a subset unto which a growth advantage is conferred thereafter. As proliferation rates were nevertheless maintained uncompromised at the same rate throughout this period and as telomerase activity was high in all lines at late passage, the indirect inference was that endogenous sheep TERT may be activated in these lines. This event may plausibly occur as a consequence of a transformation event in these lines during long-term culture. It is interesting to note that in spite of the loss of mutant hTERT expression in the late passage of those two clones which exhibited relatively aggravated telomere attrition, the telomere length in these two clones did not recover to the length comparable to the mock controls after long-term culture, rather they stabilized at the short telomere length. This indicates that in sheep cells, telomerase may maintain but cannot elongate shortened telomeres, at least in this setting. This contrasts with human cells (Delhommeau et al., 2002) and may reflect intrinsic differences between hTERT expression in human cells and hTERT expression in sheep cells.

In summary, these results support the notion that telomere maintenance requires a functional telomerase complex with hTERT monomers likely interacting in an inter-dependent manner. Furthermore the result demonstrates that although hTERT non-catalytic domains may be necessary for telomerase assembly and processivity at the telomere substrate, they are not rate-determining. Catalytic hTERT domains appear to be a crucial rate-determining factor regarding processivity. In addition the study highlights the complexity of telomerase and telomere interplay; a discrepancy arose regarding one

clone, which demonstrated high levels of mutant hTERT expression that resulted in telomerase inhibition. Rather than aggravated telomere attrition as may have been predicted, average telomere length was maintained at a length comparable to mock controls. This emphasizes the limitations of using telomerase assays that incorporate a single-strand telomeric substrate. Double-strand telomeric binding proteins cannot exert a regulatory role at the telomere substrate as a result. As telomere length homeostasis is regulated by a number of associated factors such as those that constitute the Shelterin Complex, differences in expression level of these factors may account for discrepancies such as these. A more systemic approach, which regards a composite of data with respect to all these factors, will prove more beneficial in furthering our understanding of telomere length regulation. The data presented here is consistent with many lines of recent direct and indirect evidence which implicates hTERT to be functional as an inter-dependent homodimeric complex at the telomere substrate. It will be important to elucidate the minimal number of hTERT complexes that act to maintain senescence bypass, particularly in a tumour setting. Correspondingly it will be crucial to determine how many molecules of a dominant-negative hTERT protein are sufficient to inhibit active telomerase in tumour cells. Real time qPCR may provide an accurate picture of the minimal threshold below which telomerase is compromised, by providing molar stochiometries with respect to mutant and wild-type hTERT monomers. This will be of interest in determining the efficacy and targeting strategy of hTERT dominant-negative approaches using gene therapy. Data presented here highlights the requirement of sufficiently high levels of mutant hTERT that will persist throughout treatment of cancer patients. At present telomerase assays are not highly sensitive and therefore more subtle

differences in telomerase activity are not detected. A recent development (Quantitative Telomerase Detection Kit, Allied Biotech.) that is specifically designed for Real-time PCR detection of telomerase activity, may prove an invaluable tool in future measurement of telomerase activity.

7.2   Intrinsic regulation of telomere length

Seminal work in our laboratory has shown that the proliferative lifespan and telomere shortening rate of primary sheep cells is conserved after nuclear transfer. Donor cell lines at different ages and different proliferative capacities were used to clone fetuses and animals, from which new primary lines were generated; these lines exhibited the same proliferative capacities and rates of telomere shortening as the donor lines (Clark A. J. et al, 2003). This work demonstrated the fact that at least certain aspects of telomere length regulation are intrinsically determined. The classical view of telomeric termini as passive structures subject to extrinsic regulation has been dismissed with recent advances in telomere biology research. Advances in techniques such as Q-FISH that allow measurement of telomere length at the chromosomal level have revealed that individual telomeres shorten at different rates. This heterogeneity is now believed to be crucial in determining the onset of replicative senescence, where telomere lengths of a subset of the shortest telomeres most probably serve as an indicator of senescence activation rather than average telomere length in the population as a whole. Furthermore the 3'-OH of telomeric termini has been shown to form an end-capping T-loop configuration which may be crucial in maintaining genome stability. Some groups have

suggested that it is loss of this structure that is the causal trigger of replicative senescence, but compelling evidence for this is lacking. Others have postulated the idea of telomere shortening rate being determined by 3'-OH length; i.e. telomeres shorten by an amount proportional to the size of the 3'-OH.

The current venture again uses primary sheep fibroblasts as an alternative mammalian model system in which to descriptively analyze both telomere length heterogeneity and alterations to the 3'-OH in a temporal manner as a consequence of replicative ageing. Foetal fibroblast lines derived from the Black Welsh breed (BW6F2 and BWF1) were previously shown to differ in their replicative lifespan by ~3-fold, although average telomere length was similar both after derivation and at replicative senescence (Clark et al., 2003). The considerable difference in replicative lifespan was directly attributed to a ~3-fold difference in average telomere shortening rate. The key limitation of the previous study in our laboratory was that true telomere length heterogeneity was not accounted for, taking into account telomere shortening at individual telomeres. It is likely that average telomere shortening rate only indirectly indicates the functional consequence of telomere attrition. For example, telomere shortening rate within only a subset of telomeres may be directly correlated to the onset of replicative senescence rather than average telomere length in the karyotype *per se*. Therefore it was of interest to optimize Q-FISH methodology in the sheep system to attain a description of telomere shortening in the Black Welsh fibroblasts that takes into account true telomere heterogeneity and to calculate telomere shortening rate on this basis. The Q-FISH methodology had previously been optimized for mouse and human chromosomes,

conditions which were required to be modified prior to analysis on sheep metaphase spreads. Nevertheless to our knowledge, this is the first documented demonstration of Q-FISH in ovine cells. Generally, both lines show a reasonably normal distribution of telomere lengths; i.e. – a minority subset of telomeres with very long or very short telomeres, with the majority of telomeres representing an intermediate length. Therefore we can infer that average telomere length does not differ dramatically between these lines. However, BWF1 exhibits a greater proportion of very short telomeres at each snapshot of analysis. This suggests rather superficially that although replicative senescence may be triggered at a comparable 'mean' telomere length, the telomere shortening rate in a *subset* of telomeres within the BWF1 population may be a key determinant of the much earlier onset of senescence activation in this line and provides direct evidence of intrinsic differences in telomere shortening rate between the two lines. This is certainly in accordance with the 'subset of shortest telomeres' hypothesis which postulates that the mitotic clock is determined by a subset of telomeres with aggravated telomere attrition rates relative to the whole population of telomeres (postulated by Shay & Wright). This is an intriguing observation as these two lines were derived from the same genetic breed; what is the molecular basis that determines telomere shortening rate? how is this regulated? Using solely a descriptive study renders it difficult to ascertain whether the more pronounced telomere shortening rate in BWF1 is a key determinant of a shorter proliferative lifespan relative to BW6F2 or whether telomere shortening rate in this context is consequential of alternative intrinsic and extrinsic factors that determine proliferative lifespan? Some technical caveats regarding Q-FISH will be required to be overcome before a more thorough understanding of telomere

shortening that is of direct consequence, is permitted. Namely the method at present cannot distinguish between very short telomeres and true signal free ends. If this issue is resolved, the subset of individual telomeres which are true determinants of replicative senescence could be observed. It will be interesting to determine whether it is telomeres on the same subset of chromosomes that always correlate to senescence onset within a particular cell type or even species. It may be possible to therefore predict replicative lifespan of a cell line using a Q-FISH profile, thus providing a valuable tool to determine a window of opportunity for approaches such as gene targeting via retroviral transduction.

One determinant of telomere shortening rate that has been postulated (Wright & Shay) states that telomere shortening rate is directly determined by 3'-OH length. In this respect, telomere erosion would be predicted to be directly proportional to the amount 3'-OH loss after each round of cell division. However evidence to indicate that the 3'-OH varies in length during successive rounds of cell division is not as yet compelling; some have argued for erosion of 3-OH only at M1 stage senescence (Stewart et al., 2003), whilst others have argued that this occurs as a consequence of M2 stage crisis (Chai et al., 2005). We again used the Black Welsh sheep fibroblasts to attempt to resolve these issues. The Telomere-Oligonucleotide Ligation Assay (T-OLA) was modified to investigate whether the G-rich 3'-OH alters during *in vitro* culture of normal sheep fibroblasts and if so, whether this is a direct correlate to telomere shortening rate. Telomeric overhang shortening paralleled mean telomere length shortening in both lines and was found to be a significant correlate ($r = 0.79$). This indicated that the 3'-OH alters during replicative ageing in these lines and may thus reflect species differences

between sheep and human. However there was no evidence that there is a *direct* correlation between telomere and 3'-OH shortening; telomere shortening per PD is significantly more pronounced than 3'-OH shortening per PD, thus the data does not provide evidence for telomere shortening rate being directly proportional to the size of the 3'-OH. However 3'-OH length at the initial and late stage pre-senescent stage of analysis is similar for both lines, although 3'-OH shortening rate is more pronounced in BWF1. This is consistent with a more pronounced average telomere shortening rate in BWF1. Therefore although telomeres in these lines do not shorten by the size of the 3'-OH, both the 3'-OH and overall telomere length, shorten as a consequence of cellular division. It is unclear as to the functional significance of 3'-OH length with respect to replicative lifespan and senescence onset in these sheep fibroblast lines. One factor that may determine intrinsic differences in telomere and 3'-OH shortening rate is response to oxidative stress incurred during culture conditions. The von Zglinicki lab (Newcastle, UK) have shown that peroxide levels rose significantly for both lines under conditions of hyperoxia, where levels were 3-fold more pronounced in BWF1 than for BW6F2. This indicates that BWF1 has much reduced anti-oxidative defence capabilities. We this reasoned that culture of early passage BWF1 fibroblasts in a 2% oxygen chamber would increase replicative lifespan to a duration comparable to BW6F2 due to a much lower level of oxidative stress. Although culture in 2% oxygen failed to reduce the rate of telomere shortening in this setting, this may be due to the BWF1 line being already adapted to previous conditions of culture in our laboratory and so the result does not exclude an important role of oxidative stress with respect to determining telomere and

3'-OH shortening rates. A definitive experiment will require exposing mammalian cells to various levels of oxidative stress immediately upon derivation of the lines.

We further investigated whether it there is a correlation between telomerase activity and 3'-OH in a normal cellular context. hTERT-immortalized Black Welsh sheep fibroblasts were generated in our laboratory previously and it was reported that telomere maintenance and karyotypic stability are directly correlated to levels of hTERT expression (Cui et al., 2002). The current analysis of 3'-OH in this setting revealed a significant correlation ($r = 0.702$) between maximal 3'-OH length and copies of hTERT mRNA per cell. The longest 3'-OH length, concurrent with near maximal mean telomere length and stable karyotype, was evident in lines exhibiting >300 copies of hTERT mRNA per cell. Conversely, shortest 3'-OH length, concurrent with shortest mean telomere length and grossly abnormal karyotype, was evident in lines exhibiting <0.5 copies of hTERT mRNA per cell. In particular, the lines that exhibited the lowest levels of hTERT and shortest mean telomere length also exhibited the shortest 3'-OH length and were the only lines to exhibit dicentric chromosomes. As the 3'-OH length is these lines were shorter than the 3'-OH in the late pre-senescent stage of the parental unmodified lines, this raises the question as to whether 3'-OH length in these lines is in fact sufficient to form a telomere end-capping structure such as the T-loop. Dicentric chromosomes provide evidence of end to end fusions presumably permitted by sufficient loss of 3'-OH.

The data presented on the basis of 3'-OH length in primary sheep fibroblasts suggests that 3'-OH shortens and parallels telomere shortening. In the setting of hTERT-immortalized fibroblasts, 3'-OH may correlate to hTERT expression-determined telomere length, rather than hTERT expression *per se*. Although a correlation is observed between 3'-OH shortening and overall average telomere shortening, length of shortening in the latter is not directly proportional to the size of the overhang. Therefore the precise determinant of telomere shortening rate in this setting remains unclear. The correlation between 3'-OH shortening and average telomere length shortening leads us to speculate whether the same or similar machinery (with respect to the plethora of telomere-associated factors known to function at the telomere substrate) controls both telomere length and 3'-OH length in mammalian cells.

Concluding remarks

The experimental approaches and data presented in this project underline the complexity of telomere length regulation in mammalian cells. Telomere length homeostasis is governed by a plethora of inter-dependent factors, which act both intrinsically and extrinsically at chromosomal termini. Data presented here indirectly supports the concept of the telomerase complex functioning as an inter-dependent dimer at the telomere substrate, where the reverse transcriptase domain of hTERT appears the key rate-determining factor with respect to telomere maintenance. However certain discrepancies within this study highlight the requirement to invoke studies of a multitude of telomere- and telomerase-associated factors at telomeres. Expression levels of all these factors may be crucial to determine both telomere shortening rates and telomere maintenance capabilities at particular stages of analysis. A consilient approach from groups investigating these factors will further our understanding of the complex interplay at telomeres.

Advances in techniques to analyze telomere length heterogeneity and to measure the 3'-OH, provide powerful tools to descriptively study the intrinsic factors that determine and/or are determined by telomere length. Data presented here demonstrates that telomere shortening rate and replicative lifespan are at least in part determined by telomere shortening rates within a subset of short telomeres within a population, rather than average telomere length. Moreover, the data provides evidence that the 3'-OH shortens as a consequence of cellular division, but that telomere shortening rate is not directly proportional to the size of the 3'-OH. However at present, measurement of the

3'-OH is based on analysis on a population as a whole and does not resolve 3'-OH on individual telomeres. Therefore further advances in the method of 3'-OH measurement that permits the resolution of overhangs of individual telomeres will be crucial in determining whether replicative senescence is triggered by the loss of an end-capping structure in a subset of cells, once the 3'-OH has fallen below a critical minimum length for that particular cell line. In this setting it will be important to visualize telomere ends using EM technology to verify absence/presence of an end-capping structure. The milestone for this avenue of research will be the conclusive understanding of the causal and consequential progression from senescence activation at the M1 stage, through to events at M2 crisis. At present, much of the argument is circular.

Current advances in telomere and telomerase biology will supplement novel ideas regarding cancer cell biology. What is the complete spectrum regarding the role of telomerase in tumour cells? Why are telomeres permitted to be shorter in many tumour cells than corresponding wild-type cells? Do tumour cells have sufficient 3'-OH lengths to enable a telomere-capping structure to exist? These questions will have to be regarded with respect to the hierarchical model of tumour cells. It will be crucial to ask what the key differences are in telomere length, 3'-OH length, and telomerase activity in tumour-initiating populations when compared to their non-tumourigenic progeny. These factors may be vital to maintain the unique status of a prospective cancer stem cell and therefore may provide a means for a more targeted approach for cancer therapy, such as targeting anti-telomerase drugs specifically to cancer stem cell populations.

Reference List

Al-Hajj,M., Wicha,M.S., ito-Hernandez,A., Morrison,S.J., and Clarke,M.F. (2003). Prospective identification of tumorigenic breast cancer cells. Proc. Natl. Acad. Sci. U. S. A *100*, 3983-3988.

Allsopp,R.C., Vaziri,H., Patterson,C., Goldstein,S., Younglai,E.V., Futcher,A.B., Greider,C.W., and Harley,C.B. (1992). Telomere length predicts replicative capacity of human fibroblasts. Proc. Natl. Acad. Sci. U. S. A *89*, 10114-10118.

Allsopp,R.C., Chang,E., Kashefi-Aazam,M., Rogaev,E.I., Piatyszek,M.A., Shay,J.W., and Harley,C.B. (1995). Telomere shortening is associated with cell division in vitro and in vivo. Exp. Cell Res. *220*, 194-200.

Arai,K., Masutomi,K., Khurts,S., Kaneko,S., Kobayashi,K., and Murakami,S. (2002). Two independent regions of human telomerase reverse transcriptase are important for its oligomerization and telomerase activity. J. Biol Chem. *277*, 8538-8544.

Armbruster,B.N., Banik,S.S., Guo,C., Smith,A.C., and Counter,C.M. (2001). N-terminal domains of the human telomerase catalytic subunit required for enzyme activity in vivo. Mol Cell Biol *21*, 7775-7786.

Armbruster,B.N., Linardic,C.M., Veldman,T., Bansal,N.P., Downie,D.L., and Counter,C.M. (2004). Rescue of an hTERT mutant defective in telomere elongation by fusion with hPot1. Mol Cell Biol *24*, 3552-3561.

Artandi,S.E., Alson,S., Tietze,M.K., Sharpless,N.E., Ye,S., Greenberg,R.A., Castrillon,D.H., Horner,J.W., Weiler,S.R., Carrasco,R.D., and DePinho,R.A. (2002). Constitutive telomerase expression promotes mammary carcinomas in aging mice. Proc. Natl. Acad. Sci. U. S. A *99*, 8191-8196.

Asai,A., Oshima,Y., Yamamoto,Y., Uochi,T.A., Kusaka,H., Akinaga,S., Yamashita,Y., Pongracz,K., Pruzan,R., Wunder,E., Piatyszek,M., Li,S., Chin,A.C., Harley,C.B., and Gryaznov,S. (2003). A novel telomerase template antagonist (GRN163) as a potential anticancer agent. Cancer Res. *63*, 3931-3939.

Autexier,C. and Greider,C.W. (1994). Functional reconstitution of wild-type and mutant Tetrahymena telomerase. Genes Dev. *8*, 563-575.

Autexier,C. and Greider,C.W. (1995). Boundary elements of the Tetrahymena telomerase RNA template and alignment domains. Genes Dev. *9*, 2227-2239.

Autexier,C. and Lue,N.F. (2006). The Structure and Function of Telomerase Reverse Transcriptase. Annu. Rev. Biochem.

Bachand,F. and Autexier,C. (2001). Functional regions of human telomerase reverse transcriptase and human telomerase RNA required for telomerase activity and RNA-protein interactions. Mol Cell Biol *21*, 1888-1897.

Bailey,S.M. and Murnane,J.P. (2006). Telomeres, chromosome instability and cancer. Nucleic Acids Res. *34*, 2408-2417.

Balin,A.K., Goodman,D.B., Rasmussen,H., and Cristofalo,V.J. (1977). The effect of oxygen and vitamin E on the lifespan of human diploid cells in vitro. J. Cell Biol. *74*, 58-67.

Banik,S.S., Guo,C., Smith,A.C., Margolis,S.S., Richardson,D.A., Tirado,C.A., and Counter,C.M. (2002). C-terminal regions of the human telomerase catalytic subunit essential for in vivo enzyme activity. Mol. Cell Biol. *22*, 6234-6246.

Baumann,P. and Cech,T.R. (2001). Pot1, the putative telomere end-binding protein in fission yeast and humans. Science *292*, 1171-1175.

Beattie,T.L., Zhou,W., Robinson,M.O., and Harrington,L. (2001). Functional multimerization of the human telomerase reverse transcriptase. Mol. Cell Biol. *21*, 6151-6160.

Bilaud,T., Brun,C., Ancelin,K., Koering,C.E., Laroche,T., and Gilson,E. (1997). Telomeric localization of TRF2, a novel human telobox protein. Nat. Genet. *17*, 236-239.

Blackburn,E.H. and Gall,J.G. (1978). A tandemly repeated sequence at the termini of the extrachromosomal ribosomal RNA genes in Tetrahymena. J. Mol. Biol. *120*, 33-53.

Blackburn,E.H. (2000). Telomere states and cell fates. Nature *408*, 53-56.

Blackburn,E.H. (2001). Switching and signaling at the telomere. Cell *106*, 661-673.

Blasco,M.A., Funk,W., Villeponteau,B., and Greider,C.W. (1995). Functional characterization and developmental regulation of mouse telomerase RNA. Science *269*, 1267-1270.

Blasco,M.A., Rizen,M., Greider,C.W., and Hanahan,D. (1996). Differential regulation of telomerase activity and telomerase RNA during multi-stage tumorigenesis. Nat. Genet. *12*, 200-204.

Blasco,M.A., Lee,H.W., Hande,M.P., Samper,E., Lansdorp,P.M., DePinho,R.A., and Greider,C.W. (1997). Telomere shortening and tumor formation by mouse cells lacking telomerase RNA. Cell *91*, 25-34.

Blasco,M.A. (2003). Telomeres in cancer and aging: lessons from the mouse. Cancer Lett. *194*, 183-188.

Bodnar,A.G., Ouellette,M., Frolkis,M., Holt,S.E., Chiu,C.P., Morin,G.B., Harley,C.B., Shay,J.W., Lichtsteiner,S., and Wright,W.E. (1998). Extension of life-span by introduction of telomerase into normal human cells. Science *279*, 349-352.

Bonnet,D. and Dick,J.E. (1997). Human acute myeloid leukemia is organized as a hierarchy that originates from a primitive hematopoietic cell. Nat. Med. *3*, 730-737.

Broccoli,D., Godley,L.A., Donehower,L.A., Varmus,H.E., and de,L.T. (1996). Telomerase activation in mouse mammary tumors: lack of detectable telomere shortening and evidence for regulation of telomerase RNA with cell proliferation. Mol Cell Biol *16*, 3765-3772.

Broccoli,D., Smogorzewska,A., Chong,L., and de,L.T. (1997). Human telomeres contain two distinct Myb-related proteins, TRF1 and TRF2. Nat Genet. *17*, 231-235.

Bryan,T.M., Englezou,A., la-Pozza,L., Dunham,M.A., and Reddel,R.R. (1997). Evidence for an alternative mechanism for maintaining telomere length in human tumors and tumor-derived cell lines. Nat Med. *3*, 1271-1274.

Bryce,L.A., Morrison,N., Hoare,S.F., Muir,S., and Keith,W.N. (2000). Mapping of the gene for the human telomerase reverse transcriptase, hTERT, to chromosome 5p15.33 by fluorescence in situ hybridization. Neoplasia. *2*, 197-201.

Cao,Y., Li,H., Deb,S., and Liu,J.P. (2002). TERT regulates cell survival independent of telomerase enzymatic activity. Oncogene *21*, 3130-3138.

Cawthon,R.M., Smith,K.R., O'Brien,E., Sivatchenko,A., and Kerber,R.A. (2003). Association between telomere length in blood and mortality in people aged 60 years or older. Lancet *361*, 393-395.

Chai,W., Ford,L.P., Lenertz,L., Wright,W.E., and Shay,J.W. (2002). Human Ku70/80 associates physically with telomerase through interaction with hTERT. J. Biol. Chem. *277*, 47242-47247.

Chai,W., Shay,J.W., and Wright,W.E. (2005). Human telomeres maintain their overhang length at senescence. Mol Cell Biol *25*, 2158-2168.

Chang,S. and DePinho,R.A. (2002). Telomerase extracurricular activities. Proc. Natl. Acad. Sci. U. S. A *99*, 12520-12522.

Chen,J.L., Blasco,M.A., and Greider,C.W. (2000). Secondary structure of vertebrate telomerase RNA. Cell *100*, 503-514.

Chen,J.L., Opperman,K.K., and Greider,C.W. (2002). A critical stem-loop structure in the CR4-CR5 domain of mammalian telomerase RNA. Nucleic Acids Res. *30*, 592-597.

Chen,J.L. and Greider,C.W. (2003). Determinants in mammalian telomerase RNA that mediate enzyme processivity and cross-species incompatibility. EMBO J. *22*, 304-314.

Chen,J.L. and Greider,C.W. (2003). Template boundary definition in mammalian telomerase. Genes Dev. *17*, 2747-2752.

Chen,Q. and Ames,B.N. (1994). Senescence-like growth arrest induced by hydrogen peroxide in human diploid fibroblast F65 cells. Proc. Natl. Acad. Sci. U. S. A *91*, 4130-4134.

Chiang,Y.J., Nguyen,M.L., Gurunathan,S., Kaminker,P., Tessarollo,L., Campisi,J., and Hodes,R.J. (2006). Generation and characterization of telomere length maintenance in tankyrase 2-deficient mice. Mol Cell Biol *26*, 2037-2043.

Chiu,C.P. and Harley,C.B. (1997). Replicative senescence and cell immortality: the role of telomeres and telomerase. Proc. Soc. Exp. Biol. Med. *214*, 99-106.

Chong,L., van,S.B., Broccoli,D., Erdjument-Bromage,H., Hanish,J., Tempst,P., and de,L.T. (1995). A human telomeric protein. Science *270*, 1663-1667.

Chung,H.K., Cheong,C., Song,J., and Lee,H.W. (2005). Extratelomeric functions of telomerase. Curr. Mol. Med. *5*, 233-241.

Cimino-Reale,G., Pascale,E., Battiloro,E., Starace,G., Verna,R., and D'Ambrosio,E. (2001). The length of telomeric G-rich strand 3'-overhang measured by oligonucleotide ligation assay. Nucleic Acids Res. *29*, E35.

Clark,A.J., Ferrier,P., Aslam,S., Burl,S., Denning,C., Wylie,D., Ross,A., de,S.P., Wilmut,I., and Cui,W. (2003). Proliferative lifespan is conserved after nuclear transfer. Nat Cell Biol *5*, 535-538.

Collins,K. and Mitchell,J.R. (2002). Telomerase in the human organism. Oncogene *21*, 564-579.

Connelly,J.C. and Leach,D.R. (2002). Tethering on the brink: the evolutionarily conserved Mre11-Rad50 complex. Trends Biochem. Sci. *27*, 410-418.

Cook,B.D., Dynek,J.N., Chang,W., Shostak,G., and Smith,S. (2002). Role for the related poly(ADP-Ribose) polymerases tankyrase 1 and 2 at human telomeres. Mol. Cell Biol. *22*, 332-342.

Cooke,H.J. and Smith,B.A. (1986). Variability at the telomeres of the human X/Y pseudoautosomal region. Cold Spring Harb. Symp. Quant. Biol. *51 Pt 1*, 213-219.

Counter,C.M., Avilion,A.A., LeFeuvre,C.E., Stewart,N.G., Greider,C.W., Harley,C.B., and Bacchetti,S. (1992). Telomere shortening associated with chromosome instability is arrested in immortal cells which express telomerase activity. EMBO J. *11*, 1921-1929.

Counter,C.M., Hirte,H.W., Bacchetti,S., and Harley,C.B. (1994). Telomerase activity in human ovarian carcinoma. Proc. Natl. Acad. Sci. U. S. A *91*, 2900-2904.

Counter,C.M., Hahn,W.C., Wei,W., Caddle,S.D., Beijersbergen,R.L., Lansdorp,P.M., Sedivy,J.M., and Weinberg,R.A. (1998). Dissociation among in vitro telomerase activity, telomere maintenance, and cellular immortalization. Proc. Natl. Acad. Sci. U. S. A *95*, 14723-14728.

Cristofalo,V.J., Phillips,P.D., Sorger,T., and Gerhard,G. (1989). Alterations in the responsiveness of senescent cells to growth factors. J. Gerontol. *44*, 55-62.

Cui,W., Aslam,S., Fletcher,J., Wylie,D., Clinton,M., and Clark,A.J. (2002). Stabilization of telomere length and karyotypic stability are directly correlated with the level of hTERT gene expression in primary fibroblasts. J. Biol Chem. *277*, 38531-38539.

Cui,W., Wylie,D., Aslam,S., Dinnyes,A., King,T., Wilmut,I., and Clark,A.J. (2003). Telomerase-immortalized sheep fibroblasts can be reprogrammed by nuclear transfer to undergo early development. Biol Reprod. *69*, 15-21.

dda di,F.F., Reaper,P.M., Clay-Farrace,L., Fiegler,H., Carr,P., von,Z.T., Saretzki,G., Carter,N.P., and Jackson,S.P. (2003). A DNA damage checkpoint response in telomere-initiated senescence. Nature *426*, 194-198.

de,Lange.T. (2001). Cell biology. Telomere capping--one strand fits all. Science *292*, 1075-1076.

de,Lange.T. (2002). Protection of mammalian telomeres. Oncogene *21*, 532-540.

de,Lange.T. (2004). T-loops and the origin of telomeres. Nat Rev Mol Cell Biol *5*, 323-329.

de,Lange.T. (2005). Shelterin: the protein complex that shapes and safeguards human telomeres. Genes Dev. *19*, 2100-2110.

Delhommeau,F., Thierry,A., Feneux,D., Lauret,E., Leclercq,E., Courtier,M.H., Sainteny,F., Vainchenker,W., and naceur-Griscelli,A. (2002). Telomere dysfunction and telomerase reactivation in human leukemia cell lines after telomerase inhibition by the expression of a dominant-negative hTERT mutant. Oncogene *21*, 8262-8271.

Dimri,G.P., Martinez,J.L., Jacobs,J.J., Keblusek,P., Itahana,K., Van,L.M., Campisi,J., Wazer,D.E., and Band,V. (2002). The Bmi-1 oncogene induces telomerase activity and immortalizes human mammary epithelial cells. Cancer Res. *62*, 4736-4745.

Djojosubroto,M.W., Chin,A.C., Go,N., Schaetzlein,S., Manns,M.P., Gryaznov,S., Harley,C.B., and Rudolph,K.L. (2005). Telomerase antagonists GRN163 and GRN163L inhibit tumor growth and increase chemosensitivity of human hepatoma. Hepatology *42*, 1127-1136.

Downs,J.A. and Jackson,S.P. (2004). A means to a DNA end: the many roles of Ku. Nat. Rev. Mol. Cell Biol. *5*, 367-378.

Drosopoulos,W.C., Direnzo,R., and Prasad,V.R. (2005). Human telomerase RNA template sequence is a determinant of telomere repeat extension rate. J. Biol Chem. *280*, 32801-32810.

Dunham,M.A., Neumann,A.A., Fasching,C.L., and Reddel,R.R. (2000). Telomere maintenance by recombination in human cells. Nat. Genet. *26*, 447-450.

Eickbush,T.H. (1997). Telomerase and retrotransposons: which came first? Science *277*, 911-912.

era-Bloch,L., Houghton,J., Lenahan,M., Jha,K.K., and Ozer,H.L. (2002). Termination of lifespan of SV40-transformed human fibroblasts in crisis is due to apoptosis. J. Cell Physiol *190*, 332-344.

Erdmann,N., Liu,Y., and Harrington,L. (2004). Distinct dosage requirements for the maintenance of long and short telomeres in mTert heterozygous mice. Proc. Natl. Acad. Sci. U. S. A *101*, 6080-6085.

Evans,S.K. and Lundblad,V. (2000). Positive and negative regulation of telomerase access to the telomere. J. Cell Sci. *113 Pt 19*, 3357-3364.

Fajkus,J., Sykorova,E., and Leitch,A.R. (2005). Telomeres in evolution and evolution of telomeres. Chromosome. Res. *13*, 469-479.

Feng,J., Funk,W.D., Wang,S.S., Weinrich,S.L., Avilion,A.A., Chiu,C.P., Adams,R.R., Chang,E., Allsopp,R.C., Yu,J., and . (1995). The RNA component of human telomerase. Science *269*, 1236-1241.

Ferbeyre,G., de,S.E., Lin,A.W., Querido,E., McCurrach,M.E., Hannon,G.J., and Lowe,S.W. (2002). Oncogenic ras and p53 cooperate to induce cellular senescence. Mol. Cell Biol. *22*, 3497-3508.

Fiset,S. and Chabot,B. (2001). hnRNP A1 may interact simultaneously with telomeric DNA and the human telomerase RNA in vitro. Nucleic Acids Res. *29*, 2268-2275.

Flores,I., Cayuela,M.L., and Blasco,M.A. (2005). Effects of Telomerase and Telomere Length on Epidermal Stem Cell Behavior. Science.

Flores,I., Benetti,R., and Blasco,M.A. (2006). Telomerase regulation and stem cell behaviour. Curr. Opin. Cell Biol.

Forsythe,H.L., Jarvis,J.L., Turner,J.W., Elmore,L.W., and Holt,S.E. (2001). Stable association of hsp90 and p23, but Not hsp70, with active human telomerase. J. Biol. Chem. *276*, 15571-15574.

Forsythe,H.L., Elmore,L.W., Jensen,K.O., Landon,M.R., and Holt,S.E. (2002). Retroviral-mediated expression of telomerase in normal human cells provides a selective growth advantage. Int. J. Oncol. *20*, 1137-1143.

Franco,S., Alsheimer,M., Herrera,E., Benavente,R., and Blasco,M.A. (2002). Mammalian meiotic telomeres: composition and ultrastructure in telomerase-deficient mice. Eur. J. Cell Biol. *81*, 335-340.

Frippiat,C., Chen,Q.M., Zdanov,S., Magalhaes,J.P., Remacle,J., and Toussaint,O. (2001). Subcytotoxic H2O2 stress triggers a release of transforming growth factor-beta 1, which induces biomarkers of cellular senescence of human diploid fibroblasts. J. Biol. Chem. *276*, 2531-2537.

Gilley,D. and Blackburn,E.H. (1996). Specific RNA residue interactions required for enzymatic functions of Tetrahymena telomerase. Mol. Cell Biol. *16*, 66-75.

Gorbunova,V., Seluanov,A., and Pereira-Smith,O.M. (2002). Expression of human telomerase (hTERT) does not prevent stress-induced senescence in normal human fibroblasts but protects the cells from stress-induced apoptosis and necrosis. J. Biol. Chem. *277*, 38540-38549.

Graakjaer,J., Bischoff,C., Korsholm,L., Holstebroe,S., Vach,W., Bohr,V.A., Christensen,K., and Kolvraa,S. (2003). The pattern of chromosome-specific variations in telomere length in humans is determined by inherited, telomere-near factors and is maintained throughout life. Mech. Ageing Dev. *124*, 629-640.

Graakjaer,J., Pascoe,L., Der-Sarkissian,H., Thomas,G., Kolvraa,S., Christensen,K., and Londono-Vallejo,J.A. (2004). The relative lengths of individual telomeres are defined in the zygote and strictly maintained during life. Aging Cell *3*, 97-102.

Graakjaer,J., Der-Sarkissian,H., Schmitz,A., Bayer,J., Thomas,G., Kolvraa,S., and Londono-Vallejo,J.A. (2006). Allele-specific relative telomere lengths are inherited. Hum. Genet.

Greenberg,R.A., Allsopp,R.C., Chin,L., Morin,G.B., and DePinho,R.A. (1998). Expression of mouse telomerase reverse transcriptase during development, differentiation and proliferation. Oncogene *16*, 1723-1730.

Greider,C.W. and Blackburn,E.H. (1985). Identification of a specific telomere terminal transferase activity in Tetrahymena extracts. Cell *43*, 405-413.

Greider,C.W. and Blackburn,E.H. (1987). The telomere terminal transferase of Tetrahymena is a ribonucleoprotein enzyme with two kinds of primer specificity. Cell *51*, 887-898.

Greider,C.W. (1990). Telomeres, telomerase and senescence. Bioessays *12*, 363-369.

Greider,C.W. (1999). Telomeres do D-loop-T-loop. Cell *97*, 419-422.

Griffith,J.D., Comeau,L., Rosenfield,S., Stansel,R.M., Bianchi,A., Moss,H., and de,L.T. (1999). Mammalian telomeres end in a large duplex loop. Cell *97*, 503-514.

Hackett,J.A., Feldser,D.M., and Greider,C.W. (2001). Telomere dysfunction increases mutation rate and genomic instability. Cell *106*, 275-286.

Harley,C.B., Futcher,A.B., and Greider,C.W. (1990). Telomeres shorten during ageing of human fibroblasts. Nature *345*, 458-460.

Harley,C.B. (1991). Telomere loss: mitotic clock or genetic time bomb? Mutat. Res. *256*, 271-282.

Harley,C.B. (2002). Telomerase is not an oncogene. Oncogene *21*, 494-502.

Harrington,L., McPhail,T., Mar,V., Zhou,W., Oulton,R., Bass,M.B., Arruda,I., and Robinson,M.O. (1997). A mammalian telomerase-associated protein. Science *275*, 973-977.

Harrington,L. (2004). Does the reservoir for self-renewal stem from the ends? Oncogene *23*, 7283-7289.

Harrington,L. (2004). Those dam-aged telomeres! Curr. Opin. Genet. Dev. *14*, 22-28.

Hashimoto,M., Kyo,S., Masutomi,K., Maida,Y., Sakaguchi,J., Mizumoto,Y., Nakamura,M., Hahn,W.C., and Inoue,M. (2005). Analysis of telomeric single-strand overhang length in human endometrial cancers. FEBS Lett. *579*, 2959-2964.

Hastie,N.D., Dempster,M., Dunlop,M.G., Thompson,A.M., Green,D.K., and Allshire,R.C. (1990). Telomere reduction in human colorectal carcinoma and with ageing. Nature *346*, 866-868.

Haussmann,M.F., Winkler,D.W., O'Reilly,K.M., Huntington,C.E., Nisbet,I.C., and Vleck,C.M. (2003). Telomeres shorten more slowly in long-lived birds and mammals than in short-lived ones. Proc. R. Soc. Lond B Biol Sci. *270*, 1387-1392.

Hayflick,L. and Moorehead,P.S. (1961). The serial cultivation of human diploid cell strains. Exp. Cell Res. *25*, 585-621.

Hayflick,L. (1984). Intracellular determinants of cell aging. Mech. Ageing Dev. *28*, 177-185.

Hemann,M.T., Strong,M.A., Hao,L.Y., and Greider,C.W. (2001). The shortest telomere, not average telomere length, is critical for cell viability and chromosome stability. Cell *107*, 67-77.

Herbig,U., Jobling,W.A., Chen,B.P., Chen,D.J., and Sedivy,J.M. (2004). Telomere shortening triggers senescence of human cells through a pathway involving ATM, p53, and p21(CIP1), but not p16(INK4a). Mol Cell *14*, 501-513.

Herrera,E., Samper,E., Martin-Caballero,J., Flores,J.M., Lee,H.W., and Blasco,M.A. (1999). Disease states associated with telomerase deficiency appear earlier in mice with short telomeres. EMBO J. *18*, 2950-2960.

Herskind,C. and Rodemann,H.P. (2000). Spontaneous and radiation-induced differentiationof fibroblasts. Exp. Gerontol. *35*, 747-755.

Hockemeyer,D., Sfeir,A.J., Shay,J.W., Wright,W.E., and de,L.T. (2005). POT1 protects telomeres from a transient DNA damage response and determines how human chromosomes end. EMBO J. *24*, 2667-2678.

Hockemeyer,D., Daniels,J.P., Takai,H., and de,L.T. (2006). Recent expansion of the telomeric complex in rodents: Two distinct POT1 proteins protect mouse telomeres. Cell *126*, 63-77.

Holt,S.E., Aisner,D.L., Baur,J., Tesmer,V.M., Dy,M., Ouellette,M., Trager,J.B., Morin,G.B., Toft,D.O., Shay,J.W., Wright,W.E., and White,M.A. (1999). Functional requirement of p23 and Hsp90 in telomerase complexes. Genes Dev. *13*, 817-826.

Hopfner,K.P., Putnam,C.D., and Tainer,J.A. (2002). DNA double-strand break repair from head to tail. Curr. Opin. Struct. Biol. *12*, 115-122.

Houghtaling,B.R., Cuttonaro,L., Chang,W., and Smith,S. (2004). A Dynamic Molecular Link between the Telomere Length Regulator TRF1 and the Chromosome End Protector TRF2. Curr. Biol *14*, 1621-1631.

Huard,S., Moriarty,T.J., and Autexier,C. (2003). The C terminus of the human telomerase reverse transcriptase is a determinant of enzyme processivity. Nucleic Acids Res. *31*, 4059-4070.

Huber,M.D., Lee,D.C., and Maizels,N. (2002). G4 DNA unwinding by BLM and Sgs1p: substrate specificity and substrate-specific inhibition. Nucleic Acids Res. *30*, 3954-3961.

Huffman,K.E., Levene,S.D., Tesmer,V.M., Shay,J.W., and Wright,W.E. (2000). Telomere shortening is proportional to the size of the G-rich telomeric 3'-overhang. J. Biol Chem. *275*, 19719-19722.

Huntly,B.J. and Gilliland,D.G. (2005). Leukaemia stem cells and the evolution of cancer-stem-cell research. Nat. Rev. Cancer *5*, 311-321.

Iwano,T., Tachibana,M., Reth,M., and Shinkai,Y. (2004). Importance of TRF1 for functional telomere structure. J. Biol Chem. *279*, 1442-1448.

Joeng,K.S., Song,E.J., Lee,K.J., and Lee,J. (2004). Long lifespan in worms with long telomeric DNA. Nat Genet. *36*, 607-611.

Jones,R.B., Lumpkin,C.K., Jr., and Smith,J.R. (1980). A stochastic model for cellular senescence. Part I. Theoretical considerations. J. Theor. Biol. *86*, 581-592.

Ju,Z. and Rudolph,K.L. (2006). Telomeres and telomerase in cancer stem cells. Eur. J. Cancer *42*, 1197-1203.

Kanaya,T., Kyo,S., Hamada,K., Takakura,M., Kitagawa,Y., Harada,H., and Inoue,M. (2000). Adenoviral expression of p53 represses telomerase activity through down-regulation of human telomerase reverse transcriptase transcription. Clin. Cancer Res. *6*, 1239-1247.

Karlseder,J., Broccoli,D., Dai,Y., Hardy,S., and de,L.T. (1999). p53- and ATM-dependent apoptosis induced by telomeres lacking TRF2. Science *283*, 1321-1325.

Karlseder,J., Smogorzewska,A., and de,L.T. (2002). Senescence induced by altered telomere state, not telomere loss. Science *295*, 2446-2449.

Kelleher,C., Kurth,I., and Lingner,J. (2005). Human protection of telomeres 1 (POT1) is a negative regulator of telomerase activity in vitro. Mol. Cell Biol. *25*, 808-818.

Kim Sh,S.H., Kaminker,P., and Campisi,J. (2002). Telomeres, aging and cancer: in search of a happy ending. Oncogene *21*, 503-511.

Kim,N.W., Piatyszek,M.A., Prowse,K.R., Harley,C.B., West,M.D., Ho,P.L., Coviello,G.M., Wright,W.E., Weinrich,S.L., and Shay,J.W. (1994). Specific association of human telomerase activity with immortal cells and cancer. Science *266*, 2011-2015.

Kim,N.W. and Wu,F. (1997). Advances in quantification and characterization of telomerase activity by the telomeric repeat amplification protocol (TRAP). Nucleic Acids Res. *25*, 2595-2597.

Kim,S.H., Kaminker,P., and Campisi,J. (1999). TIN2, a new regulator of telomere length in human cells. Nat Genet. *23*, 405-412.

Kim,S.H., Beausejour,C., Davalos,A.R., Kaminker,P., Heo,S.J., and Campisi,J. (2004). TIN2 mediates functions of TRF2 at human telomeres. J. Biol. Chem. *279*, 43799-43804.

Kipling,D. and Cooke,H.J. (1990). Hypervariable ultra-long telomeres in mice. Nature *347*, 400-402.

Lansdorp,P.M. (2000). Repair of telomeric DNA prior to replicative senescence. Mech. Ageing Dev. *118*, 23-34.

Lapidot,T., Sirard,C., Vormoor,J., Murdoch,B., Hoang,T., Caceres-Cortes,J., Minden,M., Paterson,B., Caligiuri,M.A., and Dick,J.E. (1994). A cell initiating human acute myeloid leukaemia after transplantation into SCID mice. Nature *367*, 645-648.

Lei,M., Zaug,A.J., Podell,E.R., and Cech,T.R. (2005). Switching human telomerase on and off with hPOT1 protein in vitro. J. Biol Chem. *280*, 20449-20456.

Lengauer,C., Kinzler,K.W., and Vogelstein,B. (1997). Genetic instability in colorectal cancers. Nature *386*, 623-627.

Li,B., Oestreich,S., and de,L.T. (2000). Identification of human Rap1: implications for telomere evolution. Cell *101*, 471-483.

Lingner,J., Hughes,T.R., Shevchenko,A., Mann,M., Lundblad,V., and Cech,T.R. (1997). Reverse transcriptase motifs in the catalytic subunit of telomerase. Science *276*, 561-567.

Lingner,J., Cech,T.R., Hughes,T.R., and Lundblad,V. (1997). Three Ever Shorter Telomere (EST) genes are dispensable for in vitro yeast telomerase activity. Proc. Natl. Acad. Sci. U. S. A *94*, 11190-11195.

Liu,D., O'Connor,M.S., Qin,J., and Songyang,Z. (2004). Telosome, a mammalian telomere-associated complex formed by multiple telomeric proteins. J. Biol Chem. *279*, 51338-51342.

Liu,D., Safari,A., O'Connor,M.S., Chan,D.W., Laegeler,A., Qin,J., and Songyang,Z. (2004). PTOP interacts with POT1 and regulates its localization to telomeres. Nat. Cell Biol. *6*, 673-680.

Loayza,D. and De Lange,T. (2003). POT1 as a terminal transducer of TRF1 telomere length control. Nature *423*, 1013-1018.

Londono-Vallejo,J.A., DerSarkissian,H., Cazes,L., and Thomas,G. (2001). Differences in telomere length between homologous chromosomes in humans. Nucleic Acids Res. *29*, 3164-3171.

Lorenz,M., Saretzki,G., Sitte,N., Metzkow,S., and von,Z.T. (2001). BJ fibroblasts display high antioxidant capacity and slow telomere shortening independent of hTERT transfection. Free Radic. Biol. Med. *31*, 824-831.

Luce,M.C. and Cristofalo,V.J. (1992). Reduction in heat shock gene expression correlates with increased thermosensitivity in senescent human fibroblasts. Exp. Cell Res. *202*, 9-16.

Lundblad,V. and Szostak,J.W. (1989). A mutant with a defect in telomere elongation leads to senescence in yeast. Cell *57*, 633-643.

Makarov,V.L., Hirose,Y., and Langmore,J.P. (1997). Long G tails at both ends of human chromosomes suggest a C strand degradation mechanism for telomere shortening. Cell *88*, 657-666.

Martens,U.M., Chavez,E.A., Poon,S.S., Schmoor,C., and Lansdorp,P.M. (2000). Accumulation of short telomeres in human fibroblasts prior to replicative senescence. Exp. Cell Res. *256*, 291-299.

Martin-Rivera,L. and Blasco,M.A. (2001). Identification of functional domains and dominant negative mutations in vertebrate telomerase RNA using an in vivo reconstitution system. J. Biol. Chem. *276*, 5856-5865.

Martin-Ruiz,C., Saretzki,G., Petrie,J., Ladhoff,J., Jeyapalan,J., Wei,W., Sedivy,J., and von,Z.T. (2004). Stochastic variation in telomere shortening rate causes heterogeneity of human fibroblast replicative life span. J. Biol Chem. *279*, 17826-17833.

Maser,R.S. and DePinho,R.A. (2002). Connecting chromosomes, crisis, and cancer. Science *297*, 565-569.

Masutomi,K., Yu,E.Y., Khurts,S., Ben-Porath,I., Currier,J.L., Metz,G.B., Brooks,M.W., Kaneko,S., Murakami,S., DeCaprio,J.A., Weinberg,R.A., Stewart,S.A., and Hahn,W.C. (2003). Telomerase maintains telomere structure in normal human cells. Cell *114*, 241-253.

Masutomi,K. and Hahn,W.C. (2003). Telomerase and tumorigenesis. Cancer Lett. *194*, 163-172.

Masutomi,K., Possemato,R., Wong,J.M., Currier,J.L., Tothova,Z., Manola,J.B., Ganesan,S., Lansdorp,P.M., Collins,K., and Hahn,W.C. (2005). The telomerase reverse transcriptase regulates chromatin state and DNA damage responses. Proc. Natl. Acad. Sci. U. S. A *102*, 8222-8227.

McClintock,B. (1939). The Behavior in Successive Nuclear Divisions of a Chromosome Broken at Meiosis. Proc. Natl. Acad. Sci. U. S. A *25*, 405-416.

McElligott,R. and Wellinger,R.J. (1997). The terminal DNA structure of mammalian chromosomes. EMBO J. *16*, 3705-3714.

Meyerson,M., Counter,C.M., Eaton,E.N., Ellisen,L.W., Steiner,P., Caddle,S.D., Ziaugra,L., Beijersbergen,R.L., Davidoff,M.J., Liu,Q., Bacchetti,S., Haber,D.A., and Weinberg,R.A. (1997). hEST2, the putative human telomerase catalytic subunit gene, is up-regulated in tumor cells and during immortalization. Cell *90*, 785-795.

Meyne,J., Ratliff,R.L., and Moyzis,R.K. (1989). Conservation of the human telomere sequence (TTAGGG)n among vertebrates. Proc. Natl. Acad. Sci. U. S. A *86*, 7049-7053.

Mitchell,J.R., Wood,E., and Collins,K. (1999). A telomerase component is defective in the human disease dyskeratosis congenita. Nature *402*, 551-555.

Moriarty,T.J., Marie-Egyptienne,D.T., and Autexier,C. (2004). Functional organization of repeat addition processivity and DNA synthesis determinants in the human telomerase multimer. Mol Cell Biol *24*, 3720-3733.

Morin,G.B. (1989). The human telomere terminal transferase enzyme is a ribonucleoprotein that synthesizes TTAGGG repeats. Cell *59*, 521-529.

Morrison,S.J., Prowse,K.R., Ho,P., and Weissman,I.L. (1996). Telomerase activity in hematopoietic cells is associated with self-renewal potential. Immunity. *5*, 207-216.

Munoz-Jordan,J.L., Cross,G.A., de,L.T., and Griffith,J.D. (2001). t-loops at trypanosome telomeres. EMBO J. *20*, 579-588.

Muntoni,A. and Reddel,R.R. (2005). The first molecular details of ALT in human tumor cells. Hum. Mol. Genet. *14 Spec No. 2*, R191-R196.

Murti,K.G. and Prescott,D.M. (1999). Telomeres of polytene chromosomes in a ciliated protozoan terminate in duplex DNA loops. Proc. Natl. Acad. Sci. U. S. A *96*, 14436-14439.

Nakamura,T.M., Morin,G.B., Chapman,K.B., Weinrich,S.L., Andrews,W.H., Lingner,J., Harley,C.B., and Cech,T.R. (1997). Telomerase catalytic subunit homologs from fission yeast and human. Science *277*, 955-959.

Nikitina,T. and Woodcock,C.L. (2004). Closed chromatin loops at the ends of chromosomes. J. Cell Biol *166*, 161-165.

Nosek,J., Kosa,P., and Tomaska,L. (2006). On the origin of telomeres: a glimpse at the pre-telomerase world. Bioessays *28*, 182-190.

Nugent,C.I. and Lundblad,V. (1998). The telomerase reverse transcriptase: components and regulation. Genes Dev. *12*, 1073-1085.

O'Connor,M.S., Safari,A., Liu,D., Qin,J., and Songyang,Z. (2004). The human Rap1 protein complex and modulation of telomere length. J. Biol. Chem. *279*, 28585-28591.

O'Connor,M.S., Safari,A., Xin,H., Liu,D., and Songyang,Z. (2006). A critical role for TPP1 and TIN2 interaction in high-order telomeric complex assembly. Proc. Natl. Acad. Sci. U. S. A *103*, 11874-11879.

Oh,H., Taffet,G.E., Youker,K.A., Entman,M.L., Overbeek,P.A., Michael,L.H., and Schneider,M.D. (2001). Telomerase reverse transcriptase promotes cardiac muscle cell proliferation, hypertrophy, and survival. Proc. Natl. Acad. Sci. U. S. A *98*, 10308-10313.

Ohki,R. and Ishikawa,F. (2004). Telomere-bound TRF1 and TRF2 stall the replication fork at telomeric repeats. Nucleic Acids Res. *32*, 1627-1637.

Olovnikov,A.M. (1973). A theory of marginotomy. The incomplete copying of template margin in enzymic synthesis of polynucleotides and biological significance of the phenomenon. J. Theor. Biol *41*, 181-190.

Ouellette,M.M., Aisner,D.L., Savre-Train,I., Wright,W.E., and Shay,J.W. (1999). Telomerase activity does not always imply telomere maintenance. Biochem. Biophys. Res. Commun. *254*, 795-803.

Ouellette,M.M., Liao,M., Herbert,B.S., Johnson,M., Holt,S.E., Liss,H.S., Shay,J.W., and Wright,W.E. (2000). Subsenescent telomere lengths in fibroblasts immortalized by limiting amounts of telomerase. J. Biol Chem. *275*, 10072-10076.

Pennock,E., Buckley,K., and Lundblad,V. (2001). Cdc13 delivers separate complexes to the telomere for end protection and replication. Cell *104*, 387-396.

Prescott,J. and Blackburn,E.H. (1997). Functionally interacting telomerase RNAs in the yeast telomerase complex. Genes Dev. *11*, 2790-2800.

Prowse,K.R. and Greider,C.W. (1995). Developmental and tissue-specific regulation of mouse telomerase and telomere length. Proc. Natl. Acad. Sci. U. S. A *92*, 4818-4822.

Rahman,R., Mo,L., and Cui,W. (2006). Telomerase with mutated catalytic motifs has dominant negative effects on telomerase activity and inhibits cell growth. Biochem. Biophys. Res. Commun. *350*, 796-802.

Robles,S.J. and Adami,G.R. (1998). Agents that cause DNA double strand breaks lead to p16INK4a enrichment and the premature senescence of normal fibroblasts. Oncogene *16*, 1113-1123.

Romero,D.P. and Blackburn,E.H. (1991). A conserved secondary structure for telomerase RNA. Cell *67*, 343-353.

Rudolph,K.L., Chang,S., Lee,H.W., Blasco,M., Gottlieb,G.J., Greider,C., and DePinho,R.A. (1999). Longevity, stress response, and cancer in aging telomerase-deficient mice. Cell *96*, 701-712.

Samper,E., Flores,J.M., and Blasco,M.A. (2001). Restoration of telomerase activity rescues chromosomal instability and premature aging in Terc-/- mice with short telomeres. EMBO Rep. *2*, 800-807.

Samper,E., Fernandez,P., Eguia,R., Martin-Rivera,L., Bernad,A., Blasco,M.A., and Aracil,M. (2002). Long-term repopulating ability of telomerase-deficient murine hematopoietic stem cells. Blood *99*, 2767-2775.

Sarin,K.Y., Cheung,P., Gilison,D., Lee,E., Tennen,R.I., Wang,E., Artandi,M.K., Oro,A.E., and Artandi,S.E. (2005). Conditional telomerase induction causes proliferation of hair follicle stem cells. Nature *436*, 1048-1052.

Schnapp,G., Rodi,H.P., Rettig,W.J., Schnapp,A., and Damm,K. (1998). One-step affinity purification protocol for human telomerase. Nucleic Acids Res. *26*, 3311-3313.

Shay,J.W. and Wright,W.E. (1989). Quantitation of the frequency of immortalization of normal human diploid fibroblasts by SV40 large T-antigen. Exp. Cell Res. *184*, 109-118.

Shay,J.W., Pereira-Smith,O.M., and Wright,W.E. (1991). A role for both RB and p53 in the regulation of human cellular senescence. Exp. Cell Res. *196*, 33-39.

Shay,J.W. and Wright,W.E. (2000). Implications of mapping the human telomerase gene (hTERT) as the most distal gene on chromosome 5p. Neoplasia. *2*, 195-196.

Shay,J.W. and Wright,W.E. (2000). Hayflick, his limit, and cellular ageing. Nat. Rev. Mol. Cell Biol. *1*, 72-76.

Shay,J.W. and Wright,W.E. (2005). Senescence and immortalization: role of telomeres and telomerase. Carcinogenesis *26*, 867-874.

Singh,S.K., Clarke,I.D., Terasaki,M., Bonn,V.E., Hawkins,C., Squire,J., and Dirks,P.B. (2003). Identification of a cancer stem cell in human brain tumors. Cancer Res. *63*, 5821-5828.

Singh,S.K., Hawkins,C., Clarke,I.D., Squire,J.A., Bayani,J., Hide,T., Henkelman,R.M., Cusimano,M.D., and Dirks,P.B. (2004). Identification of human brain tumour initiating cells. Nature *432*, 396-401.

Smith,J.R. and Whitney,R.G. (1980). Intraclonal variation in proliferative potential of human diploid fibroblasts: stochastic mechanism for cellular aging. Science *207*, 82-84.

Smith,S. and de,L.T. (2000). Tankyrase promotes telomere elongation in human cells. Curr. Biol *10*, 1299-1302.

Smogorzewska,A., van,S.B., Bianchi,A., Oelmann,S., Schaefer,M.R., Schnapp,G., and de,L.T. (2000). Control of human telomere length by TRF1 and TRF2. Mol. Cell Biol. *20*, 1659-1668.

Smogorzewska,A. and de,L.T. (2002). Different telomere damage signaling pathways in human and mouse cells. EMBO J. *21*, 4338-4348.

Smogorzewska,A. and De Lange,T. (2004). Regulation of telomerase by telomeric proteins. Annu. Rev Biochem. *73*, 177-208.

Snow,B.E., Erdmann,N., Cruickshank,J., Goldman,H., Gill,R.M., Robinson,M.O., and Harrington,L. (2003). Functional conservation of the telomerase protein Est1p in humans. Curr. Biol. *13*, 698-704.

Stampfer,M.R. and Yaswen,P. (2003). Human epithelial cell immortalization as a step in carcinogenesis. Cancer Lett. *194*, 199-208.

Stansel,R.M., de,L.T., and Griffith,J.D. (2001). T-loop assembly in vitro involves binding of TRF2 near the 3' telomeric overhang. EMBO J. *20*, 5532-5540.

Starling,J.A., Maule,J., Hastie,N.D., and Allshire,R.C. (1990). Extensive telomere repeat arrays in mouse are hypervariable. Nucleic Acids Res. *18*, 6881-6888.

Steinert,S., Shay,J.W., and Wright,W.E. (2000). Transient expression of human telomerase extends the life span of normal human fibroblasts. Biochem. Biophys. Res. Commun. *273*, 1095-1098.

Stewart,S.A., Ben-Porath,I., Carey,V.J., O'Connor,B.F., Hahn,W.C., and Weinberg,R.A. (2003). Erosion of the telomeric single-strand overhang at replicative senescence. Nat Genet. *33*, 492-496.

Stewart,S.A. (2005). Telomere maintenance and tumorigenesis: an "ALT"ernative road. Curr. Mol. Med. *5*, 253-257.

Sun,H., Karow,J.K., Hickson,I.D., and Maizels,N. (1998). The Bloom's syndrome helicase unwinds G4 DNA. J. Biol Chem. *273*, 27587-27592.

Takai,H., Smogorzewska,A., and de,L.T. (2003). DNA damage foci at dysfunctional telomeres. Curr. Biol. *13*, 1549-1556.

Tarsounas,M., Munoz,P., Claas,A., Smiraldo,P.G., Pittman,D.L., Blasco,M.A., and West,S.C. (2004). Telomere maintenance requires the RAD51D recombination/repair protein. Cell *117*, 337-347.

Tesmer,V.M., Ford,L.P., Holt,S.E., Frank,B.C., Yi,X., Aisner,D.L., Ouellette,M., Shay,J.W., and Wright,W.E. (1999). Two inactive fragments of the integral RNA cooperate to assemble active telomerase with the human protein catalytic subunit (hTERT) in vitro. Mol. Cell Biol. *19*, 6207-6216.

Ting,N.S., Yu,Y., Pohorelic,B., Lees-Miller,S.P., and Beattie,T.L. (2005). Human Ku70/80 interacts directly with hTR, the RNA component of human telomerase. Nucleic Acids Res. *33*, 2090-2098.

van,Steensel.B. and de,L.T. (1997). Control of telomere length by the human telomeric protein TRF1. Nature *385*, 740-743.

van,Steensel.B., Smogorzewska,A., and de,L.T. (1998). TRF2 protects human telomeres from end-to-end fusions. Cell *92*, 401-413.

Verdun,R.E., Crabbe,L., Haggblom,C., and Karlseder,J. (2005). Functional human telomeres are recognized as DNA damage in G2 of the cell cycle. Mol. Cell *20*, 551-561.

von,Zglinicki.T., Saretzki,G., Docke,W., and Lotze,C. (1995). Mild hyperoxia shortens telomeres and inhibits proliferation of fibroblasts: a model for senescence? Exp. Cell Res. *220*, 186-193.

von,Zglinicki.T., Serra,V., Lorenz,M., Saretzki,G., Lenzen-Grossimlighaus,R., Gessner,R., Risch,A., and Steinhagen-Thiessen,E. (2000). Short telomeres in patients with vascular dementia: an indicator of low antioxidative capacity and a possible risk factor? Lab Invest *80*, 1739-1747.

von,Zglinicki.T., Burkle,A., and Kirkwood,T.B. (2001). Stress, DNA damage and ageing -- an integrative approach. Exp. Gerontol. *36*, 1049-1062.

von,Zglinicki.T. (2003). Replicative senescence and the art of counting. Exp. Gerontol. *38*, 1259-1264.

von,Zglinicki.T., Petrie,J., and Kirkwood,T.B. (2003). Telomere-driven replicative senescence is a stress response. Nat Biotechnol. *21*, 229-230.

Vulliamy,T., Marrone,A., Goldman,F., Dearlove,A., Bessler,M., Mason,P.J., and Dokal,I. (2001). The RNA component of telomerase is mutated in autosomal dominant dyskeratosis congenita. Nature *413*, 432-435.

Vulliamy,T., Marrone,A., Szydlo,R., Walne,A., Mason,P.J., and Dokal,I. (2004). Disease anticipation is associated with progressive telomere shortening in families with dyskeratosis congenita due to mutations in TERC. Nat Genet. *36*, 447-449.

Walne,A.J., Marrone,A., and Dokal,I. (2005). Dyskeratosis congenita: a disorder of defective telomere maintenance? Int. J. Hematol. *82*, 184-189.

Wang,J., Xie,L.Y., Allan,S., Beach,D., and Hannon,G.J. (1998). Myc activates telomerase. Genes Dev. *12*, 1769-1774.

Wang,R.C., Smogorzewska,A., and de,L.T. (2004). Homologous recombination generates T-loop-sized deletions at human telomeres. Cell *119*, 355-368.

Watson,J.D. (1972). Origin of concatemeric T7 DNA. Nat New Biol *239*, 197-201.

Wenz,C., Enenkel,B., Amacker,M., Kelleher,C., Damm,K., and Lingner,J. (2001). Human telomerase contains two cooperating telomerase RNA molecules. EMBO J. *20*, 3526-3534.

Wilmut,I., Schnieke,A.E., McWhir,J., Kind,A.J., and Campbell,K.H. (1997). Viable offspring derived from fetal and adult mammalian cells. Nature *385*, 810-813.

Wright,W.E. and HAYFLICK,L. (1975). Nuclear control of cellular aging demonstrated by hybridization of anucleate and whole cultured normal human fibroblasts. Exp. Cell Res. *96*, 113-121.

Wright,W.E., Piatyszek,M.A., Rainey,W.E., Byrd,W., and Shay,J.W. (1996). Telomerase activity in human germline and embryonic tissues and cells. Dev. Genet. *18*, 173-179.

Wright,W.E., Tesmer,V.M., Huffman,K.E., Levene,S.D., and Shay,J.W. (1997). Normal human chromosomes have long G-rich telomeric overhangs at one end. Genes Dev. *11*, 2801-2809.

Wright,W.E. and Shay,J.W. (2002). Historical claims and current interpretations of replicative aging. Nat. Biotechnol. *20*, 682-688.

Wright,W.E. and Shay,J.W. (2005). Telomere-binding factors and general DNA repair. Nat. Genet. *37*, 116-118.

Wu,L., Multani,A.S., He,H., Cosme-Blanco,W., Deng,Y., Deng,J.M., Bachilo,O., Pathak,S., Tahara,H., Bailey,S.M., Deng,Y., Behringer,R.R., and Chang,S. (2006). Pot1 deficiency initiates DNA damage checkpoint activation and aberrant homologous recombination at telomeres. Cell *126*, 49-62.

Ye,J.Z. and De Lange,T. (2004). TIN2 is a tankyrase 1 PARP modulator in the TRF1 telomere length control complex. Nat Genet. *36*, 618-623.

Ye,J.Z., Hockemeyer,D., Krutchinsky,A.N., Loayza,D., Hooper,S.M., Chait,B.T., and de,L.T. (2004). POT1-interacting protein PIP1: a telomere length regulator that recruits POT1 to the TIN2/TRF1 complex. Genes Dev. *18*, 1649-1654.

Yeager,T.R., Neumann,A.A., Englezou,A., Huschtscha,L.I., Noble,J.R., and Reddel,R.R. (1999). Telomerase-negative immortalized human cells contain a novel type of promyelocytic leukemia (PML) body. Cancer Res. *59*, 4175-4179.

Yi,X., Shay,J.W., and Wright,W.E. (2001). Quantitation of telomerase components and hTERT mRNA splicing patterns in immortal human cells. Nucleic Acids Res. *29*, 4818-4825.

Zhong,Z., Shiue,L., Kaplan,S., and de,L.T. (1992). A mammalian factor that binds telomeric TTAGGG repeats in vitro. Mol. Cell Biol. *12*, 4834-4843.

Zhu,J., Wang,H., Bishop,J.M., and Blackburn,E.H. (1999). Telomerase extends the lifespan of virus-transformed human cells without net telomere lengthening. Proc. Natl. Acad. Sci. U. S. A *96*, 3723-3728.

Zhu,X.D., Kuster,B., Mann,M., Petrini,J.H., and de,L.T. (2000). Cell-cycle-regulated association of RAD50/MRE11/NBS1 with TRF2 and human telomeres. Nat. Genet. *25*, 347-352.
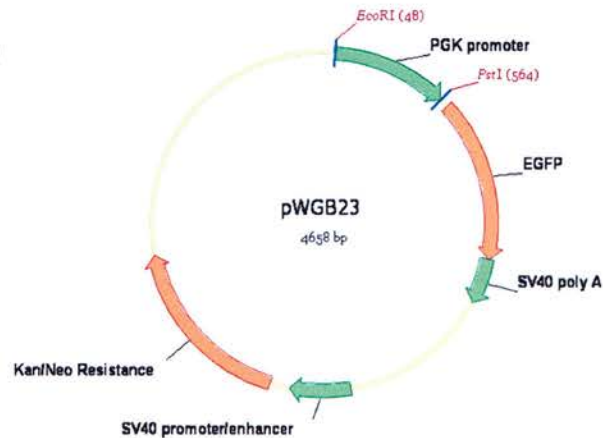
Zou,Y., Sfeir,A., Gryaznov,S.M., Shay,J.W., and Wright,W.E. (2004). Does a sentinel or a subset of short telomeres determine replicative senescence? Mol Biol Cell *15*, 3709-3718.
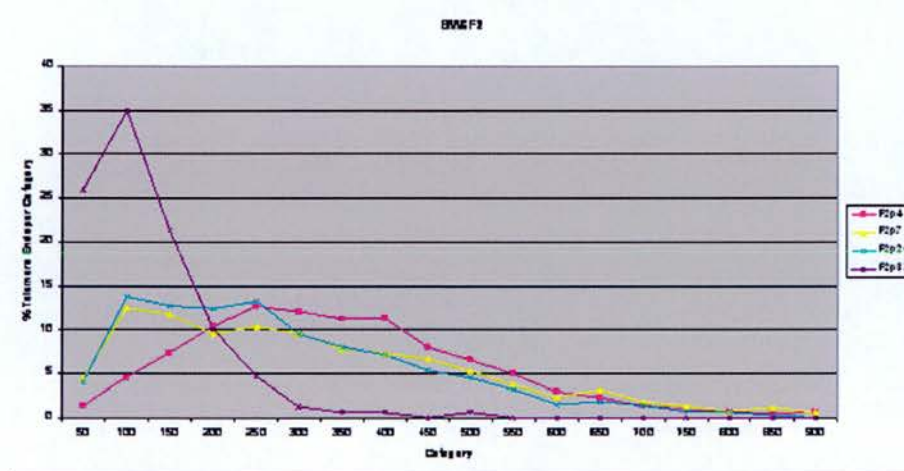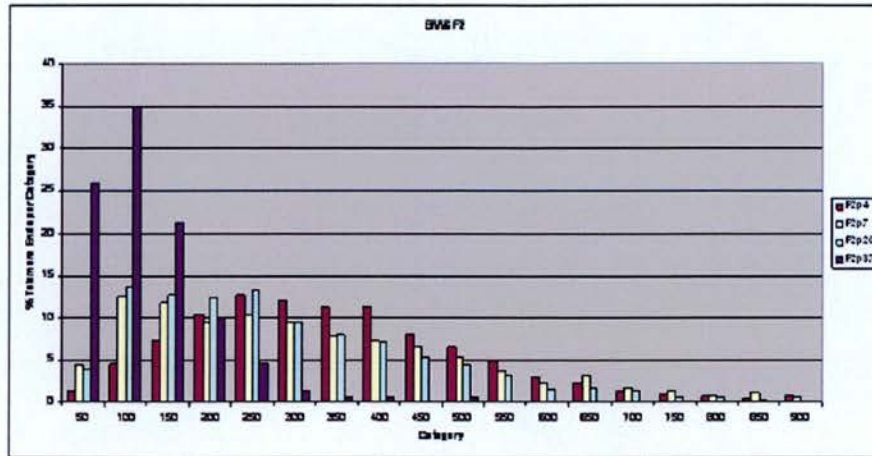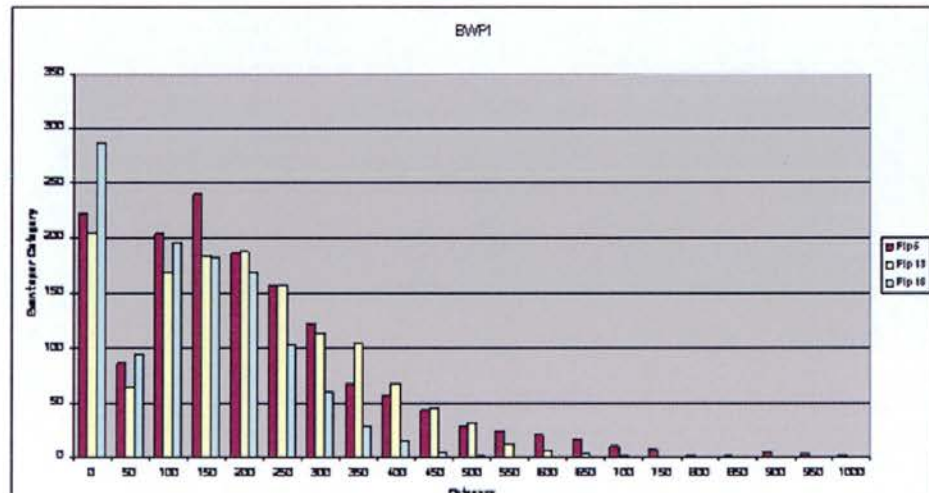
APPENDIX

A
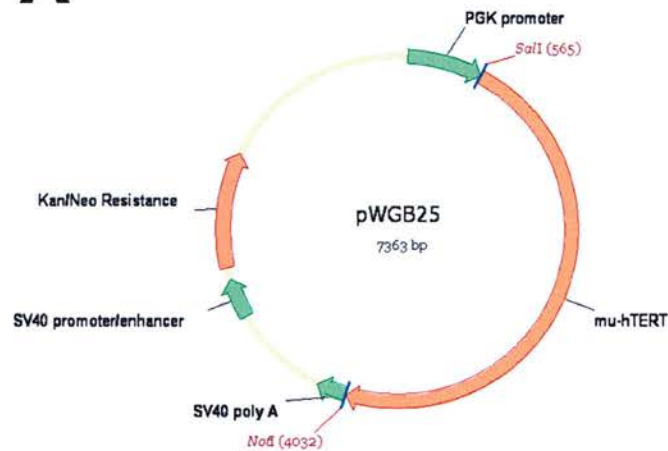
B

Appendix 1: Transgenic constructs used to transfect the GRN1-1 hTERT-immortalized line. The ~4.6Kb EGFP mock vector control construct was initially sub-cloned and placed under the control of a PGK promoter (B). The ~7.3Kb pWGB25 construct (A) was then created by replacing the EGFP transgene sequence with the mutant hTERT transgene sequence under the control of a PGK promoter. Mutant hTERT contains three independent amino acid substitutions ((R631A, D712A and D868A) in the reverse transcriptase motif of hTERT. (Constructs were developed by Dr. Wei Cui).

209

| TFU Category	F1p5 (n=380)	F1p13 (n=337)	F1p18 (n=286)		F2p4 (n=329)	F2p7 (n=323)	F2p20 (n=321)	F2p37 (n=95)
0	222	205	287		106	194	350	211
50	86	64	95		16	47	37	44
100	204	168	195		56	135	127	59
150	240	184	183		89	126	118	36
200	186	188	169		126	104	115	17
250	157	157	102		154	112	122	8
300	123	113	59		146	104	88	2
350	68	104	29		135	84	74	1
400	57	68	15		137	79	66	1
450	43	44	5		97	71	49	0
500	29	31	2		76	57	42	1
550	24	12	0		60	40	29	0
600	20	6	0		35	25	14	0
650	17	3	0		28	33	17	0
700	10	1	0		17	19	12	0
750	7	0	0		12	15	6	0
800	1	0	0		8	8	6	0
850	1	0	0		5	12	2	0
900	5	0	0		8	7	0	0
950	3	0	0		2	8	2	0
1000	2	0	0		3	2	5	0
1050	3	0	0		0	4	1	0
1100	3	0	0		0	1	1	0
1150	3	0	0		0	3	0	0
1200	1	0	0		0	0	1	0
1250	0	0	0		0	0	0	0
1300	1	0	0		0	0	0	0
1350	1	0	0		0	0	0	0
1400	1	0	0		0	0	0	0

Appendix 2: Absolute Telomere Fluorescence Units (TFU) for the BWF1 and BW6F2 sheep fibroblast lines as measured by Q-FISH analysis. TFU categories represent arbitrary TFU which correspond to actual telomere length. n denotes the number of individual chromosomes analyzed for each line.

Appendix 3: Q-FISH profile for BW6F2. Q-FISH profiles showing percentage of telomere ends per TFU category for the BW6F2 line, including the pre-senescent passage 37 stage. This passage was excluded from the main body of analysis due to the low number of quality metaphase spreads obtained from this line. Profiles are shown as a histogram (above) and line graph (below).
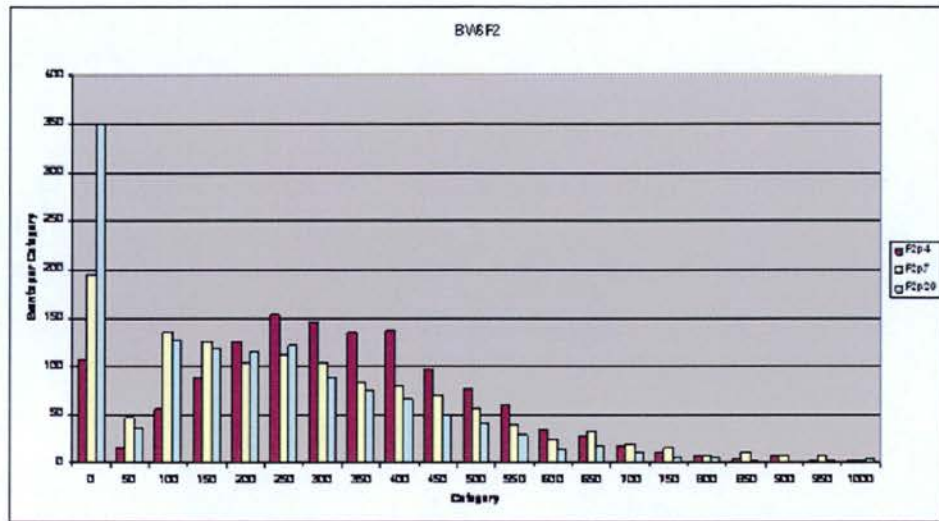
Appendix 4: Q-FISH histogram profiles showing Signal Free Ends (SFE). The SFE category was excluded from the main body of analysis so as not too confound data regarding telomere shortening rate. This represents a limitation to the Q-FISH method applied to the sheep model system; SFE detected by the Q-FISH software do not necessarily reflect true telomere SFE, but moreover, due to the quality of sheep metaphase spreads, many telomere ends remain hidden due to overlapping chromosome arms. Therefore a measure of SFE in this setting will be a substantial overestimate.
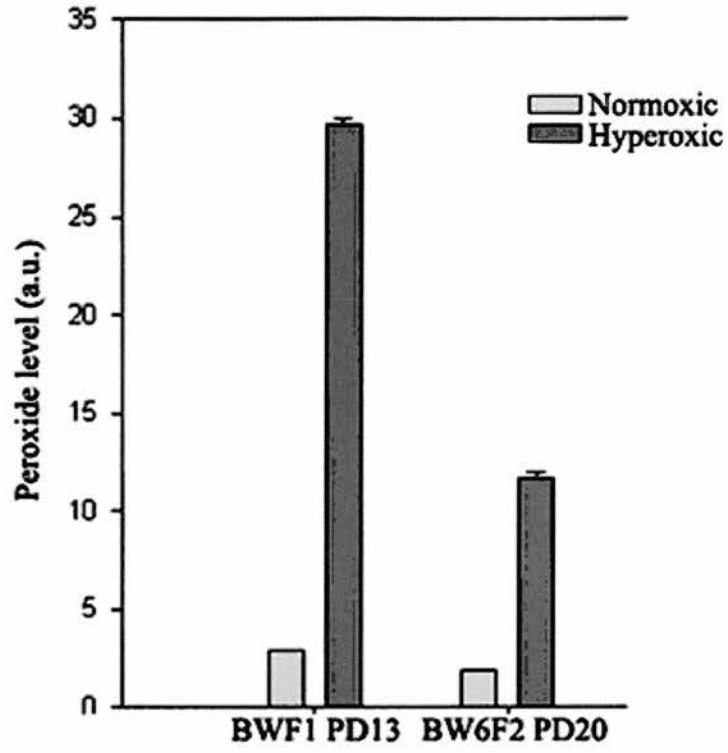
Appendix 5: Response to oxidative Black Welsh normal primary sheep fibroblasts.
Actual units of peroxide released in normoxic and hyperoxic *in vitro* culture conditions.

Publications   **Rahman R, Mo L, Cui W.** Telomerase with mutated catalytic motifs has dominant negative effects on telomerase activity and inhibits cell growth. *Biochemical and Biophysical Research Communications* **350** (2006): 796-802.

Rahman R, Forsythe N, Cui W. Telomere length is directly correlated to 3' overhang length and is a direct function of hTERT gene expression in primary ovine fibroblasts. Manuscript in preparation.

Rahman R. "The Stems of Cancer" (Winning Essay). Genetics Society Newsletter 2005; (52) 50-52.

Abstracts   **Rahman R, Mo L, Cui W.** hTERT non-catalytic function with respect to Telomere maintenance cannot be distinguished from enzymatic activity. 'Telomeres and Telomerase' Abstract Book – Cold Spring Harbour (2005).

Rahman R, Mo L, Cui W. Telomere maintenance requires a functional telomerase complex. 'Telomeres and Genome Stability' Abstract Book – Villars-sur-ollon, Geneva (2006) & 'Telomerase and Cancer Stem Cells' Abstract Book – BACR Meeting, York (2006).

Telomerase with mutated catalytic motifs has dominant negative effects on telomerase activity and inhibits cell growth

Ruman Rahman [a], Ling Mo [a], Wei Cui [b,*]

[a] Department of Gene Function and Development, Roslin Institute, Roslin, Midlothian EH25 9PS, UK
[b] Institute of Reproductive and Developmental Biology, Imperial College London, Faculty of Medicine, Du Cane Road, London W12 0NN, UK

Abstract

Telomerase catalytic subunit (TERT) seems a key factor controlling telomerase activity, telomere length, and cell growth. To further address this issue, we forced expression of a catalytically inactive mutant human TERT (hTERT) in hTERT-immortalised sheep fibroblasts to examine its effects. Expression of mutant hTERT compromised telomerase activity reconstituted by wild-type hTERT in a manner directly attributable to mutant hTERT expression level. High levels of mutant hTERT expression inhibited cell growth with a subset of cells entering replicative senescence. Furthermore, significant telomere attrition was evident in two of three clones with high levels of mutant hTERT expression. Our findings are consistent with the notion that hTERT homodimers are necessarily required to form a functional telomerase complex at the telomere substrate. We also highlight the requirement of a more thorough understanding of telomerase- and telomere-associated factors to understand fully the interplay that governs telomere homeostasis *in vitro* and *in vivo*.
© 2006 Elsevier Inc. All rights reserved.

Keywords: hTERT; Telomerase; Telomere; Senescence; Dominant-negative telomerase

Eukaryotic telomeres are specialised structures located at the ends of linear chromosomes, consisting of proteins and reiterated G-rich repeats that are conserved in all vertebrae as TTAGGG [1]. Telomeres function to protect chromosomal termini from degradation and fusion, thereby contributing to genomic stability [2,3]. In most eukaryotes, telomeric DNA is replenished by the action of telomerase—a specialised cellular ribonucleoprotein reverse transcriptase that synthesizes telomeric repeats onto chromosomal ends [4–6]. Telomerase consists of two main components that are required for core enzymatic activity, a telomerase RNA (TR) as a template for the addition of *de novo* telomeric repeats, and a catalytic protein subunit with reverse transcriptase activity (TERT). It has been reported that human telomerase structure is that of a multimer containing two cooperating hTR molecules [7,8] and most likely two hTERT

molecules [9]. hTERT has been shown to consist of two physically separable functional domains: a polymerase domain, containing RNA interaction domain 2 (RID2), reverse transcriptase (RT) motifs, and C-terminal sequences, and a major accessory domain, RNA interaction domain 1 (RID1) [10]. In humans, telomerase is preferentially expressed in germ-line cells and early embryonic tissues, but is not detected in most somatic cells [11]. Therefore, somatic cells progressively lose their telomere repeats after each round of cell division. Eventually when the telomeres on one or more chromosomes become critically short, cells stop dividing and enter an irreversible state termed replicative senescence [12–14]. However, telomerase is active in the majority of cancer cells; thereby inhibition of active telomerase could be a way to treat cancer.

TERT has been implicated as a key factor limiting telomerase activity as the RNA subunit is constitutively expressed at a low basal level [15] and ectopic expression of hTERT restored telomerase activity, extended

---

* Corresponding author. Fax: +44 20 759 42192.
  E-mail address: wei.cui@imperial.ac.uk (W. Cui).

telomeres, and indefinitely prolonged cellular lifespan [16,17]. It has been hypothesised that dimeric TERT molecules are required to form a functional telomerase complex [8]. However, telomere length is not always maintained in cells with active telomerase and many tumour cell lines are shorter than those of corresponding normal cells, indicating that telomerase activity does not necessarily imply telomere maintenance [18,19]. It has been accepted generally that telomere length in mammalian telomeres is regulated by a homeostatic mechanism that is governed in part by telomerase and a telomere-specific protein complex recently termed 'Shelterin', which consists of TRF1, TRF2, TIN2, Rap1, TPP1, and POT1 [20].

To further address the function of telomerase catalytic subunit TERT in relation to telomerase activity, telomere length, and cell growth, we expressed a catalytically dysfunctional hTERT in an hTERT-immortalised primary sheep foetal fibroblast line in which telomeres stabilise at an average length shorter than that of the untransfected parental line. This system enables us to study if hTERT non-catalytic domains have any effect on telomerase activity and telomere maintenance. Conversely the presence of a catalytically dysfunctional hTERT most likely results in both mutant/wild-type telomerase heterodimers and mutant/mutant telomerase homodimers, both of which may compete with and compromise wild-type/wild-type telomerase homodimers.

Our results showed that overexpression of non-catalytic domain decreased telomerase activity, inhibited cell proliferation, and did not enhance telomere maintenance, which may result from competitive binding to sheep TR molecules and/or disruption of hTERT homodimeric structure. Therefore, our results suggest that telomere maintenance requires a functional telomerase complex which contains hTERT homodimeric structure.

Materials and methods

Cell culture, plasmids, and transfection. Sheep fibroblasts, BW6F2, and their hTERT immortalised clonal line, GRN1-1, were prepared and cultured as described previously [19].

The mock plasmid (pWGB23) was constructed by inserting a mouse phosphoglycerate kinase (PGK) promoter into *Eco*RI/*Pst*I site of the pEGFP-1 vector (Clontech). The mutant hTERT construct (pWGB25) was then generated by replacing the EGFP fragment in pWGB23 with a mutant hTERT cDNA which was kindly provided by Geron Corporation, which contains three point mutations at reverse transcriptase motifs, resulting in three amino acid substitutions from Arginine (631) and Aspartic acid (712 and 868) to Alanine (Fig. 1A). Both vectors were linearised with *Bgl*II and transfection was performed as previously described [19] with 800 μg/ml G418 for selection.

RNA extraction and RT-PCR. Total RNA was extracted using the RNeasy kit (Qiagen) according to the manufacturer's guidelines and digested with DNase I. RT-PCR was performed as previously described [19]. The expression levels were quantified by densitometry and normalised to GAPDH. Relative stoichiometry was inferred by assigning a value of 1 to the parental GRN1-1 and GRN23(C1) mock vector control.

Telomerase activity and telomere length assays. Telomerase activity was analysed by telomeric repeat amplification protocol (TRAP) assay with a TRAPeze Telomerase Detection kit (Chemicon). The product was
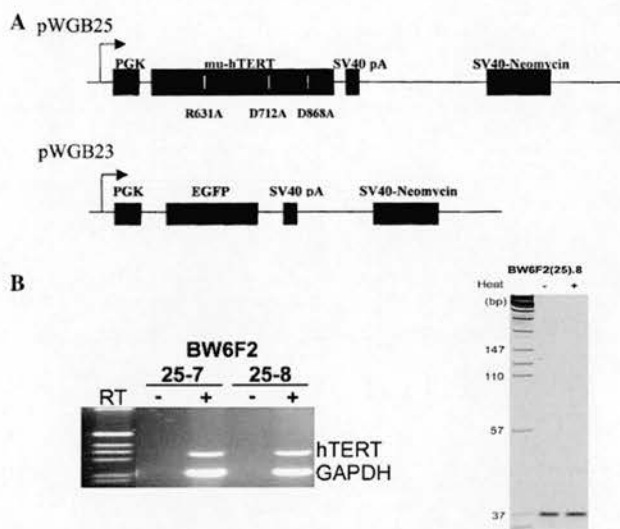

Fig. 1. Expression of mutant hTERT in primary sheep fibroblast. (A) Schematic map of transgenic constructs. pWGB25: mutant hTERT cDNA (7.3 kb) with three amino acid substitutions as indicated; pWGB23: mock EGFP vector. The PGK promoter, SV40 polyadenylation signal, and neomycin selection cassette are indicated. (B) BW6F2(25)-7 and -8 are two clones derived from parental BW6F2 sheep fibroblasts transfected with mutant hTERT, showing high levels of mutant hTERT expression (left) but no detectable telomerase activity (right).

resolved on a 10% polyacrylamide gel and visualised with a PhosphoImager (Amersham Biosciences). Telomere length was determined by telomere restriction fragment (TRF) Southern blot analysis and mean telomere length was calculated [21] and statistics done by Student's *t*-test.

Senescence-associated β-galactosidase staining. Cells were fixed in 3% formaldehyde for 5 min, then incubated for 16 h with freshly prepared senescence-associated β-gal solution after washing with PBS [22].

Results

Expression of mutant hTERT in sheep fibroblasts does not reconstitute telomerase activity

Primary cultures of sheep foetal fibroblasts show similar characteristics to those of human fibroblasts in that no telomerase activity is detectable and cells undergo a limited number of cell divisions. Forced expression of human telomerase catalytic subunit hTERT in sheep fibroblasts, BW6F2, reconstituted telomerase activity and extended their proliferative lifespan [6]. However, telomere lengths were not maintained in all hTERT-immortalised lines, rather they stabilised at various lengths dependent on hTERT expression levels [19]. To further address the effects of telomerase function on telomere maintenance, we constructed a mutant hTERT expression vector (pWGB25, Fig. 1A) in which hTERT was mutated with three point mutations at distinct reverse transcriptase motifs and its expression was under the control of a mouse PGK promoter.

To verify the functionality of this mutant hTERT, we first transfected it into the BW6F2 cells. Several colonies
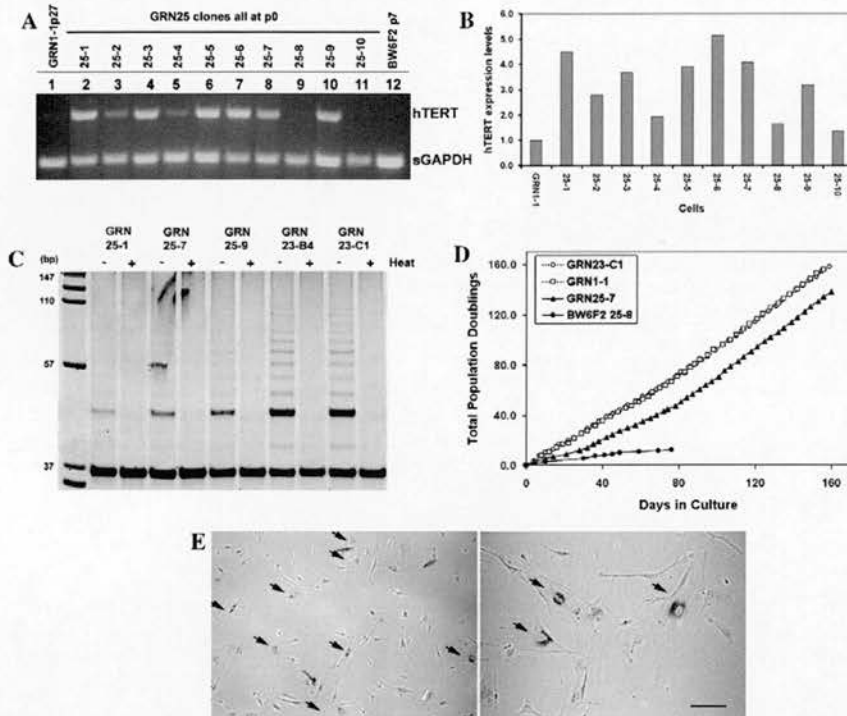
Fig. 2. Effects of mutant hTERT expression on telomerase activity and cell growth. (A) RNA expression analysis in mutant hTERT-transfected GRN1-1 clones. Passage number post-transfection is indicated. Parental BW6F2 and GRN1-1 were used as controls. (B) Histogram of densitometric analysis showing expression levels of the hTERT transgenes. (C) TRAP analysis on selected mutant hTERT positive clones shows that telomerase activity is inhibited in all three mutant hTERT positive lines in comparison to the GRN23-C1 mock vector control clone, with GRN25-1 exhibiting the highest inhibition and GRN25-9 the least. (D) Growth curve of mutant hTERT clone GRN25-7 showed a period of significant slower proliferation with PD time of 40 h. In contrast, hTERT control cells (GRN1-1 and 23-C1) exhibited steady proliferation throughout with approximately 19 h PD time. Expression of mutant hTERT alone did not bypass senescence (BW6F2 25-8). (E) Senescence-associated β-galactosidase staining on GRN25-7 cells. Scale bar represents 250 and 100 μm, respectively.

formed after selection but only two clones (BW6F2 25-7 and 25-8) were able to be expanded to obtain enough cells for transgene analysis. RT-PCR confirmed that the mutant hTERT transgene was expressed and TRAP assay showed no detectable telomerase activity (Fig. 1B). The cells did not proliferate vigorously and senesced after several passages (Fig. 2D). These results confirmed that the three point mutations in reverse transcriptase motifs of hTERT have abolished its catalytic function so that the mutant hTERT does not have the ability to reconstitute telomerase activity.

High levels of mutant hTERT expression compromise telomerase repeat addition processivity

Mutant hTERT does not reconstitute telomerase activity in sheep fibroblasts. However, what effect does it have on active telomerase activity? To test this, we transfected mutant hTERT into the hTERT-immortalized foetal sheep fibroblast line GRN1-1, in which the hTERT expression level is sufficient to immortalise the cells but not to maintain the full telomere length [19]. Ten clones were isolated after selection. We also transfected GRN1-1 with a mock vector in which mutant hTERT was replaced by EGFP.

All the colonies were expanded up to T25 flasks and 2/3 cells were frozen down and the rest further expanded for expression analysis.

The transgene expression was validated by RT-PCR. Due to only three base pairs differing between wild- and mutant-hTERT, we were unable to differentiate between their expression levels. Thus, expression of total hTERT mRNA was analysed by semi-quantitative RT-PCR. As they were all derived from clonal cell line GRN1-1 and have similar levels of wild-type hTERT, the excess of TERT above that of the controls was mainly attributed to mutant hTERT levels. The results showed that eight of 10 clones (GRN25-1, -2, -3, -4, -5, -6, -7, and -9) expressed higher levels of hTERT (Fig. 2A, lanes 2–11) than the original GRN1-1 (Fig. 2A, lane 1) and that hTERT expression in mock controls, GRN23-C1, and GRN23-C4 was similar to that in GRN1-1 (data not shown). We calculated that clone GRN25-1, -6, and -7 exhibited over 3-fold higher mutant hTERT expression than the wild-type (Fig. 2B) and clone 25-3, -5, and -9 over 2-fold. Therefore, they were grouped as the high and medium expression, respectively.

To test effects of mutant hTERT expression on telomerase activity, we carried out TRAP assay on some of these

clones, GRN25-1, 25-7, and 25-9. The results showed that telomerase activity was inhibited in all three lines in comparison to GRN23-C1 mock vector control clones (Fig. 2C). The levels of inhibition seemed related to mutant hTERT expression levels, with GRN25-1 exhibiting the highest inhibition and GRN25-9 the least, indicating that the mutant hTERT functions dominant-negatively to inhibit telomerase activity.

Effects of high mutant hTERT-expression on cell proliferation and senescence

Since the TRAP assay results showed that telomerase activity in the mutant clones was inhibited, we next examined the effect of mutant hTERT on cell growth and proliferation. We resuscitated clones exhibiting medium and high levels of mutant hTERT expression (GRN25-1, 25-5, 25-6, 25-7, and 25-9) and monitored their proliferation by recording their growth curves. All the clones, except clone GRN25-1 and GRN25-7, grew uncompromised with a steady rate of proliferation during the 160 days of culture, with about one population doubling every 19 h. There is no significant difference to the overall proliferation profile between these clones and control GRN23 clones which only expressed wild-type hTERT.

In clones GRN25-1 and GRN25-7 (particularly clone GRN25-7), however, a period of slower proliferation was evident at around 3 weeks of continuous culture, in which population doubling rate slowed to over 40 h (Fig. 2D). Concurrent with this, a subset of cells within the population adopted morphology of bigger and flat appearance with clearly visible microtubules, a characteristic of the senescent phenotype. This subset of cells represented around 30% of the total population. To further confirm that these cells were senescent, we applied the senescence-associated -galactosidase (SA-β-gal) staining assay to the GRN25-7 cells and the results indicated positive staining as expected (Fig. 2E). No such phenomenon was found

in GRN23 control cells. Since these phenomena only appeared in high expressing mutant hTERT clones, it is suggested that the high expression of mutant hTERT might play a critical role leading to cellular senescence.

However, it is interesting why not all the cells were affected as they came from a clonal population. We noticed that after a period of time of *in vitro* culture, even a clonal cell population will exhibit heterogeneity, particularly with regard to transgene expression. In some cells, the transgene expression was silenced. This occurred in both GRN23 clonal GFP clones and GRN25 mutant hTERT clones. In the former case, some cells lost GFP expression, resulting in a mosaic GFP expression pattern in the cell population even though they all expressed GFP at the beginning of *in vitro* culture. Nevertheless, GFP expression does not affect cell growth and both silenced and expressing cell types probably proliferate at a similar rate, thus maintaining the mosaic pattern for a long time. By contrast, in the latter case, the silenced mutant hTERT transgene relieved inhibition pressure in the cells, giving them a growth advantage over the cells expressing mutant hTERT. Therefore, after long-term culture and propagation, the silenced mutant hTERT cells would have been selected for and thus overwhelm the whole population. This was confirmed by RT-PCR and TRAP assay to test mutant hTERT expression and telomerase activity at early and late passage cells. The results showed a dramatic downregulation of total hTERT expression, to levels similar to wild-type hTERT levels in GRN1-1, indicating almost complete silencing of mutant hTERT (Fig. 3A). Correspondingly, the telomerase activity was restored to similar levels as in control cells (Fig. 3B).

The relationship between telomerase expression, telomerase activity, and telomere maintenance is complex

We also examined the effects of mutant hTERT expression on telomere length in these cells. Telomere lengths
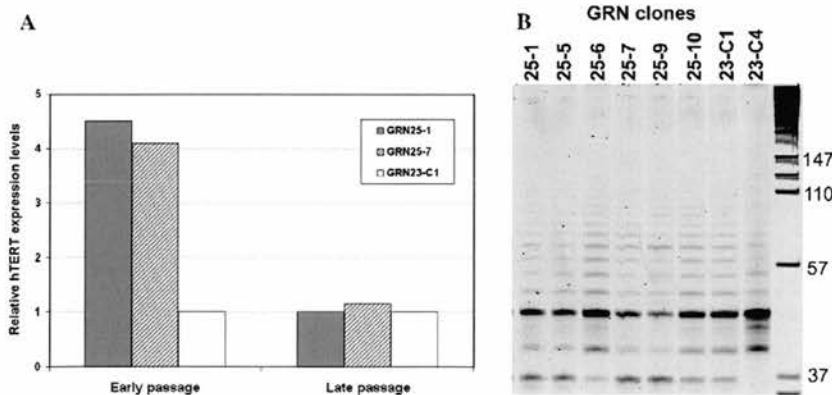

Fig. 3. Loss of mutant hTERT expression upon long-term culture. (A) Histogram of RT-PCR densitometric analysis of hTERT in early and late passage transfected clones showed a dramatic reduction in levels of total hTERT expression in mutant hTERT clones (GRN25-1 and -7) at late passage, indicating almost complete silencing of the mutant hTERT transgene. (B) Inhibition of telomerase activity in GRN25-1 and 25-7 was also lost after long-term culture (100 days), showing all GRN clones exhibiting comparable telomerase activity.
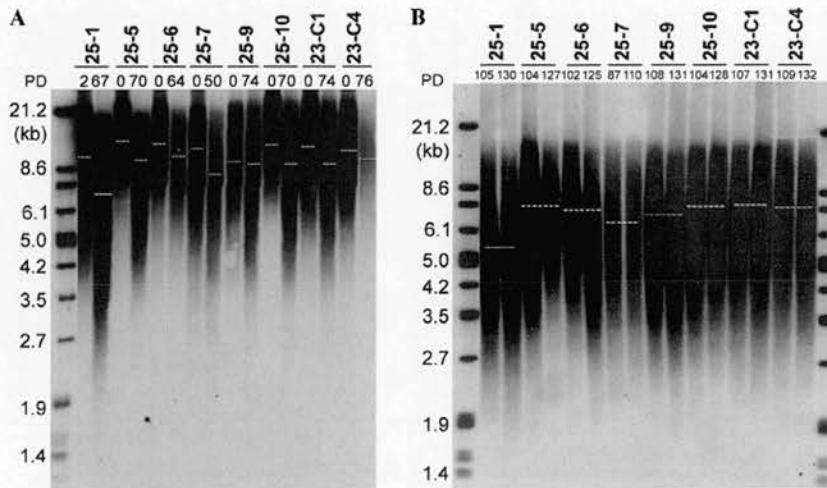
Fig. 4. Telomere length analysis in mutant hTERT clones. (A) All clones showed telomere erosion after 70 population doublings with clones GRN25-1 and -7 exhibiting the most telomere attrition. All other clones (GRN25-5, 6, 9, and 10) had similar telomere shortening in comparison to the mock controls (GRN23-C1 and C4). (B) Telomere length stabilised at a length in each clone after long-term culture. GRN25-1 and -7 still showed significantly shorter mean telomere lengths compared to the others. PD, population doublings.

were measured at multiple time points (0, 70, and 130 days) during long-term culture. The results showed that after ~70 days in culture, telomere lengths shortened in all cell lines (Fig. 4A). However, GRN25-1 and GRN25-7 exhibited significantly shorter mean telomere length (6.7 and 7.7 kb, respectively) in comparison with GRN23 control cells (9.2 and 10.1 kb, $p < 0.05$). The remaining GRN25 clones showed similar telomere shortening as GRN23 controls ($p > 0.1$).

This pattern of telomere shortening persisted throughout the culture period and mean TRF lengths in all GRN clones were stabilised after approximately 100 population doublings post-transfection. Stabilised mean TRF length in clones GRN25-5, -6, and -9 were within the range of 6.6–7.1 kb and did not differ significantly to the 7.0 and 7.2 kb of GRN23 mock controls ($p > 0.1$), whereas the mean TRF lengths in GRN25-1 and -7 were eventually stable at 5.2 and 6.3 kb, significantly shorter than that in the mock controls ($p < 0.0005$) (Fig. 4B). These results indicate that high levels of mutant hTERT expression might have accelerated the telomere shortening, probably as a consequence of inhibited telomerase activity. However, the other high expressing mutant hTERT clone GRN25-6 did not exhibit this faster telomere shortening in spite of the clear inhibition of telomerase activity. And, although telomerase activity was restored to levels comparable to the control GRN23 cells at late passage due to transgene silencing, we did not observe telomere lengthening in the GRN25-1 and 25-7 cells. These results suggest that telomere length regulation is more complicated and consideration has to be given to the plethora of factors involved.

Discussion

In this report, we forced expression of a catalytically inactive mutant hTERT in hTERT-immortalised primary

sheep fibroblasts to examine its effects on telomerase activity, telomere length, and cell proliferation. We showed that clones exhibiting high levels of mutant hTERT expression inhibited telomerase activity, whereas, clones exhibiting lower levels did not. These results indicate that the inhibition effect of mutant hTERT has a threshold and this is likely due to a dominant-negative and/or competitive inhibition effect between the wild-type and mutant hTERT proteins. Thus mutant hTERT expression compromised wild-type telomerase activity in a manner directly attributable to mutant hTERT expression level. When mutant hTERT expression is sufficiently higher than the wild-type, it competitively inhibits the binding of wild-type hTERT to telomerase RNA or the formation of TERT homodimers, hence inhibition of telomerase activity. However, we noticed that when TRAP assay was conducted using 0.5 μg rather than 0.1 μg protein lysate, low levels of telomerase activity were detectable in cells with high expressing mutant hTERT. This low level of telomerase activity could be due to a small number of cells in which mutant hTERT was silenced or expressed at low levels.

We also found that high levels of mutant hTERT expression in these immortalised cells not only inhibited telomerase activity but also affected cell proliferation and telomere length, which could be the consequence of telomerase inhibition. After a short-term in culture, a subset of cells in the high mutant hTERT expressing clones exhibited a senescent phenotype and expressed SA-β-gal. This is reflected in the growth curves, as these cells went through a period of slower growth. Unfortunately, a small number of cells lost mutant hTERT expression shortly after culturing and these cells therefore had a growth advantage over the high mutant hTERT expressing cells. Therefore, during cell propagation, they gradually took over the population. After long-term culture, hardly any mutant hTERT expression was detected.

Significant telomere attrition was evident in two of three clones with high levels of mutant hTERT expression (GRN25-1 and GRN25-7). Telomeres in these clones eventually reached mean stabilised lengths much shorter than those in mock controls. These results seem to be directly attributable to mutant hTERT expression. Mutant hTERT/mutant hTERT and mutant hTERT/wild-type hTERT dimeric complexes are likely to be in much greater abundance than wild-type/wild-type dimers within these lines. Inhibition of telomerase activity and increased telomere attrition are therefore likely to be due to the compromising of wild-type homodimeric function at the telomere substrate due to the molar ratio imbalance of hTERT complexes. This is consistent with the notion that hTERT homodimers are necessary to form a functional telomerase complex at the telomere substrate [9], where catalytic domains of both hTERT molecules may function inter-dependently. Surprisingly one clone with high mutant hTERT expression level and subsequent abrogation of telomerase activity showed comparable stabilised mean telomere length to mock controls. We believe this highlights the limitation of in vitro based telomerase activity assays to assess proper telomerase function on telomere regulation; Telomere length is not controlled by telomerase (TERT and TR) alone but requires other telomerase associated proteins and telomere binding proteins, such as POT1, TRF1, and TRF2 [20]. Therefore differences in expression level of these factors may account for this discrepancy.

It is interesting to note that in spite of the loss of mutant hTERT expression in the late passage of GRN25-1 and GRN25-7, the telomere length in these two clones did not recover to the length comparable to the mock controls after long-term culture, rather they stabilised at the short telomere length. The mechanism behind it is not clear. It was reported that loss of dominant-negative hTERT transgene expression in human leukaemia cells resulted in telomere lengthening in human leukaemia cells [23]. This discrepancy could be due to the species differences between hTERT in human cells and hTERT in sheep cells.

In summary, our results support the notion that telomere maintenance requires a functional telomerase complex with hTERT monomers likely interacting in an inter-dependent manner. Furthermore the result demonstrates that although hTERT non-catalytic domains may be necessary for telomerase assembly and processivity at the telomere substrate, they are not rate-determining. Catalytic hTERT domains appear to be a crucial rate-determining factor regarding processivity; however, a more thorough understanding of telomerase- and telomere-associated factors will be required to understand fully the interplay that governs telomere homeostasis in vitro and in vivo. Consistent with the work from other laboratories, our results also showed a potential interest of using anti-telomerase gene therapy to treat cancer but consideration has to be taken on how to overcome the transgene silencing in a small number of cells.

References

[1] J. Meyne, R.L. Ratliff, R.K. Moyzis, Conservation of the human telomere sequence (TTAGGG)n among vertebrates, Proc. Natl. Acad. Sci. USA 86 (1989) 7049–7053.

[2] C.M. Counter, A.A. Avilion, C.E. LeFeuvre, N.G. Stewart, C.W. Greider, C.B. Harley, S. Bacchetti, Telomere shortening associated with chromosome instability is arrested in immortal cells which express telomerase activity, EMBO J. 11 (1992) 1921–1929.

[3] J.A. Hackett, D.M. Feldser, C.W. Greider, Telomere dysfunction increases mutation rate and genomic instability, Cell 106 (2001) 275–286.

[4] C.W. Greider, E.H. Blackburn, The telomere terminal transferase of Tetrahymena is a ribonucleoprotein enzyme with two kinds of primer specificity, Cell 51 (1987) 887–898.

[5] J. Lingner, T.R. Hughes, A. Shevchenko, M. Mann, V. Lundblad, T.R. Cech, Reverse transcriptase motifs in the catalytic subunit of telomerase, Science 276 (1997) 561–567.

[6] W. Cui, D. Wylie, S. Aslam, A. Dinnyes, T. King, I. Wilmut, A.J. Clark, Telomerase-immortalized sheep fibroblasts can be reprogrammed by nuclear transfer to undergo early development, Biol. Reprod. 69 (2003) 15–21.

[7] C. Wenz, B. Enenkel, M. Amacker, C. Kelleher, K. Damm, J. Lingner, Human telomerase contains two cooperating telomerase RNA molecules, EMBO J. 20 (2001) 3526–3534.

[8] J. Prescott, E.H. Blackburn, Functionally interacting telomerase RNAs in the yeast telomerase complex, Genes Dev. 11 (1997) 2790–2800.

[9] T.L. Beattie, W. Zhou, M.O. Robinson, L. Harrington, Functional multimerization of the human telomerase reverse transcriptase, Mol. Cell. Biol. 21 (2001) 6151–6160.

[10] T.J. Moriarty, D.T. Marie-Egyptienne, C. Autexier, Functional organization of repeat addition processivity and DNA synthesis determinants in the human telomerase multimer, Mol. Cell. Biol. 24 (2004) 3720–3733.

[11] W.E. Wright, M.A. Piatyszek, W.E. Rainey, W. Byrd, J.W. Shay, Telomerase activity in human germline and embryonic tissues and cells, Dev. Genet. 18 (1996) 173–179.

[12] M.T. Hemann, M.A. Strong, L.Y. Hao, C.W. Greider, The shortest telomere, not average telomere length, is critical for cell viability and chromosome stability, Cell 107 (2001) 67–77.

[13] P.M. Lansdorp, Repair of telomeric DNA prior to replicative senescence, Mech. Ageing Dev. 118 (2000) 23–34.

[14] Y. Zou, A. Sfeir, S.M. Gryaznov, J.W. Shay, W.E. Wright, Does a sentinel or a subset of short telomeres determine replicative senescence? Mol. Biol. Cell 15 (2004) 3709–3718.

[15] J. Feng, W.D. Funk, S.S. Wang, S.L. Weinrich, A.A. Avilion, C.P. Chiu, R.R. Adams, E. Chang, R.C. Allsopp, J. Yu, The RNA component of human telomerase, Science 269 (1995) 1236–1241.

[16] A.G. Bodnar, M. Ouellette, M. Frolkis, S.E. Holt, C.P. Chiu, G.B. Morin, C.B. Harley, J.W. Shay, S. Lichtsteiner, W.E. Wright, Extension of life-span by introduction of telomerase into normal human cells [see comments], Science 279 (1998) 349–352.

[17] C.M. Counter, W.C. Hahn, W. Wei, S.D. Caddle, R.L. Beijersbergen, P.M. Lansdorp, J.M. Sedivy, R.A. Weinberg, Dissociation among in vitro telomerase activity, telomere maintenance, and cellular immortalization [see comments], Proc. Natl. Acad. Sci. USA 95 (1998) 14723–14728.

[18] M.M. Ouellette, D.L. Aisner, I. Savre-Train, W.E. Wright, J.W. Shay, Telomerase activity does not always imply telomere maintenance, Biochem. Biophys. Res. Commun. 254 (1999) 795–803.

[19] W. Cui, S. Aslam, J. Fletcher, D. Wylie, M. Clinton, A.J. Clark, Stabilization of telomere length and karyotypic stability are directly correlated with the level of hTERT gene expression in primary fibroblasts, J. Biol. Chem. 277 (2002) 38531–38539.

[20] L.T. de, Shelterin: the protein complex that shapes and safeguards human telomeres, Genes Dev. 19 (2005) 2100–2110.

[21] M.M. Ouellette, M. Liao, B.S. Herbert, M. Johnson, S.E. Holt, H.S. Liss, J.W. Shay, W.E. Wright, Subsenescent telomere lengths in fibroblasts immortalized by limiting amounts of telomerase, J. Biol. Chem. 275 (2000) 10072–10076.

[22] G.P. Dimri, X. Lee, G. Basile, M. Acosta, G. Scott, C. Roskelley, E.E. Medrano, M. Linskens, I. Rubelj, O. Pereira-Smith, A biomarker that identifies senescent human cells in culture and in aging skin in vivo, Proc. Natl. Acad. Sci. USA 92 (1995) 9363–9367.

[23] F. Delhommeau, A. Thierry, D. Feneux, E. Lauret, E. Leclercq, M.H. Courtier, F. Sainteny, W. Vainchenker, A. Naceur-Griscelli, Telomere dysfunction and telomerase reactivation in human leukemia cell lines after telomerase inhibition by the expression of a dominant-negative hTERT mutant, Oncogene 21 (2002) 8262–8271.